THE UNIVERSITY OF CALGARY

Sedimentology and Diagenesis of the Nisku Formation, Wayne, Alberta

by

Blake Harold Ford

A THESIS

SUBMITTED TO THE FACULTY OF GRADUATE STUDIES

IN PARTIAL FULFILMENT OF THE REQUIREMENTS FOR THE

DEGREE OF MASTER OF SCIENCE

DEPARTMENT OF GEOLOGY AND GEOPHYSICS

CALGARY, ALBERTA

DECEMBER, 1998

ABSTRACT

The Nisku Formation is divided into three sub-units in the Wayne area. The Nisku 1 contains five lithofacies that were deposited proximal to an evaporitic salina environment. The underlying Nisku 2 contains seven lithofacies that range from peritidal, to restricted shallow subtidal, to open marine subtidal. Laterally adjacent to the Nisku 2, the Nisku 3 was deposited in a NW-SE trending channel, and is comprised of four deep subtidal lithofacies. Underlying structural activity may have influenced the position of the channel as well as other Nisku deposits. Stratigraphic continuity of Nisku 2 and 3 cycles is questionable.

Diagenesis has significantly obscured primary depositional textures. Related to an intraformational unconformity at the Nisku 1 and 2 contact, early diagenesis resulted in localized dolomitization, cavity formation and sedimentation, collapse brecciation, and cementation of underlying Nisku 2 strata. Late diagenesis caused pervasive dolomitization, fossil mold development, fracturing, and cementation of pore space.

ACKNOWLEDGEMENTS

I thank PanCanadian Petroleum Ltd. for financial support with core table rental, thin section preparation, photographs, drafting, reproduction, and work space.

I thank the Natural Sciences and Engineering Research Council of Canada for providing a PGS A scholarship over the course of my Master's studies. The University of Calgary, through grants and teaching assistantships, also provided financial aid.

The assistance and patience provided by PanCanadian employees such as Wanda Nyysola, Colin Cox, Donna Berndt, Bev Morgan, Phil Argatoff, as well as the entire drafting, reproduction and library staffs is greatly appreciated.

Those who have contributed thoughtful suggestions and stimulating discussion, including John Weissenberger, Peter Boyle, Doug Hansen, Geoff Burrowes, Wayne Cox, Dan Potocki, Ian Hutcheon, Jason Squires, Marian Warren, Mark Cooper, Doug Scott, Jerry Lucia, Murray Gilhooly, Mark Hearn, and Les Eliuk, I am grateful.

Special thanks go to Melanie Kells, my not so harsh first draft editor/complaints department. To you I owe many spiced chais.

My supervisor, John Hopkins, provided the blue, black, green, and yes, RED editorial inks for my initial attempts at penmanship. The simple logic behind most arguments became much clearer through your explanations and elimination of the 'fluffy' language. Thanks for taking me on as one of your students.

I am indebted to Ian McIlreath for conceiving the thesis topic, offering such a great deal of his time to explain the basics of carbonates, assisting me in core and thin section description, sharing but not influencing me with his ideas, and for giving me a periodic kick in the !#$* (pants) to get finished. Do you think you have finally gotten rid of me?

My friends and family, particularly Mom and Dad, have been wonderfully supportive throughout my stint back at school. Can you put up with me through a Ph.D. as well? Just kidding. Many thanks to all of you.

Lastly, I am deeply grateful to my wife Lisa for carrying me through the turbulent ride of the past two years. Without your patience and encouragement I might never have completed this, what seemed to be at the time, insane work.

TABLE OF CONTENTS

LIST OF TABLES

LIST OF FIGURES

Chapter 1 INTRODUCTION

1.1 INTRODUCTION

The Frasnian Nisku Formation has been a prolific source of hydrocarbons within south-central Alberta over the past half century. Most large discoveries took place during the 1950's and include those in the Bashaw area as well as the more southerly Drumheller and West Drumheller fields. Recent exploration has concentrated on the smaller, more elusive traps in the region.

Drilled in October of 1993 by PanCanadian Petroleum Limited, the 37 m oil column of the Wayne Nisku 'A' pool discovery well was a significant find in the southern Alberta Nisku platform. Presently, four pools comprise the Wayne field (Figure 1.1) with total recoverable reserves estimated at over 20 million barrels of 32° API oil.

1.2 STUDY AREA

The study area is located in the subsurface of south-central Alberta and includes the northern thirds of Township 27 Ranges 20 and 21, all of Township 28 Ranges 20 and 21, and, the southern half of Township 29 Range 21 (Figure 1.1). The study area spans nearly 300 km^2 and is bordered by the town of Drumheller to the northeast. Focus is on the Wayne Nisku 'A' and 'B' pools because of the high concentration of wells and drillcore contained within. The Devonian strata of interest presently reside at depths ranging from 1500 m to 1900 m below ground surface. Regional dip is approximately 0.5° to the west.

1.3 OBJECTIVES

Little has been published on the Nisku Formation in the Drumheller area despite its economic significance. Wayne is a logical subject to help fill a gap in the subsurface knowledge of the Nisku Formation in the area. The principal objective of this study is to gain an understanding of the sedimentology of the formation. Specifically:

(1) To document the lithofacies present within the Nisku Formation.

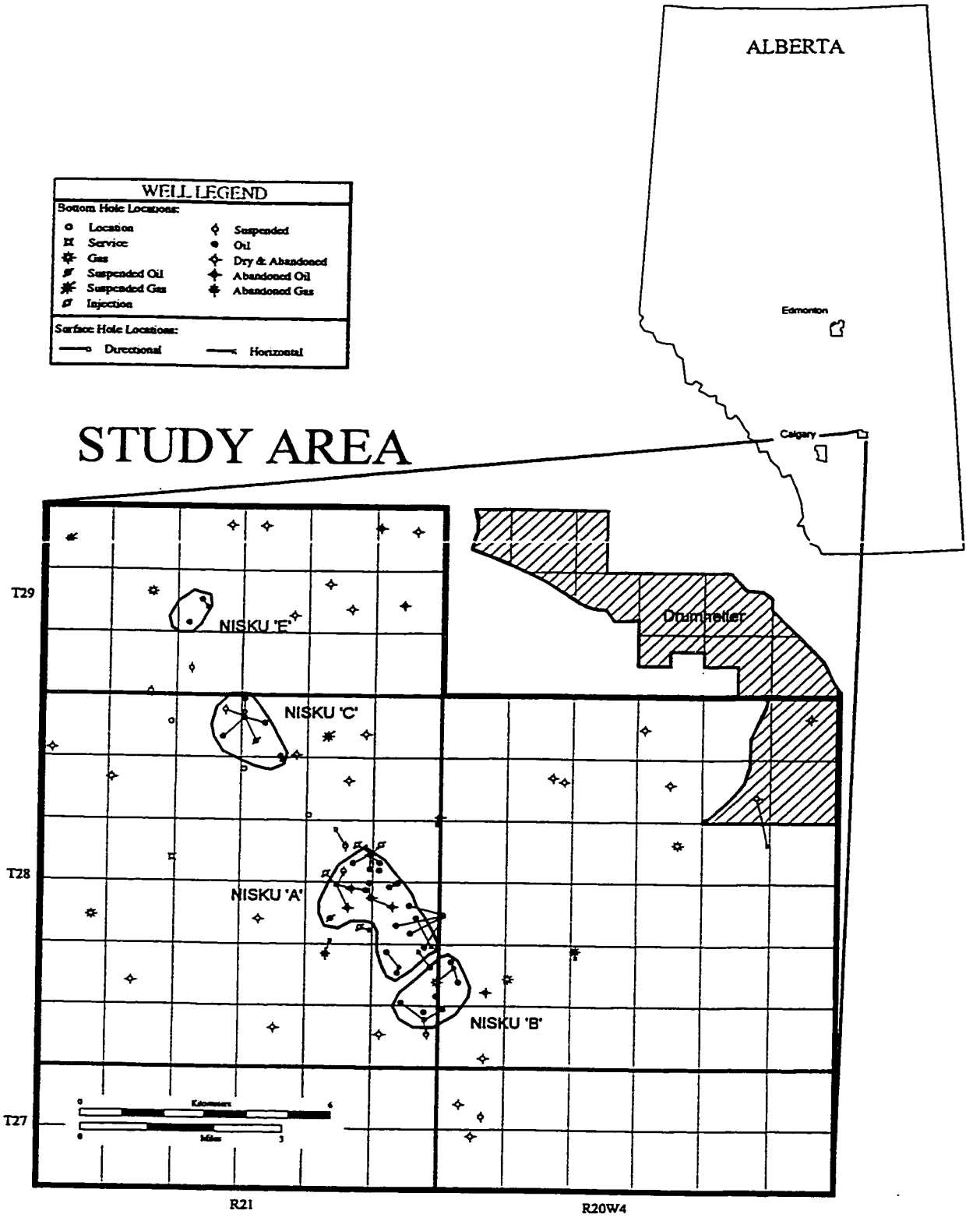

Figure 1.1 Location map of study area and positions of pools within the Wayne field.

(2) To reconstruct the paleoenvironment at the time of deposition of the Nisku Formation lithofacies.

(3) To determine the lateral and vertical associations amongst Nisku Formation lithofacies and establish their stacking patterns within a three-dimensional framework.

The second objective of this study is to examine and interpret the diagenetic alterations which have affected the Nisku Formation strata from initial burial to the present. Specific attention will be paid to dolomitization, anhydritization, and cavity-forming processes. The final goal is to establish a paragenetic sequence to determine the relative ages of diagenetic events.

A third objective is to investigate potential structural influences on the Nisku Formation in the study area, especially in relation to the positioning of the pools along the Wayne field.

1.4 METHODOLOGY

The two predominant methods used to study sedimentologic and diagenetic fabrics were: (a) direct observations of drillcore, and (b) petrographic analysis of core samples.

A total of 516 m of core from 28 wells within the study area (Figure 1.2; Table 1.1) were examined at the Calgary Core Research Centre of the Alberta Energy and Utilities Board during the summer of 1997. A sample of fourteen detailed core descriptions are included in Appendix I. All core are from within the Nisku Formation yet none contain the entire Nisku interval; no upper or lower formational contacts are present. The mean length of the cores is 18.5 m. Cores were examined to obtain information on lithology, sedimentary structures, faunal composition, colour, and diagenetic features.

Of approximately 150 core samples, 140 were made into thin sections. All thin sections were half stained with Alizarin red-S and potassium ferricyanide for standard light microscopy. Thin sections were examined for lithology, crystal/grain sizes, sedimentary structures, faunal composition, and diagenetic features.

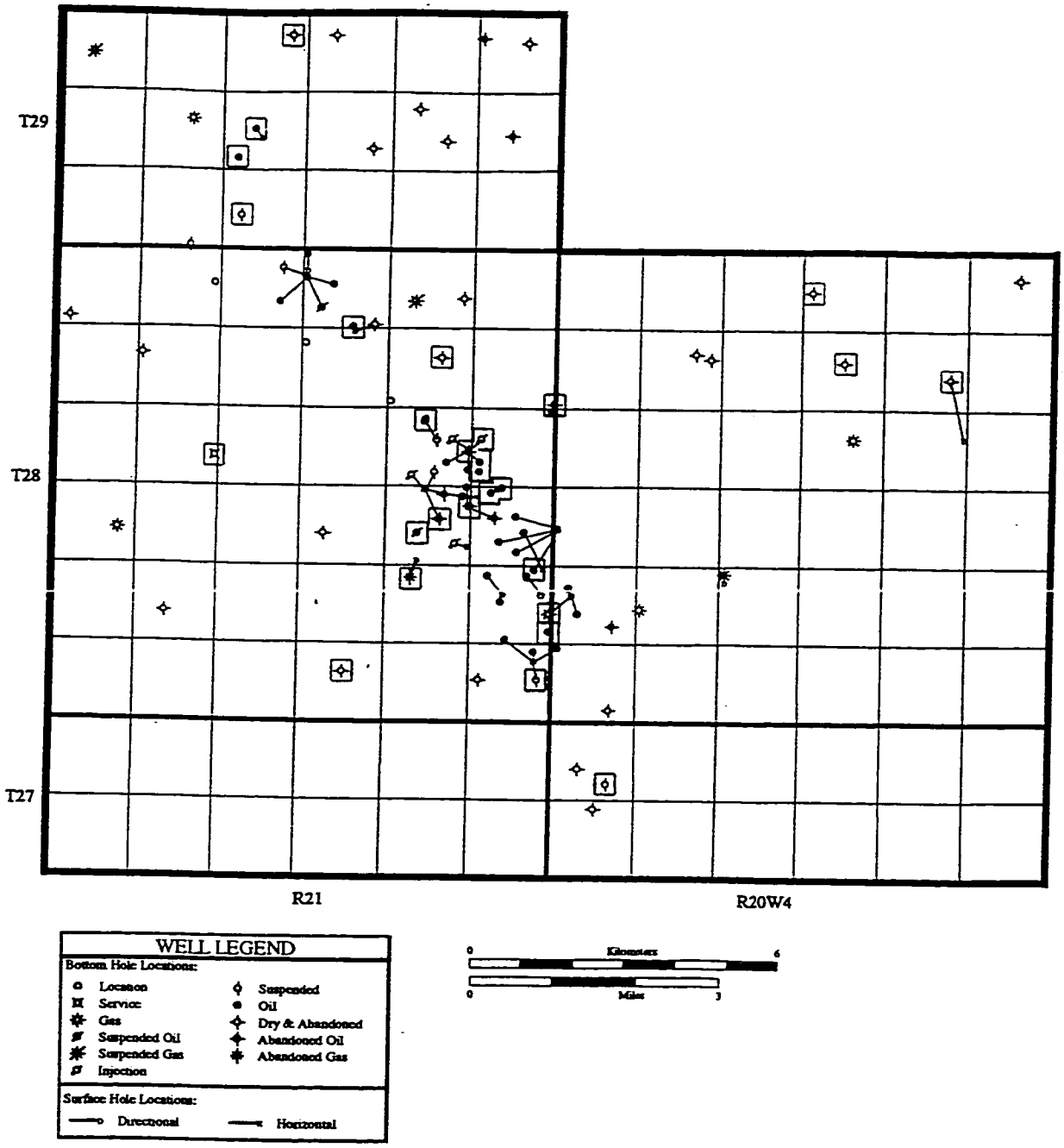

Figure 1.2 Location of wells penetrating the Nisku Formation. Wells outlined with squares contain cores that were logged for the present study.

	Well Location	Core Interval Logged (m)	No. of m logged
	02-31-27-20W4	1723-1741	18 m
	08-26-28-20W4	2247.8-2266.5	18.7 m
	10-27-28-20W4	1691.5-1709.8	18.3 m
	05-34-28-20W4	1703-1713.2	10.2 m
*	09-01-28-21W4	1826.75-1844.75	18 m
*	10-03-28-21W4	1801-1813.8	12.8 m
*	14-11-28-21W4	1835-1853.4	18.4 m
	01-12-28-21W4	1736-1751	15 m
*	08-12-28-21W4	1880.65-1898.45	17.8 m
	16-12-28-21W4	2055-2073	18 m
*	13-13-28-21W4	1767.6-1785.1, 1785.3-1802.8	35 m
*	14-13-28-21W4	1753.6-1772	18.4 m
*	06-14-28-21W4	1756.1-1778.1	22 m
	102/09-14-28-21W4	1757.2-1764.3	7.1 m
*	102/10-14-28-21W4	1946-1964.3	18.3 m
	08-20-28-21W4	1807.5-1819.5	12 m
*	08-23-28-21W4	1762-1770.95, 1784-1790.35	15.3 m
*	14-23-28-21W4	1778-1789.35	11.35 m
*	04-24-28-21W4	1757.5-1774.3, 1775-1792.4, 1793-1811	52.2 m
*	05-24-28-21W4	1829-1847.3, 1848.3-1865.55	35.55 m
*	12-24-28-21W4	1859-1877	18 m
	01-25-28-21W4	1779.8-1793.1	13.3 m
*	10-26-28-21W4	1756.9-1783.1, 1783.4-1787.7	30.5 m
	02-34-28-21W4	1799-1817.45	18.45 m
	05-04-29-21W4	1756-1763.15	7.15 m
	04-09-29-21W4	1738-1749.5, 1750.3-1759	20.2 m
	11-09-29-21W4	1750-1751.5, 1754.8-1763	9.7 m
	09-16-29-21W4	1732.5-1739	6.5 m
			TOTAL = 516.2 m

Table 1.1 Well locations and intervals of cores logged within the study area. All cores have been depth corrected to corresponding wireline log markers. Well locations marked with the symbol * have detailed core descriptions in Appendix I.

Additional information was obtained through the study of wireline well logs. Eighty four (84) wells penetrate at least the upper portion of the Nisku Formation in the study area (Figure 1.2). Most of these wells were drilled between 1993 and the present; the result is a modern database of wireline log responses. Due to the commonly limited variability in the curves of the standard log suite, especially through the carbonate intervals, high resolution logs were utilized where possible. Correlations were attempted between wells based on wireline log characteristics, and where available, enhanced by core information.

Four sulphate samples were analyzed for sulphur isotopic compositions at the University of Calgary. Sample powders were obtained from scrapings with a dental pick. Values of $\delta^{34}S$ are presented relative to Canyon Diablo Troilite (CDT) with a precision of ±0.4‰.

X-Ray diffraction analysis of one clay-rich sample was performed by Core Laboratories Canada Limited in Calgary. An automated Philips APD 3620, which uses a vertical goniometer with a variable divergence slit and copper K-alpha radiation (1.5418 degrees), was utilized for the analysis. Software developed by Philips Inc. and the Core Laboratories Research and Development Group performed peak deconvolution of the diffractogram as well as calculations of the mineral percentages.

The total organic carbon (TOC) contents of seven organic-rich samples were determined by the Geological Survey of Canada in Calgary. A Delsi Rock-Eval II pyrolysis unit outfitted with a total organic carbon analysis module was utilized on the dried and powdered samples. TOC is reported as the weight percent of the whole rock. The reader is referred to Peters (1986) for further discussion on the Rock-Eval/TOC analysis.

Three-dimensional seismic data, provided by PanCanadian Petroleum Limited, was used to support interpretations of positioning of depositional bodies as well as potential structural influence on strata of the Nisku Formation.

Chapter 2 STRATIGRAPHY AND PALEOGEOGRAPHY

2.1 REGIONAL STRATIGRAPHY

A grey to buff crystalline dolomite containing inclusions of anhydrite, silty areas, and shale partings defined the 47.5 m-thick Nisku "Member" of the Winterburn "Formation" type section in the well B.A. Pyrcz No. 1, 12-25-50-26W4 (Imperial Oil Limited, 1950). The Upper Devonian (Frasnian) Winterburn was later termed a group, and its three components, the Nisku, Calmar and Graminia, were modified to formations (Belyea, 1955). It is these descriptors that are used in the current study. The stratigraphic relationships between the Woodbend, Winterburn, and Wabamun Groups are illustrated in Figure 2.1 and are discussed below.

Stratigraphically situated below the Winterburn Group is the Frasnian-aged Woodbend Group. The Woodbend Group is underlain by the Cooking Lake Formation, a carbonate platform onto which the thick Leduc Formation carbonate complexes were built. The argillaceous Duvernay and Lower Ireton formations are basinal equivalents to the Leduc Formation. Positioned immediately below the Winterburn Group is the shaly Upper Ireton Formation, which is separated from the Lower Ireton by the relatively thin, carbonate-rich Camrose Member. The lowermost unit of the Winterburn Group, the Nisku Formation, unconformably overlies the Upper Ireton Formation. The Nisku is predominantly a carbonate rock unit that becomes increasingly evaporitic towards the top of the formation. Within the Winterburn Group, an unconformity separates the Nisku Formation from the overlying Calmar Formation, a silt- and clay-rich unit. The uppermost formation of the Winterburn Group is the Graminia Formation, which is comprised of carbonates, evaporites, and terrigenous clastics. Unconformably overlying the Winterburn Group is the Famennian-aged Wabamun Group. Carbonates and evaporites of the Stettler and Big Valley formations are prevalent in the Wabamun Group.

Correlative formations to those of the Winterburn Group include the Jean Marie, Redknife, and Kakisa formations in northwestern Alberta, the Birdbear Formation in

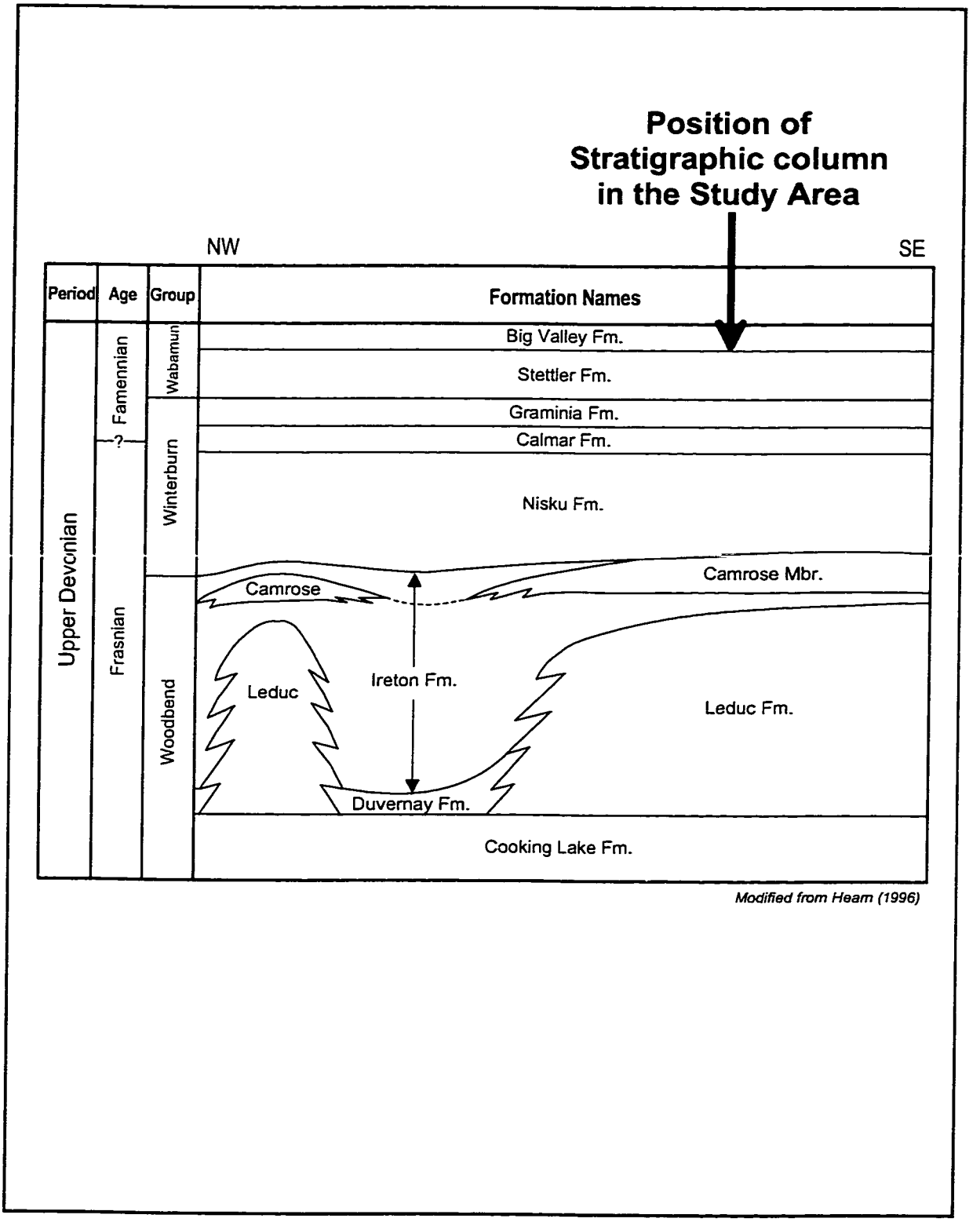

Figure 2.1 Schematic stratigraphy of the Upper Devonian in south-central Alberta.

Saskatchewan and Montana, and the Southesk and Alexo formations in the Rocky Mountain outcrops.

2.2 LOCAL STRATIGRAPHY

The contact between the Nisku Formation and the Camrose Member is not well established in the study area because: (a) the intervening Upper Ireton Formation is rarely present, (b) the Nisku Formation and the Camrose Member are indistinguishable on wireline logs, and (c) most cores do not intersect the contact between these units.

The Nisku Formation in the Drumheller area has previously been subdivided into lower dolomite and upper evaporitic sub-units (Kirker, 1959). In the present study, three sub-units of the Nisku Formation are distinguished (Figure 2.2) using the following criteria:

a) The **Nisku 1** sub-unit comprises the uppermost third of the Nisku Formation across the study area and is of mixed dolomite and evaporite lithologies. It is recognized on wireline logs as displaying a variable gamma ray (GR) response and an average photoelectric (PE) response of 5 barns per electron.
b) The **Nisku 2** sub-unit dominates the lower two thirds of the Nisku Formation in the study area and is dolomitic. It exhibits a low API gamma ray response and a PE of about 3 to 3.5 barns per electron.
c) The **Nisku 3** sub-unit is laterally restricted within the study area (based on three-dimensional seismic interpretation – Figure 2.3) and is present at the same stratigraphic level as the Nisku 2 sub-unit. The Nisku 3 sub-unit is more argillaceous than the other two sub-units and therefore displays a high API gamma ray response; yet the high dolomite content causes the PE to average 3.5 barns per electron.

A determination of the thickness of the Nisku 2 sub-unit or even the entire Nisku Formation interval is difficult due to the uncertain position of the underlying contact with the Camrose Member of the Ireton Formation. It is estimated that the Nisku Formation has an average thickness of 50 m throughout the study area.

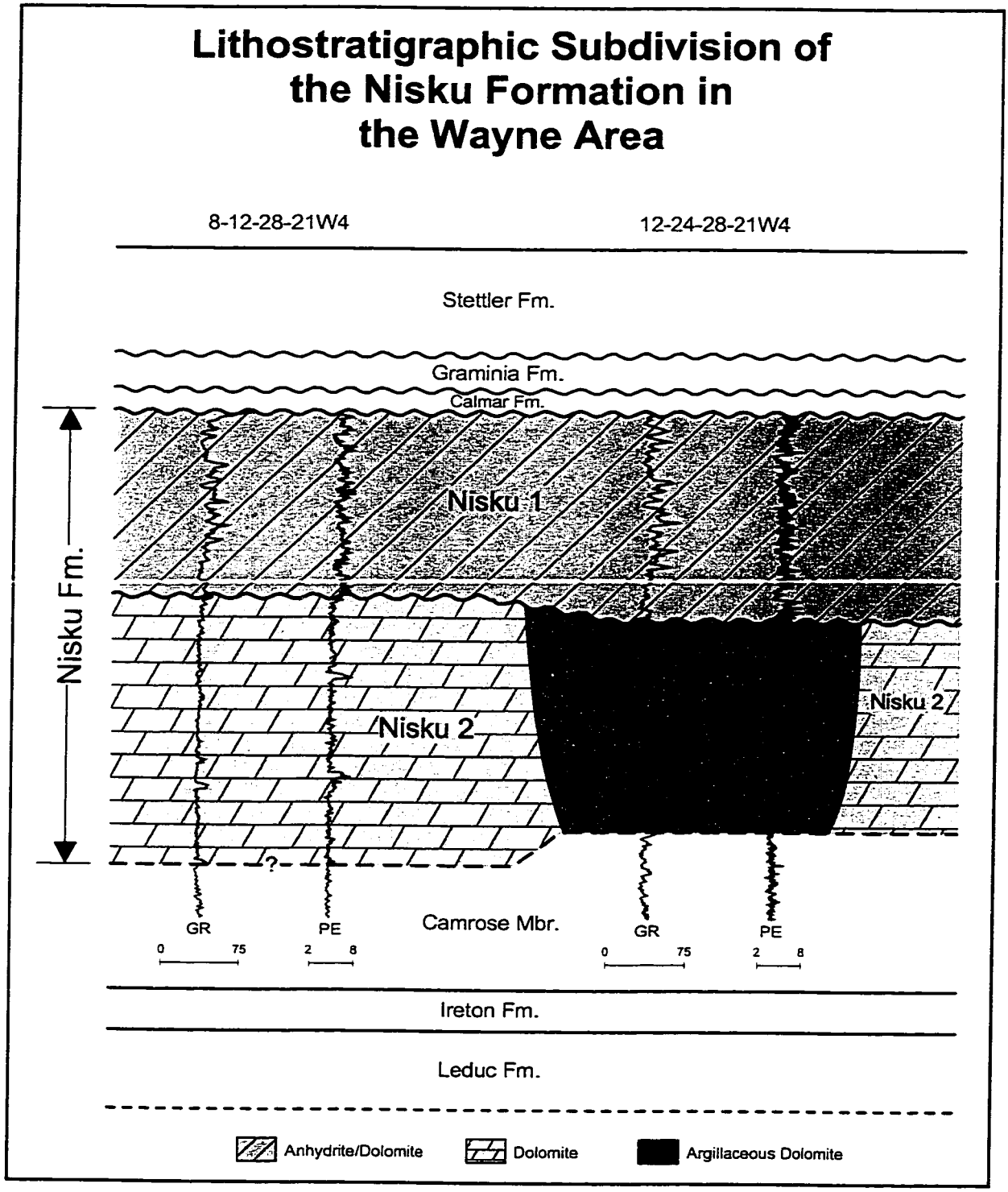

Figure 2.2 Subdivision of the Nisku Formation into three litostratigraphic sub-units based on gamma ray (GR) and photoelectric (PE) wireline log responses. Thickness of the Nisku Formation in 8-12-28-21W4 is 53m. Horizontal distance between the two wells is 3817m. Datum is the top of the Nisku Formation

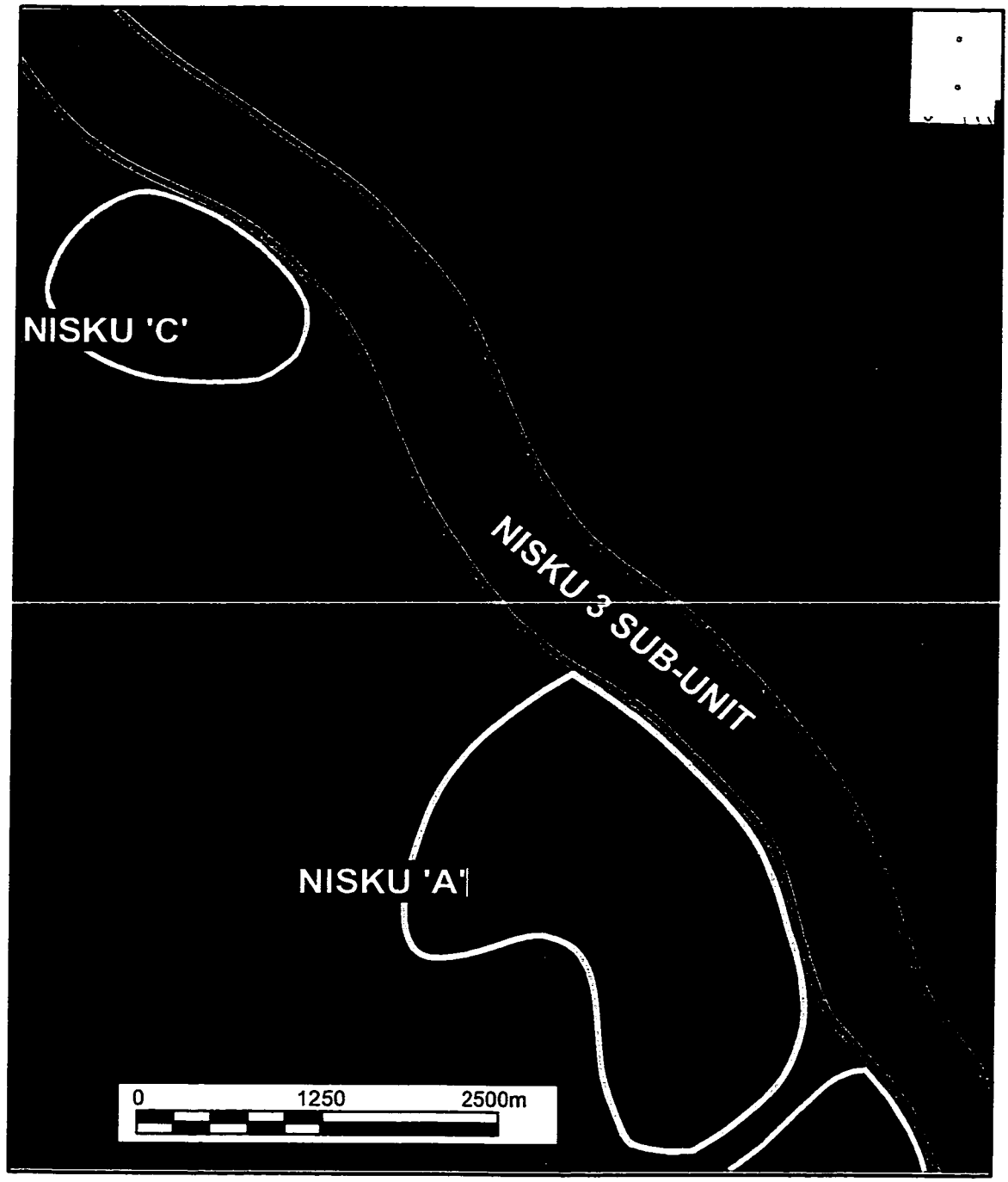

Figure 2.3 Three-dimensional seismic time horizon: second order residual structure map of the top of the Wabamun Group (Provided and interpreted by PanCanadian Petroleum Limited geophysicists). The Wabamun is utilized instead of the Nisku Formation because of poor acoustic contrast at the Nisku level as well as interference from short period multiples generated in overlying siliciclastics. Note the position and orientation of the Nisku 3 sub-unit relative to the Wayne Nisku oil pools. Contour interval = 2 milliseconds.

Regionally, the top of the Nisku Formation is an unconformity, commonly exhibiting evidence of subaerial exposure such as karst features, and is overlain by the fine-grained silt and clay of the Calmar Formation (Kissling, 1996; Whittaker and Mountjoy, 1996). No cores penetrate the unconformity or the Calmar Formation within the study area, therefore identification of the Calmar Formation is based on the sharp, high gamma log response due to its significant argillaceous content. Rarely the Calmar Formation is absent, presumably removed by erosion or possibly not originally deposited. The maximum observed thickness of the Calmar Formation in the study area is 3.5 m.

The overlying Graminia Formation has not been cored in the study area, however, the Graminia Formation elsewhere has been documented to be of siltstone, dolostone, and evaporite composition (Gilhooly, 1987). The Graminia Formation is of variable thickness throughout the study area, ranging from zero to 10 m.

Bedded evaporites of the Stettler Formation unconformably overlie the deposits of the Winterburn Group. An example of a typical wireline log over the interval from the Leduc to Stettler formations is provided in Figure 2.4.

2.3 PALEOGEOGRAPHY

At the end of deposition of the Leduc Formation a series of NE-SW trending carbonate complexes dominated the topography of central Alberta. The carbonate complexes were separated by deeper water embayments within the "East Shale Basin" and by the "West Shale Basin" to the northwest (Switzer et al., 1994; Figure 2.5). Towards the southeast existed a very widespread carbonate shelf that extended throughout southern Alberta, Saskatchewan, Manitoba, and the northern plain states. The border between the southern Alberta Shelf and the Ghost Pine Embayment to the north passes through the present Drumheller area (Figure 2.5). The shelf edge is deliniated by an abrupt reef buildup, the southernmost extension of the Killam Barrier. Sixteen kilometres south of the shelf to basin transition, but still above the raised Killam Barrier, was the site of the Nisku Formation deposition at Wayne.

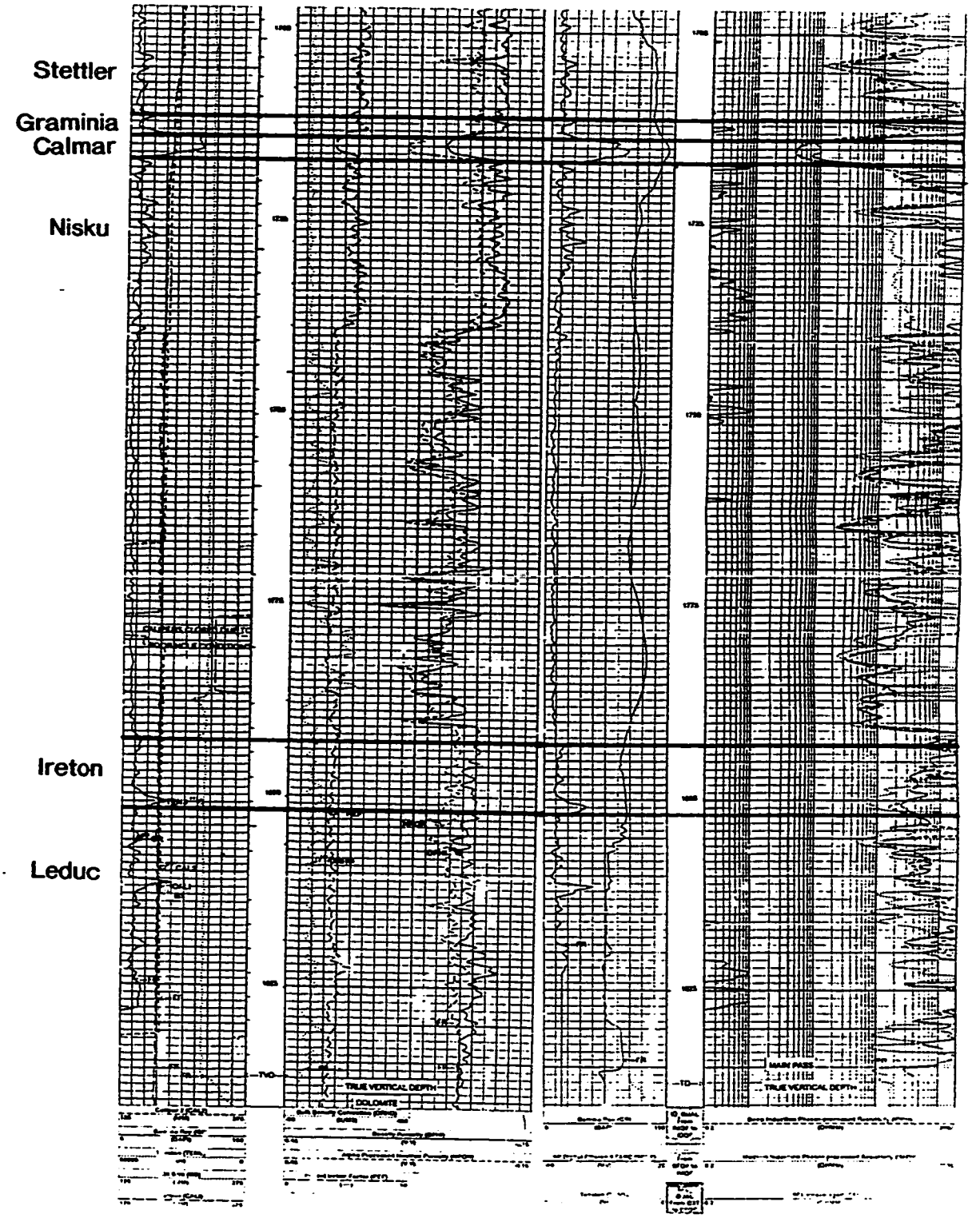

Figure 2.4 A representative suite of wireline logs from a well (100/12-07-28-20W4) within the Wayne Field. Formation names and their interpreted boundaries are indicated.

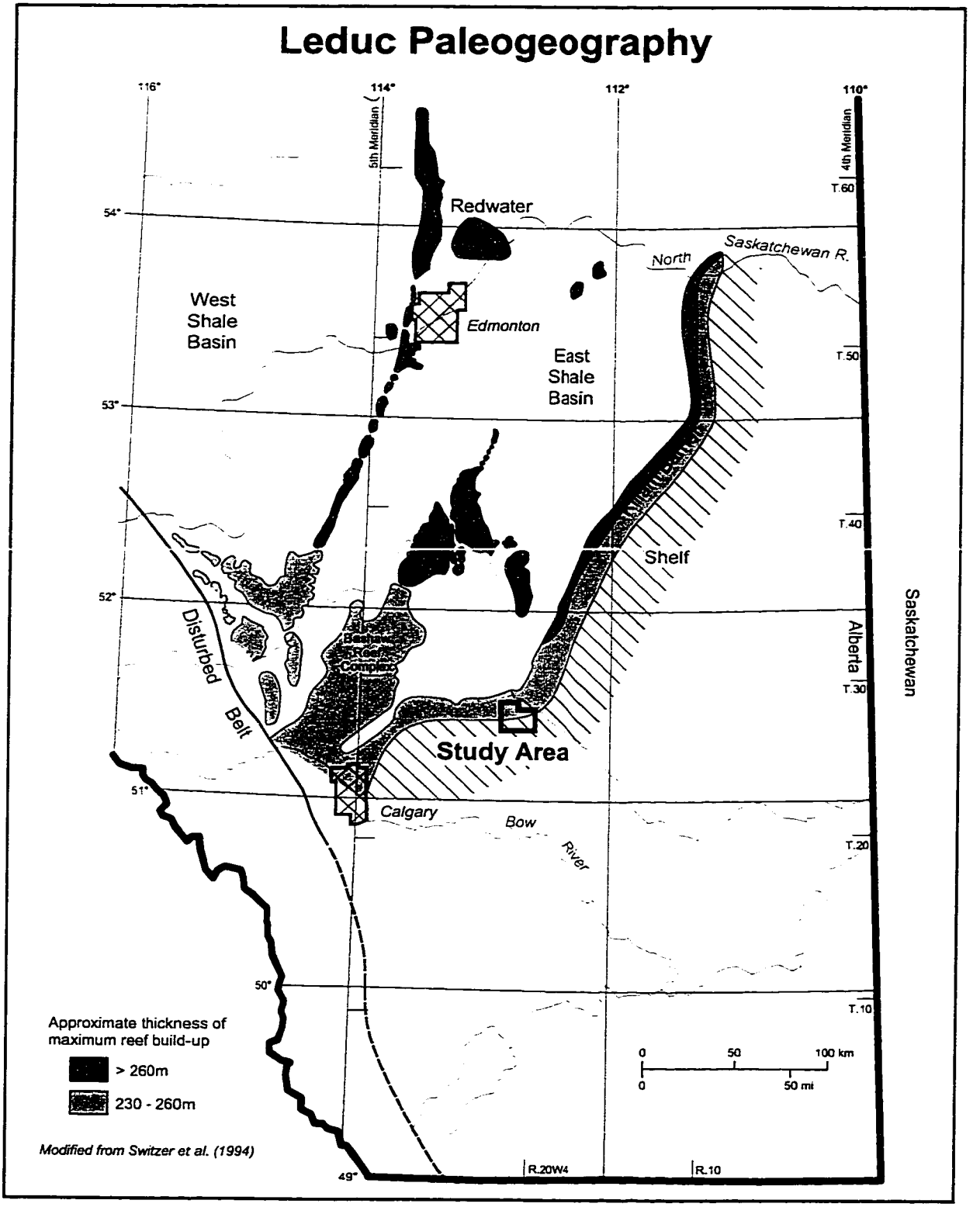

Figure 2.5 Index map of study area and paleogeographic reconstruction highlighting post-Leduc deposition.

After Ireton Formation deposition, an apparent relative rise in sea level resulted in deposition of the widespread Nisku Formation ramp across southern Alberta, Saskatchewan, Manitoba, and the northern plain states (Switzer et al., 1994). The edge of the Nisku Formation platform prograded beyond the underlying Leduc Formation reef complexes and over the deep basin fill of the West Pembina area (Figure 2.6). The development of inner-platform sub-basins, such as the Joffre and Ghost Pine, took place over older embayments of the Leduc Formation (Gilhooly et al., 1994). The sub-basins experienced deeper water deposition with only thin condensed units being deposited (Stoakes, 1992).

Initially, deposition of the Nisku Formation occurred under marine to marginal marine conditions and resulted in carbonate sediments dominating the lower portion of the platform. As the margin of the Nisku Formation platform grew to sea level, reduced circulation from the open basin was responsible for the upper, more restricted, hypersaline interval of the Nisku Formation (Stoakes, 1992). Laminated dolomudstones and bedded anhydrites were the resultant subaqueous deposits of this hypersaline phase, which entirely postdates the lower carbonate phase of the Nisku Formation (Stoakes, 1992). In the current study, an unconformity is interpreted to exist between the Nisku 1 sub-unit (upper Nisku Formation) and the Nisku 2 sub-unit (lower Nisku Formation), and is discussed further in chapter 4.

A regional lowering in sea level following deposition of the Nisku Formation (Johnson et al., 1985) caused widespread subaerial exposure across the platform and resulted in a karsted unconformity prior to deposition of the Calmar Formation. The Calmar Formation is comprised of quartz-rich sands, fine-grained silts and clays and is coalesced with the Upper Graminia silt in the southern and eastern parts of the platform (Switzer et al., 1994).

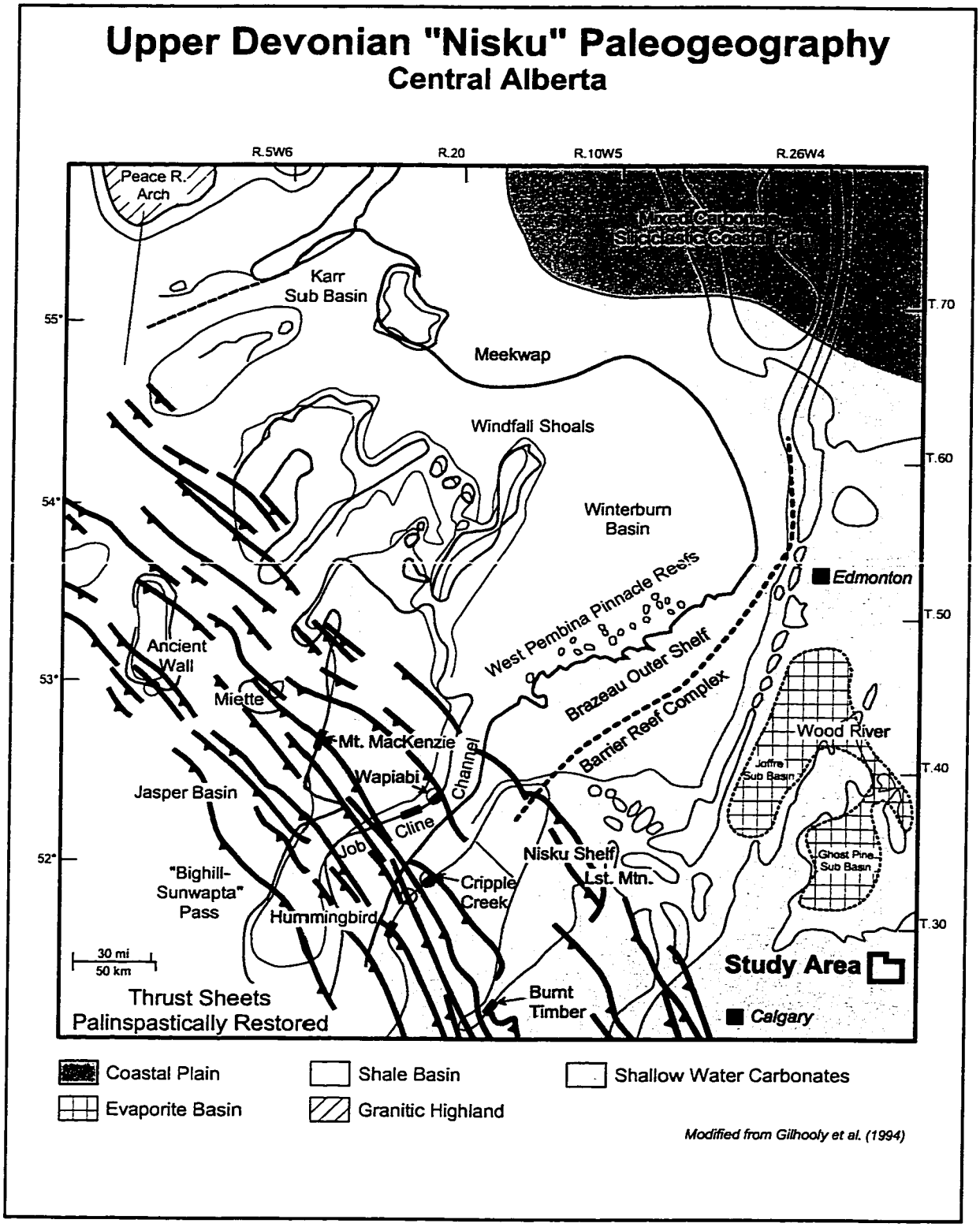

Figure 2.6 Index map of study area and paleogeographic reconstruction highlighting mid-Nisku deposition.

Chapter 3 SEDIMENTOLOGY

3.1 INTRODUCTION

Despite the existence of numerous deviated wells within and near the Wayne field, most penetrations of the Nisku Formation are vertical. All physical structures within the core are at or near original depositional orientation, give or take the present-day regional structural dip of the Nisku Formation of 0.5°.

All cores examined and photographed have been slabbed. All stated crystal sizes were obtained through petrographic analysis and refer to the average length of the long axis, unless otherwise specified. The crystal size scale distinguished by Folk (1959) is utilized throughout this study. Fractures are ubiquitous throughout all lithofacies and unless specifically addressed, are documented in Chapter 4. A modified Embry and Klovan (1971) version of Dunham's (1962) limestone classification according to depositional texture was chosen for description of the carbonate lithofacies.

Within the study area, a total of sixteen lithofacies are distinguished in the Nisku Formation on the basis of lithology, physical structure, and faunal composition.

3.2 LITHOFACIES OF THE NISKU 1 SUB-UNIT

Few cores within the study area penetrate the upper evaporitic portion of the Nisku Formation and the ones that do commonly preserve only the lowermost few metres. Most coring was likely unintentional despite the significance of the Nisku 1 sub-unit as a top seal to the petroleum reservoirs of the Wayne field. Consequently, only brief descriptions and interpretations of the five Nisku 1 sub-unit lithofacies are presented.

Lithofacies A: LAMINATED DOLOMUDSTONE AND ANHYDRITE (Figure 3.1)

Description:

Lithofacies A is characterized by light to dark brown (locally grey, green, and red) laminated to thin bedded dolomudstone and anhydrite. Volumetrically, laminated

dolomudstone and anhydrite is the most important lithology of the Nisku 1 sub-unit sediment and is present in successions up to 4 m thick.

Layers range from less than 1 mm thick laminae to beds of 3 cm thick and are usually planar to slightly undulatory (Figures 3.1a and 3.1b). Less commonly, laminae are wavy, current rippled, inclined, or discontinuous (Figures 3.1c and 3.1d). Contacts with underlying laminae are locally scoured and, in a few places, flat pebble conglomerates are present (Figures 3.1a and 3.1d). Micro-faults and fractures may offset laminae or laminae sets up to one centimetre thick (Figure 3.1c). Fossils are not present and laminae have not been disturbed by bioturbation.

In thin section, dolomite crystals are isolated within a matrix of horizontally aligned anhydrite laths. The dolomite crystals are anhedral to subhedral and have an average length of 25 μm. The felted anhydrite crystals are an order of magnitude smaller; that is, no longer than 3 μm. Larger anhydrite crystals are encountered in fracture infills and where the anhydrite alone comprises entire layers. Within most beds and laminae an upwards decrease in crystal size is evident in both the dolomite and the anhydrite.

Interpretation:

The lack of bioturbation and preserved fauna indicates that environmental conditions were detrimental to the health of any organisms living within the substrate or water column at the time of deposition of Lithofacies A. Based on the high sulphate content of the lithofacies, hypersalinity seems to be the most obvious choice to explain the stressed environment. The bedding contacts and association with current forms further indicate that laminae are the result of physical sedimentation processes as opposed to biological processes.

The dominance of laminated sulphates implies precipitation and deposition in a water body whose bottom was predominantly unaffected by wave action and currents (Kendall, 1984). In evaporite successions, laminites have been interpreted to form in deep quiet waters (Davies and Ludlam, 1973) or shallow protected lagoons (Shearman and Fuller, 1969). Evidence for deep water deposition would include: (a) laminae that can be correlated over long distances, (b) extensive aerial distribution of the evaporite unit, (c)

Figure 3.1:

Lithofacies A: LAMINATED DOLOMUDSTONE AND ANHYDRITE

a) Light to dark brown planar laminated (pl) to thin-bedded dolomudstone. Contacts between layers may be scoured (sc). A flat pebble rip-up breccias (B) displays highly angular clasts.
2-31-27-20W4, 1725.5 m.

b) Repetitive planar laminae, 1 to 5 mm thick in upper half of photograph. Darker colours correspond to areas with high anhydrite content (A).
9-1-28-21W4, 1841.2 m.

c) Minor beds of rippled (r), coarser-grained anhydrite within laminated to thin-bedded light brown dolomudstone. Early diagenetic processes include microfaulting (F) with mm-displacement as well as fracturing. Fracture (Fr) is filled by fine-grained dark sediment and clasts collapsed from surrounding host rock.
2-31-27-20W4, 1727.5 m.

d) Inclined, dark brown to grey dolomudstone and anhydrite laminae (I) above predominantly horizontally aligned flat pebble breccia clasts (B).
9-1-28-21W4, 1834.1 m.

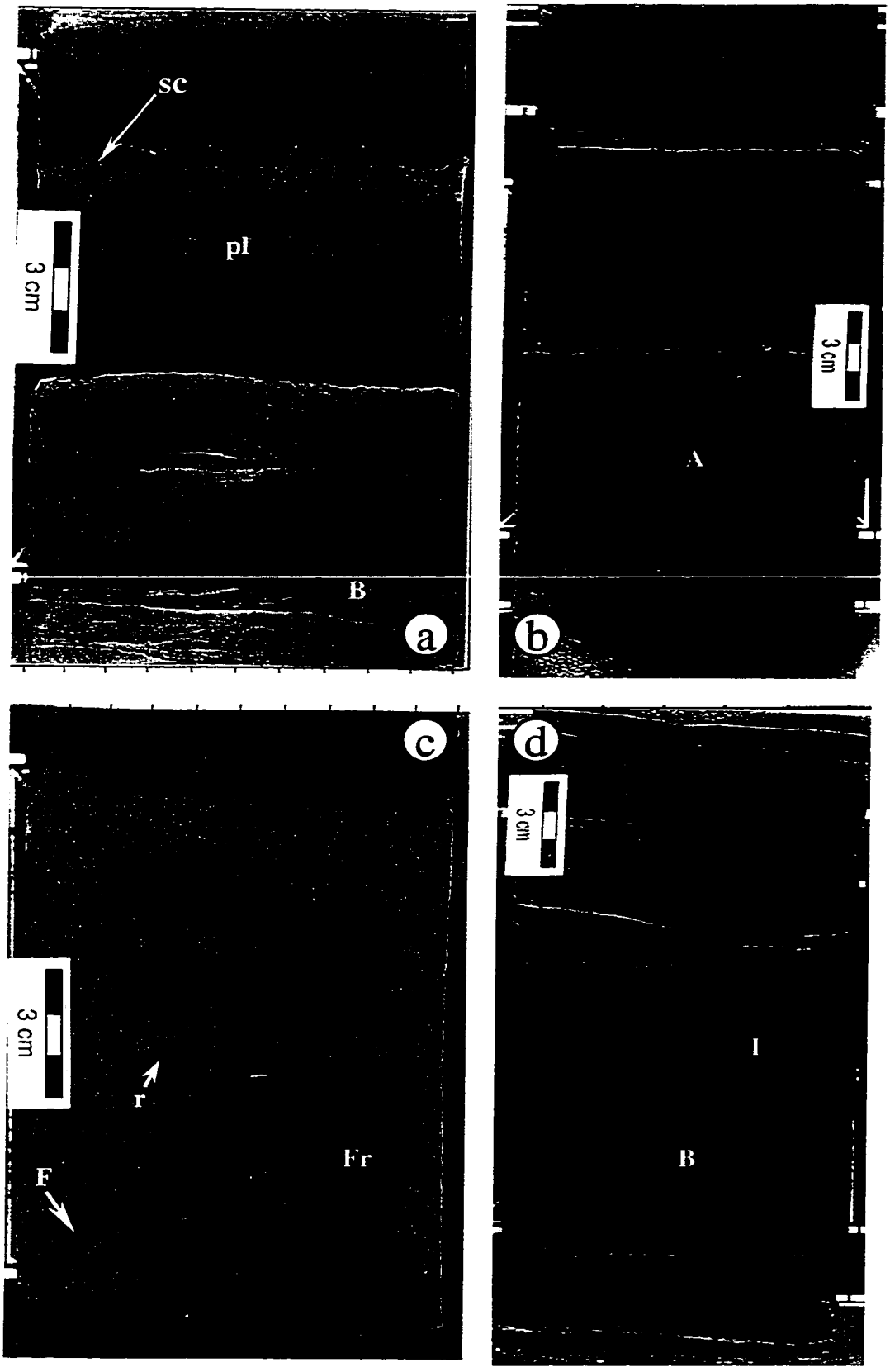
sc
pl
3 cm
B
a
3 cm
A
b
c
3 cm
r
Fr
F
d
3 cm
I
B

presence of gravity-displaced evaporites, and (d) lack of shallow water indicators (Kendall, 1984). Although Lithofacies A is widespread throughout the study area, individual laminae or bundles of laminae cannot be correlated between wells. Slump, mass-flow, and/or turbidity deposits are also absent. However, the most significant evidence against deep water deposition are the various high energy, shallow water indicators.

Hardie et al. (1983) point out that mechanical sedimentary structures are common within evaporite deposits, especially involving gypsum-anhydrite deposits. Even though both the textures and the mineralogy can be altered by recrystallization and/or replacement, the macro-structures generally remain (Hardie et al., 1983). Cut-and-fill scouring and flat-pebble conglomerates indicate higher energy disturbances of previous deposits in Lithofacies A. Ripple cross-lamination and other cross-stratification structures record traction load deposition. Graded bedding and repetitive planar laminae represent carbonate and saline mineral crystal muds settling out from suspension. It should be emphasized that these laminated muds dominate Lithofacies A despite the presence of higher energy features.

Even though anhydrite currently is present, its hydrated form of gypsum probably was the prevalent sulphate at the time of deposition. At levels of gypsum saturation (3.8 times normal seawater concentration – Kendall, 1992) crystals likely precipitated at the brine-surface and then sank to the brine floor. Episodes of dilution, possibly even seasonally, resulted in the deposition of carbonate partings between the evaporite laminae. However, variations in temperature or evaporation rate can also be responsible for interlamination of carbonates and evaporites (Kendall, 1984).

An opposing argument is one that calls for late-stage anhydrite replacement of a normal marine carbonate sequence. Although this scenario is more common in the ancient record than true salina textures (Warren and Kendall, 1985), the previously discussed lithologic and sedimentologic evidence points to a hypersaline setting.

Based on the primary structures, it seems reasonable to interpret Lithofacies A as deposited in a predominantly low energy, subaqueous environment, probably a few metres deep, such as a marginal marine salina. High energy events such as floods and storms

periodically modified the sediments, especially gypsarenites, but quiet water deposition in which mud-sized sediment accumulated was the rule, not the exception. Similar ancient evaporites developed in evaporitic lagoons of only a few metres or less of brine depth and stretched out over hundreds of thousands of square kilometres – yet there are no modern analogues (Kendall, 1992).

Lithofacies B: CRINKLY-WAVY DOLOMUDSTONE AND ANHYDRITE (Figures 3.2a and 3.2b)

Description:

Lithofacies B is characterized by light tan to grey, wavy to crinkled laminae of dolomite and anhydrite. The lithofacies is common throughout the Nisku 1 sub-unit and is present in intervals up to 2 m in thickness or as isolated beds of a few centimetres.

Wavy to crinkly laminae are generally horizontally aligned across the width of the core (Figure 3.2a), although some display slight doming of a few centimetres in height (Figure 3.2b). Layers that are made up mainly of anhydrite may display enterolithic folding within (Figure 3.2a). Evidence of bioturbation or of a preserved fauna is not apparent, nor are structures indicative of current activity.

Petrographically, most layers are comprised of isolated to interlocking dolomite crystals surrounded by poikilotopic anhydrite. The dolomite crystals are predominantly subhedral and have an average length of 40 μm. Poikilotopic anhydrite crystals may be over 100 μm in width. Smaller anhydrite crystals of less than 10 μm in size are also commonly present.

Interpretation:

The most recurrent characteristic of Lithofacies B is the repetition of the generally horizontally-oriented, crinkly-wavy laminae. Such laminae are here interpreted as cryptalgal laminites and are similar to those described in the literature (also known as algal mats, microbial mats, cyanobacterial mats, cryptomicrobial laminites, and stromatolites; e.g. Aitken, 1967; Logan et al., 1974; Pratt, 1982; Krumbein, 1983).

Figure 3.2:

Lithofacies B: CRINKLY-WAVY DOLOMITE AND ANHYDRITE

a) Light brown, crinkly-wavy dolomudstone laminae (Cr) interbedded with thicker cloudy grey anhydrite layers (A). Anhydrite is preferentially fractured and contains enterolithic folds of dolomudstone (ent).
2-31-27-20W4, 1733.6 m.

b) Crinkly-wavy dolomudstone layers in lower two thirds of photograph. Slight doming (d) of laminae near the top of the succession. Core pieces do not fit together above the domed laminae. Wide sediment-filled fracture (Fr) diagonally cut across the laminae during early diagenesis.
14-23-28-21W4, 1779.3 m.

Lithofacies C: NODULAR ANHYDRITE

c) Multisized, irregular-shaped, cloudy grey anhydrite nodules (nod) separated by light brown dolomite (D). Anhydrite has distorted original carbonate laminae in lower portion of photograph.
10-26-28-21W4, 5821.5 ft.

d) Coalesced mass of anhydrite nodules with indistinct colour variations has resulted in a cloudy overprint of original lithofacies.
9-1-28-21W4, 1839.1 m.

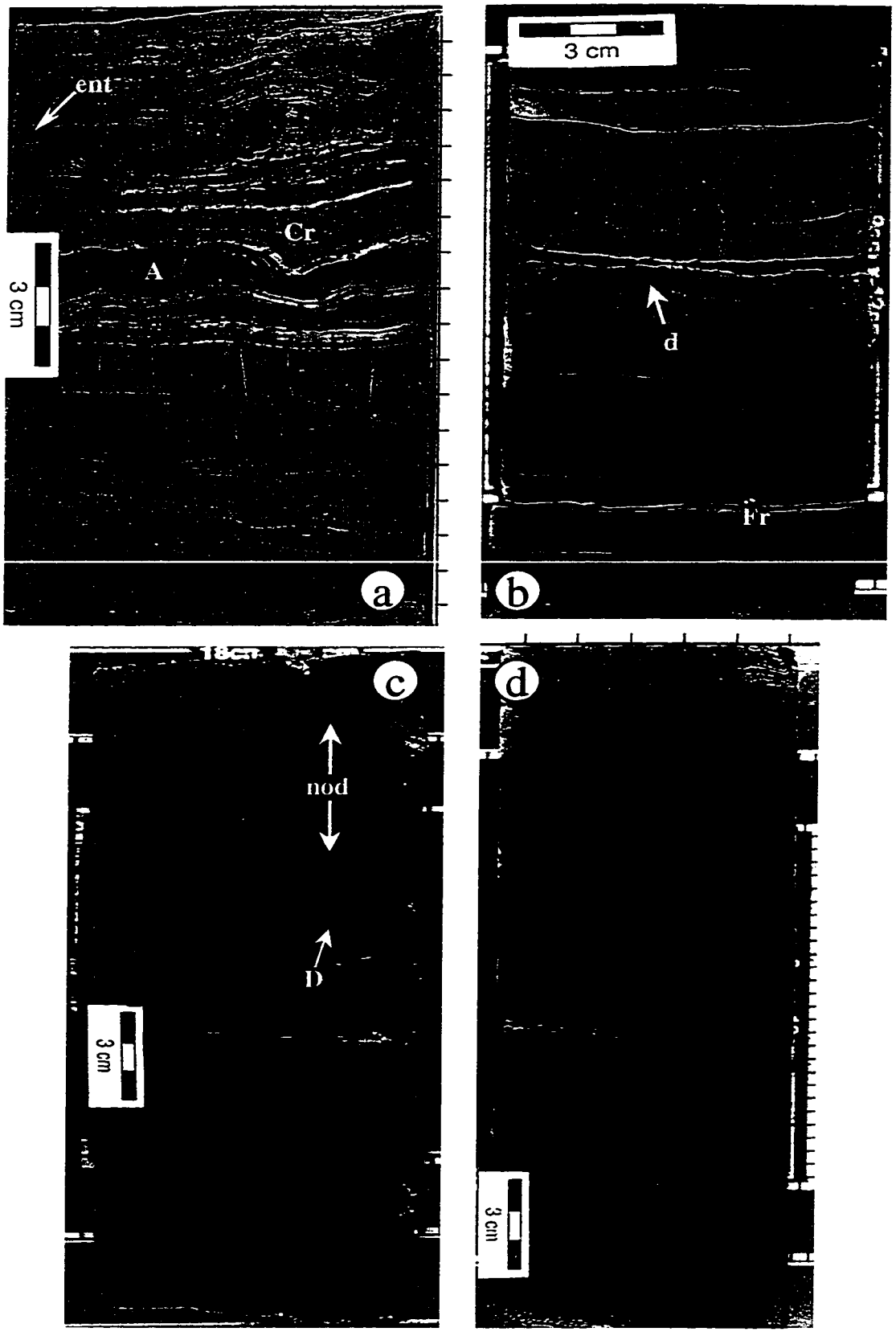
ent
Cr
A
3 cm
a
3 cm
d
Fr
b
c
nod
D
3 cm
d
3 cm

The preservation of Phanerozoic cryptalgal laminites is considered to be related to the inability of browsing animals, such as gastropods, to live within hypersaline subaqueous to supratidal environments (Logan et al., 1974). However, only below halite saturation are cyanobacterial mats ubiquitous in evaporitic flat and shallow subaqueous environments (Kendall, 1992). The close association with the evaporitic salina deposits (Lithofacies A) and the internal primary sulphate layers supports a hypersaline setting at the time of deposition of Lithofacies B. The water depth at the time of deposition is in question, however.

With respect to subtidal stromatolites, Schreiber et al. (1976) argue that in the absence of wave and current structures, algal structures record deposition in a deeper environment but one that still resides within the photic zone. Kendall (1984) counters by arguing that the photic limit in hypersaline waters is likely always shallow (decimetres) because of suspended organic residues, anaerobic bacteria, and surface nucleated evaporite crystals. Regardless, subtidal stromatolites typically display a domal morphology, a feature that is not common in Lithofacies B.

Alternatively, deposition within intertidal to supratidal environments is supported by the presence of fenestrae, desiccation fabrics, and preserved organic matter within the cryptalgal laminites. None of these peritidal features are obvious in Lithofacies B, except for rare mudcracks.

Based on the presence of mudcracks and the strong association with the shallow subaqueous laminites of Lithofacies A, Lithofacies B is interpreted to have been deposited in an upper subtidal to fringing intertidal evaporitic flat setting, marginal to the salina deposits. The lack of organic matter may be due to oxidization and the lack of fenestrae may be because of insufficient drying-out of the sediments. Warren (1982) similarly recognizes that flat, laminated algal mats may be present shoreward of salina deposits.

Lithofacies C: NODULAR ANHYDRITE (Figures 3.2c and 3.2d)

Description:

Individual and coalesced nodules of anhydrite characterize Lithofacies C. The nodular anhydrite is most common near the base of the Nisku 1 sub-unit and ranges in thickness between 1 and 1.5 m.

Where individual anhydrite nodules (typically 1 to 2.5 cm in diameter) are separated by light tan dolomite, a characteristic chicken-wire texture is apparent (Figure 3.2c). More commonly the nodules have converged to form a cloudy grey mass of anhydrite with indistinct colour variations and irregular dolomite wisps throughout (3.2d). It is not clear what the matrix was prior to nodule growth, if there was any variation in the composition of the matrix, or if there has been any remobilization of the anhydrite nodules. Rarely, crinkly layering similar to that found in Lithofacies B is at the base of Lithofacies C but it is somewhat obscured and deformed by the anhydrite (Figure 3.2c).

Interpretation:

Lithofacies C has a similar appearance as the classic chicken-wire anhydrite layers located within the Arabian Gulf sabkhas. However, before immediately tagging a sabkha interpretation to Lithofacies C it is vital to look at its total facies assemblage. Furthermore, it is important to keep in mind that anhydrite fabrics can be significantly altered by early and late diagenesis; caution should be taken when relating anhydrite fabrics to depositional environments (Kendall, 1984).

Nodular anhydrites in modern sabkha settings are either overlain by supratidal sediments with no more than 1 m total thickness, or are truncated by an erosional deflation surface (Warren and Kendall, 1985). In addition, nodular anhydrites found within both ancient and Holocene sabkhas are underlain by intertidal organic cyanobacterial mats. The nodular anhydrite of Lithofacies C ranges between 1 and 1.5 m in thickness and is overlain by either cryptalgalaminites or laminated dolosiltite, neither of which is interpreted as supratidal in origin. The most common unit below the Lithofacies C is Lithofacies A, an interpreted subaqueous salina deposit. Thus, a sabkha environment is unlikely to be responsible for the deposition of the nodular anhydrite in Lithofacies C.

A purely diagenetic origin is proposed for Lithofacies C. Ghosts of dolomite are common between the anhydrite nodules indicating the existence of carbonate prior to the growth, displacement, and coalescence of the sulphate phase. It is probable that early gypsum crystals precipitated within restricted carbonate-rich sediments, dewatered and converted to anhydrite, and displaced the original sediment to the degree that the primary bedding is no longer apparent. The original depositional environment could have been subtidal to supratidal.

Lithofacies D: BEDDED TO MASSIVE DOLOPACKSTONE (Figures 3.3a and 3.3b)

Description:

Lithofacies D is characterized by a light to dark brown dolopackstone. The lithofacies is present in only two wells as successions 60 cm thick.

Lithofacies D is comprised of a random arrangement of dolomitized mudstone lithoclasts, bioclast molds, and peloid molds all in contact with one another in a mostly muddy matrix. Patches of pure dolograinstone are also present. Of the two recorded examples of Lithofacies D, the dolopackstone in 12-24-28-21W4 is massive (Figure 3.3a) and in 10-26-28-21W4 inclined bedding, up to 20°, is displayed (Figure 3.3b). In both cores the packstones abruptly grade upward into thin finer-grained dolowackestone beds, maximum 3 cm in thickness. These thin beds have a reduced faunal content and may be laminated to clotted in texture. The dolowackestones have sharp upper contacts with the overlying dolopackstones as opposed to their slightly gradational lower contacts.

In thin section, bladed anhydrite cement (mean crystal length of 0.4 mm) fills the molds of the leached allochems, most of the interparticle pore space of the dolograinstones, and a large portion of the dolomitized mud matrix (mean dolomite crystal length of 40 μm) in the dolopackstones. Much finer dolomite crystals, less than 2 μm in length, outline the allochem molds. A few of the allochems appear to have undergone deformation, resulting in irregular shapes and further contributing to the general lack of orientation throughout. Sorting is poor. The largest allochems are the highly angular mudstone lithoclasts, which

may reach lengths up to 2 cm. Irregularly-shaped leached bioclasts range between 1 cm to less than 1 mm in diameter. Peloid molds average 1.5 mm in diameter.

Interpretation:

As a poorly sorted mixture of lithoclasts, bioclasts and peloids, most leached and cemented, Lithofacies D is enigmatic. Bedding may be crudely visible or totally absent. With the displaced nature and large size of many of the allochems, especially the mudstone lithoclasts, relatively high energy currents must be invoked to transport the debris. Yet a fine-grained matrix prevails throughout most of the packstone, implying later quiet water infiltration of mud through the interparticle pore space. Thin beds of much finer-grained sediment also indicate periods of significantly lower energy deposition. Such abrupt upward transitions into these mud- and wackestone deposits does not imply normal waning flow but rather virtually instantaneous reductions in current energy. The sharp upper contacts provide evidence for early lithification prior to the next high energy event. Episodic high energy, probably generated by storm activity, is the most likely cause of deposition for the bulk of Lithofacies D.

Spatially, Lithofacies D appears to have been deposited only over the underlying Nisku 3 sub-unit channel (see page 59). This distribution, along with the above listed sedimentary features, likely indicates that local bank-derived debris accumulated within a bathymetrically deep (relative to the surrounding bank) sediment trap. It is thus implied that the Nisku 3 sub-unit channel still maintained a vestige of its earlier presence at the time of deposition of the Nisku 1 sub-unit. Periodic high energy storm activity was intense enough to rip-up and transport litho- and bioclasts from the bank region and into the channel, ultimately deposited as poorly consolidated, unsorted masses of coarse-grained debris. At the same time, dilution of the channel's water column likely took place, allowing for the growth of a limited fauna. Post-storm quiet water conditions were responsible for the deposition of the thin laminated to slightly mottled fine-grained layers and also for the infiltration of mud into the open pore space of the coarse-grained packstone deposit. The succession of flat-bedded deposits of Lithofacies A atop of Lithofacies D signified the resumption of quieter hypersaline conditions.

Figure 3.3:

Lithofacies D: BEDDED TO MASSIVE DOLOPACKSTONE

a) Vertical arrows indicate two successions of massive, unsorted dolopackstone (P) abruptly grading upwards (gr) into thin, light brown dolowackestone beds (W). Sharp overlying contact (sh) and dolopackstone infill of fracture (Fr) implies lithification of dolowackestone before deposition of overlying dolopackstone. Sharp contact (sh) with Lithofacies A (L.A) above.
12-24-28-21W4, 1860.3 m.

b) Multiple fining upwards successions (arrows) from faintly bedded dolopackstone (P) into mottled dolowackestone (W). Sharp, irregular contact (sh) with darker beds of Lithofacies A (L.A) above.
10-26-28-21W4, 5815 ft.

Lithofacies E: LAMINATED DOLOGRAINSTONE

c) Millimetre-scale fining-upward packages of light brown dolograinstone to dolomudstone has resulted in a planar laminated (pl) appearance. Black carbonaceous partings are present between laminae. Poikilotopic anhydrite (p) commonly cross-cuts laminae. Sharp, scoured contact (sh) with underlying dark coloured beds of Lithofacies A.
9-1-28-21W4, 1838.2 m.

d) Ripple cross-stratification (r) in light brown dolograinstone at top of photograph. Truncated poikilotopic anhydrite (p) at contact between laminae. Darker portions are anhydrite cements (Ac) along porous dolograinstone laminae.
12-24-28-21W4, 1861.3 m.

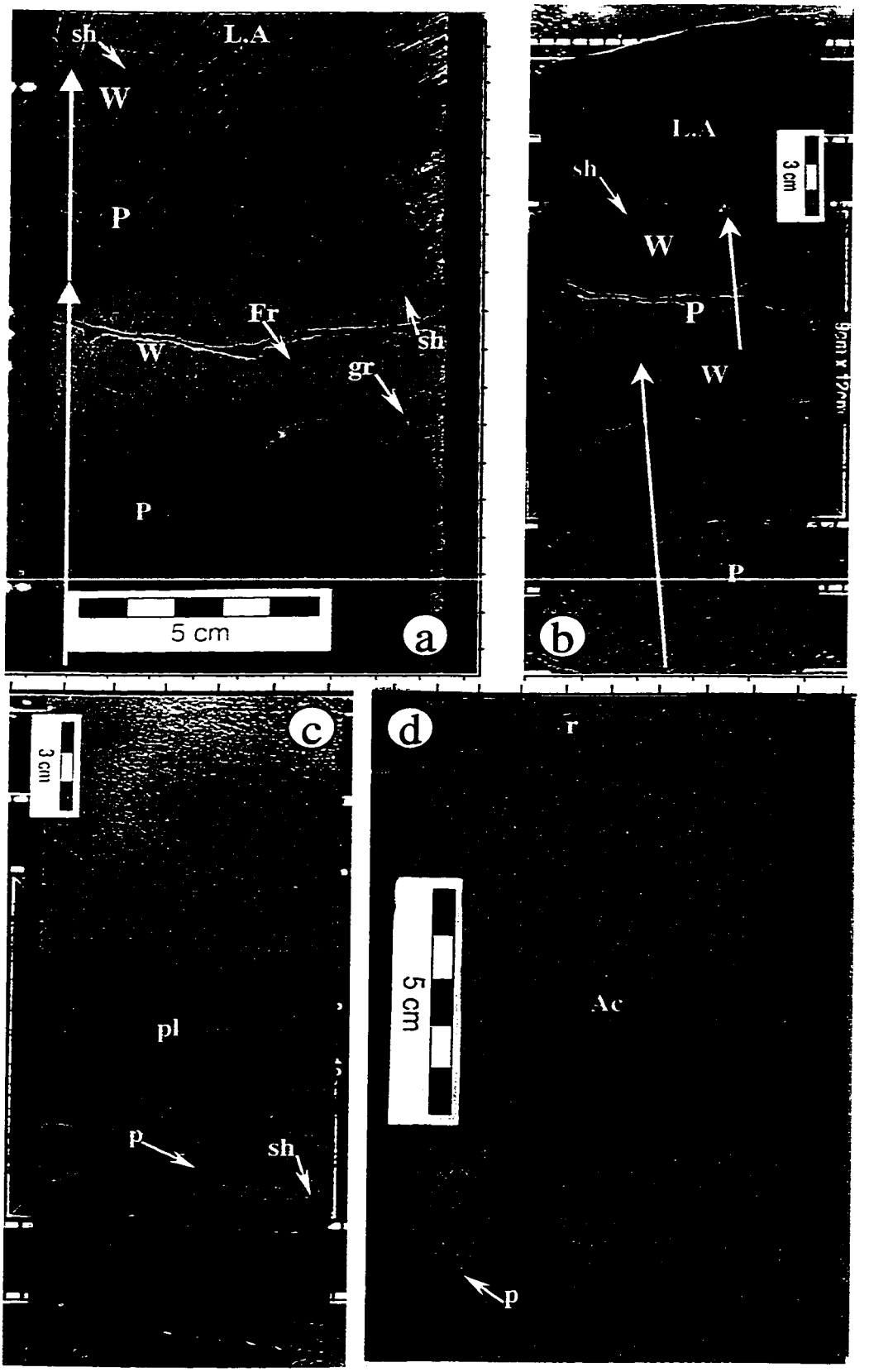
sh
L.A
W
P
Fr
W
sh
gr
P
5 cm
a
L.A
sh
3 cm
W
P
W
P
b
3 cm
c
pl
p
sh
d
r
5 cm
Ac
p

Lithofacies E: LAMINATED DOLOGRAINSTONE (Figures 3.3c and 3.3d)

Description:

A faintly laminated, light tan porous dolomite characterizes Lithofacies E. The lithofacies is present only in the lower portion of the Nisku 1 sub-unit in successions averaging 75 cm in thickness.

Laminae are planar, less than 1 cm in thickness, and are defined by thin horizontal accumulations of carbonaceous material (Figure 3.3c). Wave ripples up to 1 cm in height may be present locally (Figure 3.3d). Microscopic open subspherical molds of unknown origin are present throughout the lithofacies, however, no conclusive evidence of fauna or bioturbation is present.

In thin section, abundant intercrystalline porosity is present between subhedral to euhedral dolomite crystals that range between 100 μm in length at the base of small scale fining upward packages to 20 μm in length at the top of such packages. These normally graded packages average 1 cm or less in thickness and have sharp upper and lower contacts. Detrital dolomite is not present. Poikilotopic anhydrite is patchy in distribution; crystals can reach over 1 cm in length and may be truncated by overlying laminae (Figure 3.3d) but more commonly vertically cross-cut the laminations (Figure 3.3c).

Interpretation:

The relatively coarse dolomite crystal sizes, the sharp scoured bases, and the evidence of cross-stratification in the form of wave ripples indicates that Lithofacies E was deposited under slightly higher energy conditions than the bulk of the Nisku 1 sub-unit lithofacies. The presence of regular fining upward packages suggest a rhythmic occurrence of lower energy conditions as well. Interlocking mosaics of dolomite crystals and lack of detrital grains indicate complete dolomite replacement of the original sediment.

The absence of fauna and the existence of undisturbed laminae (lack of bioturbation) implies that environmental conditions were not suitable for any biotic community. Hypersalinity, based on the presence of early truncated poikilotopic sulphate crystals, was the likely reason for the inhospitable environment. Organic-rich laminae may indicate a

very high organic content in the water column, a high sedimentation rate, or anoxic conditions at the time of deposition.

It is interpreted that Lithofacies E was deposited in a very shallow subtidal to lower intertidal environment with moderate energy conditions. Salinity was lower than that during most of the Nisku 1 sub-unit deposition, but was still too high for the presence of any fauna.

3.3 LITHOFACIES OF THE NISKU 2 SUB-UNIT

Examination of core and thin sections representing the Nisku 2 sub-unit in the Wayne study area reveals pervasive dolomitization of the strata. Numerous other diagenetic overprints have removed or masked the primary fabrics as well, making lithofacies descriptions and interpretations difficult and likely over-simplified compared to the original depositional facies. Despite the descriptive complexities, seven lithofacies of the Nisku 2 sub-unit can be distinguished in core.

Lithofacies F: FENESTRAL LAMINATED DOLOMUDSTONE (Figure 3.4)

Description:

Lithofacies F is characterized by a light to medium brown fenestral laminated dolomitized mudstone. Volumetrically, Lithofacies F is a minor component of the Nisku 2 sub-unit and averages 35 cm in thickness.

Bedding parallel, aligned planar isolated vugs and subspherical vugs typify the fenestrae. Vugs are predominantly 1 mm or less in diameter but may be up to 4 mm across where individual voids have coalesced or become enlarged by solution (Figure 3.4a). The small voids (1 mm or less) are commonly spherical to ovoid in shape whereas the larger ones have outlines that are more irregular. Cementation by anhydrite is rare – most voids are open. Laminae may not be visible but more commonly are present as indistinct crinkly layers (Figure 3.4d), planar horizontal layers (Figures 3.4a, 3.4b, and 3.4c), or planar but slightly inclined layers across the core.

Figure 3.4:

Lithofacies F: FENESTRAL LAMINATED DOLOMUDSTONE

a) Bedding parallel, aligned fenestral vugs (av) and coalesced or solution-enlarged fenestrae (se) within a medium brown dolomudstone. A flooding surface demarcates a sharp transition (sh) into overlying Lithofacies G (L.G). In contrast to the fenestral voids of Lithofacies F, biomolds (bm) are the dominant void in Lithofacies G.
10-3-28-21W4, 1803.3 m.

b) Gradual transition from dark brown, mottled dolowackestone of Lithofacies G at base of photograph (L.G) into medium brown, fenestral laminated (lam) dolomudstone in upper two thirds of photograph
16-12-28-21W4, 2058 m.

c) Dark brown dolomudstone contains aligned subspherical vugs (sph) in lower half of photograph grading upwards into smaller bedding parallel fenestral vugs and laminae (lam). Diagenetic colour variations are apparent at the top of the photograph.
8-12-28-21W4, 1892.6 m.

d) Faint crinkly laminae (Cr) and associated bedding parallel fenestral vugs. Some larger voids may be fossil molds (fm). Vertically-oriented solution-enlarged fractures (Fr) cross-cut the fenestral laminated medium brown dolomudstone.
1-12-28-21W4, 1744.8 m.

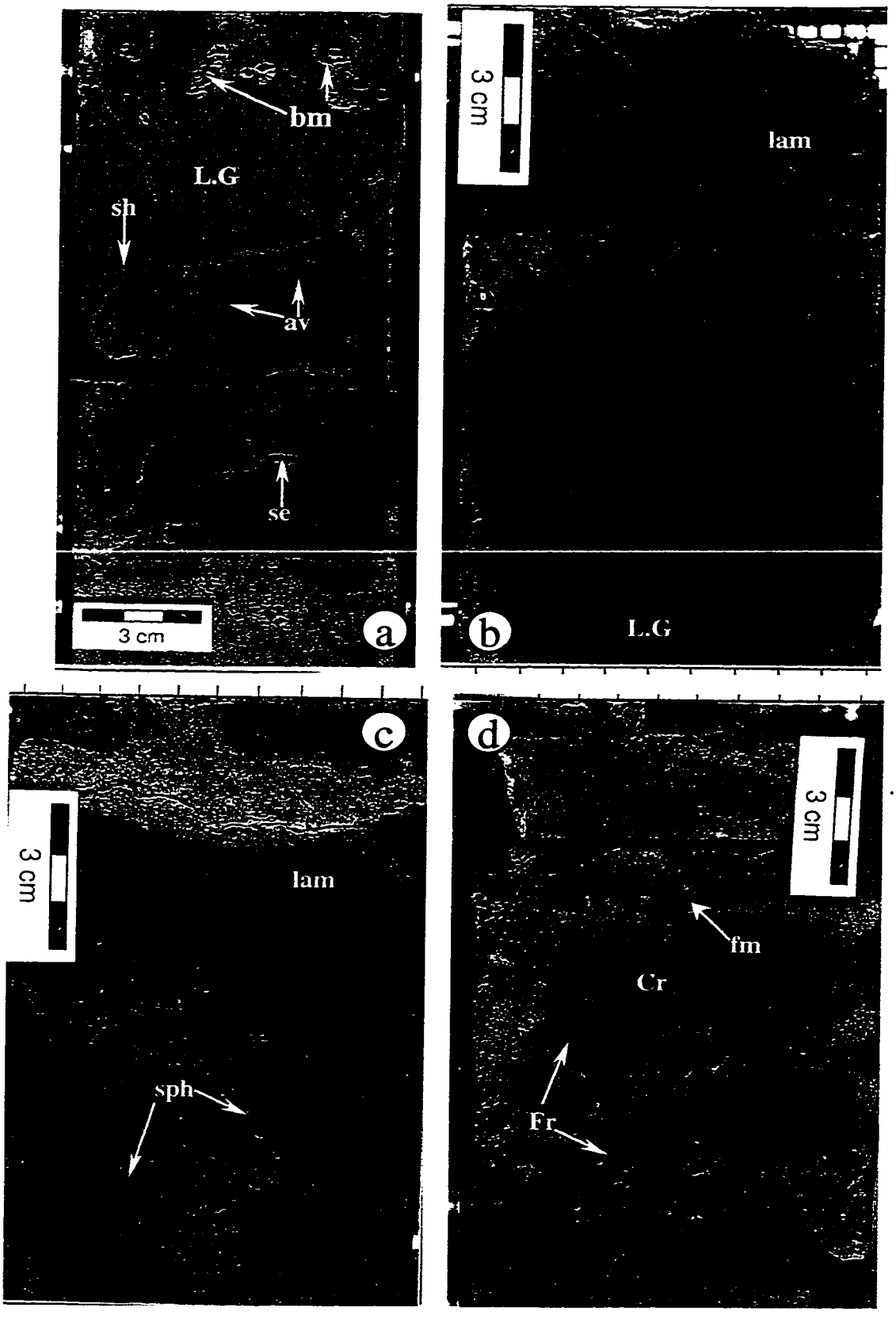
bm
L.G
sh
av
se
3 cm
a
3 cm
lam
b
L.G
c
3 cm
lam
sph
d
3 cm
fm
Cr
Fr

The dolomitized mudstone matrix has a mean crystal length of 60 μm in thin section. However, dolomite crystal sizes significantly vary between samples, with a range between 40 and 100 μm. Dolomite crystals are subhedral and appear as interlocking mosaics.

Interpretation:

Lithofacies F displays the characteristic fenestral fabric of planar isolated vugs and bubblelike vugs parallel to bedding. Fenestrae are generally indicative of tidal-flat environments (as opposed to subtidal), especially when in fine-grained sediment such as mud or syndepositional dolomite (Shinn, 1983). According to Shinn (1968), fenestrae may exist as planar isolated vugs 1 to 3 mm high by several millimetres in width or as isolated spherical voids 1 to 3 mm in diameter. Internal shrinkage (because of desiccation of exposed sediments) and gas bubbles, respectively, were experimentally determined to be the most probable means of formation (Shinn, 1968).

The high proportion of mud in the matrix of Lithofacies F supports a tidal flat interpretation. However, the mudcracks, stromatolites, and storm layers commonly associated with peritidal sediments (Shinn, 1983) are not readily apparent in Lithofacies F. Thin fractures that cross into overlying lithofacies are due to post-burial stresses rather than early mudcracks. The dolomudstone matrix displays rare indistinct crinkly laminae, similar to the interpreted cryptalgal laminites of Lithofacies B, but less obvious. Storm layers *may* be present as thin beds containing larger molds of allochems, reduced concentrations of fenestral vugs, and coarser dolomite crystal sizes.

Fenestral voids can be completely obliterated by compaction unless preburial cementation of the matrix or early cementation of the vugs takes place (Shinn et al., 1980). Most voids within Lithofacies F lack any evidence of previous cement fills, implying that syndepositional cementation must have taken place in order to preserve the open voids from the effects of burial compaction. Shinn (1968) maintains that supratidal sediments are commonly cemented syndepositionally, and that fenestral fabrics are most abundant in supratidal sediments.

It is interpreted that Lithofacies F was deposited in a mud-rich upper intertidal to supratidal setting in which early cementation of the matrix took place. Algal layers were

likely present but degraded upon death and/or have been obscured by the severe dolomite overprint.

Lithofacies G: MOTTLED GASTROPOD DOLOWACKESTONE (Figure 3.5)

Description:

Lithofacies G is a light to dark brown dolomitized wackestone with irregular dark mottled patches and numerous gastropod molds. The lithofacies constitutes a large proportion of the rock volume of the Nisku 2 sub-unit and is present mainly in the upper half of the interval in successions up to 2.5 m thick.

Predominantly dolomitized mud, the only abundant fauna that can be identified with certainty are the spiralled molds of leached gastropods which are typically 10 mm or less in length. Rarely, the gastropod shells have been replaced by dolomite. Molds of shell fragments of unknown origin comprise a very small proportion of the lithofacies and appear as randomly oriented, curving to straight voids less than 5 mm in length (Figure 3.5b). Most of Lithofacies G is comprised of small, rarely aligned (Figure 3.5a), subspherical voids less than 2 mm in diameter, hence the wackestone classification. Comprised of a tight interlocking mosaic of subhedral dolomite crystals, the dolomitized mud matrix has a mean crystal length of 50 μm.

The origin of the small voids is enigmatic. Possible spiralling of interior walls suggest small gastropod molds while other subspherical voids offer no clues towards their heritage. The majority of the small voids are randomly positioned but in some examples they are aligned in curved or straight rows. Rarely, the molds of large (up to 5 cm in length) single megalodont valves are present within the matrix. Overall, the fabric is massive with only hints of faint laminae in the upper portions of Lithofacies G. Patches of dark irregular mottling are present throughout.

Interpretation:

Lithofacies G is unique in that the only abundant recognizable fauna it contains are gastropods, animals that are not singularly indicative of any depositional environment either today or during the Devonian (Murray, 1966). Klovan (1964) also recognized the

Figure 3.5:

Lithofacies G: MOTTLED GASTROPOD DOLOWACKESTONE

a) Rare gastropod molds (g) with numerous spherical molds and aligned voids (av) in a medium brown dolomudstone matrix. Most molds are of unknown origin. White patches are diagenetic anhydrite.
4-9-29-21W4, 1740.8 m.

b) Millimetre- to centimetre-sized gastropod molds (g) randomly distributed along with small subspherical voids and shell fragment molds (sf) in a slightly mottled, light brown-green dolomudstone matrix.
8-23-28-21W4, 1765.2 m.

c) Mottled, light brown dolowackestone accentuated by rare shell debris and small gastropod molds (g) amongst numerous subspherical voids.
5-24-28-21W4, 1831.5 m.

d) Highly mottled dolomudstone supporting relatively few gastropod molds (g) and voids. Colours vary with location of mottling and diagenetic alteration.
4-24-28-21W4, 1763.8 m.

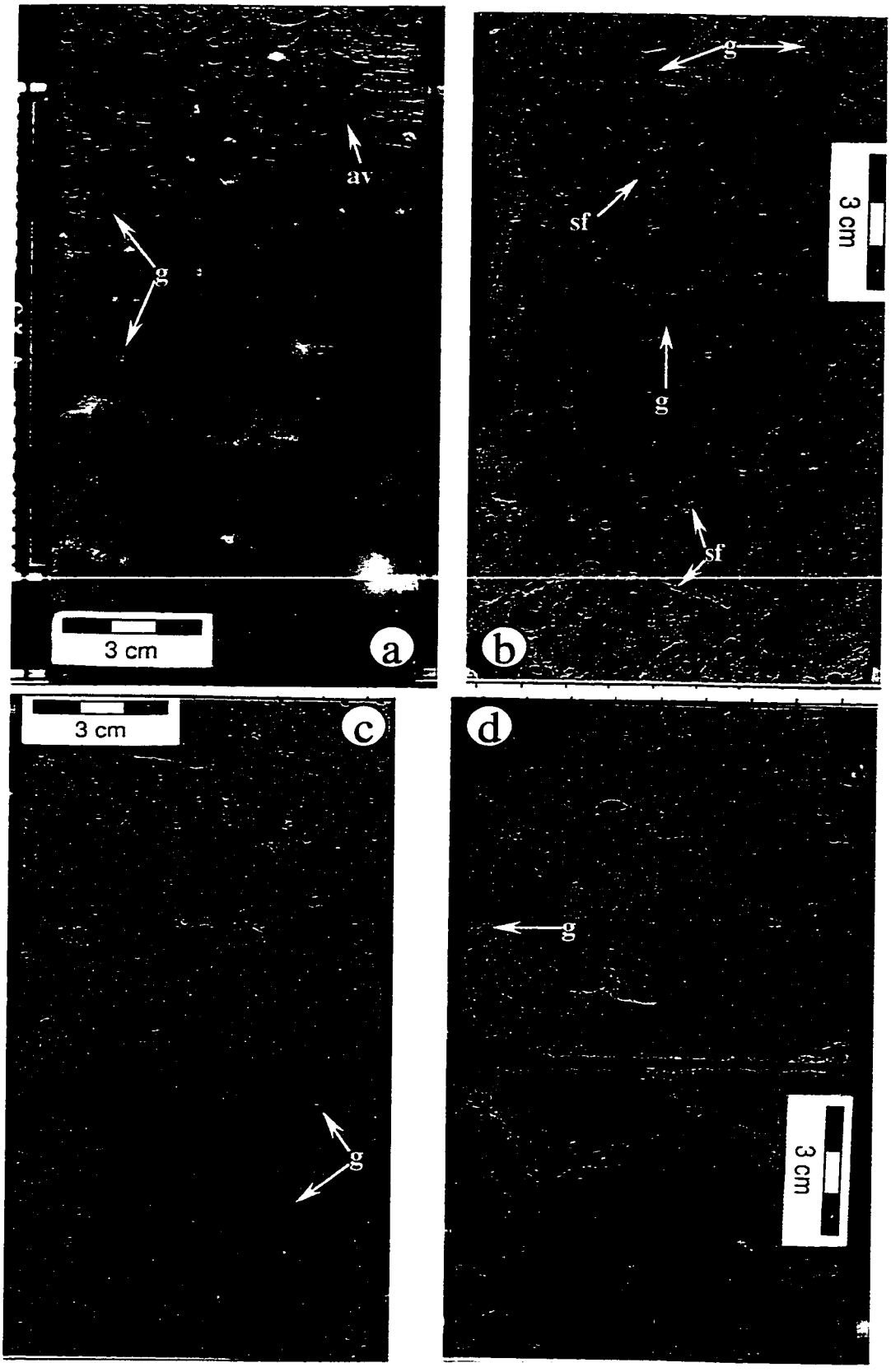
av
g
3 cm
a
g
sf
3 cm
g
sf
b
3 cm
c
g
g
3 cm
d

ubiquitous presence of gastropods and their tolerance for water conditions ranging anywhere between very quiet to very high energy, and fresh to higher than normal salinities.

The massive dolomitized mud matrix offers no clues towards the original composition of the mud or the small voids. The dominance of mud does indicate that energy conditions were quite subdued, but not so quiet as to totally inhibit the presence of small shell fragments. Mottling is common within the matrix of Lithofacies G, indicating an active infauna. But unlike many other lithofacies of Nisku 2 sub-unit, which display thoroughly bioturbated, massive, non-mottled mud matrices, the infaunal churning is not as complete in Lithofacies G. Less than ideal environmental conditions for the infaunal community in Lithofacies G may explain the less intense activity.

Pratt et al. (1992) recognize that in modern tropical carbonate environments, the lowermost intertidal zone in quiet water settings of normal salinity tends to be a thoroughly bioturbated mixture of lime mud, pellets, and bioclasts. During low tide the sediment tends to be covered with an ephemeral algal slick, the source of food for grazing animals such as gastropods (Bathhurst, 1975).

In Recent sediments of south Bonaire, Lucia (1968) identifies an intertidal pelleted mud deposit composed of lime mud, 0.1-0.2 mm pellets, foraminifera, ostracods, gastropods, a small pelecypod, and a few pisolites. Pelleted lime muds with restricted faunas of myliolid forams and gastropods are typical of Recent intertidal deposits (Lucia, 1968). This modern dolomitized pelleted mud, which originates from the intertidal environment on the shores of the hypersaline Lake Pekelmeer in south Bonaire (Figure 3.6 – F.J. Lucia, personal communication) displays a striking resemblance to Lithofacies G of the Nisku 2 sub-unit.

It is interpreted that Lithofacies G developed in the lower intertidal zone of a low energy, mud-rich environment. The low faunal diversity, the presence of the hardy gastropods, the incompletely bioturbated matrix, and the similarity to a modern intertidal deposit in a hypersaline setting suggests that at least moderately restricted conditions

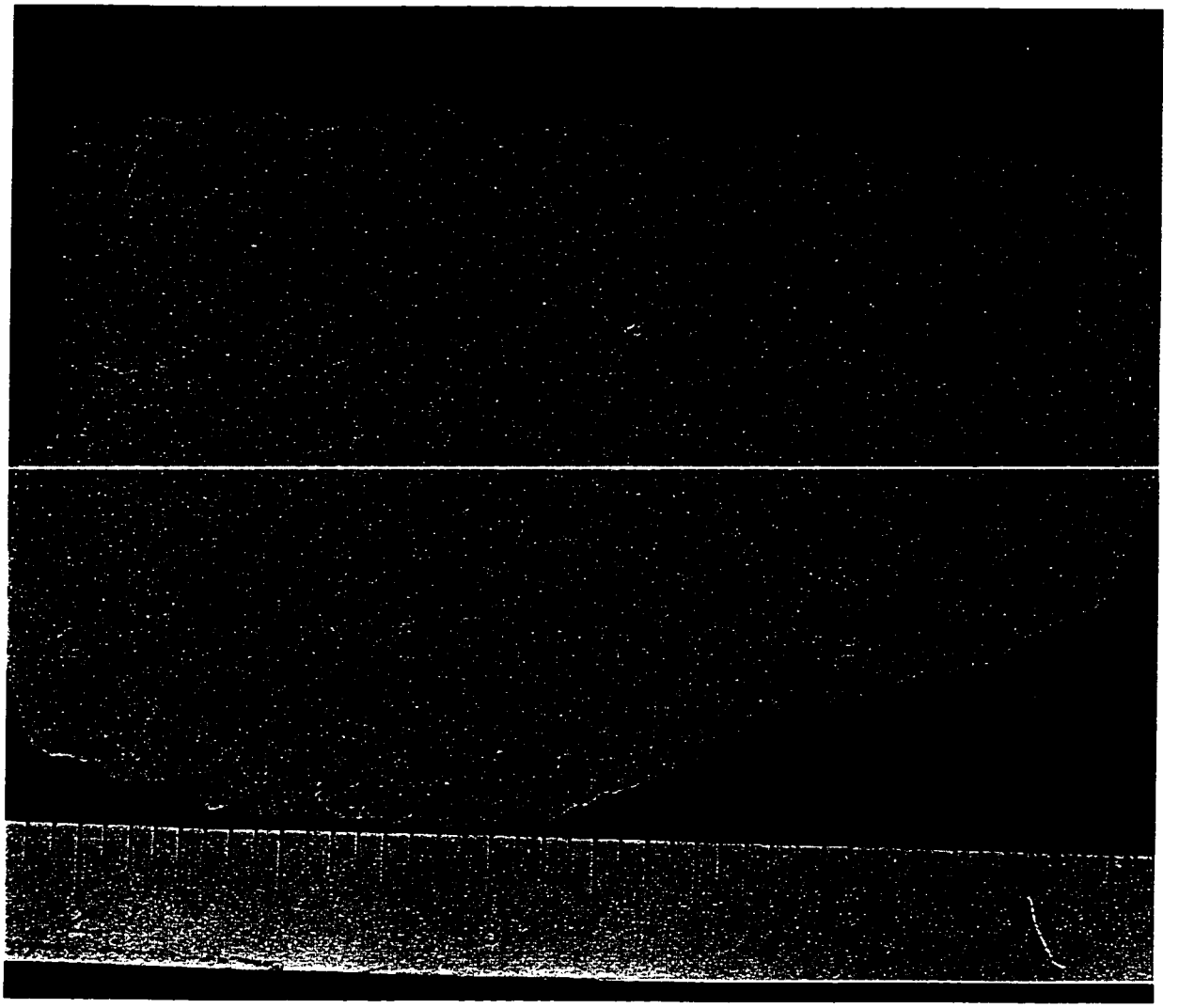

Figure 3.6: Dolomitized pelleted mud from a modern intertidal environment in Bonaire. Abundant small fossil molds including spiralled gastropods (g). Scale bar is in inches. Photograph courtesy of F.J. Lucia.

prevailed at the time of deposition. Microbial (algal) mats, upon which the gastropods grazed, were likely present but no evidence has been preserved.

Lithofacies H: MEGALODONT DOLOFLOATSTONE (Figure 3.7)

Description:

Articulated and disarticulated megalodont clams within a light to medium brown dolomudstone to dolowackestone matrix characterize Lithofacies H. Individual accumulations are up to 2.5 m thick and are concentrated along the flanks of the Nisku 3 sub-unit channel.

The megalodont bivalve shells may achieve dimensions up to 10 cm in length and 2.5 cm in thickness. The state of preservation of the megalodonts widely varies. Individuals may be: (i) completely replaced with dolomite (Figure 3.7a), (ii) replaced by dolomite then partially dissolved (Figure 3.7d), (iii) completely leached resulting in empty molds (Figure 3.7c), (iv) moldic with isopachous cement linings, or (v) cemented by anhydrite at any of the above stages (Figures 3.7b and 3.7d). Where articulated, the thick hinge area typically points downward while the rest of the valve thins in an upward direction (Figure 3.7d). The bulk of the megalodonts, however, are disarticulated with individual valves randomly oriented. Very little shell fragmentation or bio-erosion is apparent. In some zones the megalodonts may be so concentrated as to be in contact with one another. Yet the matrix is always a dolomudstone to dolowackestone. The dolowackestone has a similar appearance as Lithofacies G, but with larger, non-aligned voids and gastropods reaching widths of 3 cm. Overturned bulbous stromatoporoids, up to 15 cm in diameter, are very rare. Biomolds, possibly of brachiopod and ostracod shell fragments, are present sporadically.

In thin section, the dolomudstone to dolowackestone matrix is comprised of cloudy interlocking crystals with a mean length of 70 μm. Pore-filling anhydrite crystals may be either coarse and blocky or as very fine-crystalline interlocking mosaics.

Figure 3.7:

Lithofacies H: MEGALODONT DOLOFLOATSTONE

a) Large gastropod (g) and megalodont (meg) shells replaced by cream coloured dolomite within a medium brown dolowackestone matrix. Supported by the matrix, the fossils are randomly oriented.
1-12-28-21W4, 1750 m.

b) A combination of empty and filled molds of disarticulated megalodont bivalves (meg). Cloudy white anhydrite (A) cements the interiors of select molds.
13-13-28-21W4, 1768.5 m.

c) Highly porous megalodont dolofloatstone. The molds of megalodonts (meg) and other shell debris lack any cement fill.
14-13-28-21W4, 1757.7 m.

d) Upright articulated bivalve (ameg) amongst partially dissolved and cemented solitary valves in a light brown dolowackestone matrix.
8-23-28-21W4, 1770 m.

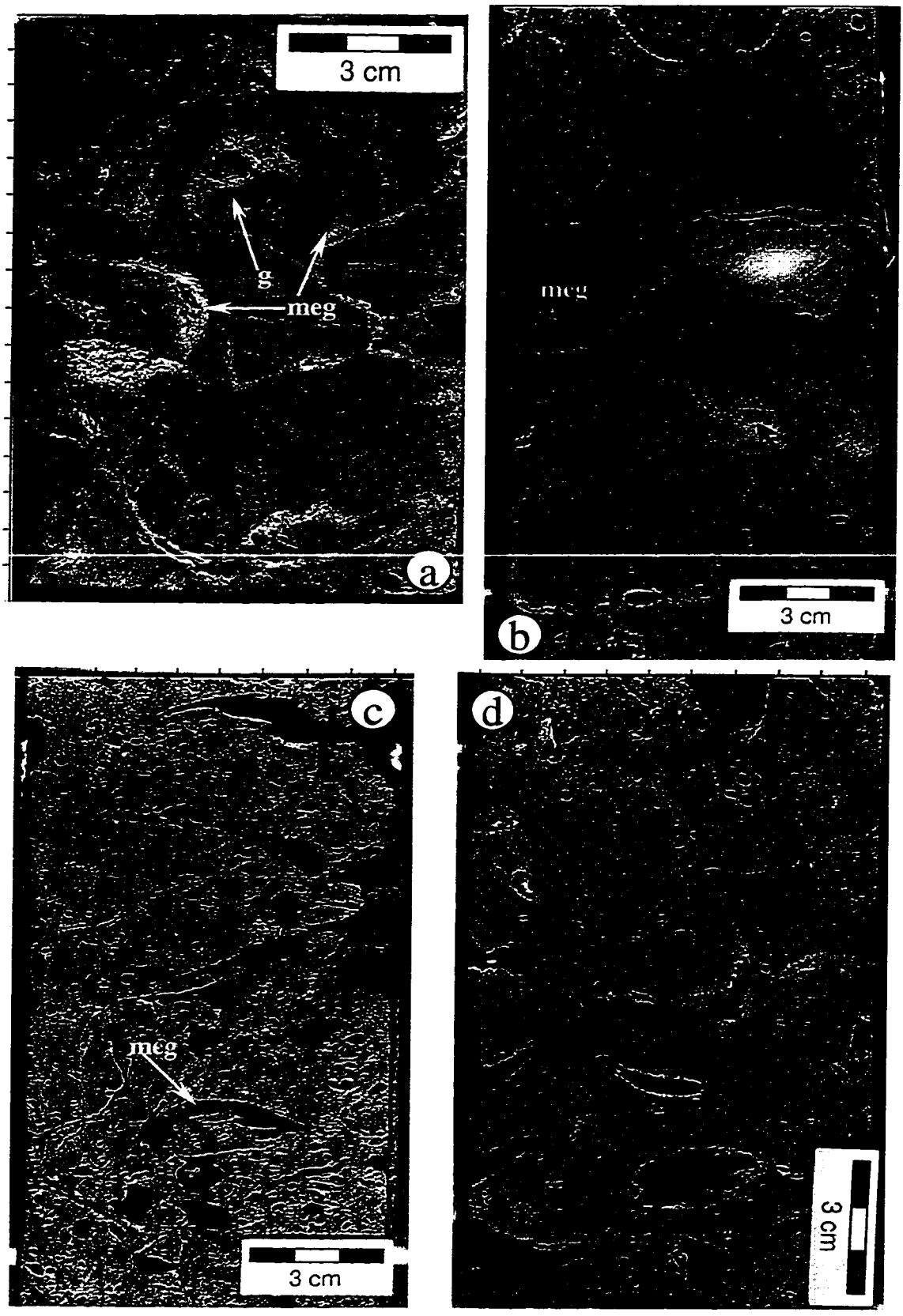
3 cm
g
meg
a
meg
b
3 cm
c
meg
3 cm
d
3 cm

Interpretation:

A significant volume of the Nisku 2 sub-unit in the Wayne field is comprised of Lithofacies H, yet the megalodont bivalve is considered to be a minor contributor in relation to the entire Devonian fossil assemblage. The cause of the prolific growth of these robust clams along the channel margin is in question.

Due to the degree of dolomitization and masking of primary fabrics, it is speculative to identify the original lime-mud composition of Lithofacies H. Where present in limestones elsewhere, megalodonts are commonly preserved in peloidal mudstone or wackestone matrices and are interpreted to have inhabited shallow-water, protected back-barrier, lime mud-rich settings (de Freitas et al., 1993). Most of the megalodont valves in Lithofacies H are disarticulated, solitary, and randomly oriented. It is common to encounter disarticulated bivalves in the ancient record since the soft elastic ligaments which hold the valves together decompose after death (Clarkson, 1993). Hence, high energy conditions do not have to be invoked to physically separate the valves. With the lack of shell fragmentation and the abundance of mud in the matrix of Lithofacies H, marine energy conditions were likely very low at the time of deposition.

There are numerous examples within Lithofacies H of articulated bivalves preserved in upright, natural life positions. Apparently the valves were unable to separate upon death of the organism, perhaps because of extremely high sedimentation rates quickly covering the epifaunal megalodonts. As well, the overall lack of shell bio-erosion further supports an interpretation of rapid burial in mud.

Thick-shelled megalodonts were mud-resting, epifaunal suspension feeders that probably contained photosynthetic algal symbionts (de Freitas et al., 1993). Such a symbiotic relationship could supplement the metabolic energy required to maintain the high skeleton-to-body ratios that were needed to resist disturbances such as predation, bioturbation, and storm influx in an epifaunal environment. Despite the great stability provided by such robust shells, de Freitas et al. (1993) further hypothesized that the sediment bearing strength of lagoonal calcimudstone could not easily have supported the large epifaunal clams, and that an increase in strength would have been a prerequisite for

megalodont growth. Through the addition of biogenic calcite, microbial colonization could have stabilized the mud-sized sediment, increased the substrate bearing strength, and reduced turbidity, all advantageous to the light-dependent megalodonts. No evidence of algae or cyanobacteria has been discovered in the dolomitized Lithofacies H.

The recurrent observation that large megalodonts are preserved with low diversity fossil assemblages in lime mud-rich settings suggests that the conditions in which megalodonts flourished were not ideal for most reef inhabitants (de Freitas et al., 1993). It is generally accepted that megalodont bivalves inhabited shallow lagoons and were well adapted to temperature, salinity, and turbidity stresses (Eliuk, 1998). The only other abundant fossils recognized within Lithofacies H are large gastropods, creatures recognized for their ability to thrive in virtually any depositional setting. Eliuk (1998) confirms that a common association of megalodonts and large gastropods exists throughout select Devonian and Jurassic localities of Canada, but also in association with algae (including cyanobacteria and microbialites). He proposes that the enhanced algal presence indicates a further stress of nutrient enrichment. That is, increased suspended and dissolved inorganic materials and organic matter acted as fertilizers for the growth of algae. In nutrient enriched environments, soft substrate communities are favored over reef coral framebuilders (Wood, 1993). The supply of nutrients from the land to the marine realm is interpreted to have intensified during the Late Devonian because of the surge of vascular plants and development of thicker soils (Algeo and Maynard, 1993).

The megalodont bivalves are most abundant along the edge of the Nisku 3 sub-unit channel, likely laterally equivalent to the organic-rich channel-filling deposits of Lithofacies O and P. Although organic matter would have been oxidized in the relatively shallow bank setting, the preserved organic matter in the adjacent channel may hint at a more widespread distribution of nutrients and subsequently increased algal/microbial influence – that is, beyond the confines of the channel (see discussion of Lithofacies P). It may be no coincidence that the seemingly rare megalodont was able to thrive in the Wayne area during the late Frasnian.

Lithofacies H is interpreted to have been deposited in a low energy, shallow subtidal environment proximal to the Nisku 3 sub-unit channel. Sedimentation rates were probably rapid at times. Environmental conditions were not conducive to the growth of normal reef-dwellers; stresses such as high salinity, temperature, and/or nutrient influx likely influenced the depositional environment.

Lithofacies I: AMPHIPORA DOLOFLOATSTONE (Figure 3.8)

Description:

Lithofacies I is typified by *Amphipora* within a tan to dark brown dolomudstone matrix. The lithofacies is most common away from the Nisku 3 sub-unit channel margin in successions up to 2.7 m.

Narrow central canals running the length of the stick-like fossils support the identification of the dolomitized *Amphipora* (Figure 3.8a), but most examples are as circular to tubular molds randomly oriented (Figures 3.8b and 3.8c). Anhydrite cement is a common fill of the molds. Fossil diameters range between 1.5 and 3 mm and increase to 4 mm where solution enlarged. The maximum observed length of the long axis is 3.5 cm. Rarely the amphiporoids are in contact with one another as rudstones, but in general the fauna are mud-supported. The massive dolomudstone matrix lacks laminae and mottling. Thamnoporoid corals are local accessory fossils (Figure 3.8d).

Petrographically, anhedral to subhedral interlocking dolomite crystals of the matrix have a mean length of 50 μm. Some *Amphipora* are either replaced or cemented by significantly larger dolomite crystals (average of 100 μm).

Interpretation:

"*Amphipora* was a sessile, benthonic animal growing most abundantly in sheltered, slightly restricted waters..." (Murray, 1966). Back-reef, bank interior, and lagoonal are some of the names for the protected environments in which the stick-like stromatoporoid, *Amphipora*, is interpreted to have inhabited within Devonian successions of the Western Canada Sedimentary Basin (Murray, 1966; Leavitt, 1968; Wilson, 1975). All of these settings have in common low energy, quiet water conditions in which lime mud is the

Figure 3.8:

Lithofacies I: AMPHIPORA DOLOFLOATSTONE

a) Randomly oriented, stick-like *Amphipora* (a) fossils (outlined in pencil) display their characteristic central canals. Locally the fossils support one another in the light brown dolomudstone matrix.
8-12-28-21W4, 1887.6 m.

b) Sparsely distributed *Amphipora* molds (am) within a massive medium brown dolomudstone matrix. White patch of diagenetic anhydrite is present at the top of the photograph.
8-12-28-21W4, 1889.5 m.

c) A dense concentration of *Amphipora* molds in upper two thirds of photograph. Locally, the molds are solution enlarged (se). White anhydrite fills the molds and dissolution cavities at the base of the photograph.
13-13-28-21W4, 1794.9 m.

d) A combination of *Amphipora* molds and fossils in a light brown-green dolomudstone matrix. Thamnoporoid corals (th) are a rare accessory fossil.
4-24-28-21W4, 1793.5 m.

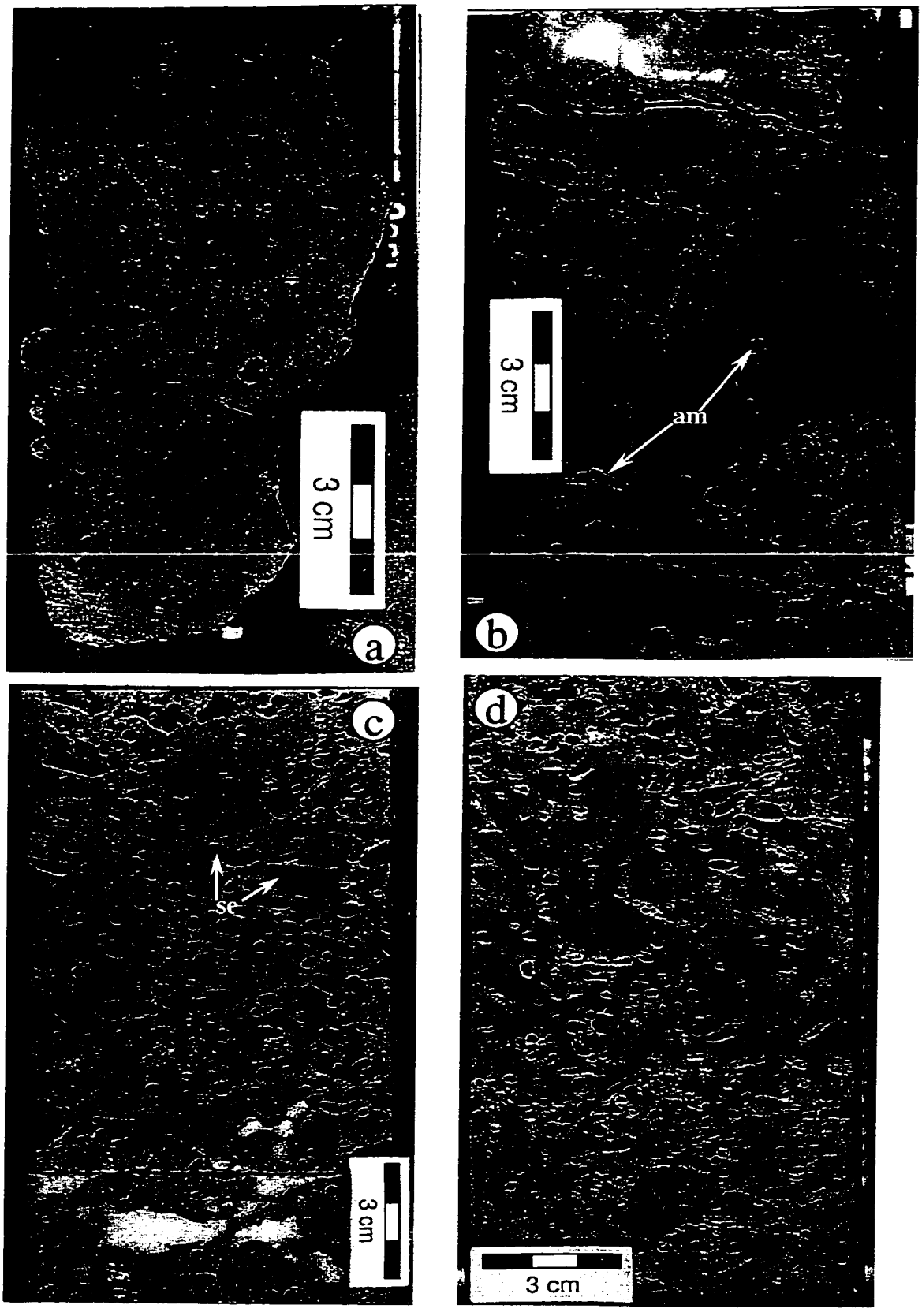
a
3 cm
b
3 cm
am
c
se
3 cm
d
3 cm

predominant deposit. In fact, the elongate stick-like morphology is believed to be an adaptation to prevent smothering by mud suspended in water (Wilson, 1975).

Natural growth position does not appear as an unquestionable state of preservation, however, instances where the *Amphipora* are intertwined suggest that densities were high enough to form thickets. The scarcity of extensive bioclast fragmentation, the lack of physical bedding structures, and the high proportion of mud indicate that little current reworking took place. In addition, the absence of preserved laminae or mottling suggests that either extensive churning of the sediment by a well developed infauna took place, or simply random deposition of mud occurred around the randomly-oriented stick-like fossils.

Within the upper Nisku 2 sub-unit, *Amphipora* tend to be most numerous away from the Nisku 3 sub-unit channel margin. Although the *Amphipora* likely tolerated slight restrictions in circulation and salinity, they probably could not handle the variety or degree of stresses that the megalodont bivalves endured at the Nisku 3 sub-unit channel margin. The rare presence of thamnoporoid corals within Lithofacies I confirms a preference amongst the *Amphipora* for more normal marine conditions, since "*Thamnopora* are interpreted as having lived in well aerated, moderately turbulent, shallow waters" (Leavitt, 1968). Based on the lack of shell fragments and gastropods, Lithofacies I was likely deposited in lower energy and slightly deeper subtidal conditions compared to the laterally adjacent megalodont-rich lithofacies.

It is interpreted that Lithofacies I was deposited in a moderately shallow yet low energy, protected subtidal environment such as a lagoon. Minor restrictions in salinity and circulation likely influenced the *Amphipora* thickets atop the bioturbated muddy substrate.

Lithofacies J: MASSIVE DOLOMUDSTONE (Figure 3.9)

Description:

A light tan to dark brown massive dolomudstone distinguishes Lithofacies J. Individual accumulations are no thicker than 1 m and have a similar spatial distribution to that of Lithofacies I.

The massive dolomudstone of Lithofacies J resembles the matrix of Lithofacies I. It is petrographically similar to the matrix of Lithofacies I with an average dolomite crystal length of 50 μm. Laminae are absent and mottling is not prevalent. Patches of *Amphipora* are the only fossils present. Small open voids, less than 1.5 mm in diameter, are sporadic and in low concentrations. More common are vugs that contain dark layered mud geopetal bases and anhydrite cemented, irregular-shaped upper portions (Figures 3.9a, 3.9c, and 3.9d). These mesopores are greater than 1 cm in diameter and may be isolated or three-dimensionally linked. Anhydrite-filled and thin open fractures are common (Figure 3.9b) and may connect many of the large vugs.

Interpretation:

Lithofacies J commonly has gradational contacts with the *Amphipora*-rich Lithofacies I, and in fact the two lithofacies tend to alternate with one another. In essence, Lithofacies J is equivalent to the matrix of Lithofacies I. Because of the common association with Lithofacies I, it is assumed that Lithofacies J was deposited in a comparable setting as that of Lithofacies I. That is, a moderately shallow yet low energy, protected subtidal environment where infaunal activity removed any evidence of primary laminae within the muddy substrate. The lower concentration of *Amphipora* likely indicates that conditions were periodically unsuitable for colonization, possibly because of variations in sedimentation rate, turbidity, salinity, temperature, and/or other environmental factors.

Within the Nisku Formation of the Bashaw area, Gilhooly's (1987) "Massive Light Fine Dolomite" (Lithofacies 5) displays a light buff colour, has a vaguely colour mottled appearance, lacks any laminae, and shows a strong association with *Amphipora*-dominated lithofacies. All of these features are common to Lithofacies J of this study. Gilhooly (1987) interprets his Lithofacies 5 as deposited in a restricted shallow subtidal setting, subject to extensive infaunal churning and periodic storm reworking. Unlike Gilhooly's (1987) Lithofacies 5, a wide range of crystal sizes (and inferred original grain sizes) was not observed in Lithofacies J of this study, suggesting lesser importance of storm reworking. Otherwise, both depositional environment interpretations are very similar.

Figure 3.9:

Lithofacies J: MASSIVE DOLOMUDSTONE

a) Massive medium brown dolomudstone with rare millimetre-scale molds is similar to the massive matrix of Lithofacies I. Large cavities (cav) with dark brown dolomudstone geopetals (geo) and anhydrite cements (A) are common in Lithofacies J.
8-20-28-21W4, 1810.1 m.

b) Randomly oriented fractures (Fr) cross-cut the massive dolomudstone.
1-25-28-21W4, 1785.3 m.

c) Light and dark brown mottling of dolomudstone in upper part of photograph. In the lower half of the photograph are abundant dissolution cavities (cav) with dark brown dolomudstone geopetals (geo) and white anhydrite cements (A).
102/10-14-28-21W4, 1962 m.

d) Massive dark brown dolomudstone with rare isolated biomolds. Hairline fractures and dissolution cavities (cav) with geopetals (geo) and anhydrite cements (A) are post-depositional features.
4-9-29-21W4, 1756.5 m.

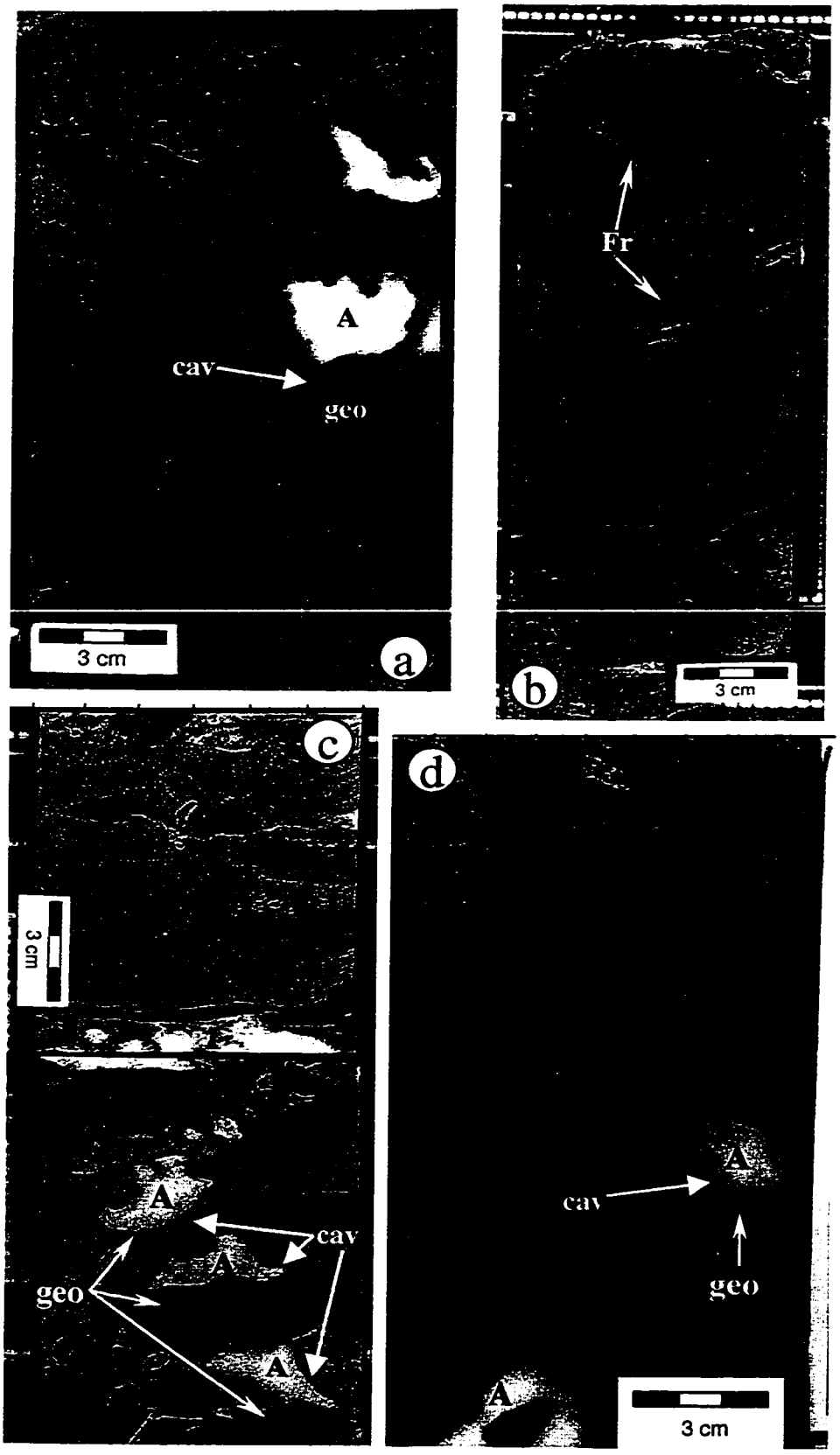
A
cav
geo
3 cm
a
Fr
b
3 cm
c
3 cm
A
cav
A
geo
A
d
A
cav
geo
A
3 cm

The large vugs with geopetal bases and anhydrite cements are interpreted to be post-depositional cavities and are discussed in detail in chapter 4.

It is interpreted that Lithofacies J was deposited in a low energy, shallow subtidal setting prone to stresses which restricted Amphipora colonization yet allowed for thorough churning by a well developed infaunal community.

Lithofacies K: THAMNOPORA DOLOFLOATSTONE/DOLORUDSTONE (Figure 3.10)

Description:

Thamnoporoid corals set within a medium to dark brown dolomudstone to dolowackestone matrix characterize Lithofacies K. The lithofacies is abundant only in the lower half of the Nisku 2 sub-unit in successions up to 3 m thick.

The corals have been replaced by dolomite yet the internal structure of the bioclasts is preserved well enough to confidently identify as *Thamnopora*. Cross-sectional widths range between 5 and 10 mm; long axis lengths reach up to 2.5 cm. Bioclast sizes tend to be larger where individuals are in contact with one another within dolorudstone beds (Figure 3.10b). Long axes appear to be randomly oriented in the bioclast supported intervals versus a somewhat sub-horizontal alignment in the mud-supported zones (Figure 3.10d). The matrix may be massive to mottled and contain numerous small voids/vugs.

In thin section, the mean dolomite crystal length in the matrix is 70 μm. The interlocking crystal mosaic contains replaced, yet well preserved *Thamnopora* skeletons throughout.

Interpretation:

Thamnopora were branching tabulate corals which inhabited shallow marine waters, but in moderately turbulent, well aerated conditions (Leavitt, 1968). Open platform conditions prevailed for similar Frasnian coral-dominated lithofacies (Dooge, 1978). Since *Thamnopora* is most abundant in mud matrices, it is believed that this dendritic coral lived on soft muddy bottoms (Murray, 1966). Gilhooly (1987) also observed a fine-grained matrix supporting the *Thamnopora* in the Nisku Formation and concluded that the corals

Figure 3.10:

Lithofacies K: THAMNOPORA DOLOFLOATSTONE/DOLORUDSTONE

a) Well preserved thamnoporoid corals (th) supported by a medium brown dolomudstone matrix. The corals (outlined in pencil) are aligned horizontally to sub-horizontally.
14-11-28-21W4, 1851.5 m.

b) *Thamnopora* dolorudstone. The thamnoporoid corals are randomly oriented. Cross-sectional widths of individual corals (th) are larger than those within floatstones. White patches are diagenetic anhydrite (A).
13-13-28-21W4, 1799.4 m.

c) Sparse distribution of thamnoporoid corals (th) within a highly fractured and diagenetically altered dark brown dolowackestone matrix.
14-11-28-21W4, 1850.1 m.

d) Sub-horizontally aligned *Thamnopora* (th) at the base of the photograph. Some corals are supported by the medium brown dolomudstone matrix whereas others are surrounded by diagenetic anhydrite (A).
14-13-28-21W4, 1762.2 m.

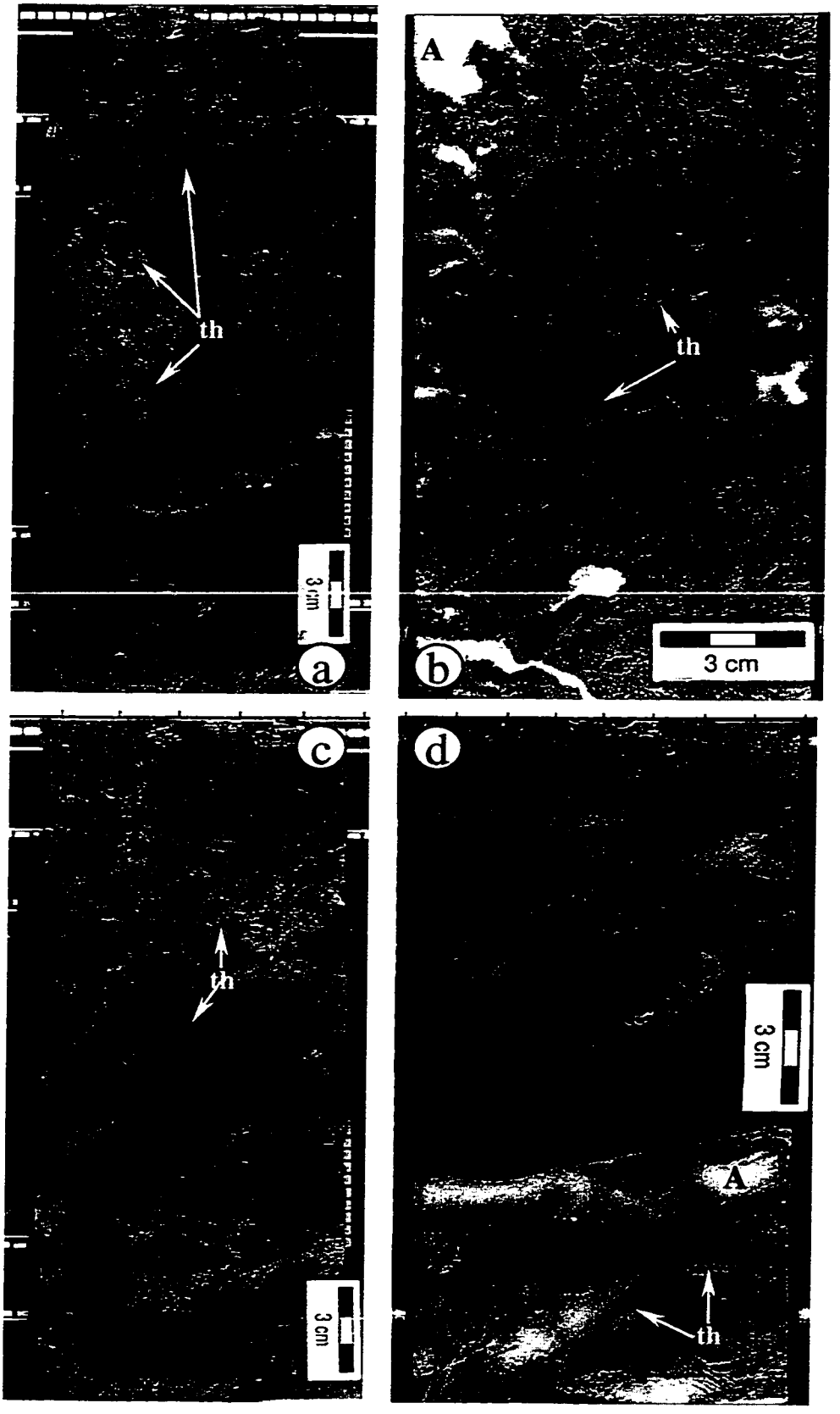
th
3 cm
a
A
th
b
3 cm
c
th
3 cm
d
3 cm
A
th

likely inhabited water depths below wave base, with storms as the main mechanism for transport of mud and fossil material.

For the most part, the thamnoporoid corals of Lithofacies K are supported by a massive to slightly mottled dolomudstone to dolowackestone matrix. The mud may not have been laminated originally or an active infaunal community could have removed all traces of laminae. Thin beds comprised entirely of the corals, similar to that recognized by Gilhooly (1987), probably were the result of storm deposition. However, the larger coral sizes in such beds may also indicate a higher energy environment in which conditions favoured the growth of more robust *Thamnopora*. It is difficult to determine whether the coral-supported beds occupy cycle capping positions.

The bulk of Lithofacies K is interpreted to have been deposited in an open marine, non-restricted platform setting below normal wave base. However, the presence of larger corals supporting one another may be the result of higher growth rates in an environment of increased energy. An active infauna bioturbated the mainly muddy substrate upon which the *Thamnopora* grew.

Lithofacies L: COARSE-CRYSTALLINE DOLOSTONE (Figure 3.11)

Description:

Lithofacies L is characterized by a fabric of light to medium brown coarse dolomite crystals supporting one another. The lithofacies is present only in the lower half of the Nisku 2 sub-unit and consequently few cores have been cut. The thickest succession is 3 m.

Lithofacies L is generally massive with no physical sedimentary structures, bioturbation, or identifiable fossils. Spherical- to peloidal-shaped molds are locally abundant and range in diameter from 0.1 mm to over 3 mm (Figures 3.11a and 3.11b), however completely massive crystalline fabrics lacking in molds are most common (Figures 3.11c and 3.11d). Where present, the molds locally may be in contact with one another.

Figure 3.11:

Lithofacies L: COARSE-CRYSTALLINE DOLOSTONE

a) Light brown coarse-crystalline dolostone contains numerous subspherical and peloid-shaped molds (m). The molds are not aligned in bedding parallel or any other orientations.

5-24-28-21W4, 1856.6 m.

b) Abundant intercrystalline pore space is present between the light brown coarse-crystalline dolomite crystals. Non-aligned molds are sporadic in distribution. Cloudy white patches are diagenetic anhydrite (A) surrounded by buff coloured coarse-crystalline dolomite.

4-24-28-21W4, 1781 m.

c) Massive light brown coarse-crystalline dolostone contains a few small subspherical molds (m) and rare fractures (Fr).

4-24-28-21W4, 1789.8 m.

d) A low amplitude stylolite (sty) separates massive medium brown coarse-crystalline dolostone in the lower half of the photograph from a combination of medium brown coarse-crystalline dolostone (cd) and light brown fine-crystalline dolostone (fc) in the upper half of the photograph.

14-11-28-21W4, 1852.4 m.

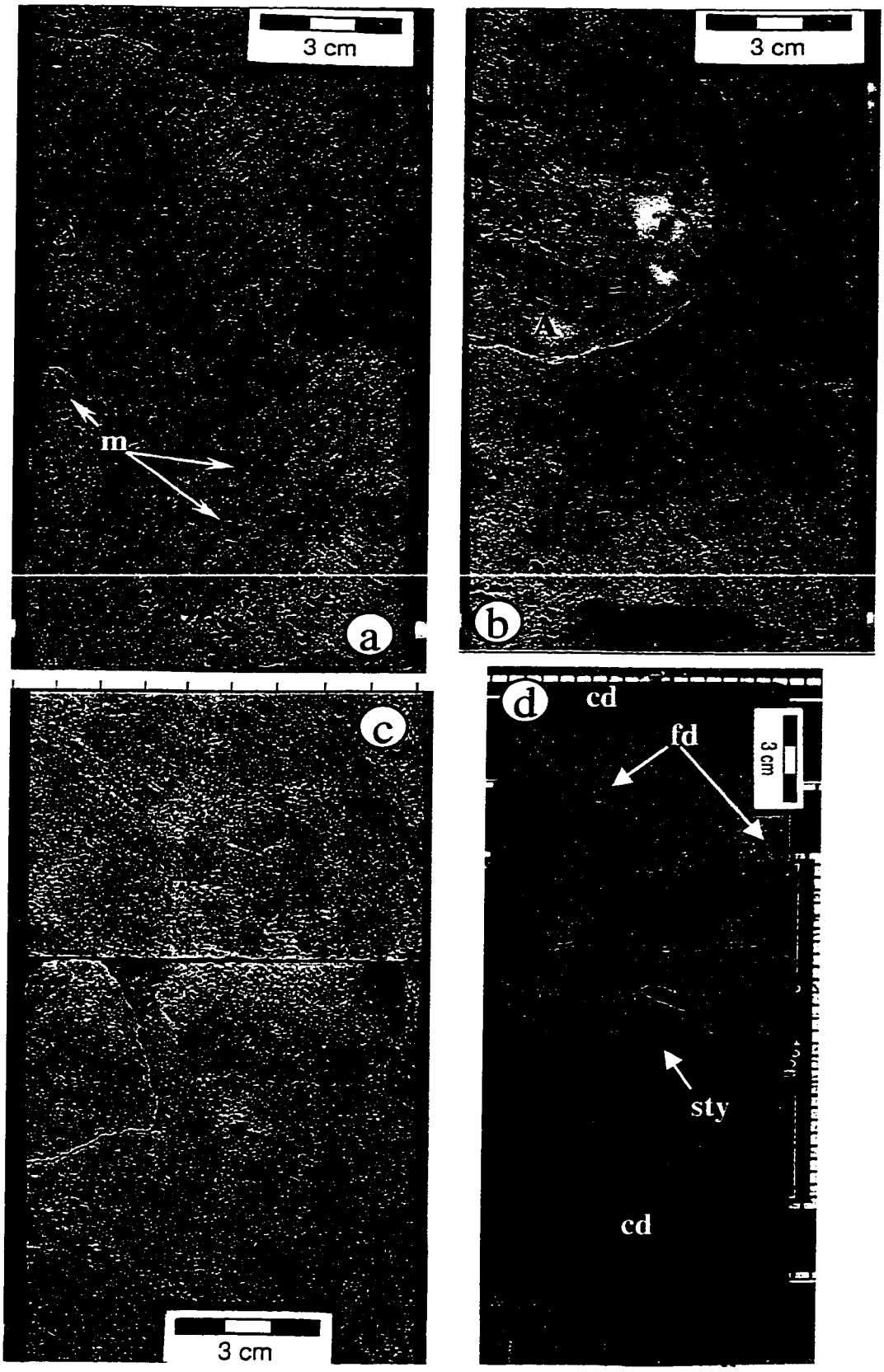
3 cm
m
a
3 cm
A
b
c
3 cm
d
cd
fd
3 cm
sty
cd

In thin section, Lithofacies L is made up of generally euhedral dolomite crystals in contact with one another. Intercrystalline pore space is abundant. Anhydrite cement rarely occludes the pores. The dolomite rhombs have an average crystal length of 120 μm. Less common are patches of finer interlocking dolomite crystals in which the subhedral crystals have a mean length of 50 μm (Figure 3.11d).

Interpretation:

Some carbonate workers believe that dolomite crystal size has no relation to the grain size of the precursor limestone (e.g. Dolphin and Klovan, 1970). It is important to note, however, that the coarse-crystalline Lithofacies L is the only Nisku 2 sub-unit lithofacies that contains such a loose fabric of dolomite rhombs with abundant intercrystalline pore space. The dolomudstone matrices of the other Nisku 2 sub-unit lithofacies contain finer interlocking dolomite crystal mosaics without large intercrystalline pores. Rather than an anomalously coarse-crystalline dolomite replacement of mud it makes more sense to suggest that an originally coarser-grained fabric was replaced in Lithofacies L. The minor patches of more densely packed dolomite mosaics present in Lithofacies L further imply that muddier zones existed within a predominantly coarser-grained deposit. It is less logical to argue for random coarse- and fine-crystalline dolomite replacement separately taking place in the same homogenous rock. Lithofacies L was likely deposited in a relatively high energy environment, but either the energy was not too great as to remove all of the muddier sediment or mud infiltrated the coarse-grained deposit subsequent to the high energy deposition.

It is difficult to pinpoint an environment of deposition without any bedding or faunal indicators. Accumulations as thick as 3 m rule out the possibility of a short-lived tempestite. Lithofacies L caps coarsening upward cycles and is likely related to shallow water deposition above normal wave base.

3.4 LITHOFACIES OF THE NISKU 3 SUB-UNIT

The deposits of the Nisku 3 sub-unit have an aerially restricted distribution along a linear and narrow seismic anomaly (Figure 2.3) and are significantly more argillaceous

than the laterally adjacent Nisku 2 sub-unit deposits. Based on these observations and the following depositional interpretations, the Nisku 3 sub-unit is interpreted as a channel fill.

Only three wells within the study area, 12-24-28-21, 10-26-28-21, and 8-26-28-20W4, have core which contain lithofacies of the Nisku 3 sub-unit. None of the cores penetrate the complete thickness of the channel, therefore the following lithofacies may not be a true representation of what filled the entire channel. Regardless, four distinct carbonate lithofacies are distinguished as representative of the Nisku 3 sub-unit.

Lithofacies M: FINING UPWARD DOLOPACKSTONE TO DOLOWACKESTONE (Figure 3.12a and 3.12b)

Description:

Lithofacies M is comprised of small scale fining-upward packages of peloidal light brown dolopackstones to dark brown dolowackestones. Lithofacies M dominates the upper portion of the channel fill and ranges in thickness from 4 m in 12-24-28-21W4 to over 6 m in 10-26-28-21W4.

The dolopackstones generally have sharp, slightly erosive lower contacts with the underlying litho-units (Figure 3.12a) and gradually become more mud-rich upwards (Figure 3.12b). Where well developed, these normally-graded packages are between 10 and 60 cm in thickness. However, the packstones tend to dominate near the top of the lithofacies, resulting in poorly defined fining-upward packages and reduced mud content. Bedding is commonly at a horizontal but may reach an angle of 25 degrees in the 10-26-28-21W4 core. Faint organic-rich laminae are common within the packstones. Subspherical molds, 0.3 to 1 mm in diameter, are interpreted as peloids (Figure 3.12a). Anhydrite commonly cements the molds and is also present as isolated nodules 5 to 20 mm in diameter. Calcite is a much rarer cement. No definite fauna are present but rare tubular anhydrite-cemented molds are likely leached *Amphipora.*

Petrographically, the size of the dolomite crystals within the matrix widely varies. Crystal lengths range between 20 and 100 μm, with an average of 50 μm. The dolomite crystals are cloudy and tightly interlocking throughout. Cements are most commonly very

fine-crystalline mosaic anhydrite, although very coarse-crystalline calcite occludes some molds as well.

Interpretation:

The base of each fining-upward package is erosively scoured and filled by a peloid-rich yet mud-dominated packstone. Peloid abundance decreases and mud content increases upwards until the next erosive contact. Such normal grading generally indicates waning flow conditions and implies that episodic high-energy events initially scoured underlying units, followed by progressive decreases in current energy. Based on the dark colour, near lack of fauna, and absence of exposure indicators, resumption of quiet-water, subtidal deposition took place at the top of cycles until the following high-energy event.

It is likely that the *Amphipora* present in Lithofacies M were derived from the bank and did not inhabit the channel. This assertion is based on the fossil's abundance in the Nisku 2 sub-unit and the generally inhospitable environment interpreted at the time of deposition in the lower channel (see interpretations of the other Nisku 3 sub-unit lithofacies).

Considering the deeper water channel position it is probable that most of the coarser-grained sediment of Lithofacies M was also bank-derived and was swept into the channel by high energy currents. Storm events are a possible explanation for the high energy cut and fill, however no evidence for tempestites has been identified within the Nisku 2 sub-unit bank deposits. Another possibility is intermittent sediment-gravity flows, which could be related to slope failure. The steeply inclined bedding displayed in the 10-26-28-21W4 core may indicate slope deposition at that location.

Overall shallowing seems to take place over the duration of Lithofacies M deposition, represented by the increased packstone content and culminating in a sharp transition into Nisku 1 sub-unit deposits. Shoaling may be related to a drop in sea level across the entire study area at the end of deposition of the Nisku 2 sub-unit (see Chapter 4).

In summary, Lithofacies M was deposited under relatively deep subtidal conditions in the Nisku 3 sub-unit channel. Quiet water mud deposition was repeatedly disturbed by

Figure 3.12:

Lithofacies M: FINING UPWARD DOLOPACKSTONE TO DOLOWACKESTONE

a) Sharp erosive contact (er) between underlying Lithofacies N (L.N) and overlying medium brown dolopackstone (P) of Lithofacies M. The isolated molds in Lithofacies M are interpreted to be those of peloids.
8-26-28-20W4, 2254.4 m.

b) Fining-upward succession (fu) from buff coloured peloidal dolopackstone (P) to dark grey dolowackestone (W). The sharp contact (sh) with the overlying dolopackstone marks the base of the younger succession.
10-26-28-21W4, 5858 ft.

Lithofacies N: DARK MOTTLED DOLOMUDSTONE

c) High amplitude stylolites (sty) and anhydrite concentrations (A) within mottled dark brown dolomudstone. Buff coloured alterations of the host rock are common near anhydrite patches.
8-26-28-20W4, 2266.5 m.

d) Highly mottled medium to dark brown dolomudstone. Accumulations of green and black argillaceous minerals (arg) are common along stylolites (sty). Patches of cloudy white diagenetic anhydrite (A) are common.
12-24-28-21W4, 1872.6 m.

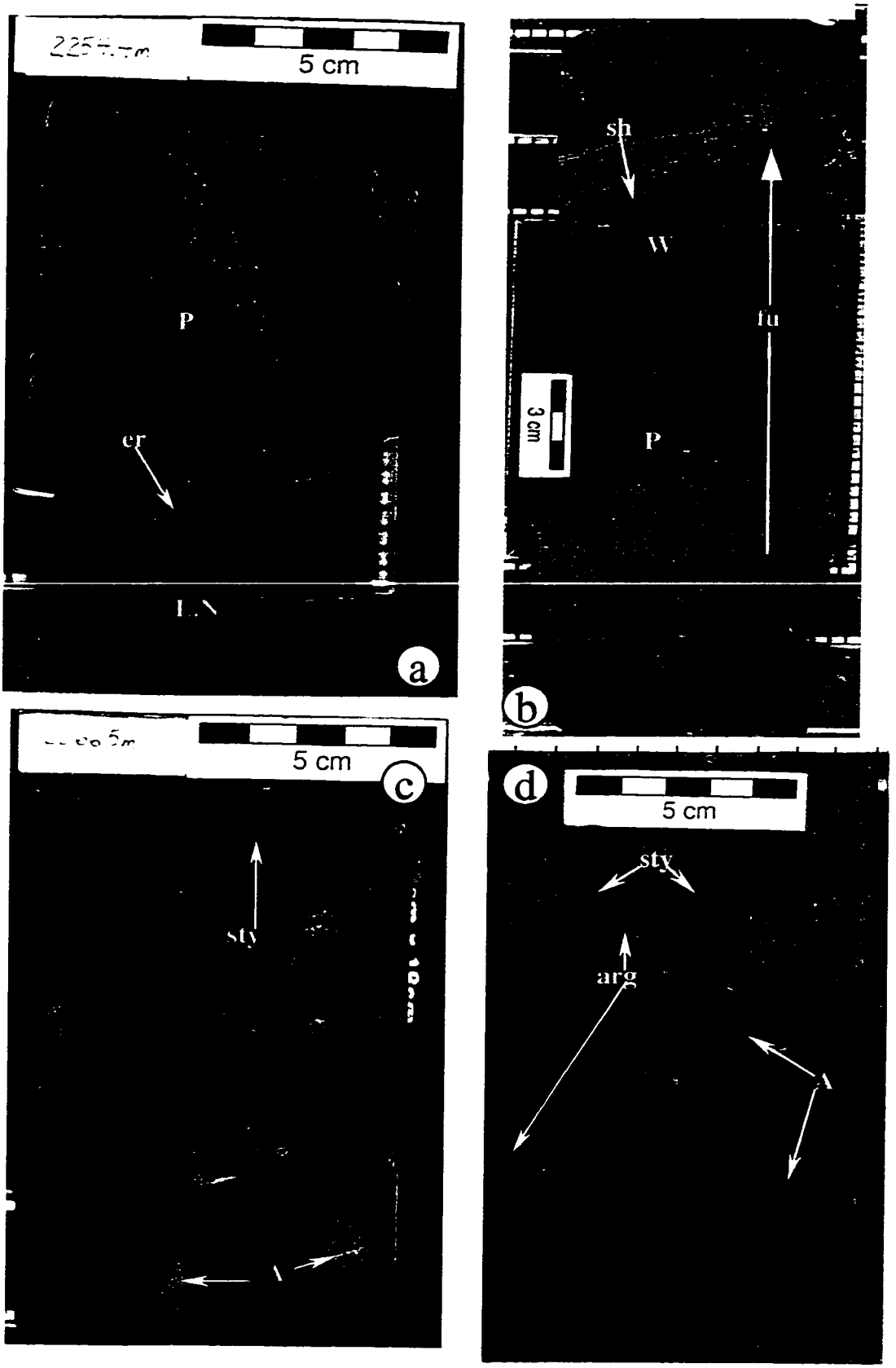
5 cm
P
er
a
sh
W
fu
3 cm
P
b
5 cm
sty
c
d
5 cm
sty
arg

high energy currents due to episodic storm activity or intermittent sediment-gravity flows sweeping sediment into the channel.

Lithofacies N: DARK MOTTLED DOLOMUDSTONE (Figure 3.12c and 3.12d)

Description:

Mottled medium to dark brown dolomudstone characterizes Lithofacies N. The lithofacies makes up the bulk of the lower part of the Nisku 3 sub-unit with individual successions ranging between 1 and 4 m in thickness.

The dolomudstone is highly mottled and lacking in laminae or other sedimentary structures. No burrow traces or vugs can be recognized. Irregular anhydrite patches with argillaceous linings are common and are associated with low-amplitude stylolites (Figure 3.12c). Most argillaceous material is black, or less commonly, green in colour and is present along stylolites (Figure 3.12d). Adjacent to the anhydrite patches the groundmass is commonly lighter brown, resulting in 1 to 5 mm haloes. Rare circular-shaped anhydrite-filled molds, 3 to 5 mm in diameter, may be biomolds, but evidence is weak.

In thin section, the fine dolomite crystals that make up the mottled mudstone matrix have a mean length of 40 μm. The crystals are cloudy and form a tight interlocking mosaic. Patches of anhydrite may be comprised of coarse bladed crystals, very fine-crystalline mosaics, or a combination of both.

Interpretation:

The dark colour, high mud content, small crystal sizes, lack of exposure indicators, and strong association with other subtidal lithofacies indicate that Lithofacies N was likely deposited in a subtidal setting of low energy. The lack of fossil evidence does not point to a healthy environment for fauna. However, the mottled appearance and lack of laminae suggest that conditions were possibly favorable for some bioturbators.

Although not apparent petrographically, the dark colour of the lithofacies may be due to dispersed organic matter throughout the mud, preserved because of a reduced oxygen content (see Lithofacies O and P). Increased salinity may also have been a potential

environmental stress, although most anhydrite patches are associated with stylolites and thus, are of deeper burial origin.

It is interpreted that Lithofacies N was deposited in a relatively deep subtidal environment. Stresses such as a reduced oxygen content and enhanced salinity may have limited the faunal community but did not totally restrict it.

Lithofacies O: BIOTURBATED LAMINATED DOLOMUDSTONE (Figure 3.13a)

Description:

Lithofacies O is a dolomudstone with wavy black laminae separated by white to tan burrow traces. Lithofacies O is present only in 12-24-28-21W4 as a 1.3 m interval within the lower channel fill.

Dark concentrations of carbonaceous-rich organic matter define wavy, commonly discontinuous laminae in Lithofacies O (Figure 3.13a). Between sets of laminae are lighter coloured burrow traces lacking in organic matter (Figure 3.13a). Most of the preserved burrowing is the result of *Chondrites isp.*, evident by branching burrows approximately 1 mm in diameter. The traces are aligned approximately parallel to the horizontal axis. Also present in lower abundance are the traces of *Phycosiphon isp.*, characterized by mud-lined burrows. No other fossils are present.

In thin section, the dolomite crystal length of the burrow infills is an average of 60 μm, noticeably coarser than the 30 μm of the interlocking matrix. All dolomite crystals are cloudy and generally subhedral. Organics are dispersed throughout the matrix and concentrated along wavy layers, yet they are absent in the burrows. There is, however, a noticeably higher concentration of opaque minerals, likely pyrite, within the burrow traces.

Interpretation:

A low diversity of traces and partial preservation of organic-rich laminae indicate that environmental conditions were not ideal for an infaunal community at the time of deposition of Lithofacies O. The most abundant traces are that of *Chondrites isp.*, a burrower characteristic of the distal *Cruziana* ichnofacies (Pemberton et al., 1992). Such branching traces are developed in sediment at or near storm wave base but below

Figure 3.13:

Lithofacies O: BIOTURBATED LAMINATED DOLOMUDSTONE

a) Light brown *Chondrites* trace fossils (Tf) are abundant in the black dolomudstone. Dark concentrations of organic matter define wavy, commonly discontinuous laminae (lam).
12-24-28-21W4, 1870.7 m.

Lithofacies P: PLANAR LAMINATED DOLOMUDSTONE

b) Rare white anhydrite nodules (nod) have displaced some of the predominantly planar, organic-rich dolomudstone laminae (pl).
12-24-28-21W4, 1875.1 m.

c) Preservation of highly organic-rich dolomudstone laminae results in a near black appearance of the entire core photograph. Laminae are inclined and a microfault (mf) offsets laminae by approximately 2 mm. A total organic carbon content of 3.5% was obtained from this sample – see discussion in text.
8-26-28-20W4, 2263 m.

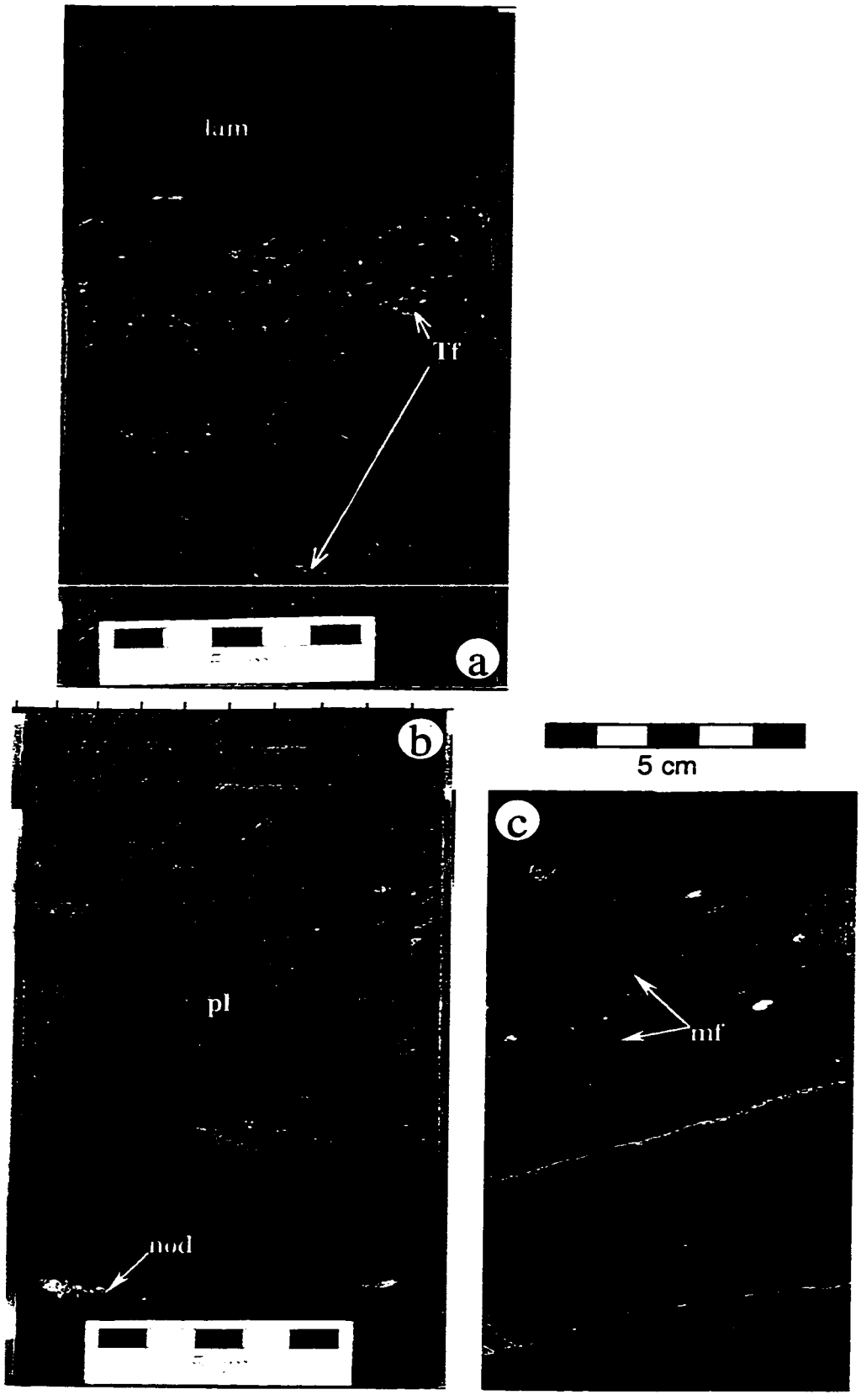
lam
Tf
a
b
pl
nod
5 cm
c
mf

fairweather wave base (Pemberton et al., 1992). The next most common traces are *Phycosiphon isp.*, part of the ambiguous *Zoophycos* ichnofacies with an extremely broad paleobathymetric range (Pemberton et al., 1992). The *Zoophycos* animal was tolerant of variations in water depth, substrate type, food source, energy and oxygen level, and could survive in *Cruziana* through to *Nereites* ichnofacies (Pemberton et al., 1992). Based on the abundance of associated *Chondrites isp.* traces, it seems reasonable to assume that *Phycosiphon isp.* survived in the *Cruziana* ichnofacies. The waviness of the laminae may be due to storm current modification, infaunal disruption, or a combination of both.

The "common denominator" of the *Zoophycos* ichnofacies is a stressed, quiet water setting exhibiting lowered oxygen levels (Pemberton et al., 1992). The preservation of slightly wavy organic-rich laminae and absence of fossils further indicates that bottom-water anoxia was periodically present during the deposition of Lithofacies O. Pemberton et al. (1992) believe the *Zoophycos*-related anoxia to be associated with an abundance of organic material. It is not clear whether the authors mean that the high content of organic material itself caused anoxia or if algal blooms fed on the organic material and subsequently used up all of the available oxygen.

It is interpreted that Lithofacies O was deposited in a quiet water subtidal setting, at or near storm wave base, which experienced periods of bottom-water anoxia.

Lithofacies P: PLANAR LAMINATED DOLOMUDSTONE (Figure 3.13b and 3.13c)

Description:

Repetitious banding of planar black and light brown laminae characterize Lithofacies P. The laminated dolomudstone is present in the lower portion of the channel fill with a maximum thickness of 1.8 m.

High concentrations of organic matter define the planar laminae. Total organic carbon content ranges between 0.75% and 3.56% within selected samples of Lithofacies P (Table 3.1). The flat (Figure 3.13b) to inclined (Figure 3.13c) laminae generally parallel one another across the core, except where slightly scoured or offset by microfaults by a few millimetres (Figure 3.13c). Disturbance of the layers by infaunal activity is not

WELL LOCATION	SAMPLE DEPTH	TOC %
08-26-028-20W4	2256.5 m	0.75
08-26-028-20W4	2257 m	1.48
08-26-028-20W4	2263 m	3.56
08-26-028-20W4	2263.3m	1.72
08-26-028-20W4	2263.4 m	2.25
12-24-028-21W4	1875.1 m	1.22
12-24-028-21W4	1877 m	0.83

Table 3.1 Total organic carbon contents reported as weight percentages of rock samples obtained from two Nisku 3 channel wells. All samples are from Lithofacies P.

evident nor are any fossils present within the lithofacies. Minor disruption of laminae is due to small anhydrite nodules, less than 10 mm in diameter, which commonly displace the laminae (Figure 3.13b).

In thin section, the cloudy dolomite crystals fine upwards in size within individual layers. The crystals are interlocking and have a mean length of 50 μm. Rather than being evenly dispersed throughout the matrix, black organic matter concentrates between the dolomite crystals along specific laminations. The result is a very rhythmic pattern of banding.

Interpretation:

With respect to energy conditions at the time of deposition, the thin, generally undisturbed planar laminae indicate that low energy sediment fall-out from suspension was the dominant form of deposition. A subtidal environment below storm wave base is a likely explanation for the planar laminae. Furthermore, the association with other interpreted deeper-water channel lithofacies supports a subtidal interpretation. Contemporaneous soft-sediment deformation, which can be a characteristic of deep-water carbonate slope environments (Cook and Mullins, 1983), was likely responsible for the microfaulting and local inclination of laminae.

The planar laminae and lack of preserved traces indicate that environmental conditions were not suitable for burrowing organisms to live in. Any significant infaunal activity would have churned the sediment and removed most, if not all, traces of laminae. Even if only one tolerant species of burrower had been present, the laminae would likely have been somewhat disturbed, such as in Lithofacies O.

The high total organic carbon content of Lithofacies P may shed some light on the kinds of stresses affecting the local depositional environment. Depositional processes that influence the accumulation of organic carbon are: (a) sedimentation rates, (b) bottom-water anoxia independent of organic productivity, and (c) high primary productivity (Chow et al., 1995).

(a) An anomalously high sedimentation rate burying the organic matter before it can be completely oxidized is an unlikely explanation for the high organic carbon content of

Lithofacies P. The rhythmic alternation of organic-rich laminae does not support the possibility of periodic high volume influxes of sediment quickly burying the organic matter.

(b) Bottom-water anoxia through density stratification is produced by the thermocline or the halocline and results in preservation of organic matter within underlying fine-grained sediment because of restricted scavenging and bioturbation (Chow et al., 1995). Within the Devonian of the Western Canada Sedimentary Basin it is commonly believed that organic-rich facies developed in deep (e.g. water depths greater than 100 m for the Duvernay Formation), anoxic basins (Stoakes and Creaney, 1984, 1985). Lithofacies P is 12 m below the Nisku 1 and 3 contact in the 12-24-28-21W4 well. Even taking into account differential compaction, the channel water depth would have been no where near that of typical Devonian basins with bottom-water anoxia. There is no evidence to support the development of a sluggish thermocline at the time of deposition. Proof for the presence of salinity stratification is also lacking considering the absence of primary sulphate or halite layers within Lithofacies P or any of the other Nisku 3 sub-unit lithofacies. The early displacive anhydrite nodules within Lithofacies P are the only signs of increased salinity.

(c) High organic production in surface waters is considered to be the dominant mechanism for organic matter accumulation in modern and ancient seas (Pederson and Calvert, 1990). In such a model nutrient influx to the photic zone increases the production of planktonic organisms (algal blooms) and results in a greater amount of organic matter to fall to the seabed (Chow et al., 1995). Chow et al. (1995) also postulate that aerobic bacterial degradation of the settling organic material uses up the available oxygen and creates a midwater oxygen minimum zone below which anoxic bottom waters reside. Pederson and Calvert (1990) do not, however, believe conditions of oxygen minima enhance preservation of organic matter; instead the cause of organic-rich sediments is predominantly high primary production. In the Lower Keg River Member, Chow et al. (1995) interpret algal blooms to have taken place in water depths as little as 20 m.

Organic petrology was not performed on Lithofacies P to either confirm or discount the presence of "bloom" organic facies. However, indirect support for the high organic production mechanism exists: (i) The water depth of the Nisku 3 sub-unit channel is shallow, (ii) The presence of *Phycosiphon isp.* burrow traces in Lithofacies O are interpreted to indicate anoxic conditions related to increased organic matter. Lithofacies P is texturally similar to Lithofacies O but with an even higher concentration of organic carbon, and (iii) The megalodont bivalves of Lithofacies H preferentially inhabit a narrow band along the channel margin. The large clams throve in conditions of high nutrient influx and increased algal presence (Eliuk, 1998) and may be an indicator of such conditions within the channel itself. The organic matter was presumably oxidized and therefore not preserved in the shallower environment of Lithofacies H versus the deeper water, likely anoxic setting of Lithofacies P.

It is interpreted that Lithofacies P was deposited subtidally, below storm wave base, in an anoxic setting that allowed for the preservation of organic-rich laminae. Anoxia was likely not independent of primary productivity of organic matter. Algal blooms responding to periodically high levels of nutrient influx were the probable source of the organic carbon in Lithofacies P, as well as the cause of bottom-water anoxia, which preserved the organic matter.

3.5 FACIES SUCCESSIONS AND CYCLES

Lithofacies of the Nisku Formation in the Wayne area are grouped into three distinct facies associations that are interpreted as having formed in three depositional settings:
Nisku 1 sub-unit – a shallow evaporitic salina to marginal salina.
Nisku 2 sub-unit – a relatively shallow subtidal to peritidal carbonate platform.
Nisku 3 sub-unit – a deep subtidal carbonate channel.

Within each of the facies associations vertical facies successions can be recognized. Facies successions may be interpreted as cycles (James, 1979) or parasequences (Van Wagoner et al., 1988), however, in the Wayne area it is difficult to correlate individual facies successions from well to well. The main hindrances to lateral tracing of facies

successions are: (1) the difficulty in recognizing cycle contacts between successions in subtidal areas, particularly the identification of flooding surfaces, (2) the severe diagenetic overprint over many facies, and (3) the possibility that the successions do not correlate even over distances of a few kilometres.

This section provides a description of the stacking characteristics of the lithofacies of the Nisku Formation, their interpretation as cycles, and stratigraphic continuity of cycles. Facies successions and cycles in the Nisku 1 sub-unit are not discussed due to the limited data.

Nisku 2 sub-unit:

Based on lithofacies characteristics, the Nisku 2 sub-unit can be informally divided into two separate portions within the study area: (a) the lower Nisku 2 sub-unit, comprised of Lithofacies I, J, K, and L (mainly open-marine, subtidal lithofacies), and (b) the upper Nisku 2 sub-unit, comprised of Lithofacies F, G, H, I, and J (restricted shallow subtidal and tidal-flat lithofacies). The Nisku 2 sub-unit is the most fossiliferous unit of the Nisku Formation in the Wayne area, therefore, faunal variation is used to distinguish successions within the unit. Variations in fauna were caused by changes in energy levels and relative water depths (see facies interpretations, above). Hence, a faunal-based facies succession can be used here to record progressive changes in water depths in a specific vertical direction.

(a) The lower Nisku 2 sub-unit is dominated by Lithofacies K (*Thamnopora* floatstones and rudstones) and L (coarse-crystalline dolostones). Lithofacies I (*Amphipora* dolofloatstone) and J (massive dolomudstone) are subordinate. As previously discussed, all of these lithofacies were deposited subtidally under low to high-energy conditions. The lower Nisku 2 sub-unit was thus deposited in a subtidal platform environment of low to high energy and generally open marine circulation conducive to the growth of fauna, particularly thamnoporoid corals.

An idealized shallowing-upward facies succession consists, from base to top, of: (a) Lithofacies K (*Thamnopora* dolofloatstone), (b) a combination of Lithofacies I (*Amphipora* dolofloatstone) and Lithofacies J (massive dolomudstone), and (c) Lithofacies

L (coarse-crystalline dolostone). Grain-dominated Lithofacies L likely capped the shallowing-upward successions due to the raising of the sediment-water interface to a position above the fair-weather wave base as sedimentation filled accommodation space. The facies successions of the lower Nisku 2 sub-unit may reach up to 5 m in thickness. Flooding, in response to an increase in accommodation, perhaps as a consequence of a relative rise in sea level, lead to the deposition of the next facies succession.

(b) Similar to the lower Nisku 2 sub-unit, upper Nisku 2 sub-unit shallowing-upward successions are dominated by subtidal lithofacies, Lithofacies H, I, and J (megalodont dolofloatstone, *Amphipora* dolofloatstone, and massive dolomudstone); however, tidal-flat lithofacies, Lithofacies F and G (fenestral laminated dolomudstone and mottled gastropod dolowackestone) commonly cap the successions. The upper Nisku 2 sub-unit lithofacies were deposited in mud-rich shallow subtidal to peritidal settings of predominantly low energy. Environmental stresses, including increased temperature, salinity and/or nutrient influx, caused restrictions in the faunal diversity. A restricted *Amphipora*-rich lagoonal environment dominated, with gastropod tidal-flats and megalodont banks present to a lesser degree.

Shallowing-upward successions can be recognized where relatively deeper-water lithofacies are overlying shallow-water lithofacies. An idealized shallowing-upward succession of upper Nisku 2 sub-unit lithofacies (Figure 3.14) consists of, from base to top: (a) a combination of Lithofacies I (*Amphipora* dolofloatstone) and Lithofacies J (massive dolomudstone), (b) Lithofacies H (megalodont dolofloatstone) (c), Lithofacies G (mottled gastropod dolowackestone), and (d) Lithofacies F (fenestral laminated dolomudstone). However, the proportions of different lithofacies within shallowing-upward successions vary according to geographic position within the study area.

In the area of the Wayne 'A' pool, where the highest concentration of upper Nisku 2 sub-unit cores exist, three types of shallowing-upward successions are distinguished: (i) I-J-G successions, (ii) G-F successions, and (iii) H-G successions (Figure 3.14). Each is discussed further:

UPPER NISKU 2 SUB-UNIT FACIES SUCCESSIONS

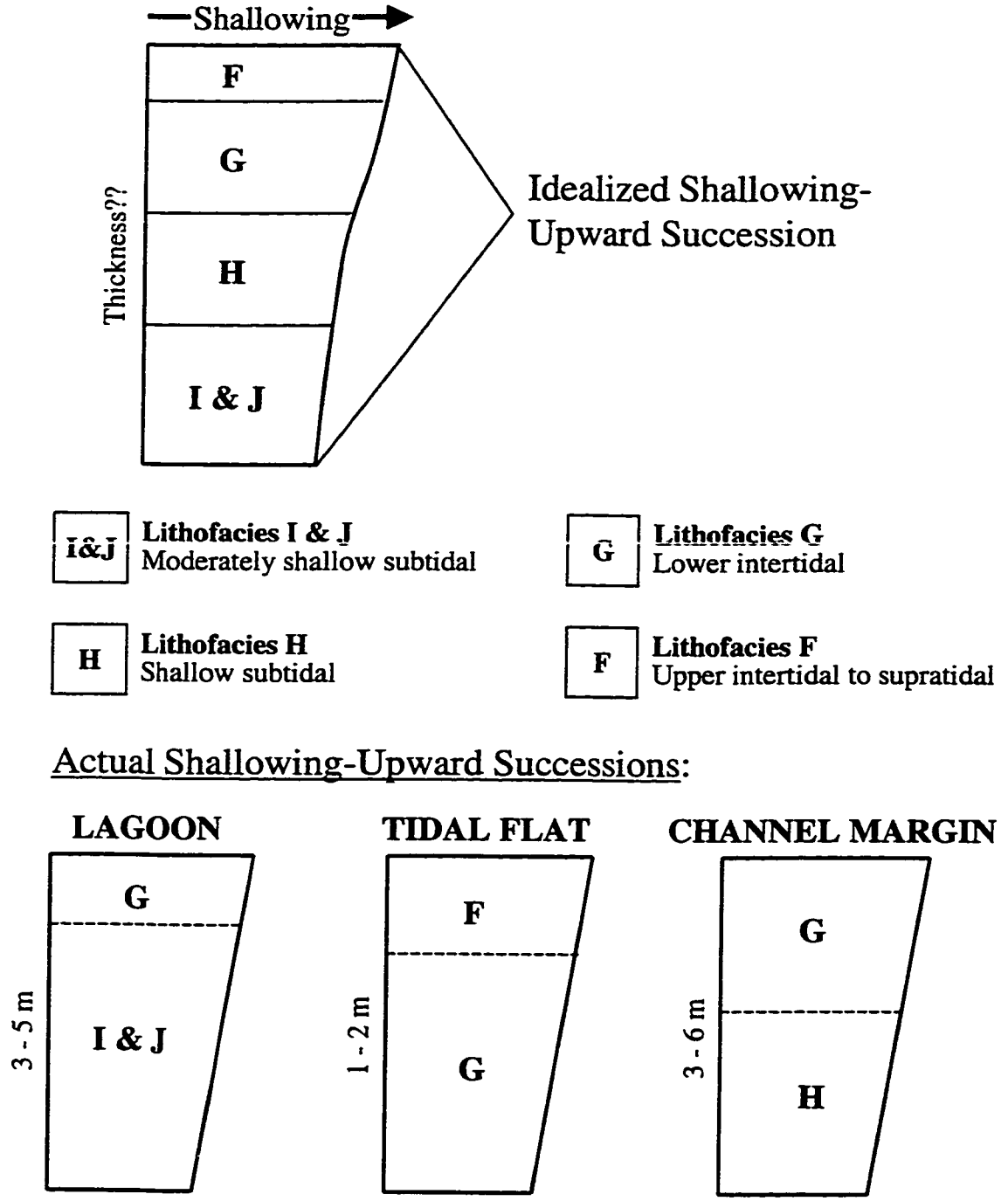

Figure 3.14: Schematic of development of upper Nisku 2 sub-unit facies successions. The idealized succession represents the composite shallowing-upward succession of upper Nisku 2 sub-unit lithofacies. The three successions at the bottom represent the actual lithofacies successions based on their paleodepositional positions within the study area.

(i) I-J-G successions: The base of an I-J-G succession is comprised of a thick interval of subtidal Lithofacies I (*Amphipora* dolofloatstone) and J (massive dolomudstone), and is commonly overlain by a much thinner interval of lower intertidal Lithofacies G (mottled gastropod dolowackestone). I-J-G successions, which range between 3 and 5 m in thickness, are relatively widespread throughout the Wayne area. The I-J-G successions are interpreted as lagoonal because of their dominance by subtidal lithofacies, their high proportion of *Amphipora*, and their presence adjacent to tidal flats. Lagoonal I-J-G successions are stacked vertically and therefore can be termed cycles.

(ii) G-F successions: The basal portion of a G-F succession is occupied by the lower intertidal Lithofacies G (mottled gastropod dolowackestone), which grades upward into thin intervals of the capping upper intertidal to supratidal Lithofacies F (fenestral laminated dolomudstone). G-F successions are laterally isolated from one another by lagoon and/or channel margin successions. Ranging between 1 and 3 m in thickness, the thin tidal flat successions had less accommodation space than their mainly subtidal counterparts. G-F cycles were primarily deposited above low mean tide level, likely due to the accumulation of sediment washed in from subtidal areas. G-F successions tend to repeatedly build upon one another, therefore they are cyclic.

(iii) H-G successions: H-G successions are generally comprised of subtidal Lithofacies H (megalodont dolofloatstone) in the basal portions and lower intertidal Lithofacies G (mottled gastropod dolowackestone) in the upper portions. Successions range between 3 and 6 m in thickness and are present adjacent to the Nisku 3 sub-unit channel. Megalodonts and gastropods were the dominant fauna due to their tolerance of higher salinity, increased nutrient influx, and/or turbid waters associated with the Nisku 3 sub-unit channel.

Discussion:

It has been established that peritidal cycles are commonly laterally discontinuous (Pratt and James, 1986; Adams and Grotzinger, 1996). The discontinuity is explained by the tidal island facies model where scattered tidal flat islands and intertidal banks are separated by contemporaneous subtidal areas (Pratt and James, 1986). In the model,

simple vertical accretion takes place on islands stable in their position until the depositional surface reaches the supratidal zone, whereby lateral progradation of the islands then occurs. Pratt and James (1986) argue that hydrographic forces cause the focus of sedimentation to constantly shift, resulting in a discontinuous facies mosaic.

The idea of vertically accreting peritidal facies on stable islands (with slight lateral progradation) explains the nature of the tidal flat cycles observed in the Wayne area. However, the constant shifting of tidal island positions across the shelf, resulting in a discontinuous facies mosaic, does not correspond to the observed tidal flat cycle stacking at Wayne. In the Wayne area, tidal flat cycles tend to stack on top of one another at specific locations, similar to the stacking of lagoon cycles and of channel margin cycles in specific areas. No evidence for shifting locations of tidal flat deposition has been observed in the study area. Such stacking patterns are interpreted to be the result of local subsidence (see Chapter 5). Therefore, it is interpreted that isolated tidal flat islands experienced vertical accretion yet limited lateral progradation, and maintained their positions in the Wayne area during deposition of the upper Nisku 2 sub-unit, a result of autocyclic mechanisms. Stratigraphic continuity between tidal flat islands likely exists, however, recognition of the continuity is not straightforward.

A general schematic of upper Nisku 2 sub-unit two-dimensional facies relationships in the Wayne Nisku 'A' pool is presented in Figure 3.15. The upper Nisku 2 sub-unit depositional model for the entire Wayne area, in the form of a block diagram of the three-dimensional facies relationships, is presented in Figure 3.16. The main elements include: (i) the deep subtidal Nisku 3 sub-unit channel deposits laterally adjacent to the relatively shallow upper Nisku 2 sub-unit deposits, (ii) the megalodont-rich shallow subtidal bank deposits present, but not continuous along the channel, (iii) the isolated tidal flat islands, and (iv) the extensive subtidal lagoon deposits across the study area.

Nisku 3 sub-unit:

The Nisku 3 sub-unit is an accumulation of mainly low energy, deep subtidal channel deposits. Periodic anoxia contributed to the stressed channel environment of which there is basically no fauna present. Three cores penetrate the Nisku 3 sub-unit and none contain

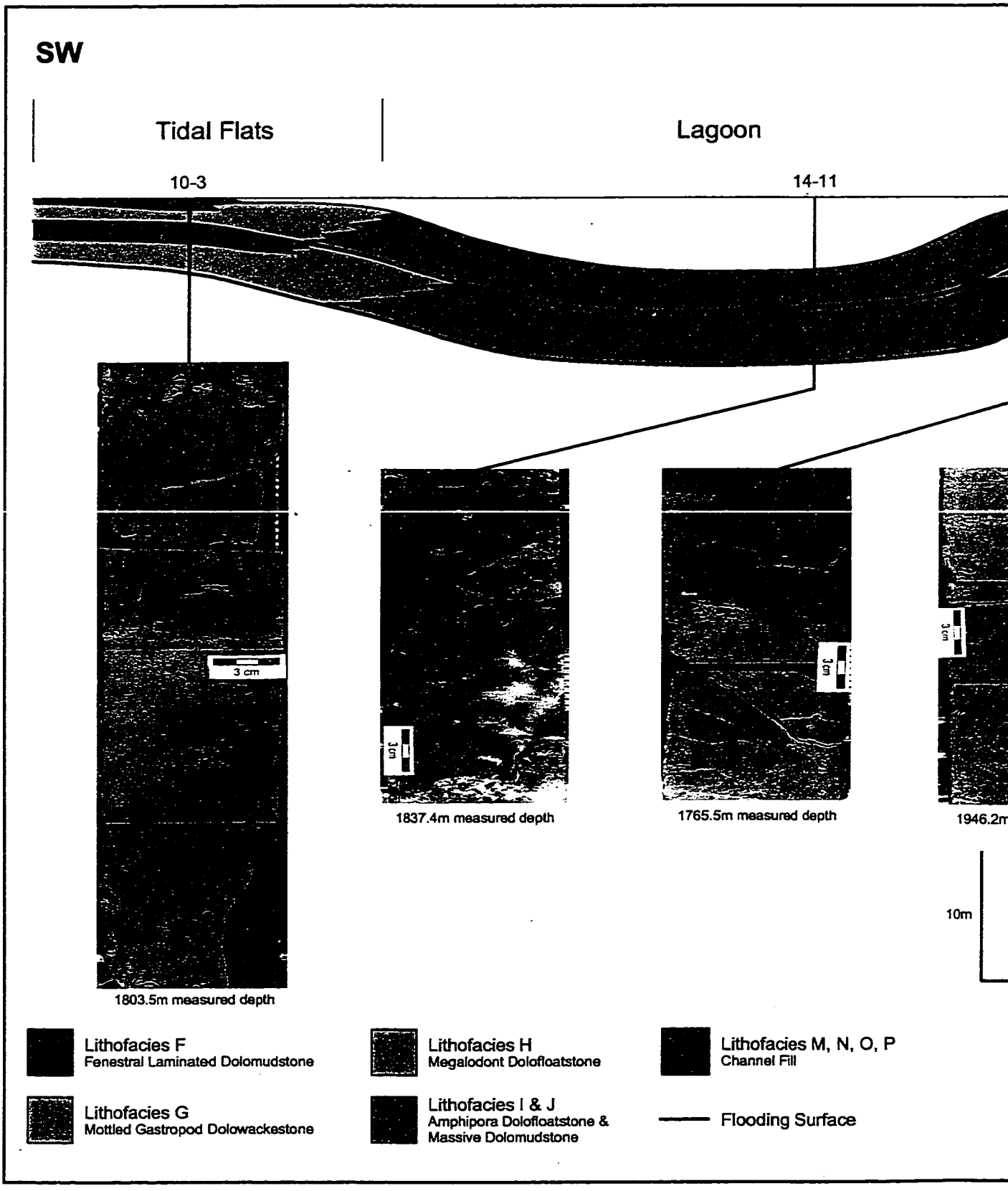
SW
Tidal Flats
Lagoon
10-3
14-11
3 cm
3cm
3cm
3cm
1803.5m measured depth
1837.4m measured depth
1765.5m measured depth
1946.2m
10m
Lithofacies F
Fenestral Laminated Dolomudstone
Lithofacies G
Mottled Gastropod Dolowackestone
Lithofacies H
Megalodont Dolofloatstone
Lithofacies I & J
Amphipora Dolofloatstone &
Massive Dolomudstone
Lithofacies M, N, O, P
Channel Fill
Flooding Surface

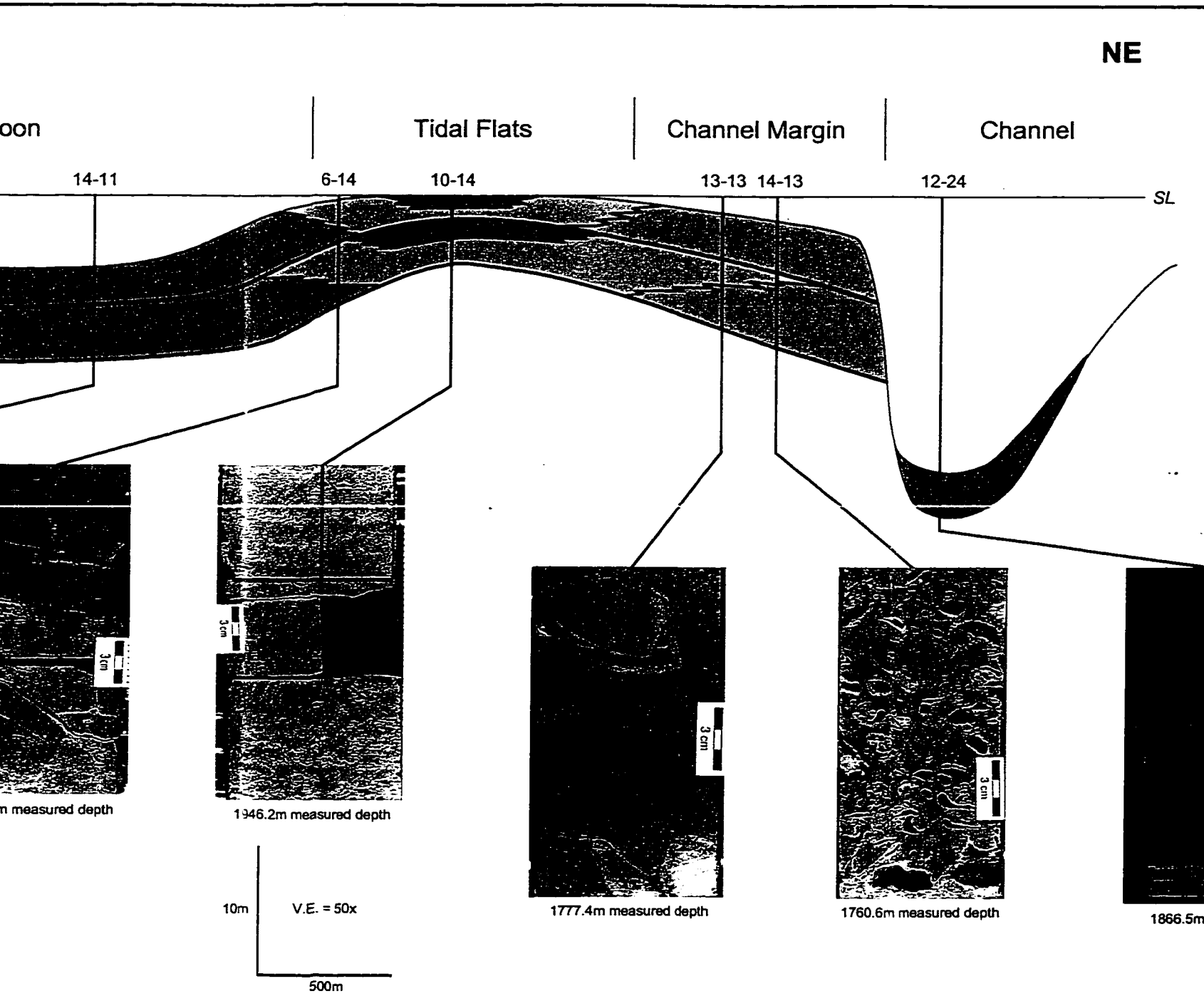

Lithofacies M, N, O, P
Channel Fill

Flooding Surface

Upper Nisku 2 & 3 Depositional Facies

Figure 3.15 Two-dimensio
relationships o
and 3 sub-units
'A' pool,with re
photographs.

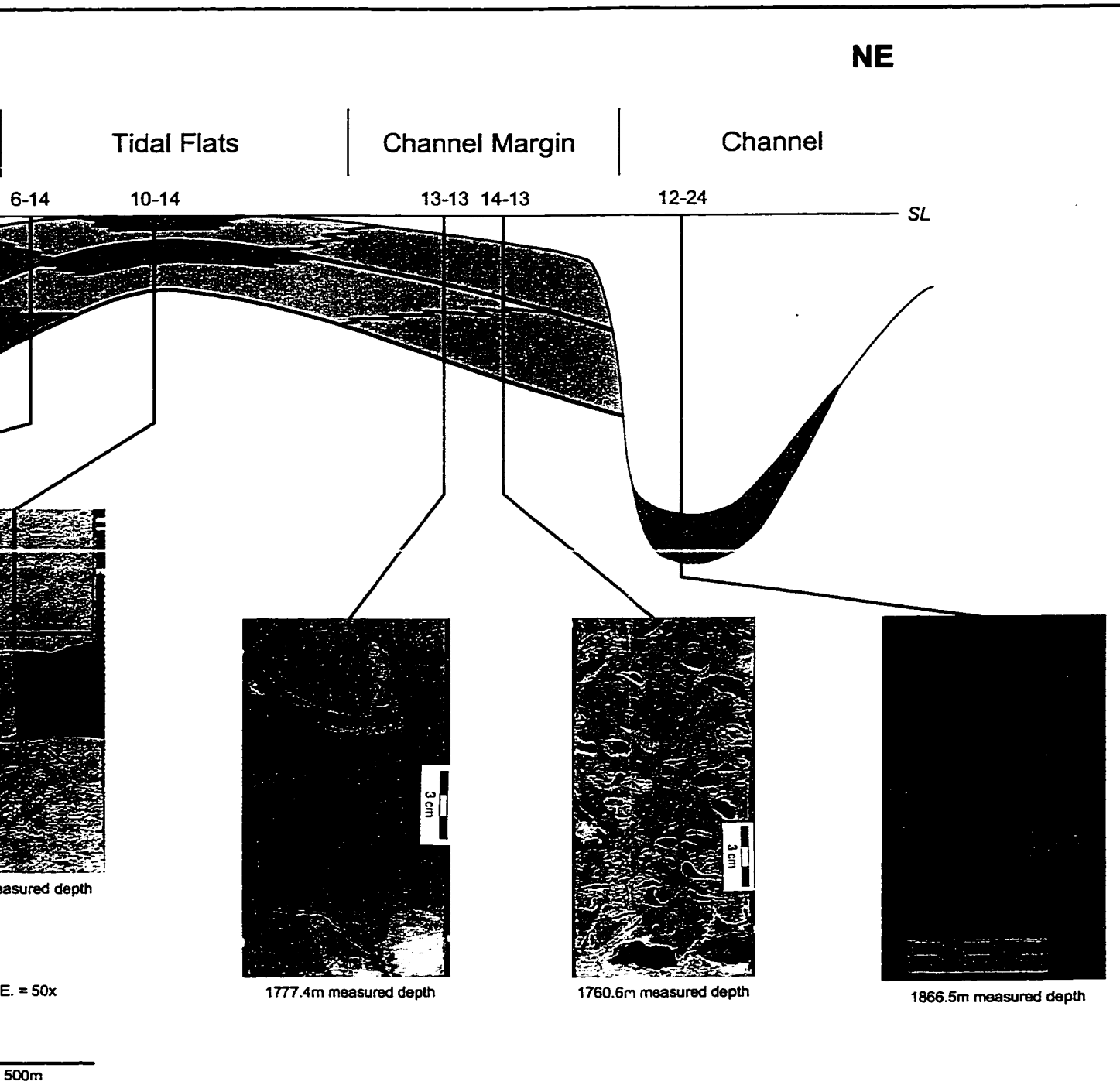

Upper Nisku 2 & 3 Depositional Facies

Figure 3.15 Two-dimensional facies relationships of the upper Nisku 2 and 3 sub-units across the Wayne 'A' pool,with representative core photographs.

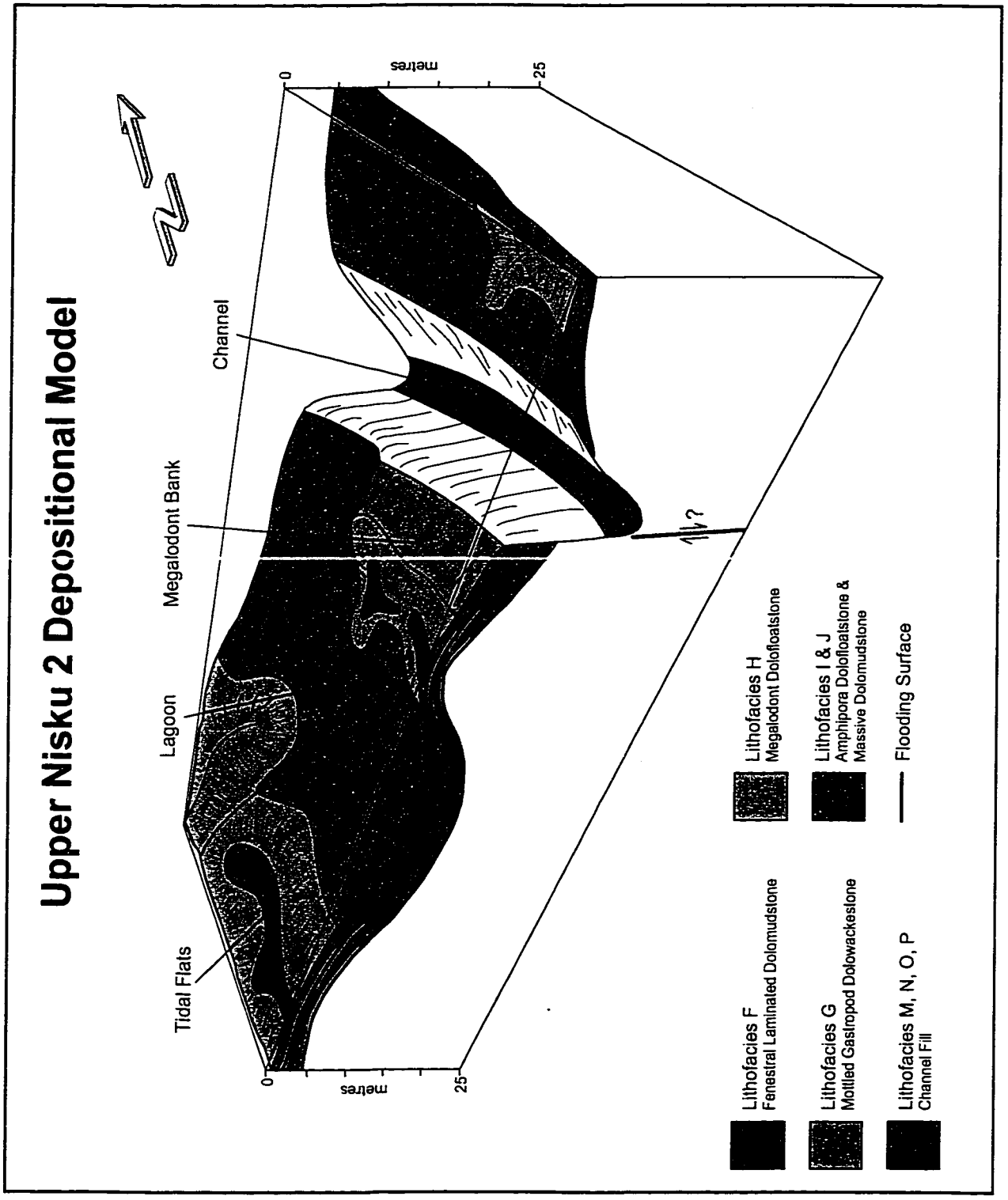

Figure 3.16 Block diagram of upper Nisku 2 and 3 facies distribution within the Wayne area. Vertical scale bars represent approximate water depths at the time of deposition.

the entire Nisku 3 sub-unit interval. Lithofacies N (dark mottled dolomudstone) dominates the lower Nisku 3 sub-unit; also present but to a much lesser degree, and commonly over single, thin intervals in each well, are Lithofacies O (bioturbated laminated dolomudstone) and P (planar laminated dolomudstone). Separated from the lower Nisku 3 sub-unit by a sharp erosional surface, the upper Nisku 3 sub-unit is comprised only of Lithofacies M (fining-upward dolopackstone to dolowackestone).

An idealized shallowing-upward succession in the lower Nisku 3 sub-unit is comprised of Lithofacies P at its base, Lithofacies O in the middle, and Lithofacies N capping the succession. Realistically, however, Lithofacies P and O do not contribute to the facies succession. With only one lithofacies dominant and only two cores penetrating the lower Nisku 3 sub-unit, cycles cannot be recognized.

Recognition of facies successions in the upper Nisku 3 sub-unit is not possible based on the presence of only one lithofacies. Therefore, upper Nisku 3 sub-unit cycles are not apparent.

3.6 DISCUSSION OF REGIONAL PALEOGEOGRAPHY

It has been established in the literature (e.g. Gilhooly et al., 1994; Whittaker and Mountjoy, 1996) that regional depositional dip of the Nisku platform in southern and central Alberta was towards the Winterburn Basin to the northwest (Figure 2.5). Within the platform, sub-basins such as the Ghost Pine also influenced local depositional orientations (Figure 2.5). The highly organic laminites of the Ghost Pine sub-basin are considered to be deposited at a transition between the Ireton Formation and the evaporites of the upper Nisku Formation (Hearn, 1996). These organic-rich laminites display a striking resemblance to those of Lithofacies P in the Wayne area. Considering the NW orientation of the Nisku 3 sub-unit channel (Figure 2.3), it is proposed that the channel was connected with the Ghost Pine sub-basin and was filled contemporaneously. It is thus interpreted that the Nisku 3 sub-unit channel was a localized depositional sub-basin during deposition of the laterally adjacent Nisku 2 sub-unit.

Interpretations of the depositional environments and their associated deposits within the southern Alberta Nisku platform vary among workers and locations of study (e.g. Gilhooly, 1987; Slingsby and Aukes, 1989; Hunter, 1995; Kissling, 1996; Whittaker and Mountjoy, 1996). A brief summary of published interpretations is provided:

The southernmost region of the Nisku platform in Alberta is comprised of muddy to grainy sediments with limited fauna, deposited in a combination of mixed tidal flat sabkhas and restricted hypersaline lagoon environments (Kissling, 1996). The cause of restriction was a NE-SW trending barrier-like carbonate sand bank to the north and NW of the tidal flat/lagoon (Kissling, 1996). Northward of the arcuate-shaped barrier the depositional environment was either shallow restricted marine with sparse fauna (Whittaker and Mountjoy, 1996) or marine with tabular stromatoporoids, tabulate corals, *Amphipora*, and numerous other faunal types (Kissling, 1996). To the south of the Ghost Pine sub-basin, and atop the Leduc Formation shelf boundary, exists the Swalwell area where Hunter (1995) interprets the Nisku Formation to be deposited in a platform edge barrier reef setting. Tabular stromatoporoids and tabulate corals, along with bulbous stromatoporoids in a skeletal wackestone to grainstone matrix comprise the lower portion; a shoal of fenestral mudstone with leached brachiopods overlain by laminated evaporites and dolomudstones comprise the upper portion of the Nisku "reef" at Swalwell (Hunter, 1995). In the Bashaw area, Gilhooly (1987) interprets the Nisku Formation to consist of deep carbonate ramp coral-crinoid deposits, ramp-platform transition tabular stromatoporoid and coral buildups, platform interior "lagoonal" *Amphipora* floatstones, and restricted platform interior shallow water to peritidal carbonates and evaporites with low faunal diversities.

The Nisku Formation in the Wayne area has some distinct depositional characteristics in comparison to other areas: (i) Dolomudstone dominates the matrices of most lithofacies in the Wayne area, implying that low energy conditions were the norm at the time of deposition. Allochem-supported lithofacies are rare, and even where present, they commonly contain dolomudstone matrices. In contrast, packstones and grainstones deposited under high energy conditions are common to many other study areas (e.g. Southern Alberta – Kissling, 1996; Swalwell – Hunter, 1995). Apparently, low energy

conditions and mud domination were anomalously prevalent during deposition at Wayne. (ii) The low diversity of fauna present in the Wayne area indicates restricted environmental conditions were present at the time of deposition. The open marine tabular stromatoporoids common to other study areas are conspicuously absent at Wayne whereas the megalodont bivalve is common in the Wayne area. Apparently, unusual stresses affected faunal development at Wayne. (iii) A narrow but deep water channel was present through most of Nisku platform deposition in the Wayne area. Deposits in the Nisku 3 sub-unit channel have distinctly high total organic carbon contents. No other southern Alberta studies report the presence of deep water, anoxic channel deposits.

Apart from identifying the Nisku Formation as a single regressive, shallowing-upward succession, most workers on the Nisku Formation in southern Alberta do not distinguish smaller scale cycles or correlate between them. One exception is Slingsby and Aukes (1989) who recognize that in the Enchant area, three informal members of the Nisku Formation are comprised of one or more shallowing-upward cycles. Another exception is Gilhooly (1987) who identifies 2 to 8 m thick, small scale shallowing-upward platform interior cycles within the Nisku Formation in the Bashaw area. Fossiliferous cycles range from subtidal *Amphipora* floatstones at the bases to peritidal laminites at the tops. Restricted, non-fossiliferous cycles are comprised of massive subtidal carbonates and laminated peritidal carbonates and evaporites. Gilhooly (1987) concludes that correlation of platform interior cycles is impossible at Bashaw. He attributes the problem to a complex system of shifting depositional highs and lows resulting in a complex mosaic of facies patterns.

There are limitations to the sedimentologic interpretations in the present study. Preferential zones of core penetration and sporadic distribution of cored wells have contributed to a bias towards the upper Nisku 2 sub-unit in the Wayne 'A' and 'B' pools. The greatest limitation on study of the Nisku Formation sedimentology, however, is the severe diagenetic overprint. Original depositional textures have been masked by dolomitization, cavity formation, anhydritization, and fracturing. Clearly, a key to

understanding the Nisku Formation in the Wayne area is to unravel the diagenetic events that have concealed the depositional facies.

3.7 SUMMARY

Sixteen carbonate and evaporite lithofacies are present within the Nisku Formation in the Wayne area. Lithofacies are distinguished based on colour, lithology, physical structure and faunal composition.

Lithofacies A, B, C, D, and E are associated with the hypersaline depositional environment of the Nisku 1 sub-unit. Lithofacies A is a laminated dolomudstone and anhydrite deposited in a salina environment. Lithofacies B was deposited in a shallow subtidal to lower intertidal setting as cryptalgal laminites. The nodular anhydrites of Lithofacies C are diagenetic in origin. Lithofacies D is a poorly sorted dolopackstone deposited by high energy currents in a subtidal setting over the Nisku 3 sub-unit channel. Lithofacies E is a laminated dolograinstone deposited in a high energy upper subtidal to lower intertidal environment.

Lithofacies F through L represent restricted peritidal to open marine subtidal deposits of the Nisku 2 sub-unit. The deposits of the shallowest setting are the fenestral laminated dolomudstones of Lithofacies F. Lithofacies G is a mottled gastropod dolowackestone deposited in a lower intertidal environment. Megalodont bivalves comprise the bulk of the restricted, shallow subtidally deposited Lithofacies H. Lithofacies I and J are both moderately shallow mud-rich lagoonal deposits that contain abundant and low amounts of *Amphipora*, respectively. Lithofacies K is a more open marine deposit comprised mainly of thamnoporoid corals. Lithofacies L is a coarse-crystalline dolostone deposited in an ambiguous environment of high energy.

The Nisku 3 sub-unit channel environment is comprised of four relatively deep subtidal lithofacies. The shallowest is Lithofacies M, which consists of multiple packages of fining upward dolopackstones to dolowackestones deposited by high energy storm or debris flow events. Lithofacies N is a dark mottled dolomudstone deposited in a deep subtidal environment near storm wave base. Lithofacies O and P are both deep subtidal

laminated dolomudstones containing high total organic carbon contents. The laminae of Lithofacies O are wavy due to the disturbance of burrowing fauna, evident by traces of *Chondrites isp.* and *Phycosiphon isp.* The planar horizontal laminae of Lithofacies P display no signs of disturbance by infauna or currents, and was deposited below storm wave base.

No attempt was made to identify Nisku 1 sub-unit cycles due to the limited penetration and distribution of cores. Cycles are difficult to distinguish in the Nisku 2 sub-unit mainly due to the significant diagenetic overprint. The Nisku 2 sub-unit is divided into a lower and an upper portion. The lower portion consists of subtidal cycles of Lithofacies K to L that are up to 5 m in thickness. The upper portion contains tidal flat capped subtidal cycles that vary with paleodepositional position. Comprising tidal flat islands, cycles of Lithofacies G to F are the thinnest at no more than 2 m. Widespread lagoon cycles of mainly Lithofacies I and J capped by Lithofacies G are thicker with a 3 to 5 m range. The thickest upper Nisku 2 sub-unit cycles exist at the margin of the Nisku 3 sub-unit channel where successions of Lithofacies H to G may reach up to 6 m in thickness.

The Nisku 3 sub-unit can also be divided into a lower and an upper portion. The lower portion is dominated by the dark mottled dolomudstone of Lithofacies N. Cycles are not readily apparent due to the limited presence of Lithofacies O and P. The upper portion of the Nisku 3 sub-unit is comprised only of Lithofacies M, which does not allow for the recognition of facies successions or cycles.

Chapter 4 DIAGENESIS

4.1 INTRODUCTION

Three important aspects of Nisku Formation diagenesis for the southern Alberta area have been established: (a) dolomitization, (b) cavity formation, and (c) anhydritization (Slingsby and Aukes, 1989; Kissling, 1996; Whittaker and Mountjoy, 1996). It is generally agreed that these three processes occur during early diagenesis, however, the interpretations of timing and relationships among the products of diagenesis remain uncertain.

In this chapter the diagenetic features observed within the Wayne study area are described and interpreted. The goal is to determine the processes causing diagenesis and establish a sequence of diagenetic events through the rock-fabric relationships observed in core and thin section.

4.2 DOLOMITE

4.21 INTRODUCTION

Three main types of dolomite are present in the Nisku Formation in the study area: (1) Replacement dolomite (RD), (2) Pore-filling dolomite (PFD), and (3) Dolomite sediment (DS). Each differ in size and form of their crystals and the style and timing of their origin.

4.22 REPLACEMENT DOLOMITE (RD)

Two types of replacement dolomite exist in the study area: (A) Fine-crystalline replacement dolomite, and (B) Coarse-crystalline replacement dolomite. Both are described and discussed in detail in the following paragraphs.

(A) Fine-Crystalline Dolomite (RD1)

Designated as RD1, the dominant type of replacement dolomite is an interlocking mosaic of cloudy, irregular-shaped crystals ranging in length between 10 and 200 μm

Figure 4.1:

Photomicrograph of a fine-crystalline interlocking mosaic of cloudy dolomite crystals that have pervasively replaced the rock matrix (RD1). Megalodont fossil retains its relict texture following dolomite replacement (RDfr). Very fine-crystalline mosaic anhydrite (Am) is a common later diagenetic feature. Scale bar = 2 mm.
16-12-28-21W4, 2070.3 m.

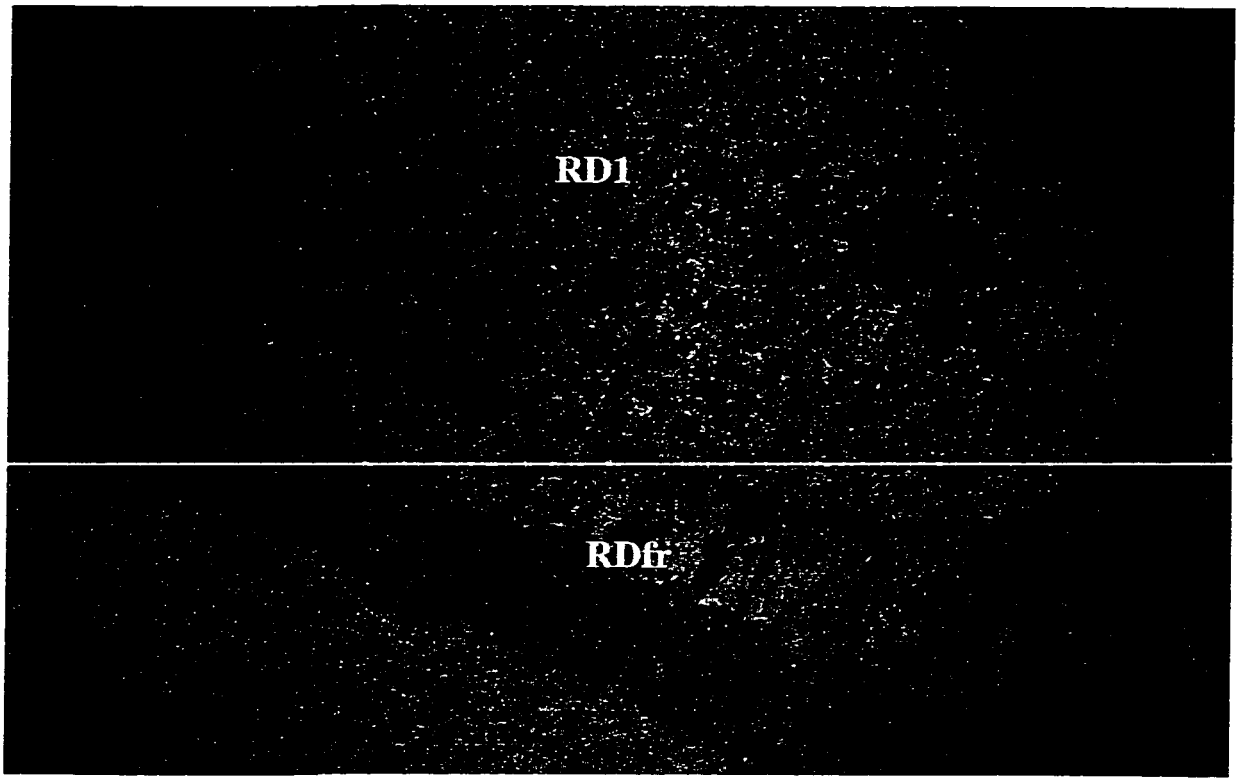
RD1
RDfr

(Figure 4.1). The mean crystal length is 60 μm, hence the classification as a fine-crystalline dolomite. Original matrix compositions and textures are not apparent because of masking by dolomite replacement. However, some fossil types within the matrices retain relict textures after dolomitization, especially megalodonts (Figure 4.1) and thamnoporoid corals, but most fauna are recognized only by their mold shapes. It is thought that the bulk of the dolomite crystals are closer to the mean length of 60 μm because of the dominance of mud as a precursor matrix. Coarse-crystalline dolomite fabrics, such as in Lithofacies L, are interpreted to be the result of replacement of coarser-grained deposits (see interpretation of Lithofacies L).

RD1 dolomite pervasively overprints all previous limestone textures to the extent that, throughout the study area, every lithofacies has been affected by the replacement phase. Hearn (1996) recognizes similar matrix replacement dolomites as abundant in the Nisku Formation of the Bashaw area.

In this study, there is no attempt to determine the origin or timing of the pervasive RD1 dolomite overprint. Most other workers on the Nisku Formation conclude that the main mechanism for the pervasive dolomitization is through seepage reflux of overlying hypersaline brines (Shields and Brady, 1995), which were likely Famennian-aged (Whittaker and Mountjoy, 1996). No results from the present study indicate an alternative mechanism.

(B) Coarse-Crystalline Dolomite (RD2)

The second type of replacement dolomite, distinguished by its coarse crystal size and stratigraphic position, is present in two forms:

(a) Designated as RD2a, the first form is an interlocking patchwork of zoned, cloudy crystals with irregular boundaries; individual crystals are coarse to very coarse and range between 0.3 and 1 mm in length (Figure 4.2). The average crystal length is 0.6 mm, therefore the classification of coarse-crystalline dolomite is given. The RD2a dolomite targets the fine-grained matrices of the host sediments and avoids the coarser-grained allochems (Figure 4.3).

Figure 4.2:

Photomicrograph of two forms of coarse-crystalline replacive RD2 dolomite. RD2a is the first form and is present in upper part of photo as a tight interlocking network of cloudy dolomite crystals (RD2a). Separated by the dashed line is the second form, RD2b dolomite (RD2b), which is the partially dissolved and corroded remnants of the RD2a dolomite. RD2b dolomite crystals are loosely packed and commonly display corrosion (corr) along both their interiors and exteriors. White patches of very fine-crystalline mosaic anhydrite (Am) fill the inter- and intracrystalline pore space. Scale bar = 1 mm. 14-23-28-21W4, 1784.8 m.

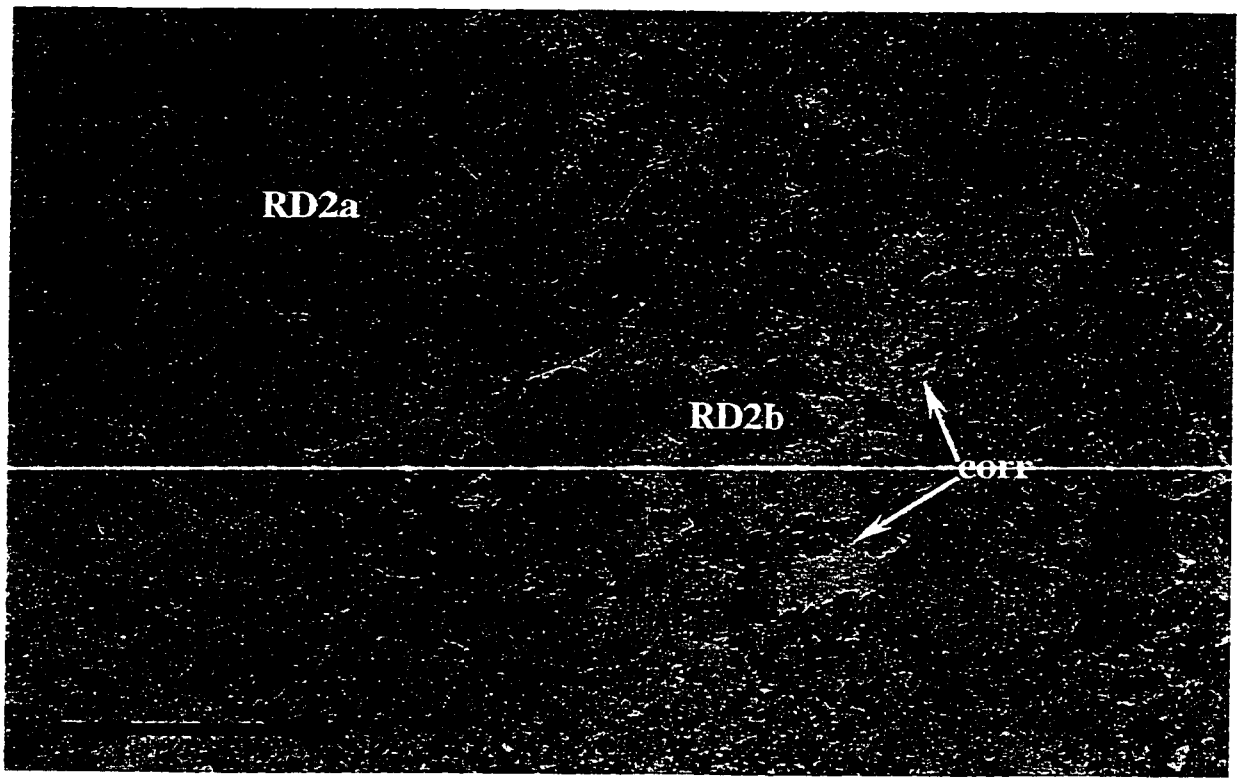
RD2a
RD2b
corr

Figure 4.3:

Core photograph of light tan coloured interlocking coarse-crystalline RD2a dolomite (RD2a) having preferentially replaced the sediment matrix. Dark brown *Amphipora* fossils (a) have been spared by the coarse-crystalline RD2a dolomite. White mosaic anhydrite (A) is common throughout as a later diagenetic phase.
6-14-28-21W4, 1758.4 m.

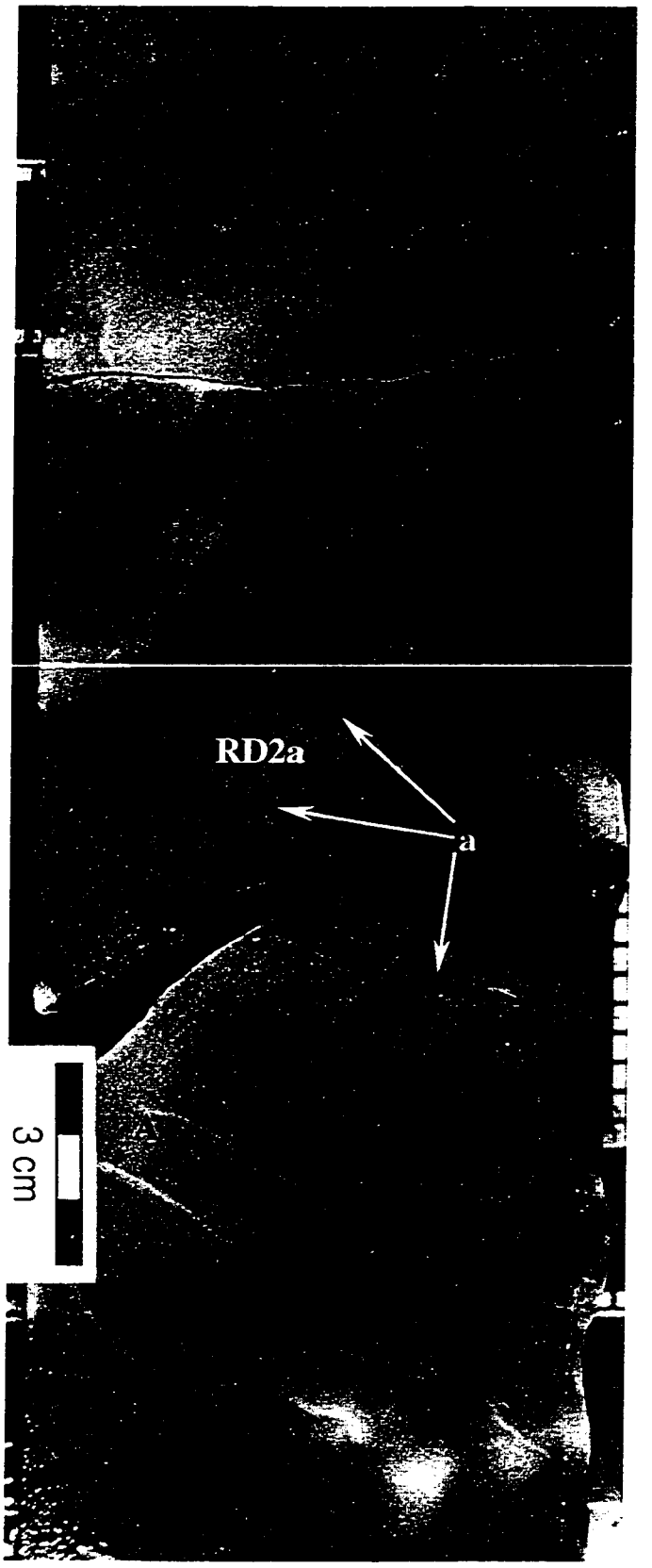
RD2a
a
3 cm

(b) Designated as RD2b, the second form is a loose framework of coarse dolomite crystals supporting one another (Figure 4.4). In thin section the crystals are cloudy, zoned, corroded along their exteriors, less commonly corroded within their interiors, and range in length between 10 μm and 1 mm (mean length of 0.5 mm) (Figure 4.5). The smaller crystals are fragments of the larger ones. Pressure solution contacts between crystals are common. Anhydrite and green clay commonly fill the abundant intercrystalline pore space.

Both forms of the coarse-crystalline RD2 dolomite are in close contact with one another. They are laterally widespread throughout the study area yet their vertical distribution is restricted to a 4 to 5 m thick horizon near the top of the Nisku 2 sub-unit, centimetres below the contact between the Nisku 1 and 2 sub-units. Together, the RD2a and RD2b dolomites comprise an interval designated as the coarse-crystalline RD2 dolomite horizon.

It is proposed that the RD2b dolomite is the corroded remnant of the interlocking RD2a dolomite. Evidence is in the fact that the crystals of both forms are cloudy, zoned, and of similar large dimensions. Furthermore, both dolomite forms can be present in the same sample with only a dissolution edge separating the two (Figure 4.2). It is then interpreted that at some time after coarse-crystalline RD2a dolomitization of the uppermost Nisku 2 sub-unit a corrosive fluid selectively attacked areas of the RD2a dolomite, resulting in patches of loose corroded RD2b dolomite.

Green clay commonly occupies the pore space between the corroded RD2b dolomite crystals (Figure 4.6). The law of crosscutting relationships makes corrosion of the dolomite crystals an earlier event than green clay infiltration. The most likely source for the green clay is the subaerial exposure surface that separates the Nisku 1 and 2 sub-units (see section 4.35). Since corrosion took place prior to green clay infiltration, corrosion likely was caused by meteoric fluids that were derived from the subaerial exposure surface. It is therefore interpreted that the original coarse-crystalline RD2a dolomitization of the uppermost Nisku 2 sub-unit took place prior to or very early in the period of subaerial

Figure 4.4:

Core photograph of a loose framework of light brown coarse-crystalline RD2b dolomite crystals (RD2b). Cloudy white anhydrite cement (Acem) occludes most of the intercrystalline pore space. Low amplitude stylolites (sty) are common in upper portion of photo.

14-23-28-21W4, 1784.8 m.

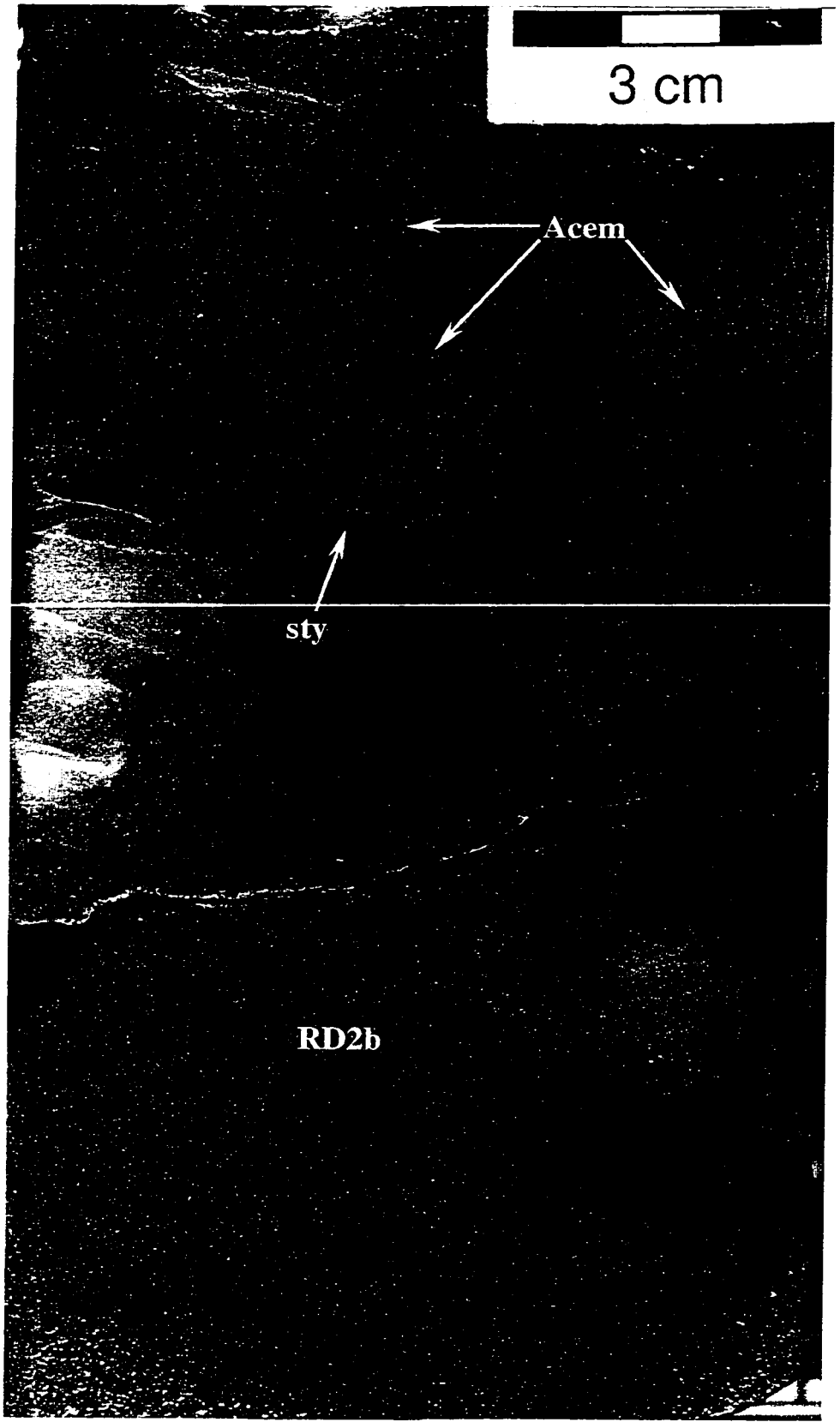
3 cm
Acem
sty
RD2b

Figure 4.5:

Photomicrograph of a loose framework of cloudy, corroded, coarse-crystalline RD2b dolomite. Pressure solution contacts (ps) are common between individual crystals. The green clay, illite (ill), is a common intercrystalline pore filler. Scale bar = 1 mm.
8-12-28-21W4, 1882.75 m.

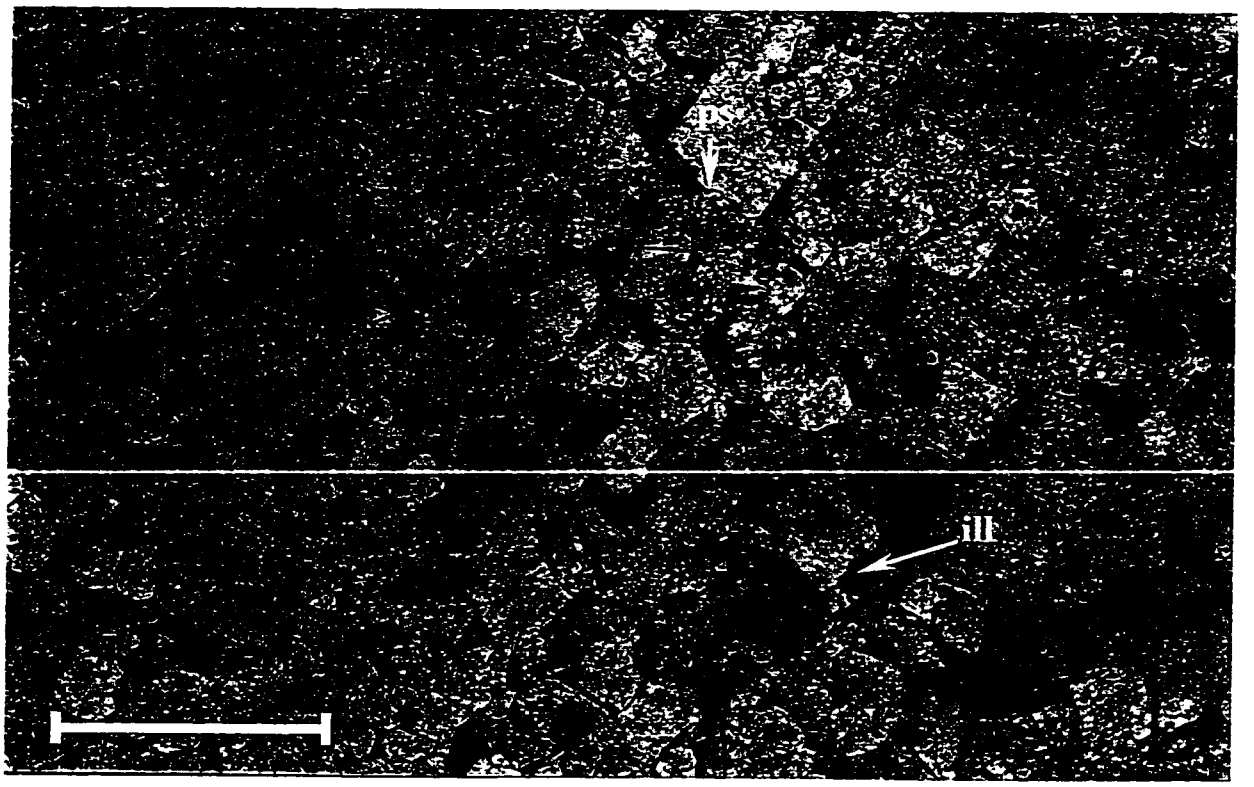
ps
ill

Figure 4.6:

Photomicrograph of corroded, coarse-crystalline RD2b dolomite (RD2b). Faint zoning (z) is apparent in larger RD2b dolomite crystals. Smaller crystals are fragments of the larger ones. Pressure solution contacts (ps) are common between dolomite crystals. Illite (ill) occupies much of the pore space between the RD2b dolomite crystals. Very fine-crystalline mosaic anhydrite (Am) is present in the upper portion of the photo. Scale bar = 1 mm.

6-14-28-21W4, 1760 m.

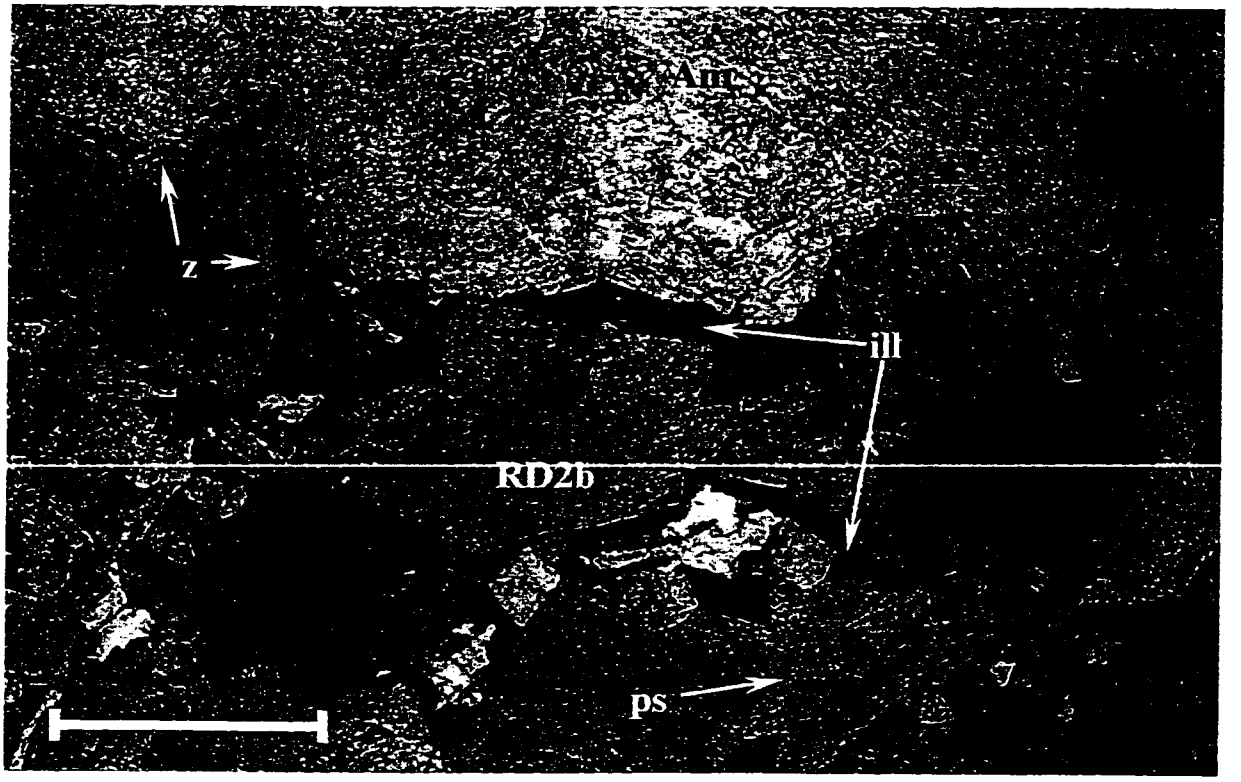
Am
z
ill
RD2b
ps

exposure between the Nisku 1 and 2 sub-units. Consequently, an early near-surface mechanism for the formation of the coarse-crystalline RD2 dolomite horizon is required.

Two current dolomitization models are considered here as possibilities for the creation of the near-surface coarse-crystalline RD2 dolomite horizon: (a) seepage reflux, and (b) mixed water. The feasibility of both models, as applied to the Wayne area, are discussed below.

(a) *Hypersaline lagoon and seepage reflux origin*

In the seepage reflux dolomitization model (Adams and Rhodes, 1960) the required source for magnesium is hypersaline lagoonal water. As the brine evaporates its density increases enough to cause seepage through the underlying deposits and reflux in a seaward direction. Sulphate precipitates from the brine resulting in high enough Mg/Ca and CO_3/Ca ratios to bring about dolomitization of the sediment.

Based on the limited fauna in the upper Nisku 2 sub-unit deposits and the dominance of anhydrite in the overlying Nisku 1 sub-unit sediments, it is not unreasonable to suggest that hypersaline lagoonal waters were prevalent in the study area near the end of Nisku 2 sub-unit deposition. As base level lowered, ultimately towards subaerial exposure, the density of the surface brine could have increased by way of evaporation to cause seepage of the dense fluid through the underlying sediment. Precipitation of sulphates would have resulted in an increased Mg/Ca ratio in the brine and caused dolomitization of the underlying lime muds. Anhydrite nodules present throughout the Nisku 2 sub-unit support this theory. The dolomitizing mechanism would have halted with the eventual subaerial exposure, resulting in the relatively thin, but aerially extensive, coarse-crystalline RD2 dolomite horizon that is now present.

Examples of near surface reflux dolomitization are common in the literature. On the island of Bonaire, Deffeyes et al. (1965) recognize a seepage reflux-related dolomite as present only in the upper part of Recent lime mud sediment. With Mg sourced from the overlying hypersaline lagoon, the modern replacement dolomite of Bonaire preferentially targets the mud matrix of the underlying sediment. Another example of near surface reflux dolomitization is described in the northern Michigan reefs. Sears and Lucia (1980)

interpret a cloudy brownish dolomite with varying crystal sizes and irregular crystal boundaries to be caused by refluxing hypersaline brines. As the result of an overlying tidal flat Mg source, the dolomite replacement is most abundant in the upper portion of the body and decreases downward.

(b) *Mixed water origin*

In the mixed water ("Dorag") dolomitization model proposed by Badiozamani (1973), within the zone of mixing between meteoric groundwater and phreatic seawater, undersaturation of the pore fluids with respect to calcite takes place. Convesely, dolomite saturation increases steadily and results in replacement of calcite by dolomite. In the model, the Mg/Ca ratio is not required to be greater than one.

Since a subaerial exposure surface is established to have been present at the end of Nisku 2 sub-unit deposition within the study area, it is entirely possible that meteoric water penetrated the sediment of the upper Nisku 2 sub-unit and came into contact with Mg-rich marine groundwater. Dolomitization could have taken place in such a mixing zone.

Various examples of interpreted mixing zone dolomitization occurring beneath subaerial exposures exist in the literature. For example, in the Abenaki Formation on the Nova Scotian shelf, Eliuk (1978) interprets that freshwater lenses developed beneath exposed paleotopographic highs. At the bases of such lenses mixing of marine and freshwater phreatic-zone waters resulted in the precipitation of thick dolomite zones. Above the Abenaki dolomite is a limestone that contains features characteristic of meteoric diagenesis. In Northern Michigan pinnacle reefs, Sears and Lucia (1980) interpret clear dolomite rhombs to have precipitated at the base of a lowered freshwater lens during emergence of the reefs. In a more local study, the Chevron Exploration Staff (1979) interpret the Nisku pinnacle reefs of the West Pembina area to have undergone mixing zone dolomitization during a major lowering of sea level and exposure at the end of Bigoray deposition.

However, there are certain characteristics of the coarse-crystalline RD2 dolomite horizon from this study that the mixed water model cannot explain: (a) First is the presence of sulphates above and below the coarse-crystalline RD2 dolomite horizon. Ancient

platforms with mixed water dolomites lack evaporites (Land, 1973). (b) Second is the horizontal geometry of the entire coarse-crystalline RD2 dolomite horizon beneath the Nisku 1 and 2 contact. Dolomite bodies created in the mixing zone display lenticular or saucer-shaped geometries (Lucia and Major, 1994). (c) Lastly, is the presence of the subaerial exposure surface directly above the coarse-crystalline RD2 dolomite horizon. Undolomitized sediments of the freshwater phreatic zone, rather than a subaerial exposure surface, should be encountered immediately above mixing zone dolomite (Lucia and Major, 1994).

It therefore appears as though shallow seepage reflux is the only feasible dolomitization model to explain the coarse-crystalline RD2 dolomite horizon. However, without isotope and fluid inclusion data a definitive dolomite mechanism cannot be chosen.

Sulphates are the final phase to significantly affect the coarse-crystalline RD2 dolomite horizon. Where illite was not present, anhydrite filled any remaining intercrystalline pore space. The anhydrite probably originated from the calcium sulphate-rich fluids that likely penetrated the Nisku 2 sub-unit from the Nisku 1 sub-unit and/or Stettler Evaporites. Based on the near total lack of porosity within the coarse-crystalline RD2 dolomite horizon, it is likely that the sulphate occluded the pore space prior to the pervasive RD1 dolomitization of the rest of the Nisku 2 sub-unit.

It is interpreted that the coarse-crystalline RD2 dolomite replacement phase formed through a near-surface seepage reflux mechanism just prior to the unconformity between the Nisku 1 and 2 sub-units. Subsequent meteoric diagenesis caused corrosion and displacement of many of the RD2a dolomite crystals, resulting in patches of corroded RD2b dolomite crystals. As green clay filtered down from the subaerial exposure surface it selectively filled the intercrystalline pore space of the RD2b dolomite. Finally, anhydrite occluded most of the remaining pore space within the coarse-crystalline RD2 dolomite horizon.

4.23 PORE-FILLING DOLOMITE (PFD)

There are two types of pore-filling dolomite in the study area: (A) Zoned dolomite, and (B) Non-zoned dolomite.

(A) Zoned Dolomite (PFD1)

Designated as PFD1, the first form of pore-filling dolomite is characterized by zoned dolomite crystals that range in length from 100 μm to over 1 mm (Figure 4.7). The interiors of the medium to coarse crystals are cloudy in comparison to the generally clearer outside rims. PFD1 dolomite crystals commonly have been corroded along their exteriors, particularly where anhydrite cement has filled in the remaining pore space. Where green muds occupy the floors of cavities as geopetals, it is common to encounter the PFD1 dolomite crystals as isopachous linings of the upper cavity chambers. Apart from lining pore walls, PFD1 dolomite may also loosely fill dissolution cavities (Figure 4.8) or be entirely supported by cavity-filling mosaic anhydrite (Figure 4.9). PFD1 dolomite crystals are also present within breccias matrices, commonly with their outermost rims mechanically separated from the original zoned crystal (Figure 4.10).

PFD1 dolomite is present within the Nisku 2 sub-unit, although it is not lithofacies specific. PFD1 dolomite is most abundant in dissolution cavities and breccia matrices, rare in fossil molds.

At least three options exist to explain the origin of the PFD1 dolomite crystals: (a) growth within the rock matrix, (b) replacement of pore-filling calcite cement, or (c) pore-filling.

(a) *Matrix Replacive Origin*

The cloudy, zoned PFD1 dolomite crystals with clearer exterior rims are similar in appearance to those which are described and interpreted by others to be matrix replacive in origin (cf., Wendte et al., 1998). However, the PFD1 dolomite crystals of the present study have been recognized to fill dissolution cavities. The fact that the crystals have precipitated in what was at one time open void space rules out the possibility of a replacive

Figure 4.7:

Photomicrograph of highly zoned, planar PFD1 dolomite crystals (PFD1) which line the walls of a void. The host rock is comprised of a tight interlocking matrix of cloudy RD1 dolomite crystals (RD1). Within the interior of the void is a large, continuous bladed crystal of anhydrite (Ab). Scale bar = 1 mm.
14-11-28-21W4, 1839.3 m.

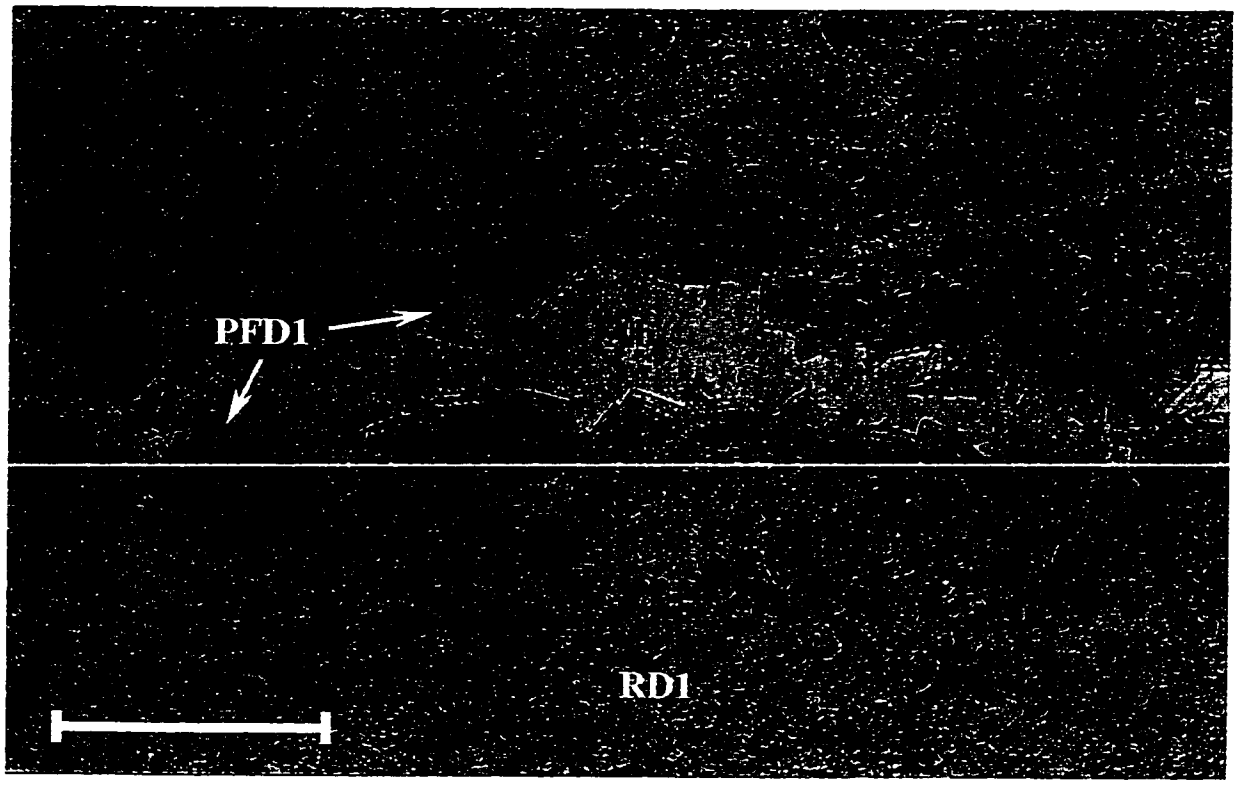
PFD1
RD1

Figure 4.8:

Cream coloured, loosely cemented PFD1 dolomite crystals (PFD1) occupy most of the volume of dissolution cavites (Cav). Green clay-rich sediment (sed) is positioned as a geopetal at the base of a cavity. The PFD1 dolomite has abundant intercrystalline pore space except where anhydrite cement (Acem) is present in the upper portions of the photograph. Cavities have been outlined in pencil in order to distinguish them from the dolowackestone host rock (Host).
5-24-28-21W4, 1851 m.

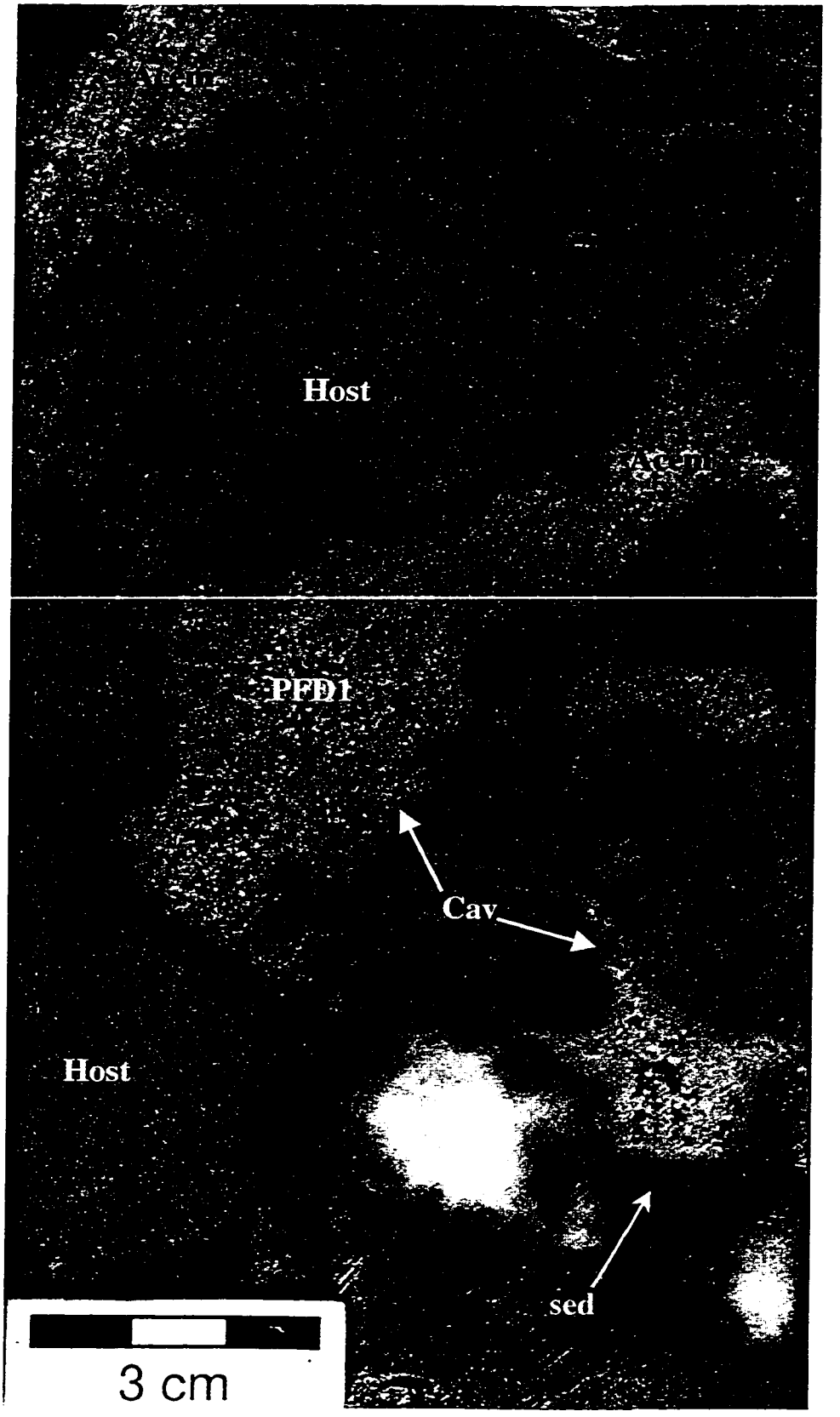
Host
PFD1
Cav
Host
sed
3 cm

Figure 4.9:

Photomicrograph of cloudy, zoned PFD1 dolomite crystals (PFD1) supported by a very fine-crystalline mosaic of anhydrite cement (Am). Both cements occupy the interior of a cavity. Fractures (frac) and corrosion on exteriors of dolomite crystals indicate that anhydrite is a later diagenetic phase. Scale bar = 1 mm.
4-24-28-21W4, 1776.3 m.

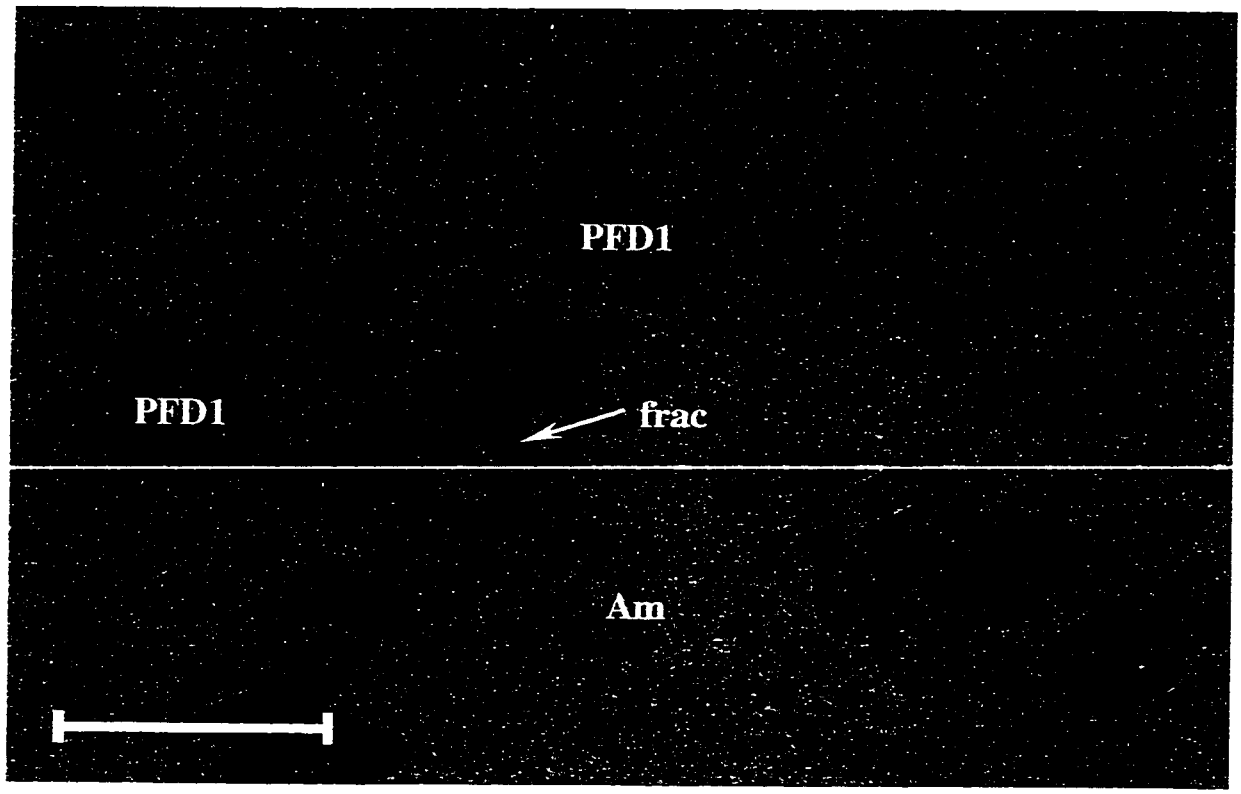
PFD1
PFD1
frac
Am

Figure 4.10:

Photomicrograph of cloudy, interlocking matrix replacive RD1 dolomite crystals (RD1) and corroded, pore-lining PFD1 dolomite cement (PFD1). The outer rims of the zoned PFD1 dolomite crystals are commonly detached from their host crystals and result in isolated dolomite crystal shards (Dsh). Bladed anhydrite cement (Ab) occupies the interior of the pore space. Scale bar = 1 mm.
4-24-28-21W4, 1778.5 m.

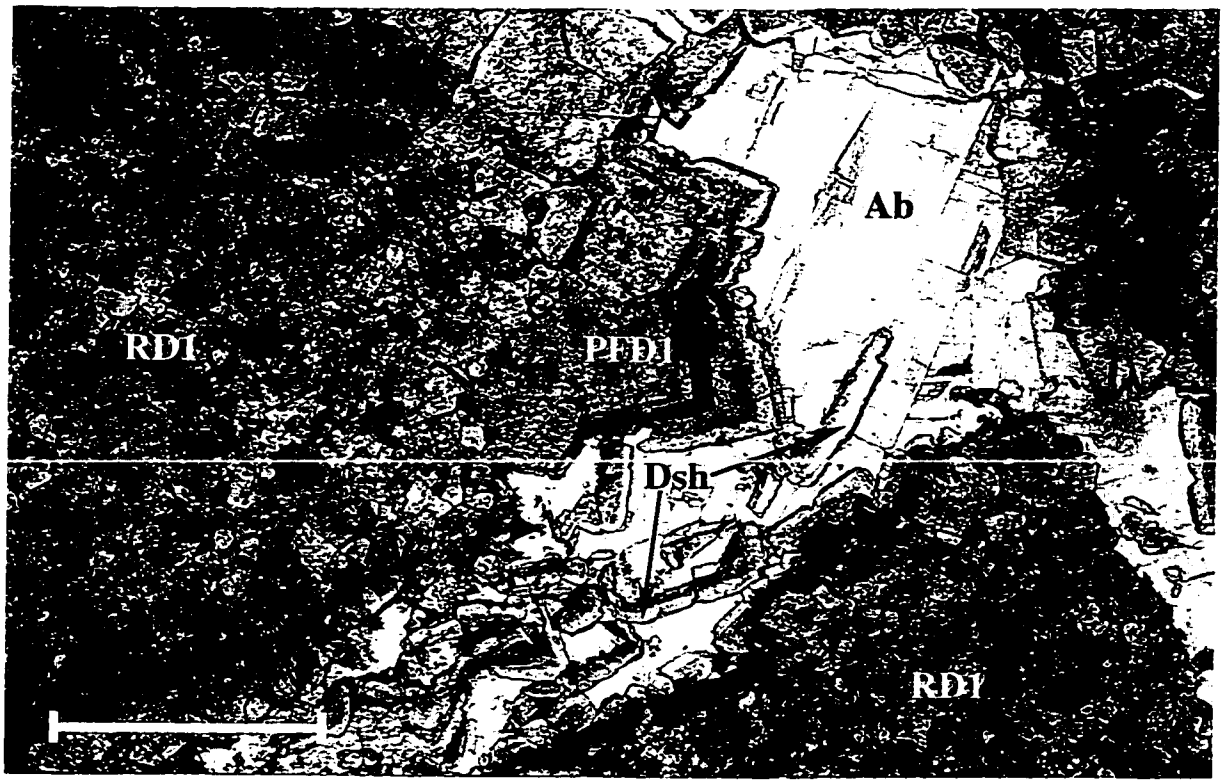
Ab
RDI
PFDJ
Dsh
RDI

origin. In addition, the distinct boundaries and differences in cloudiness existing between the matrix replacive RD1 dolomite crystals and the PFD1 dolomite crystals of the present study (Figure 4.11) imply separate origins.

(b) *Calcite Cement Origin*

It is possible that the PFD1 dolomite crystals present in the study area were previously cements of calcite mineralogy that were replaced by dolomite at some later time. Fluid inclusion and isotope analysis would likely assist in resolving the question.

(c) *Dolomite Cement Origin*

The simplest explanation for the origin of the PFD1 dolomite crystals is that they precipitated as dolomite cement into open voids. The coarse size of the crystals is partially a result of the open space in which the crystals could grow. The zonation is likely due to slight differences in chemical composition of the successive phases of cement growth. It is therefore concluded that the PFD1 dolomite crystals originated as dolomite cements.

Relative timing of cement precipitation is constrained by fabric relationships. The PFD1 dolomite cement postdates formation of dissolution cavities, deposition of cavity flooring sediment, and development of collapse breccias. Based on the mechanically displaced outer crystal rims and the corrosive contacts with the anhydrite cement, the PFD1 dolomite cement predates both burial compaction and the precipitation of anhydrite. It is therefore interpreted that PFD1 dolomite cement precipitated relatively early in the history of the Nisku Formation – following karst and breccia development but before mechanical burial compaction and anhydrite cementation.

(B) Non-zoned Dolomite (PFD2)

Designated as PFD2, the second form of pore-filling dolomite is characterized by coarse to very coarse (average of 1 mm in length) crystals that are euhedral, cloudy, and non-zoned. PFD2 dolomite is a cement that is located only within fossil molds throughout the Nisku 2 sub-unit. The reader is referred to section 4.35 for an interpretation of the origin and timing of PFD2 dolomite cementation.

Figure 4.11:

A distinct boundary (bndy) separates the dark, interlocking mosaic of RD1 dolomite crystals (RD1) from the much coarser-crystalline, euhedral PFD1 dolomite crystals (PFD1). The PFD1 dolomite crystals are highly zoned, indicating numerous phases of cement precipitation. The outermost rims of the PFD1 dolomite crystals are clearer than the crystal interiors. Corroded contacts (corr) separate the PFD1 dolomite cement crystals from the very fine crystals of the mosaic anhydrite (Am) in the interior of the void. Photomicrograph scale bar = 1 mm.
5-24-28-21W4, 1838 m.

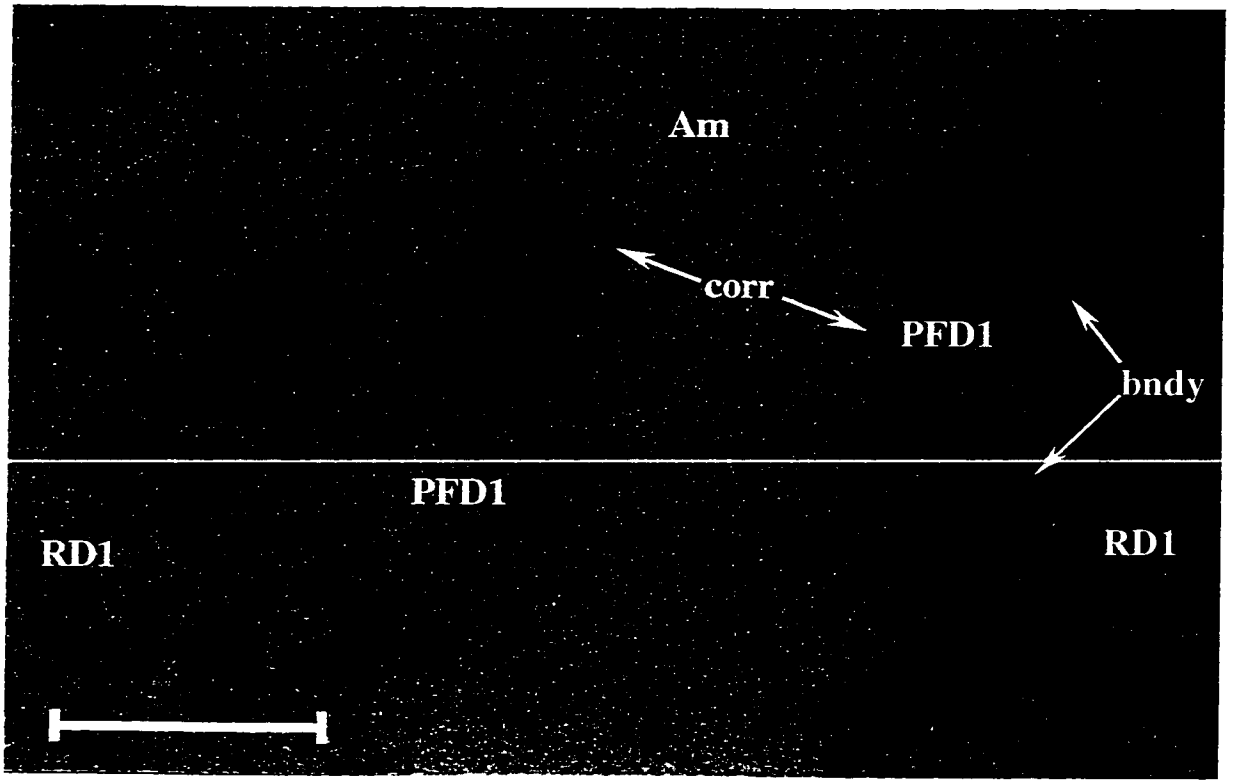
Am
corr
PFD1
bndy
PFD1
RD1
RD1

4.24 DOLOMITE SEDIMENT (DS)

Dolomite sediment (DS) is present as a sediment fill of cavities within the Nisku 2 sub-unit. The dolomite sediment is comprised of well-sorted, subspherical grains of corroded crystalline dolomite in contact with one another (Figure 4.12). The crystals are cloudy and zoning is not apparent due to the fine crystal diameter of 25 μm. The reader is referred to section 4.35 for an interpretation of the origin of the DS dolomite sediment, termed *crystal silt*.

4.25 DISCUSSION

Rock fabric relationships reveal strong evidence for early dolomitization of the Nisku Formation in the Wayne area. Other Nisku studies in southern Alberta either do not elaborate on the timing of dolomitization (e.g. Slingsby and Aukes, 1989; Kissling, 1996) or only discuss the mechanism and timing of large scale dolomitization of the Nisku Formation (Whittaker and Mountjoy, 1996).

Although the findings of early dolomitization of Wayne strata are significant, further geochemical work on the dolomites is needed to determine the composition of the dolomitizing fluids, temperatures of precipitation, and exact mechanisms of dolomitization.

4.3 CAVITY FORMATION

4.31 INTRODUCTION

The carbonates of the Wayne Nisku display various expressions of post-depositional dissolution. Fossil molds are host-specific voids that result from differences in solubility between the rock matrix and fossils. Vugs, cavities, and solution breccias are interpreted to be non fabric-related phenomena that express different interactions, rates, and intensities between the rock matrix and the dissolving fluids. A vug is an incipient cavity and a solution breccia is simply a cavity system that has collapsed, thus all are considered as cavities (Figure 4.13). For the purposes of this study, however, each cavity expression is

Figure 4.12:

Photomicrograph of the contact (dashed line) between cavity-flooring dolomite sediment (sed) and mosaic RD1 dolomite that replaced the host rock matrix (RD1). The sediment is comprised mainly of well sorted, corroded grains of crystal silt dolomite (Dcs). Scale bar = 1 mm.
6-14-28-21W4, 1771.3 m.

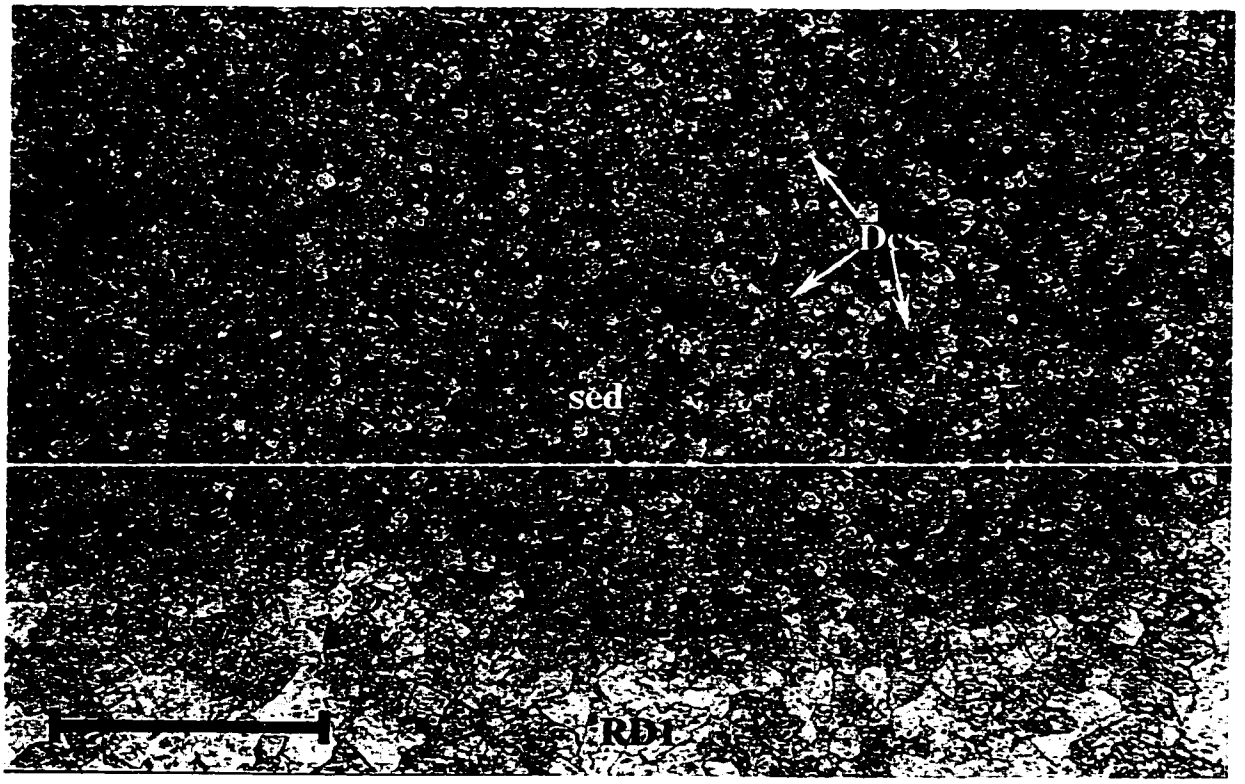
Dcs
sed
RDt

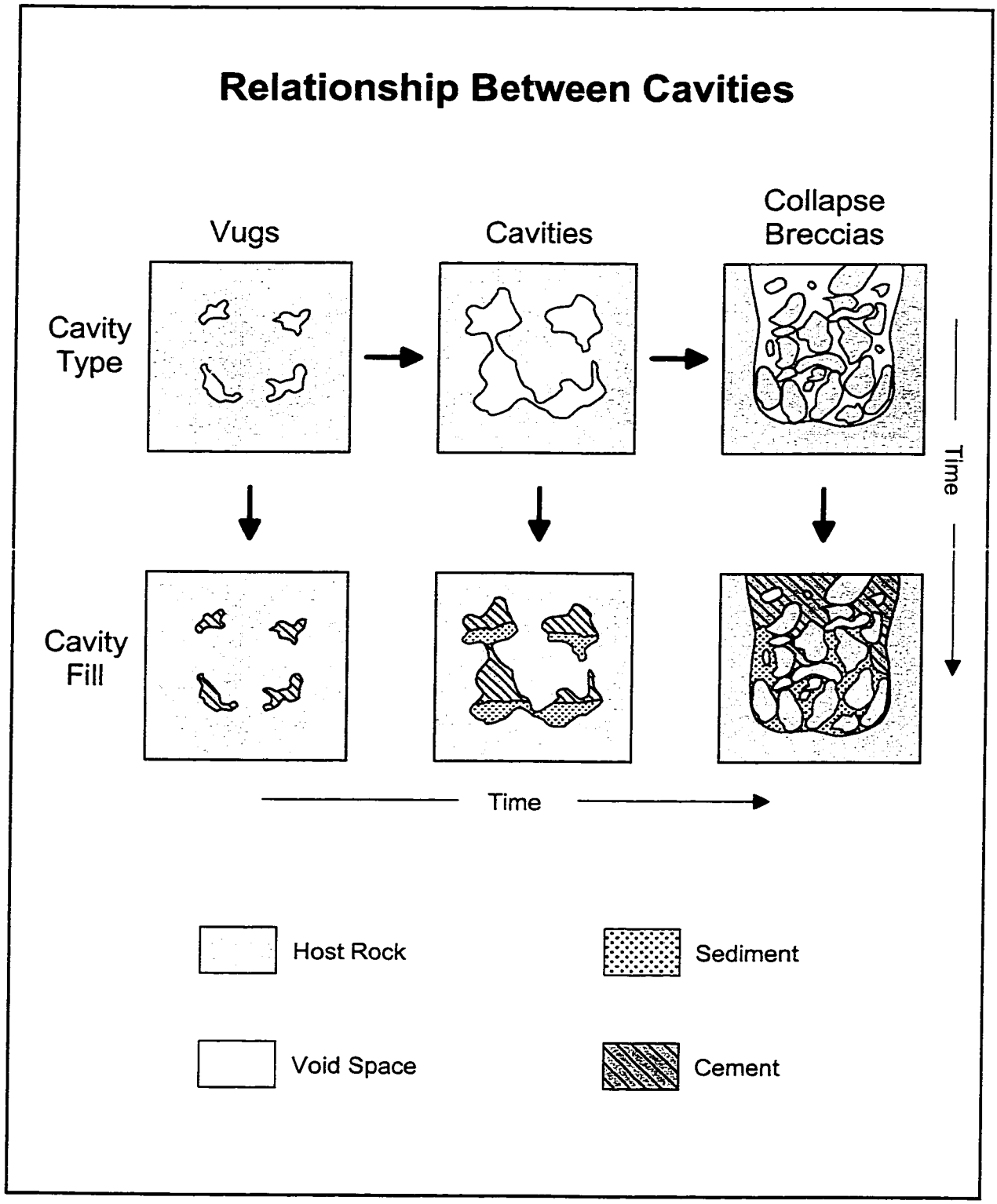

Figure 4.13 Schematic of cavity evolution from vugs to collapse breccias and the styles of cavity fill observed in the study area.

discussed separately. Void fills include allochthonous or autochthonous sediment, as well as direct precipitants from the pore fluids.

Throughout the following section the breccia terminology in the classification by Norton (1917) is utilized, except for the replacement of *founder* breccia by *collapse* breccia. Due to the insignificant development or lack of void space in the Nisku 1 and 3 sub-units, all of the following descriptions, interpretations, and discussions refer to rocks of the Nisku 2 sub-unit.

4.32 VUGS, CAVITIES, BRECCIAS, AND MOLDS

(A) *Vugs*:

The majority of vugs are less than 1 cm in diameter, highly irregular in shape, and lack any predominant orientation (Figure 4.14). They may be isolated or connected with one another.

(B) *Cavities*:

Cavity chambers are generally irregular in shape and range in diameter from less than 1 cm to over 10 cm (Figure 4.15). Solution-enlarged fossil molds may be incorporated into the cavity system (Figure 4.16), however, most dissolution cavities do not display fabric selectivity. The cavities lack any definite orientation, although a stronger horizontal component is apparent rather than vertical. Dissolution cavities are connected in three-dimensions and have distinctly sharp-edged walls, implying lithification of the matrix prior to dissolution. The host rock is not lithofacies specific.

(C) *Breccias*:

Collapse breccias may be clast- (Figure 4.17) or matrix-supported (Figure 4.18). Clasts are commonly angular and range between 0.25 and 9 cm in diameter. Clast compositions amongst collapse breccias vary with the type of host rock but all are oligomictic and of dolomite lithology. Fossils may obtrude from the clasts or country rock into the breccia matrices. Other breccias appear as a mix of crackle and mosaic types. Clasts range between 0.5 and 15 cm in diameter. The clasts are slightly separated, angular,

Figure 4.14:

Irregular-shaped vugs (Vug) are randomly oriented throughout the host rock. Most vugs contain light brown isopachous PFD1 dolomite cement (PFD1). The interiors of some vugs are filled by white anhydrite cement (Acem). A dark colour alteration is present along the perimeter of many of the vugs.
1-25-28-21W4, 1790.6 m.

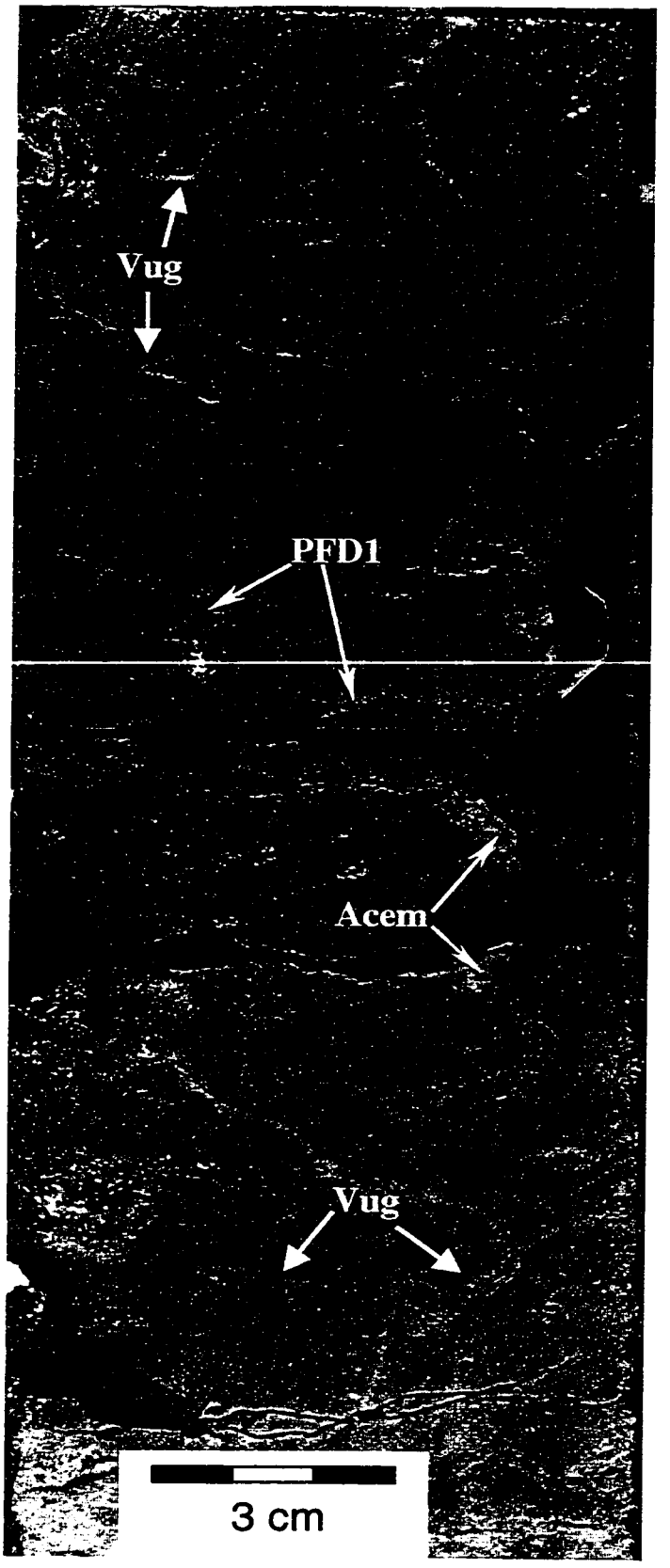
Vug
PFD1
Acem
Vug
3 cm

Figure 4.15:

Irregular-shaped non fabric-related dissolution cavities (Cav) are generally horizontally elongate across the width of the core. Most cavities contain green coloured sediment floorings (sed) and a combination of PFD1 dolomite (PFD1) and anhydrite (Acem) cement fills in the upper chambers. A megalodont valve (meg) has become incorporated into the cavity system and contains similar sediment and cement fills.
4-24-28-21W4, 1776.3 m.


meg
sed
Cav
3 cm

Figure 4.16:

A large megalodont bivalve is part of the cavity system (Cav/meg). Dissolution created extra cavity space beyond the confines of the fossil and into the rock matrix. Green sediment floorings (sed) are geopetals. Lining the cavity walls above the sediment is an isopachous form of PFD1 dolomite (PFD1). The final cavity fill is cloudy white mosaic anhydrite cement (Acem).
4-24-28-21W4, 1776.7 m.

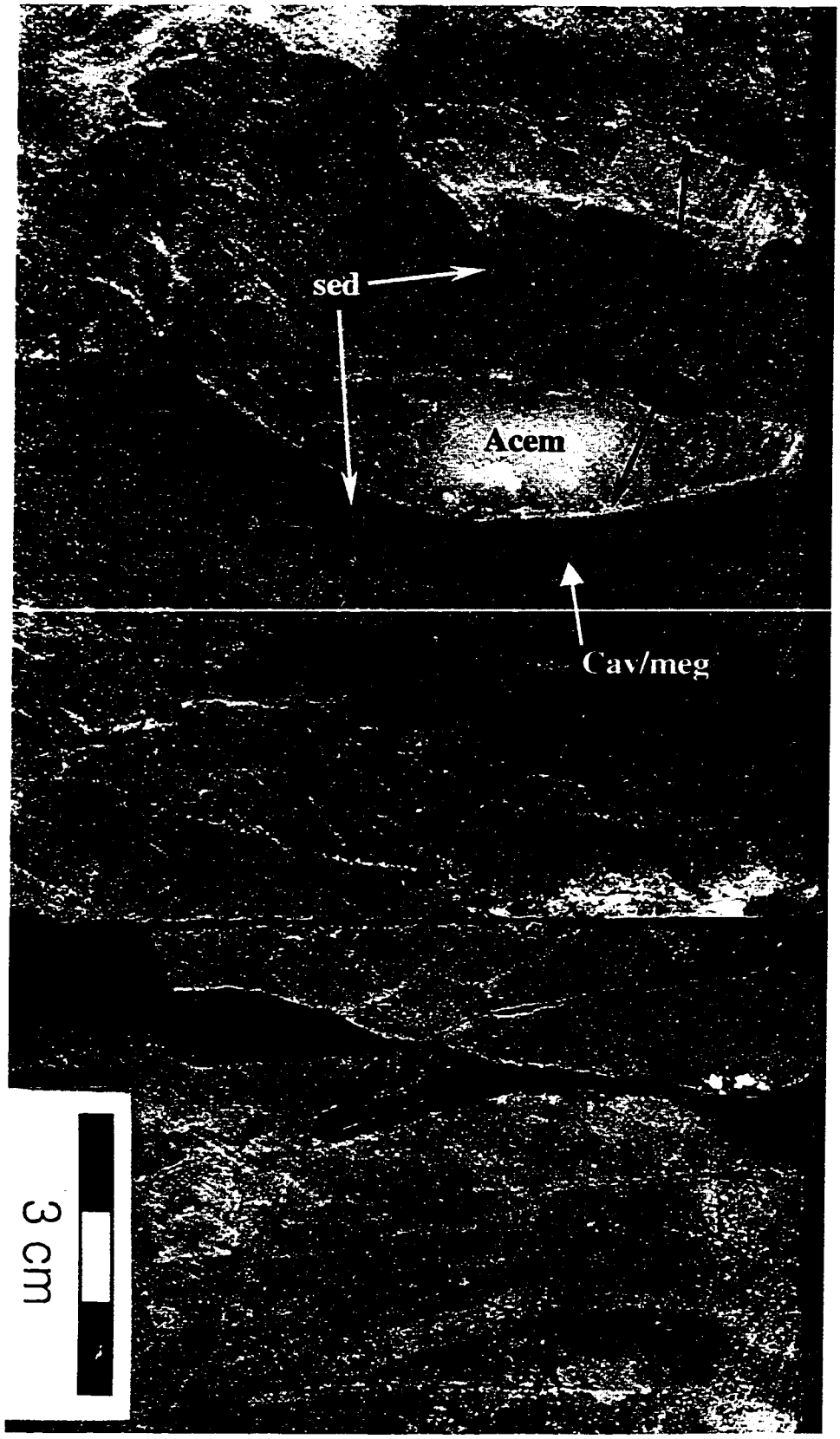
sed
Acem
Cav/meg
3 cm

Figure 4.17:

Collapse breccia at the base of the cavity system. The angular breccia clasts (clast) support one another within a light brown matrix (Bmatx) of fine-grained carbonate detritus and corroded PFD1 dolomite.
4-24-28-21W4, 1778.5 m.

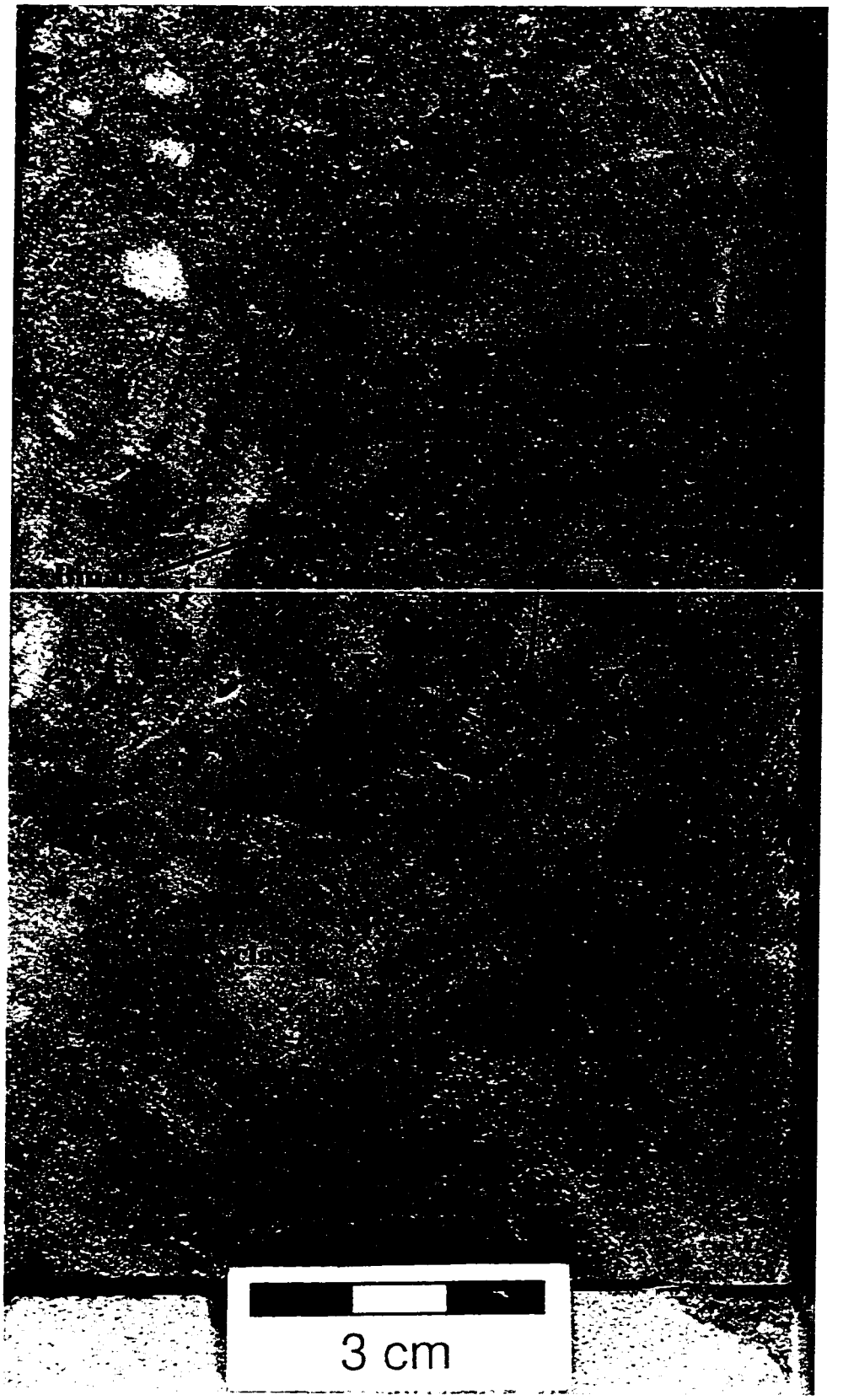
3 cm

Figure 4.18:

A collapse breccia in which the angular clasts (clast) are supported of a poorly sorted matrix (Bmatx) of fossil fragments, corroded PFD1 dolomite, and fine-grained carbonate detritus. A distinct boundary exists between the collapsed cavity system (Cav) and the dark brown host rock (Host). Megalodonts (meg) are resistant to dissolution and protrude into the breccia matrix. Massive white anhydrite (A) is a later diagenetic phase.
1-12-28-21W4, 1743.9 m.

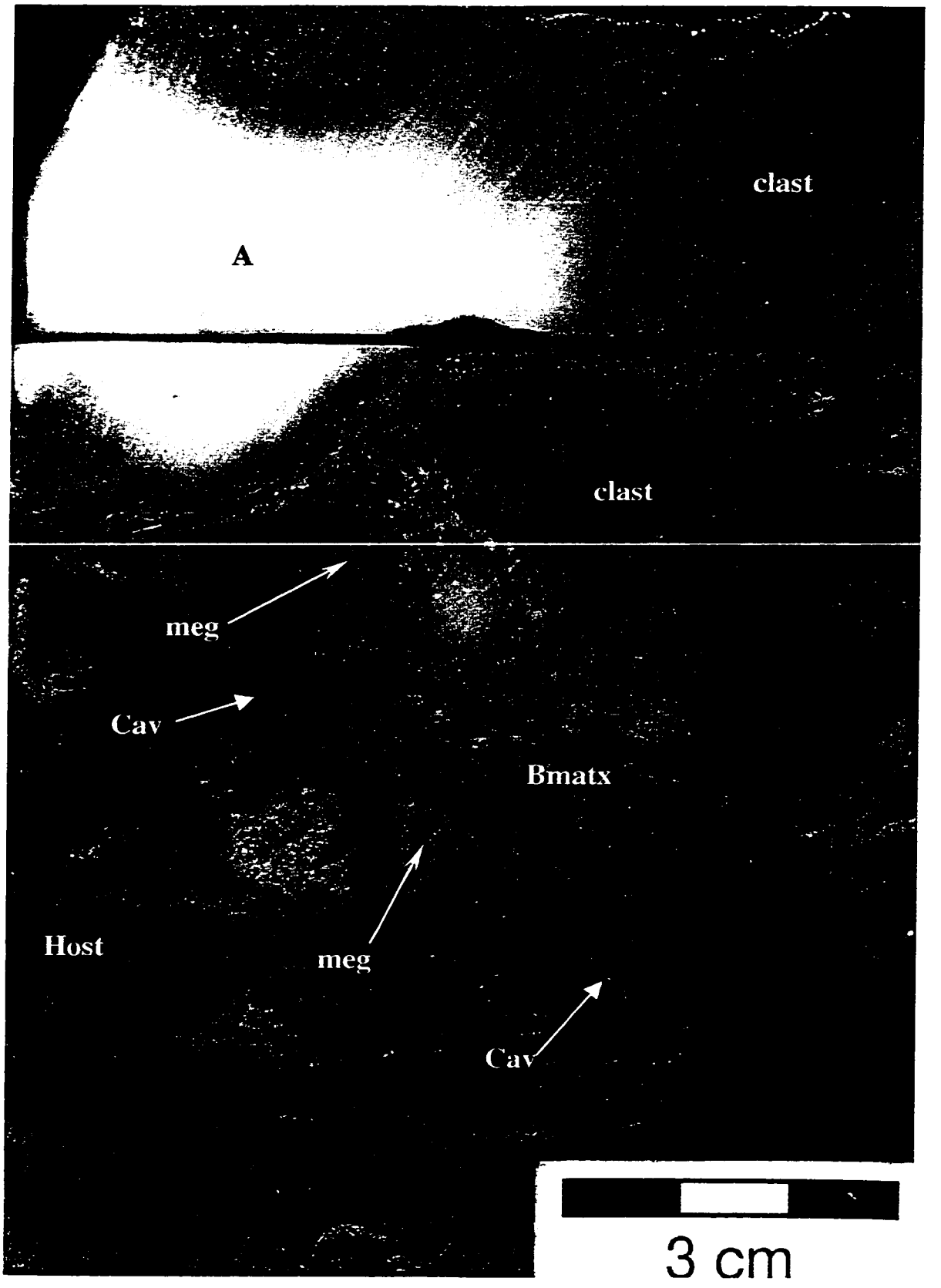
clast
A
clast
meg
Cav
Bmatx
Host
meg
Cav
3 cm

and display minor displacement. Fractures commonly extend from the breccias into the country rock.

(D) *Fossil Molds*:

Fossil molds vary in shape and size depending upon the type of fauna present prior to dissolution. Many fossils are only partially dissolved, resulting in incomplete molds. All molds display sharp boundaries with their encasing rock matrices. Most fossil molds are isolated, although some are connected in three dimensions. Descriptions and photographs of fossil molds are present in Chapter 3, with specific reference to Lithofacies G, H and I (Figures 3.5, 3.7 and 3.8, respectively).

4.33 CAVITY AND BRECCIA FILLINGS

(A) *Vugs*:

Vugs are generally open, although partial fill by PFD1 dolomite and anhydrite cements is common (Figure 4.14). The PFD1 dolomite cements are isopachous. Individual crystals are euhedral, zoned, and have an average length of 1 mm. Anhydrite crystals may either be blocky and greater than 1 mm in length or the crystals may be part of very fine-crystalline mosaics and less than 5 μm in length.

(B) *Cavities*:

Cavities are generally completely filled by sediments and/or cements. Two main types of cavity fill are distinguished based on sediment characteristics: (a) green clay-rich sediment, and (b) dark brown dolomudstone sediment.

(a) The first type of cavity filling sediment is medium to dark green in colour. The sediment ranges from vaguely laminated inclined floorings (Figure 4.19) to complete massive fill of the cavities (Figure 4.20). Thin section analysis reveals that the sediment is made up of: (i) well sorted, corroded DS dolomite crystals with a mean diameter of 25 μm (see description in section 4.24), and (ii) illitic clay (too fine to resolve form and crystal sizes) (Figure 4.12). The presence of the illite causes the overall green colour although the clay is volumetrically much less significant as an intercrystalline pore filler. However, where the illite does dominate the sediment, large euhedral dolomite crystals with a mean

Figure 4.19:

Green coloured illite-rich sediment (sed) floorings of cavities (Cav) are inclined (incl) in various directions throughout the core. Not only are the upper sediment surfaces inclined but internal tilting is apparent as well. Above the sediment floors are PFD1 dolomite and anhydrite cements (cem).
13-13-28-21W4, 1782 m.

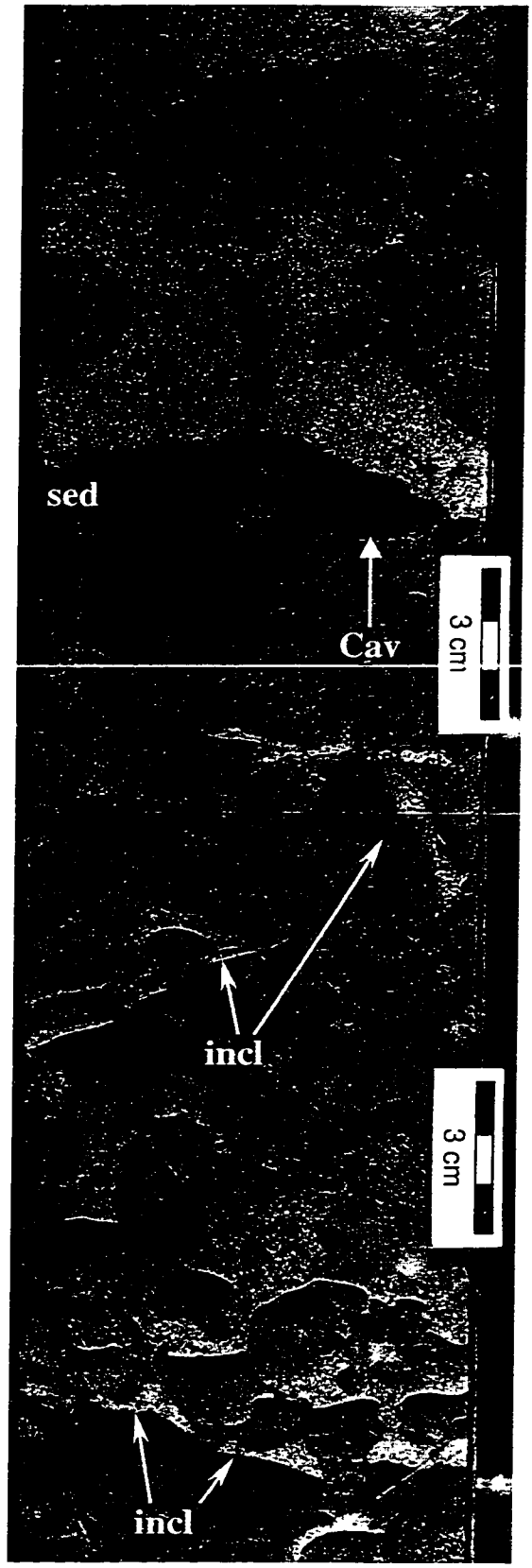
sed
Cav
3 cm
incl
3 cm
incl

Figure 4.20:

Connected dissolution cavities (Cav) have been entirely filled by green illite and dolomite sediment (sed). No cements occupy the interior of the cavities. White anhydrite (Arep) has replaced portions of the cavity fill, as well as the rock matrix, and is a later diagenetic phase. Cavities in lower portion of photograph have been outlined in pencil.
14-11-28-21W4, 1839 m.

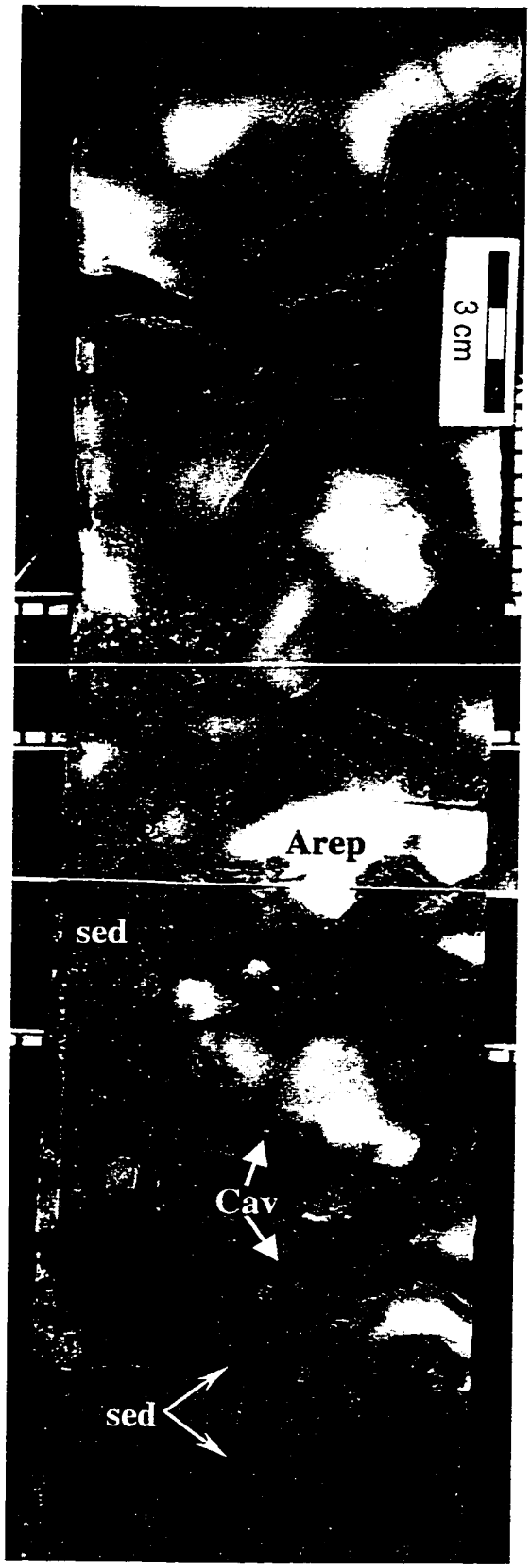
3 cm
Arep
sed
Cav
sed

diameter of 100 μm may be present within the clay (Figure 4.21). Under cross-polarized light, alignment and uniform extinction of the illite takes place on opposite sides of the large dolomite rhombs. Also present within the cavity sediment, although rare, are randomly oriented tubular fossils up to 4 mm in cross-sectional width.

Filling the remaining void space above the sediment fill, or in places completely filling entire cavities, are PFD1 dolomite and anhydrite cements (Figure 4.15). The PFD1 dolomite cement is commonly isopachous, with individual zoned crystals displaying corrosion along their outermost zoned edges. Patches of blocky anhydrite may precipitate directly against the corroded PFD1 dolomite. More commonly filling the remaining upper cavity space, and adjoining the corroded PFD1 dolomite, is a mosaic of very fine interlocking anhydrite crystals with mean crystal diameters less than 5 μm . Individual corroded PFD1 dolomite crystals also may be completely surrounded by the mosaic anhydrite (Figure 4.9).

(b) The second type of cavity fill includes sediment that is recognizable by its generally flat and horizontally-aligned dark brown dolomudstone floors (Figure 4.22). Faint laminae may be present within the dark mud but, more commonly, the cavity sediment is massive. Petrographically, the dark mud is indistinguishable from the RD1 dolomitized muds of the surrounding host rock. Both display tight mosaics of fine crystalline dolomite with mean dolomite crystal lengths of 50 μm. A slight increase in the amount of organic insolubles is responsible for the dark colour of the sediment relative to the host rock.

Overlying the dark brown cavity sediment is a white anhydrite cement comprised of a very fine mosaic of crystals each less than 5 μm in size. Anhydrite-filled fractures commonly connect the anhydrite cement fills between cavities. No dolomite is present in the fill above the dark brown cavity sediment.

(C) *Breccias*:

The matrices of the collapse breccias are comprised of various cements and fills, including: microcrystalline carbonate detritus, blocky and mosaic anhydrite cements, PFD1 dolomite cements with zoned crystals averaging 200 μm in length, minor fossil fragments,

Figure 4.21:

Photomicrograph of crystal silt dolomite (Dcs) within a cavity. The very fine-crystalline green clay illite fills much of the intercrystalline pore space between the crystal silt. Within concentrated pockets of the illite (ill) are coarse, euhedral dolomite crystals (De) that have precipitated after illite infiltration and deposition. The dashed line demarcates the contact between the cavity and the mosaic RD1 dolomite that replaced the host rock matrix (RD1). Scale bar = 1 mm.
14-11-28-21W4, 1839.3 m.

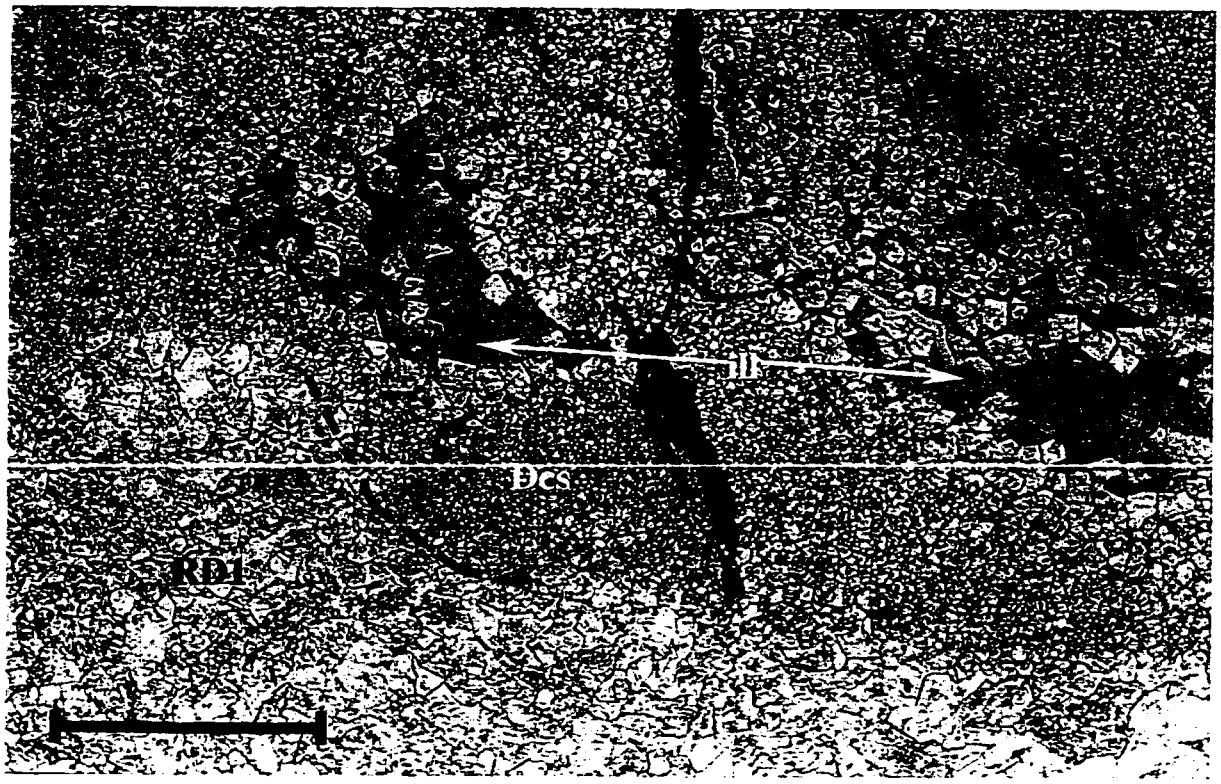
DCS
RD1

Figure 4.22:

Irregular-shaped dissolution cavities (Cav) within a light brown host dolomudstone. The cavities are floored by dark brown dolomudstone sediment (sed). White mosaic anhydrite (Am) is the only type of cement fill of the upper portions of the cavities.
5-24-28-21W4, 1865.4 m.

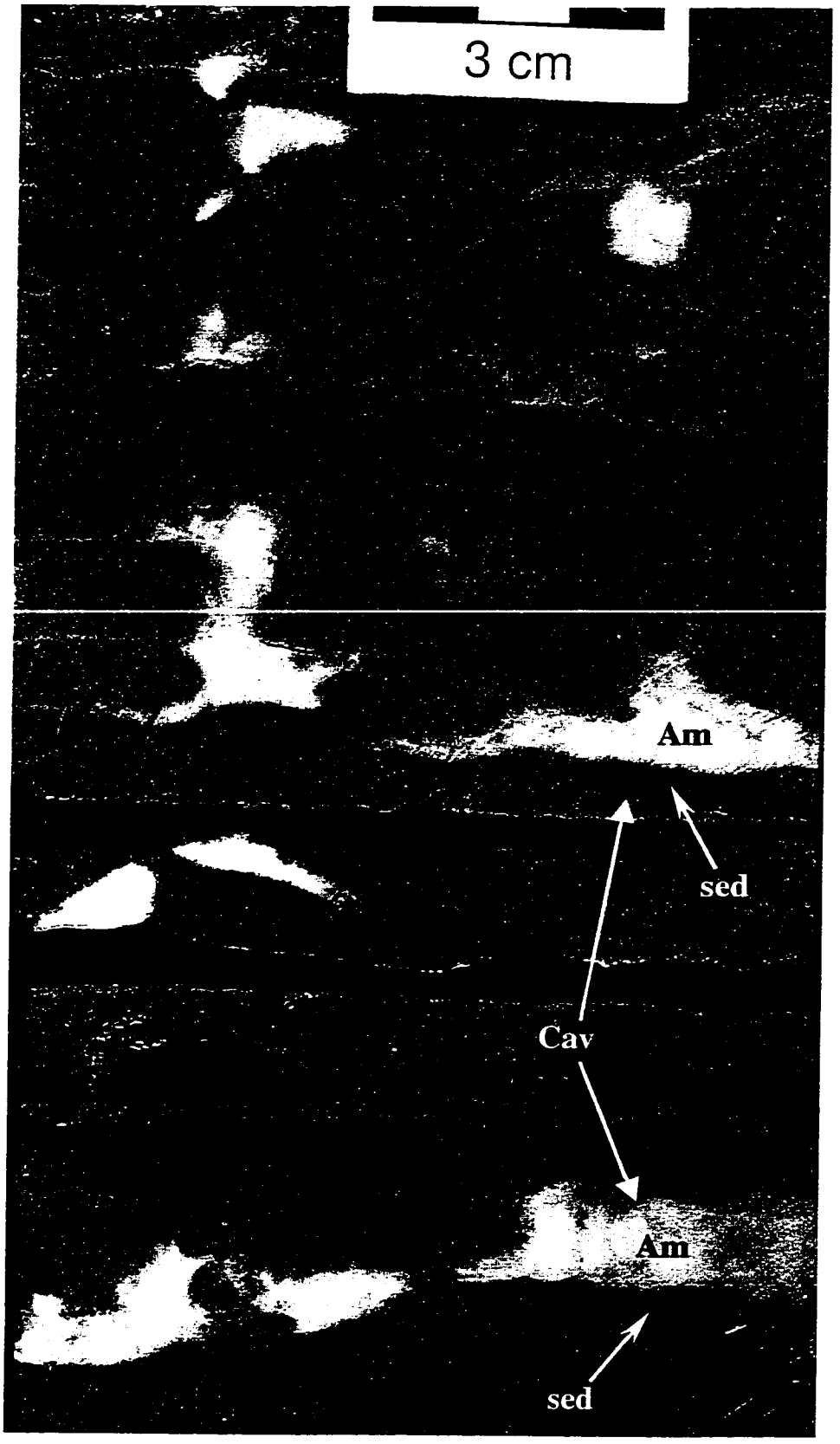
3 cm
Am
sed
Cav
Am
sed

rare replacive chalcedony, and the exterior shards of zoned PFD1 dolomite cement crystals that average 150 μm in length (Figure 4.23). In crackle/mosaic breccias, the majority of the matrices are comprised of mosaic anhydrite cement, less commonly of microcrystalline carbonate detritus and PFD1 dolomite cement. Components of all breccia matrices lack any order. Clays are not present in any of the breccia matrices.

(D) *Fossil Molds*:

Most fossil molds are completely open, however, a minor proportion have been partially to completely filled by dolomite and/or anhydrite. Of the fills, most common are planar, non-zoned dolomite crystals which simply line the pore walls and are of similar appearance and dimensions to those of the dolomitized (RD1) host rock (60 to 100 μm in length). However, significantly larger (average 1 mm in length) PFD2 dolomite crystals may completely fill the interiors of the fossil molds. Anhydrite cement may be present as coarse (crystals greater than 1 mm in length), blocky crystals crossing the width of the molds or as very fine-crystalline (crystals less than 5 μm in length) mosaics completely filling the molds.

4.34 CAVITY AND BRECCIA DISTRIBUTION

(A) *Vugs*:

Vugs are common to all lithofacies.

(B) *Cavities*:

(a) The cavities containing the green sediment fill are not lithofacies specific but instead are positioned along a stratigraphic horizon. In the Wayne 'A' pool, the top of the horizon is 14 to 22 m below the contact between the Nisku 1 and Nisku 2 sub-units. The illite-rich green sediment fill, recognized on wireline logs as a high gamma marker (up to 15 API positive shift on gamma ray logs) (Figure 4.24), occupies the upper portion of a cavity system. Laterally, the entire cavity system ranges between 6.5 m thick near the Nisku 3 sub-unit channel margin (13-13-28-21W4) to zero thickness towards the southwest (10-3-28-21W4). Proximal to the channel edge (e.g. 13-13, 4-24, 5-24-28-21W4), cements of D3a dolomite and/or anhydrite commonly occupy the upper cavity space above the

Figure 4.23:

Dashed line marks the contact between mosaic RD1 dolomite of a breccia clast (RD1) and the poorly sorted crystals of the breccia matrix. Shards from the exterior rims of zoned PFD1 dolomite cement crystals (Dsh) are abundant in the breccia matrix and are separated by dark microcrystalline carbonate detritus. Photomicrograph scale bar = 1 mm.
4-24-28-21W4, 1778.5 m.

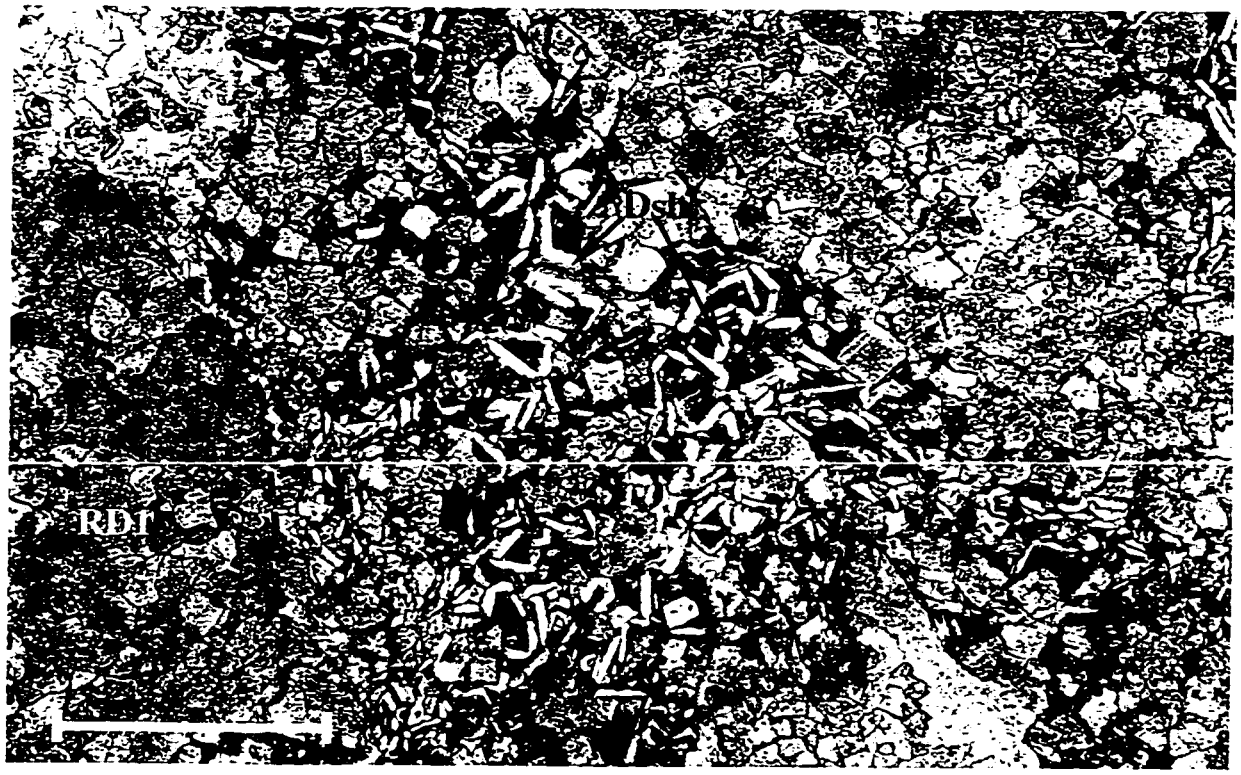
Dsh
RD
TD

SW

Wayne 'A' Pool: C
Dissolutio

100/14-11-028-21-W4

102/10-14-0

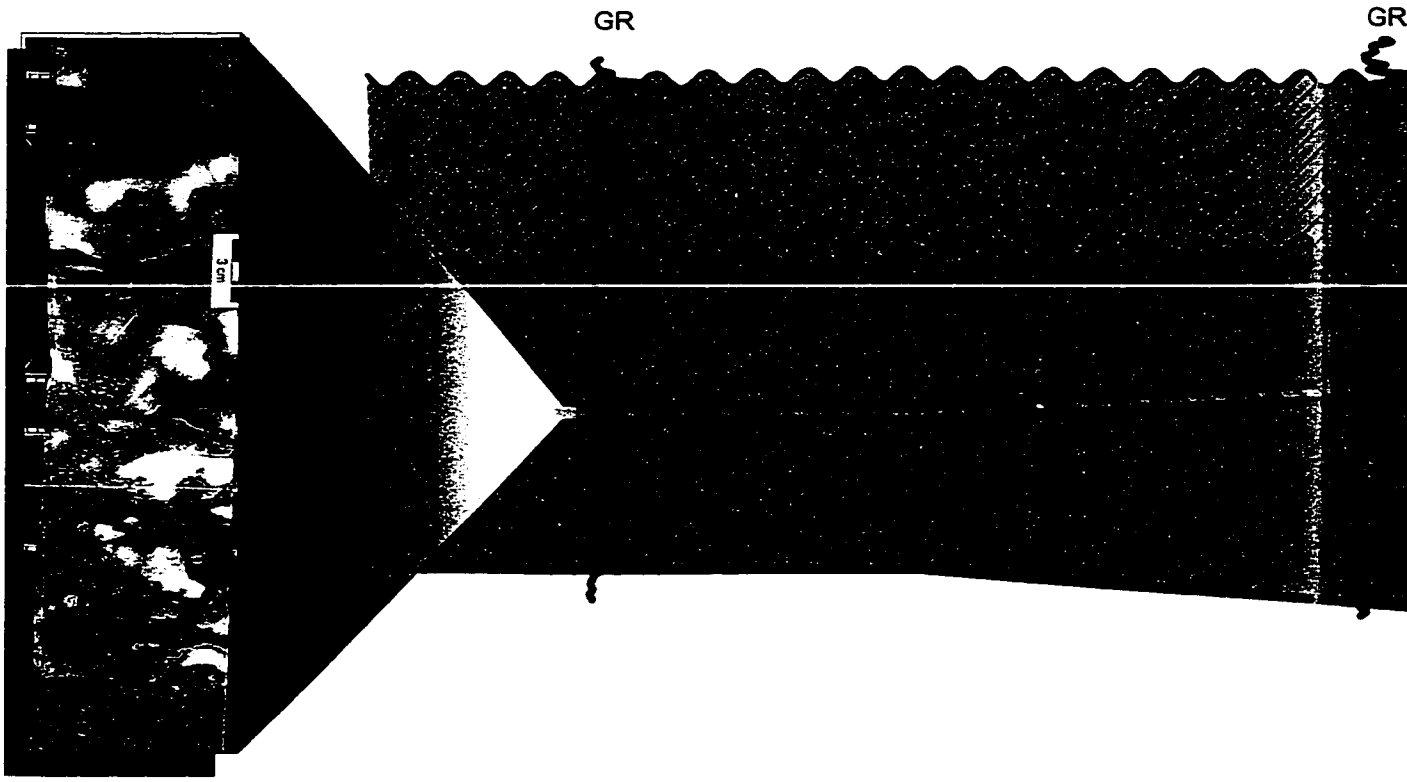

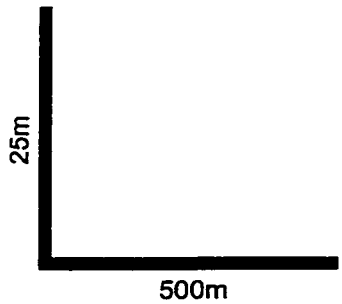

A' Pool: Green Sediment - Filled Dissolution Cavity System

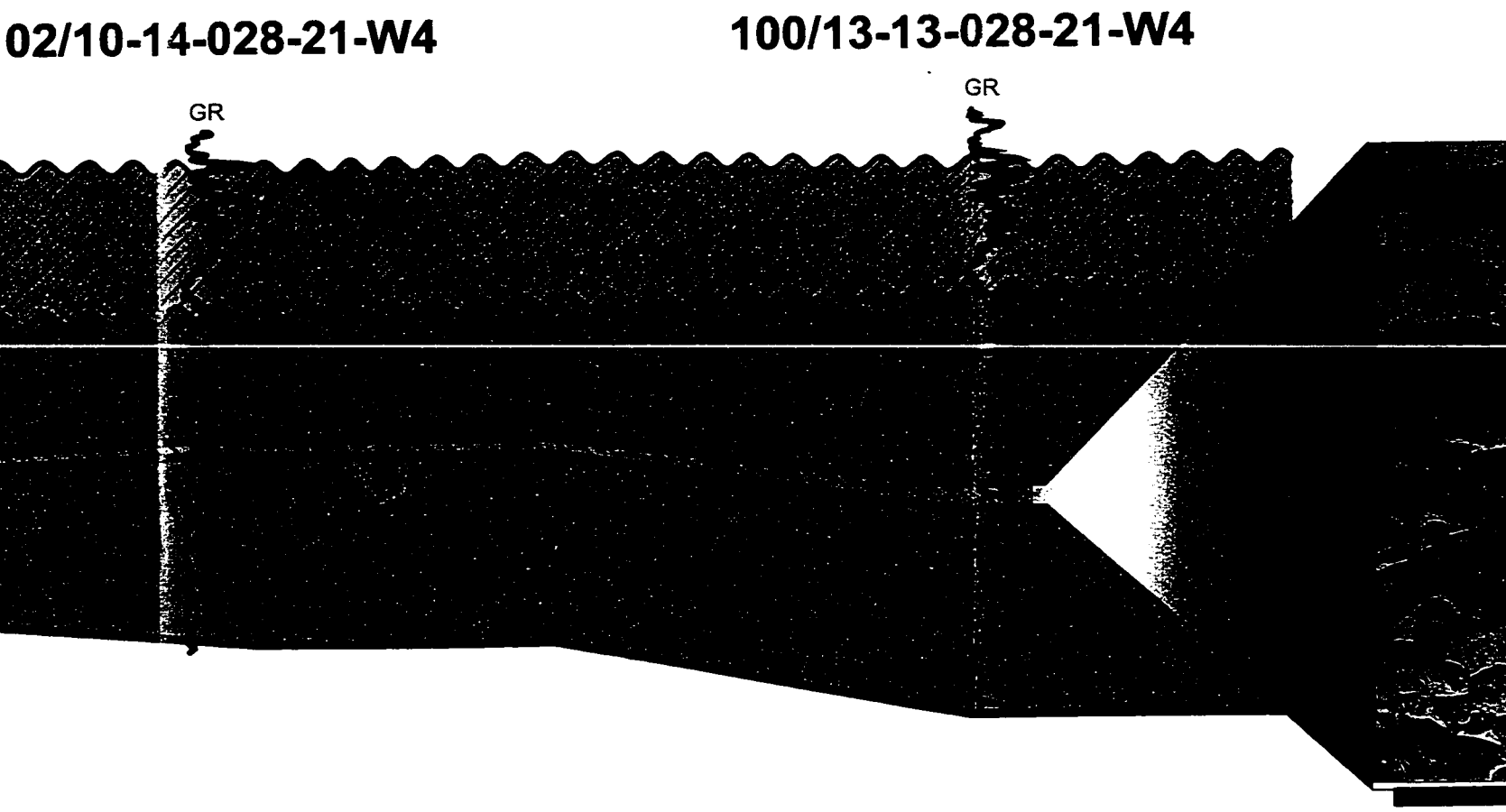

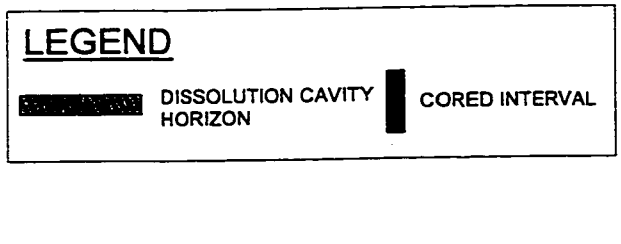

Figure 4.24 Stratigraphic cross-sect
(datum = top of the Nis
accentuates the depth a
thickness of the green
sediment-filled cavity l
within the Wayne 'A' p
Core photographs displ
differences in cavity fil
between the SW and N
of the pool.

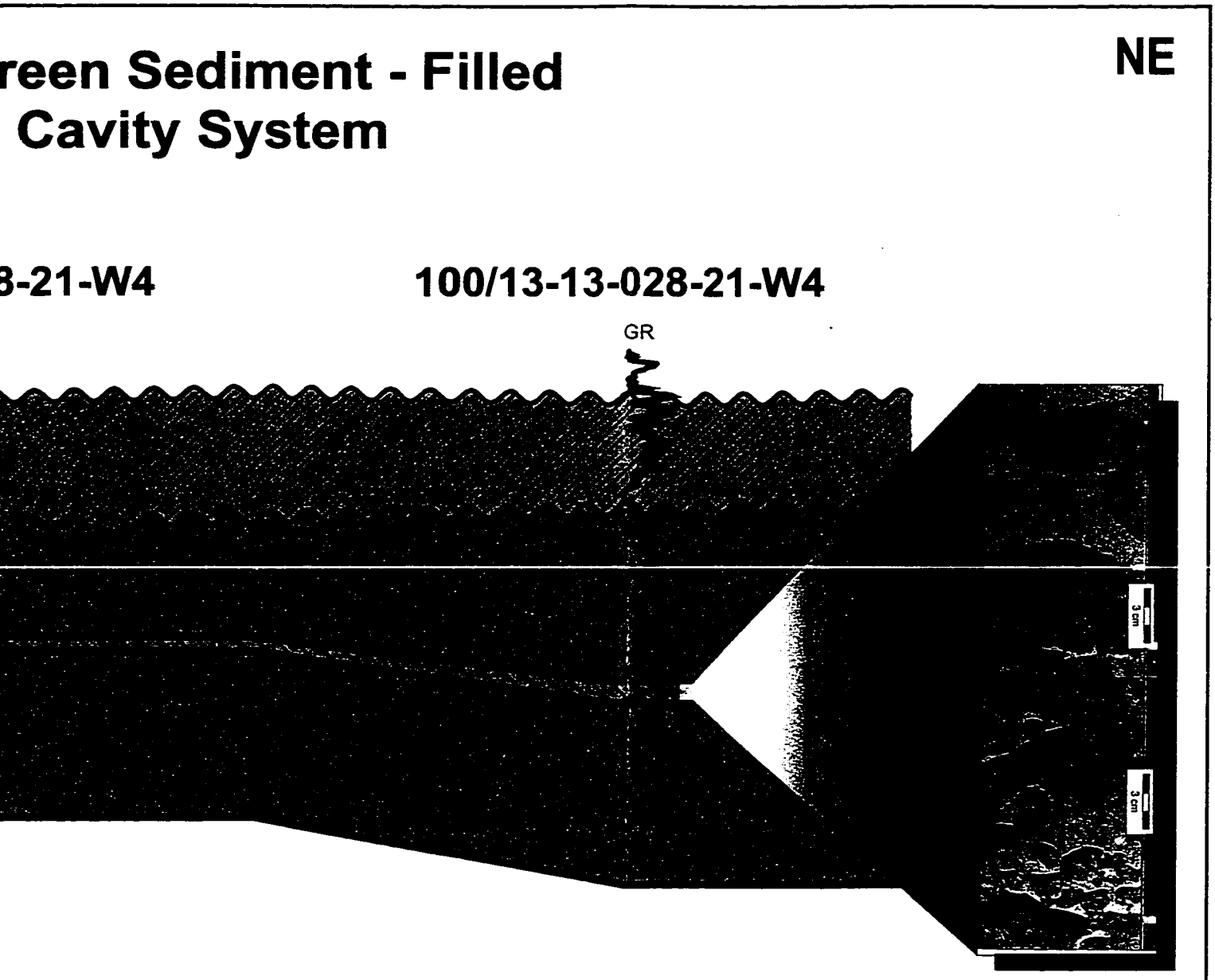

Figure 4.24 Stratigraphic cross-section (datum = top of the Nisku 1) accentuates the depth and thickness of the green sediment-filled cavity horizon within the Wayne 'A' pool. Core photographs display the differences in cavity fills between the SW and NE ends of the pool.

inclined sediment floors. As well, such cements completely fill the cavities in the lower portions of the cavity system along the channel margin. Only inward from the Nisku 3 sub-unit channel margin (e.g. 14-11, 6-14, 102/10-14-28-21W4) does the green sediment completely fill each cavity over the entire thickness of the cavity system. Green sediment-filled cavities are also present in the Wayne 'B' pool in one cored well, 8-12-28-21W4, but only 6 m below the Nisku 1 and 2 contact.

(b) In contrast to the cavities containing the green sediment, the cavities containing the dark brown dolomudstone sediment are facies specific yet not constrained to a specific stratigraphic level. This cavity system is present at various stratigraphic levels but only within the massive mudstones of Lithofacies J.

(C) *Breccias*:

Collapse breccias are common at the base of the green sediment-filled cavity system, but mainly near the Nisku 3 sub-unit channel margin. Such breccias are laterally continuous along the length of the channel edge in the Wayne 'A' pool. Other collapse breccias, as well as crackle/mosaic breccias, are present at various horizons and cannot be laterally correlated.

(D) *Fossil Molds*:

The distribution of fossil molds is related to the lithofacies they are present in. The reader is referred to Chapter 3 for information on their distribution.

4.35 INTERPRETATION

(A) *Vugs*:

As stated in section 4.31, vugs are incipient cavities and it is believed that the vugs are preserved as a result of the premature completion of the cavity-forming process. That is, the pore fluids initially responsible for dissolution are no longer corrosive enough to continue to create larger vugs. Either the pore fluids are saturated with respect to the chemistry of the host rock or the source of the dissolving fluids is no longer in contact with the isolated vug systems. The lack of allochthonous sediment fill confirms the isolated nature of the vugs. However, the same PFD1 dolomite and anhydrite cements that fill the

pore spaces of cavities and breccias also occupy many of the vugs. It is therefore interpreted that the vugs not only formed through the same processes and at the same time as cavities, but vugs were also cemented at the same time and in the same manner as the genetically-related cavities and breccias.

(B) *Cavities*:

(a) Green Sediment-Filled Cavities: Most of the green sediment fill in the study area is comprised of well sorted, corroded DS dolomite crystals with a mean diameter of 25 μm. In combination with illite, the green sediment may occupy the bases of the cavities as inclined floorings or the sediment may completely fill the cavities. The inclined floorings are not due to post-depositional structural tilting because the surfaces of the sediment may be mounded, bumpy, and do not tilt in the same direction (Figure 4.19). The inclined floorings are interpreted to be geopetals formed under special conditions, as discussed in the following.

The description of the DS dolomite crystals can be likened to that offered by Dunham (1969) for crystal silt. Crystal silt, as defined by Dunham (1969), is comprised of well-sorted, silt-sized (10 to 25 μm in diameter) calcite crystals derived from island-rock within the vadose diagenetic realm below a subaerial surface. *Vadose* silt is a synonymous term to crystal silt, as current velocities only high enough in the vadose zone can produce the commonly encountered inclined floors or complete fillings of voids by the crystal silt (Dunham, 1969). Crystal (vadose) silt contains few sand-sized particles, clay-size particles, or small fossils likely because of selective mechanical screening of the coarse fraction and chemical attack on the finer fraction (Dunham, 1969). However, skeletal particles could readily wash out of the surrounding host rock and become incorporated in the vadose sediment (Dunham, 1969).

It is therefore interpreted that the DS dolomite crystals comprising the bulk of the green sediment-filled dissolution cavities of the present study have a similar vadose origin to Dunham's (1969) crystal silt. Characteristics of the sediment less easily explained, however, are: (i) the sand-sized (100 μm), euhedral dolomite crystals, (ii) the source of the

crystal silt, (iii) the significant clay-size fraction, and (iv) the identification of the overlying subaerial exposure surface. All are discussed:

(i) The sand-sized, euhedral dolomite crystals are interpreted to have crystallized in place rather than to have been physically transported in similar fashion to the dolomite crystal silt. Had the large dolomite crystals been transported they would not retain euhedral shapes nor would the surrounding clay display preferential extinction patterns interpreted to be caused by displacement.

(ii) The source of the DS dolomite crystal silt is interpreted to be the 4 to 5 m thick coarse-crystalline RD2 dolomite horizon just below the contact between the Nisku 1 and 2 sub-units (see section 4.22). Based on the corrosion of RD2b dolomite and infiltration of green clay between the RD2b dolomite crystals, it is proposed that these coarse dolomite crystals formed through an early dolomitization mechanism and were a source for the DS dolomite crystal silt found in the underlying cavity sediment.

(iii) The explanation for the clay-sized fraction and identification of an overlying subaerial surface are best discussed together. It is proposed that the clay was not transported simultaneously with the DS dolomite crystal silt but instead infiltrated the intercrystalline pore space after deposition of the DS dolomite crystal silt. The source of the clay is interpreted to be a subaerial exposure surface at the contact between the Nisku 1 and 2 sub-units (Figure 4.25), the only widespread surface in core that displays characteristics of an unconformity. Using criteria from Esteban and Wilson (1993), evidence for the unconformity-related subaerial exposure surface is based on: (a) the distinctly different lithologies and styles of deposition above and below the surface, (b) the presence of early dolomite (RD2a and RD2b) beneath the surface, and (c) the presence of a thin horizon of layered green clay and quartz silt immediately below the Nisku 1 sub-unit (Figure 4.26). X-Ray diffraction of green clay sampled from the contact revealed a 37% bulk volume of undegraded illite and 20% quartz (Table 4.1). While the highly crystalline illite likely recrystallized upon burial and is not representative of the original clay deposit, the subrounded quartz silt grains are interpreted to be windblown in origin and transported from a distal source. Numerous

Figure 4.25:

Core photograph of the unconformable contact (unc) between the Nisku 2 and overlying Nisku 1 (N.1) deposits. Although the core is broken at the contact, the core pieces fit together, indicating that the contact is real. Along the contact is a thin layer of the green clay, illite (ill), interpreted to be deposited during subaerial exposure. The underlying Nisku 2 contains replacive anhydrite (Arep) and isolated remains of the host rock (Host). 9-1-28-21W4, 1842 m.

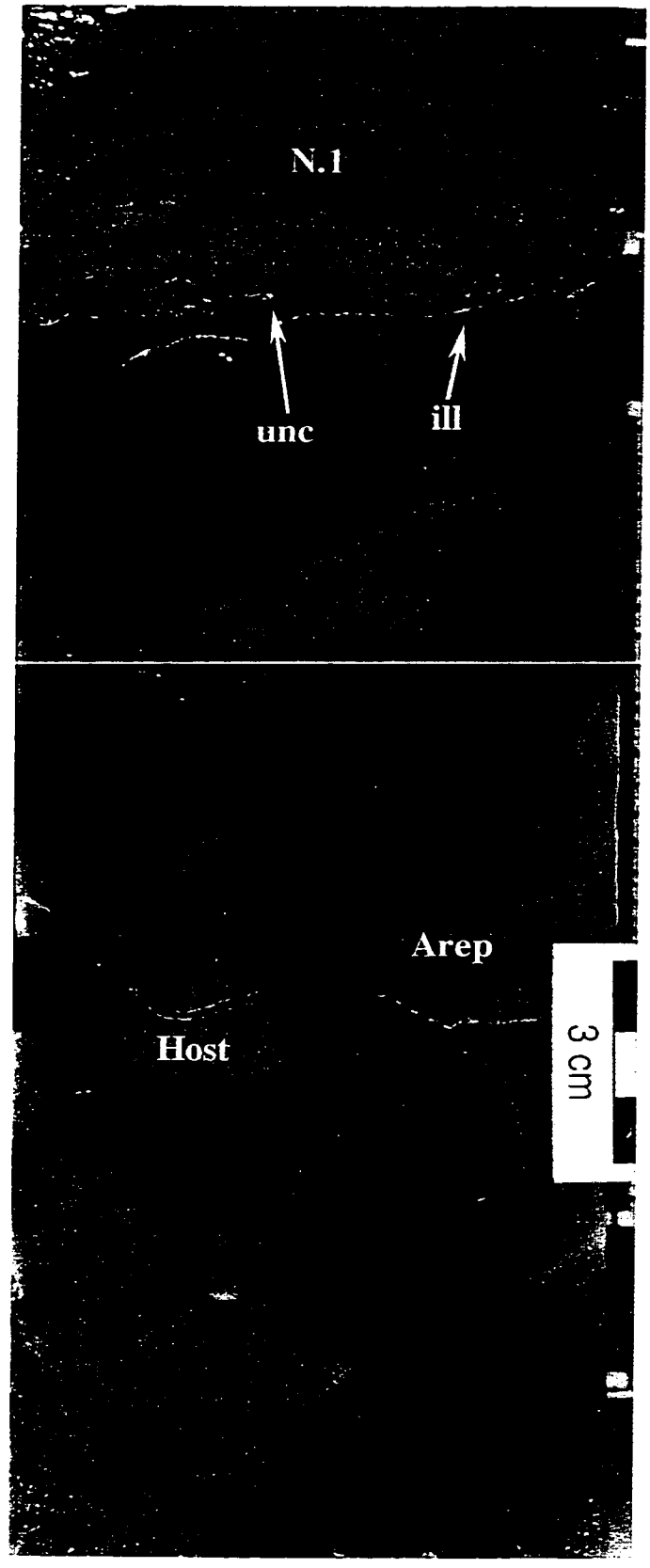
N.1
unc
ill
Arep
Host
3 cm

Figure 4.26:

Photomicrograph under cross-polarized light of the illite-rich layer (ill) at the Nisku 1 and 2 unconformable contact shown in Figure 4.25. The cryptocrystalline illite displays a straw yellow birefringence. Rounded quartz grains (qtz) are prominent along a layer in the upper part of the photomicrograph. Disseminated pyrite (pyr) is common throughout the illite. Scale bar = 250 μm.

9-1-28-21W4, 1842 m.

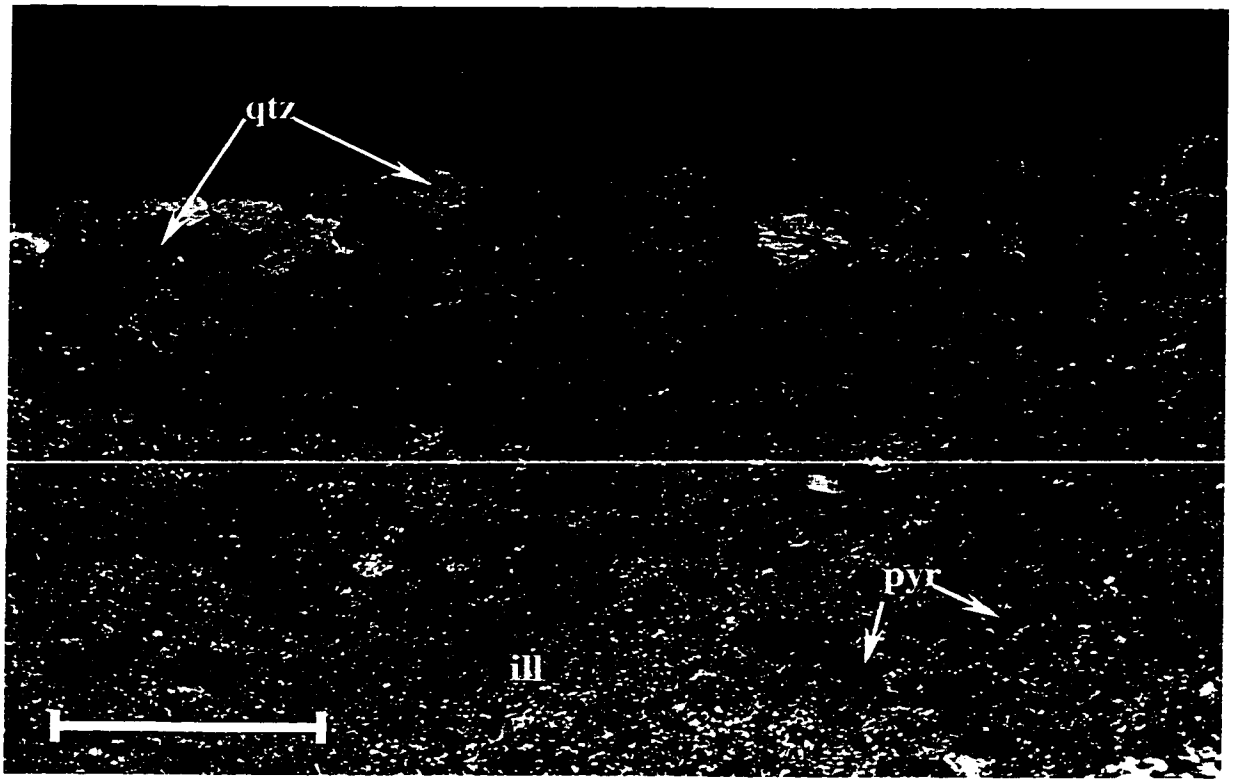
qtz
pyr
ill

WELL LOCATION: 9-1-28-21W4
DEPTH OF SAMPLE: 1842 m

MINERAL	< 2 Micron Fraction	> 2 Micron Fraction	Bulk Composition
Illite	92%	22%	37%
Anhydrite	0%	38%	31%
Quartz	8%	24%	20%
Pyrite	0%	11%	8%
Orthoclase	0%	5%	4%

Percent Material < 2 Microns: 21.8%
Percent Material > 2 Microns: 78.2%

Table 4.1 Results of X-Ray diffraction analysis of a sample from the Nisku 1 and 2 contact. Illite comprises the majority of the fine fraction and 37% of the bulk composition. Anhydrite and quartz are the next most abundant minerals.

other workers have also recognized a connection between illite-rich "green shale" and subaerial exposure (Klovan, 1964; Murray, 1966; Leavitt, 1968; Havard, 1974). It is this thin exposure horizon of green clay and quartz silt, an average of 50 cm above the coarse-crystalline RD2 dolomite horizon and 14 to 22 m above the dissolution cavity horizon, from which it is interpreted the green clay infiltrated.

The final cavity fill is in the form of PFD1 dolomite and anhydrite cements either completely infilling the entire cavity or only the portion above the inclined green sediment floors. Only near the Nisku 3 sub-unit channel margin do the dissolution cavities contain such cements. James and Choquette (1990) recognize that isopachous and blocky cements are indicative of phreatic zone precipitation. It is interpreted that the cavity filling cements precipitated in the phreatic zone with the ensuing rise in base level. No evidence of vadose precipitates, such as pendant or meniscus cements, are present to prove otherwise.

Based on the sediment-fill of the cavities, it is possible to determine the relative age and mechanism responsible for the creation of the cavity system. Dissolution of the cavities obviously took place before deposition of the DS dolomite crystal silt, thus constraining cavity formation to a period prior to or during subaerial exposure between the Nisku 1 and 2 sub-units. Evidence supporting the formation of cavities during subaerial exposure is discussed below.

In the study area, the cavity system aerially extends at least 8 km^2, is developed over a narrow vertical range, is laterally correlatable, and maintains a consistent range in depth below the Nisku 1 and 2 contact. James and Choquette (1990) state that minor exposure can result in relatively deep penetration of meteoric water and associated meteoric diagenesis. As a result, three main zones are affected by dissolution (corrosion) during this time. The three zones are: (i) the exposure surface itself through physical and biogenic corrosion, (ii) the vadose-phreatic interface where changing Pco_2 causes corrosion, and (iii) the mixing zone where changing salinity between fresh and marine waters causes corrosion.

Evidence indicating surface corrosion, such as rhizoliths, paleosoils, calcretes, vertical pipes or small karren, is not present within or near the dissolution cavity horizon. Therefore is is not believed that the cavity system formed via surface corrosion.

Evidence for or against mixing zone corrosion is less easily obtained, although the large-scale lenticular shape expected to be encountered in a mixing zone model is not apparent along the length of the dissolution cavity system. Therefore, a mixing zone dissolution mechanism is not believed to be responsible for the cavity system.

Evidence for dissolution at the vadose-phreatic interface is supported by the generally flat, widespread horizon of horizontally elongate dissolution cavities. The narrow vertical range of the cavity system is consistent with a slightly shifting water table below an unconformable subaerial exposure surface. It is then interpreted that the green sediment-filled cavity system was created at or near the water table present beneath the unconformity-related subaerial exposure surface which followed deposition of the Nisku 2 sub-unit.

(b) Dark Brown Sediment-Floored Cavities: The similarity of the cavity flooring sediment to its surrounding RD1 dolomitized matrix suggests a very local origin for the dark muds. Evidence of crystal silt or other vadose-transported materials is not apparent within the dark muds. The presence of dark organic insolubles likely indicates a residual origin from the dissolved matrix. It is then proposed that the dark brown sediment represents the remains of the dissolved host rock as the cavities were created. The similar appearance of the fine dolomite crystals in the sediment to that of the host rock suggests that cavity dissolution and sediment fill took place prior to pervasive RD1 dolomitization of the Nisku Formation.

The most striking feature of these dark mud-based dissolution cavities is that they are lithofacies specific, although not every instance of Lithofacies J contains the cavities nor are they specific to one stratigraphic horizon. Based on the cavity distribution and sediment fills, a subaerial exposure surface likely did not determine the distribution of the cavities. A more random control, yet only affecting Lithofacies J, must have been at work.

The choice of non-fabric selective dissolution mechanisms that do not involve the direct influence of vadose meteoric waters is limited. The mixing zone, where phreatic fresh and marine waters meet, is recognized as a highly corrosive environment in carbonates (James and Choquette, 1990). However, mixing zone dissolution displays an overall lenticular shape along a specific horizon, not a patchy distribution throughout the platform. Nor is mixing zone dissolution restricted to one lithofacies but instead corrodes all rock types along its path. Mixing zone dissolution is likely not responsible for the dark mud-floored cavity system.

The other dissolution possibility is the burial diagenetic environment. Non-fabric selective cavities can be created in the subsurface by reactions involving organic compounds such as liquid hydrocarbons and/or organic acids (Choquette and James, 1990). Termed *hypogenic*, such cavities lack any genetic relationships to recharge from the overlying subaerial surface (Palmer, 1991). For dissolution cavities to be initiated, pre-existing pore networks such as fractures or bedding partings are required to allow undersaturated water to flow past the soluble walls (Palmer, 1991). Lithofacies J is somewhat unique in the high density of fractures throughout. It is possible that this extensive fracture network influenced the initiation of hypogenic dissolution cavities only within Lithofacies J. Furthermore, the random positioning of the cavities is better explained by a hypogenic origin rather than a near surface meteoric control.

It is then interpreted that the dark mud-floored dissolution cavities unique to Lithofacies J were created and filled in a relatively deep subsurface diagenetic environment.

(C) *Breccias*:

Considering the position of the collapse breccias at the base of the dissolution cavity system, it is interpreted that these breccias are the result of collapse of the lower portion of the cavity system. Supporting evidence comes from specific core examples. Laterally adjacent to the collapse breccia in the 4-24-28-21W4 well is a thick interval of intact anhydrite-filled dissolution cavities in 13-13-28-21W4. Furthermore, the upper green sediment-filled cavities in the 4-24-28-21W4 well are over 2 m lower than their lateral

counterpart. Based on the lack of green clay in the breccia matrix, collapse of the lower cavity system took place after green sediment deposition in the upper cavity zone. Zoned PFD1 dolomite cements precipitated in the void spaces after initial collapse of the strata. Burial compaction and/or further dissolution likely resulted in the preferential preservation of the stoichiometrically more stable exteriors of the zoned PFD1 dolomite crystals and their displacement into the remaining pore space. The fossil fragments and carbonate detritus are interpreted to be undissolved remains of the host rock. The replacive chalcedony and anhydrite cement are both later diagenetic phases.

The thickest interval of dissolution as well as the greatest amount of collapse is present along the Nisku 3 sub-unit channel margin. It is proposed that this area experienced the greatest exposure, that is, was uplifted the highest (discussed in Chapter 5), at the time of the Nisku 1 and 2 unconformity. Consequently, shifts in the water table were the most pronounced and resulted in a wider band and denser concentration of dissolution cavities along the Nisku 3 sub-unit channel margin than areas to the southwest. In combination with the thickest amount of overburden, collapse of the cavity system was more common and pronounced along this less competent, near-channel area.

Determination of the origin of randomly positioned crackle/mosaic breccias is not straightforward but it is likely that most are related to dissolution associated with the subaerial exposure at the Nisku 1 and 2 contact. Conversely, some breccias may be tectonic in origin, especially those that are highly fractured yet display no obvious features associated with collapse.

(D) *Fossil Molds*:

Unless incorporated into a cavity system, fossil molds lack the internal sediment and zoned PFD1 dolomite cement fills common to the non fabric-selective cavities. Considering that the development and sediment fill of most cavities is interpreted to be related to the subaerial exposure between the Nisku 1 and 2 sub-units, it is unlikely that the fossil molds were formed through the same process yet were not filled by similar sediments or cements. It is then interpreted that the formation of fossil molds had to have taken place after the subaerial exposure at the Nisku 1 and 2 contact.

Some fossil molds are completely filled by coarse-crystalline, non-zoned PFD2 dolomite cement. However, the majority of molds contain only a lining of smaller dolomite crystals similar in appearance to the RD1 dolomite. Based on the similar appearance and dimensions, it is likely that the mold-lining dolomite crystals are a continuation of the matrix replacement RD1 dolomite and precipitated during pervasive RD1 dolomitization of the host rock. Therefore, fossil molds were either open prior to or were created during RD1 dolomitization. During dolomite replacement, skeletal fragments are commonly dissolved out in order to contribute carbonate to the dolomitization process (F.J. Lucia, personal communication). Similar mechanisms of porosity creation during dolomitization have been documented in the literature (e.g. Weyl, 1960; Lucia, 1962; Purser et al., 1994). If taken too far however, dolomitization can result in occlusion of pore space by dolomite cement. It is interpreted that both processes affected the Nisku strata during pervasive dolomitization. Fossil molds were formed through dolomitization, but in some areas they were locally cemented by PFD2 dolomite because RD1 dolomitization reached a pore-filling stage.

As previously discussed, the author accepts the commonly held pervasive dolomitization model of seepage-reflux during the Famennian. Therefore, formation of fossil molds and precipitation of mold-lining/filling dolomite is interpreted to be of Famennian age.

4.36 DISCUSSION

Slingsby and Aukes (1989) state that during deposition of three Nisku members, multiple subaerial exposures caused meteoric diagenesis. Various dissolution and collapse features including vugs, molds, crackle breccias and collapse breccias are present. A regionally extensive solution collapse breccia is identified as forming the top of the middle Nisku member, with unconformable contacts above and below.

Kissling (1996) also recognizes repeated exposures, erosion, and karst development throughout three Nisku members. The karsting resulted in extensive leaching, collapse

brecciation and calcium sulphate cementation, and was especially prevalent during middle, upper, and post- Nisku Formation deposition.

Agreement exists between previous work and the present study with regard to the occurrence and general effects of early diagenesis on the Nisku Formation. However, the present study goes beyond simple identification and interpretation of cavity formation and attempts to determine the specific mechanisms and timing of the products of diagenesis. A significant contribution from the present study is the identification of an intraformational unconformity within the Nisku Formation and its association with dolomitization, dissolution, sediment fill, and collapse brecciation. Furthermore, it is also concluded that voids were created and filled after deposition of the Nisku Formation, indicating that diagenesis has been a dynamic process throughout the history of the formation.

4.4 ANHYDRITE

4.41 DESCRIPTION, DISTRIBUTION, AND INTERPRETATION

Four types of diagenetic anhydrite are recognized within the Nisku Formation: (a) poikilotopic, (b) nodular, (c) replacive, and (d) pore-filling, and are briefly discussed below. However, before specifically addressing each it is important to note that the presence of the mineral anhydrite does not necessarily mean that anhydrite was the original sulphate precipitate. It is common for anhydrite to replace gypsum through de-watering and/or burial (Kendall, 1992).

(a) Poikilotopic anhydrite is distinguished where coarse anhydrite cement crystals enclose smaller grains of dolomite. The anhydrite crystals can be over 100 μm in size but most are smaller. Poikilotopic anhydrite is present only within Lithofacies B and E, both members of the hypersaline Nisku 1 sub-unit. Distribution is scattered and patchy along bedding planes. Truncation of individual anhydrite crystals is common at bedding contacts within Lithofacies E, implying the presence of calcium sulphate saturated brines early in the history of the sediment.

(b) Nodular anhydrite is recognized in thin section by very fine (less than 5 μm) anhydrite crystals forming tight interlocking mosaics. At the macro scale, expressions of nodular anhydrite vary with the lithofacies they are found in. In Lithofacies P the nodules are isolated, less than 1 cm in diameter, and displace sedimentary laminae. In Lithofacies C the nodules are 1 to 2.5 cm in diameter and are coalesced to such a degree that only wisps of dolomite separate the nodules. Most Nisku 2 sub-unit lithofacies contain anhydrite nodules as well, but in less dense concentrations. Nodular anhydrite is interpreted to form through postdepositional replacement and displacement of the host sediment.

(c) Replacement anhydrite is petrographically similar to nodular and pore-filling anhydrite with the very fine-crystalline mosaic of randomly-oriented crystals. At the macro scale the anhydrite may exist as isolated patches cross-cutting previous lithological boundaries (Figure 4.20). In other examples the replacive anhydrite may appear to form the matrix of a breccia (Figure 4.27). In this breccia-like example the anhydrite contains wisps of dolomite, the edges of the clasts are significantly faded, clasts do not support one another, and no displacement of the clasts is apparent. This breccia-like body is present immediately below the Nisku 1 and 2 contact over a thickness of 20 cm. It is interpreted that the anhydrite originated through replacement of dolomite based on: (i) the ghosts of precursor dolomite within the anhydrite, (ii) the faded reaction rims on the clasts, (iii) the fact that a cement would not be able to support breccia clasts, and (iv) the lack of clast displacement. Other minor zones of anhydrite within the Nisku 2 sub-unit display similar features but are more random in distribution. Similar to the conclusion made by Whittaker and Mountjoy (1996), replacement anhydrite is not as abundant as pore-filling anhydrite within the Nisku Formation.

(d) Pore-filling anhydrite is recognized in thin section in two forms. The first is blocky with large, commonly corroded crystals over 1 cm in length. The blocky crystals are typically adjacent to the pore wall or else completely fill the void. The second form is a very fine-crystalline mosaic with crystals less than 5 μm in size. The mosaic anhydrite commonly occupies the remaining pore space in conjunction with the first blocky type or

Figure 4.27:

Medium brown host dolomudstone (Host) has been partly replaced by cloudy white anhydrite (Arep). Where in contact with the anhydrite, the edges of the host rock are faded to a cream colour.
14-23-28-21W4, 1781.2 m.

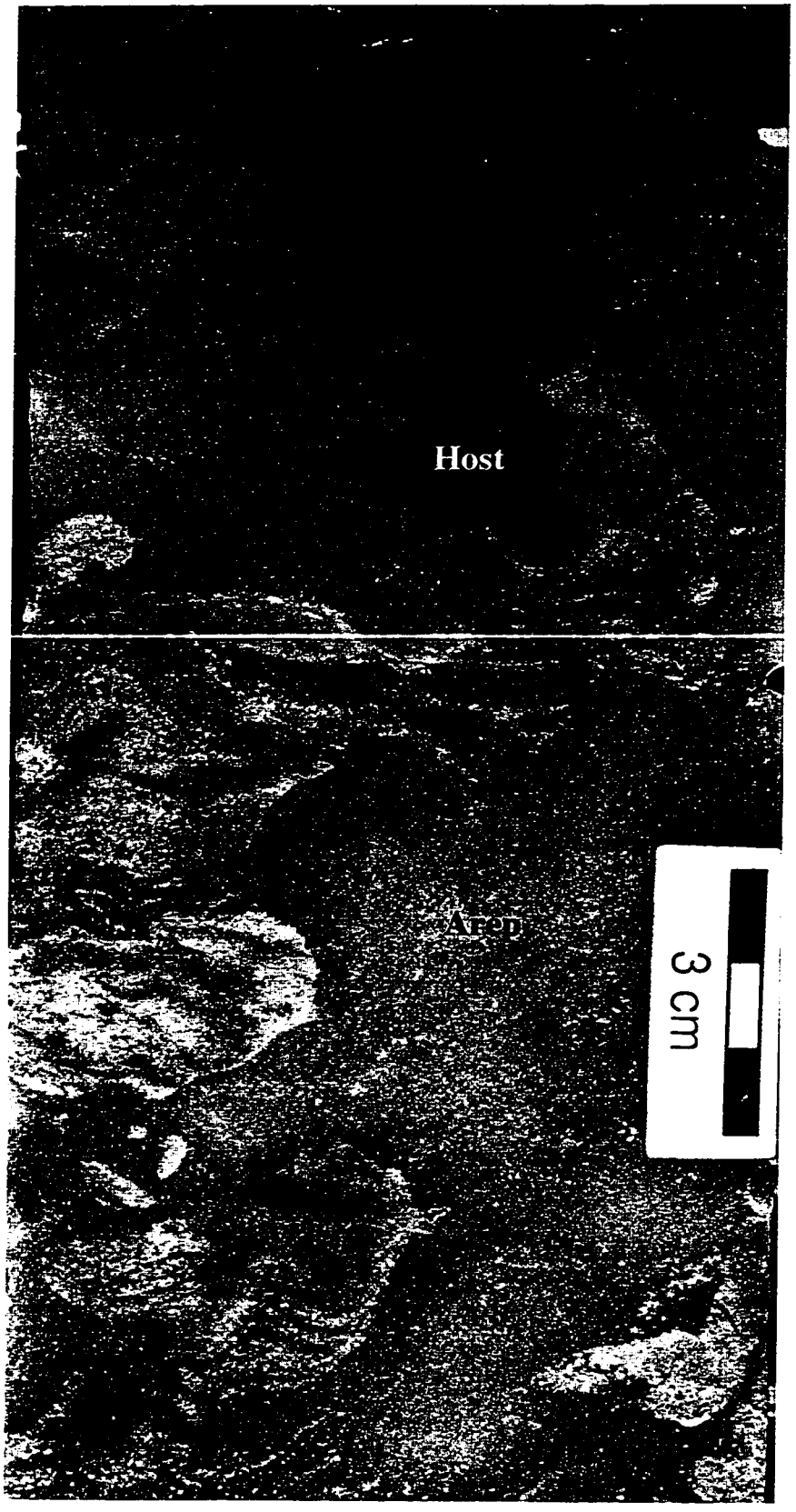
Host
3 cm

else completely fills the pores on its own. At the macro scale the blocky anhydrite crystals are well formed and nearly transparent, whereas the mosaic anhydrite appears as a snow-white dense mass. Both anhydrite forms may partially or completely fill all pore types including fossil molds, fractures, solution-enlarged fractures, vugs, cavities, breccias, intrafossil pore space, intercrystalline pore space, and intracrystalline pore space. Both forms are present in virtually every carbonate lithofacies of the Nisku and are the most abundant type of anhydrite in the study area. Based on the corrosion as well as its preference to line the pore walls, it is likely that the blocky anhydrite precipitated before the mosaic anhydrite (Figure 4.28). Various anhydrite-filled diagenetic features crossing over one another indicate multiple stages of influx of sulphate-rich fluids and anhydrite precipitation. Considering the variety and ages of voids that anhydrite cements are present in, pore-filling anhydrite is interpreted to have precipitated repeatedly over the diagenetic history of the Nisku Formation.

Sulphur isotope analysis was performed on a small number of anhydrite samples to determine if values would differ to a high enough degree to warrant further analysis of a larger sample size. Isotopically, none of the anhydrite phases analyzed display any significant differences in $\delta^{34}S$ values (Table 4.2) despite their petrographic variations. All samples are near +25‰, the same $\delta^{34}S$ value recognized by Claypool et al. (1980) to be characteristic of Frasnian-aged evaporites. Considering that the sulphur-oxygen bonds are virtually impossible to break once the original sulphate forms, it is not surprising to encounter diagenetic anhydrite with isotopes similar to their original Late Devonian source (I. Hutcheon, personal communication). Therefore, distinguishing when separate diagenetic phases were precipitated within the Nisku Formation is not possible based on isotopic analysis of sulphur.

4.42 DISCUSSION

Whittaker and Mountjoy (1996) recognize fibrous to bladed anhydrite cements as common pore-fillers of the Nisku Formation and believe they precipitated over a wide time

Figure 4.28:

Photomicrograph under cross-polarized light of very coarse-crystalline blocky (Ab) and very fine-crystalline mosaic (Am) anhydrite cements adjacent to zoned PFD1 dolomite cement crystals (PFD1). Corroded edges (corr) are present on the PFD1 dolomite crystals as well as the blocky anhydrite crystals. Scale bar = 250 μm.
14-11-28-21W4, 1839.3 m.

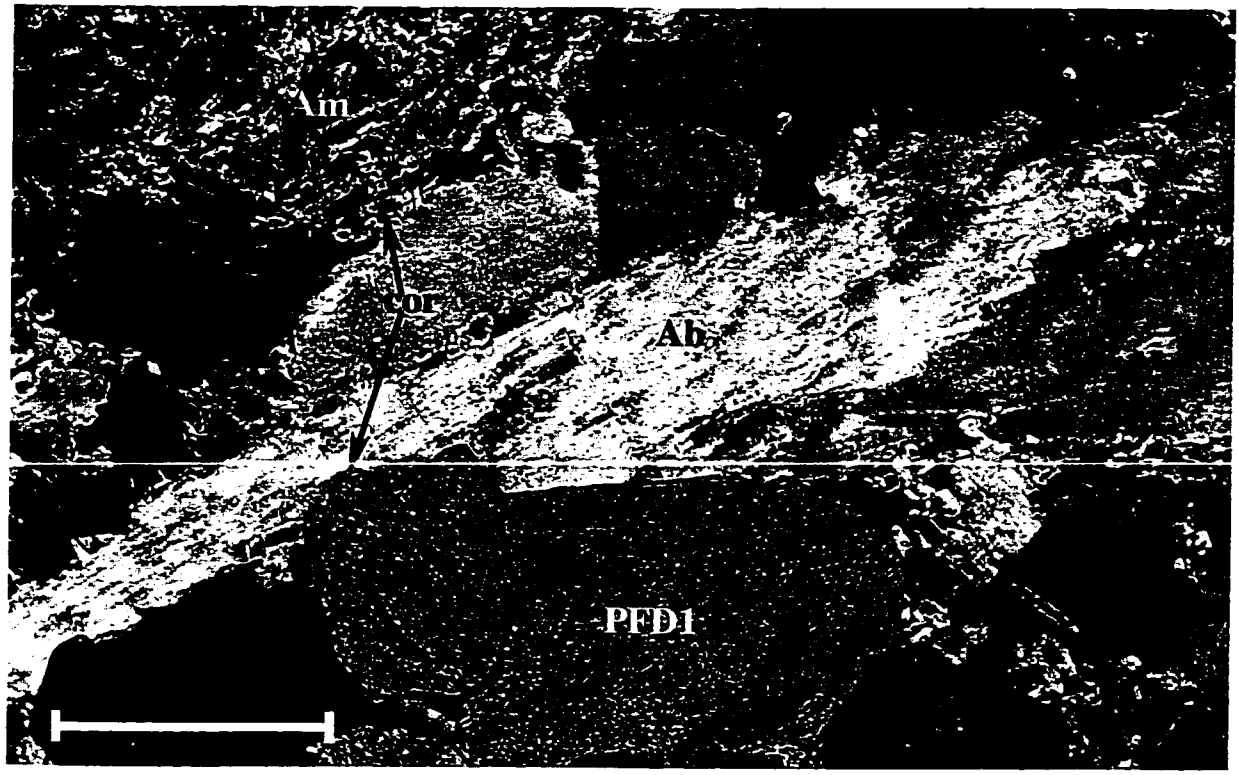
Am
or
Ab
PFD1

WELL LOCATION	DEPTH	ANHYDRITE PHASE	$\delta^{34}S$
09-01-028-21W4	1842 m	Replacement	+25.11, +25.28
10-03-028-21W4	1801.4 m	Replacement	+25.11
10-03-028-21W4	1803.25 m	Bladed Cement	+24.89
16-12-028-21W4	2062.8 m	Mosaic Cement	+24.50

Table 4.2 Sample location, depth, and sulphur isotopic composition of three phases of diagenetic anhydrite. All values are near +25 $\delta^{34}S$.

frame, including the Late Devonian to Permian and the Cretaceous to Tertiary. Replacement anhydrite, however, is considered rare by the workers and is not discussed.

In the present study a variety of diagenetic anhydrites are recognized, but pore-filling anhydrite is by far the most abundant. Fabric relationships reveal multiple stages of precipitation of the cement, unfortunately the precise timing is beyond the scope of this study.

4.5 OTHER DIAGENETIC FEATURES

4.51 FRACTURES

Most fractures present within the study area are open and of hairline widths. However, solution-enlarged or completely cemented fractures are also present. No consistent pattern of fracture orientation, aperture, or length is apparent in core. Fractures commonly cross-cut one another as well as most other diagenetic features. Larger fractures are generally associated with breccias.

Fractures are ubiquitous throughout the Nisku 2 and 3 sub-units, although their density tends to vary with location, age, and even host lithofacies (Lithofacies J). Within the Nisku 2 sub-unit, fractures are most abundant immediately adjacent to the Nisku 3 sub-unit channel and become less numerous progressively further away from the channel edge.

Most near-channel fractures are thought to be related to the collapse of the main dissolution cavity system as well as other less significant collapse breccia zones. Some of these fractures may also have been created through local tectonics. If the position of the Nisku 3 sub-unit channel is in fact controlled by a fault (to be discussed in chapter 5), it may be possible for the fault to have reactivated following Nisku deposition and to have caused fracturing in the immediate zone of stress. All of the Nisku deposits, regardless of location, were fractured to some degree during burial due to episodes of regional tectonism.

4.52 MISCELLANEOUS

Other diagenetic features present within the Nisku Formation are mentioned but not described or interpreted in detail:

Calcite cement is rare, but where present it commonly displays crystals near 200 μm in length, with some over 4 mm in length. The calcite occupies pore spaces adjacent to corroded portions of the coarse-crystalline replacement dolomite (D2b), especially in fractures and near stylolites. Some crystals may completely surround corroded anhydrite crystals. Calcite is most common, but in small amounts, just below the Nisku 1 and 2 contact. Based on fabric relationships with other cements, fractures, and stylolites, calcite is interpreted to be a late-stage pore filler.

Pyrite is petrographically recognized as disseminated opaque particles prevalent within green clay zones, breccias, and along stylolites. Pyrite is interpreted to be the result of the combination of iron and sulphur that were residual components of green clay zones, breccias, and stylolites.

Chalcedony crystals, most over 1 mm in diameter, are recognized in thin section as displaying radial extinction and quartz-like birefringence. Crystals nucleate around rock fragments and are most common in the matrices of breccias and along stylolites. Chalcedony is interpreted to be a relatively late stage replacement phase.

Stylolites are recognized as irregular- and jagged-shaped concentrations of green clay and other insolubles. Amplitudes are rarely higher than 1 cm. No other diagenetic phases have been observed to cross-cut stylolites. Stylolites are common throughout the Nisku Formation, especially the more carbonate-rich Nisku 2 and 3 sub-units. Stylolites are interpreted to be the insoluble remnants of pressure solution. The observation that calcite, pyrite, and chalcedony congregate in close proximity to stylolites implies that the stylolites periodically acted as conduits for the fluids precipitating these later diagenetic phases. Formation of stylolites is believed to initiate at a few hundred metres of burial depth (Wendte, 1998). Since all dolomite crystals are cross-cut by stylolites, latest D1 dolomitization must have occurred before stylolitization in depths of a few hundred metres or less.

4.6 PARAGENESIS AND SEQUENCE OF DIAGENETIC EVENTS

The following sequence is an interpretation of the paragenesis and relative timing of diagenetic events. No attempt is made to place the occurrence of phases into strict temporal periods. The simple classification of either *Early* or *Late* diagenesis correspond to eogenetic and mesogenetic stages, respectively.

EARLY DIAGENESIS

1. Coarse-crystalline dolomitization (RD2)
2. Meteoric corrosion of coarse-crystalline dolomite (creation of RD2b)
3. Cavity formation at or near vadose-phreatic contact
4. DS dolomite crystal silt migration into cavities
5. Green clay infiltration between RD2b dolomite crystals and into cavities
6. Collapse brecciation
7. Dolomite cementation (PFD1)
8. Anhydrite replacement and cementation (?)
9. Pyritization (?)
10. Burial compaction and fracturing

LATE DIAGENESIS

11. Cavity formation and insitu deposition of dark brown sediment
12. Anhydrite cementation (?)
13. Pervasive dolomitization (RD1)
14. Formation of fossil molds
15. Dolomite cementation (PFD2)
16. Compaction and fracturing
17. Anhydrite cementation (?)
18. Pressure solution
19. Chalcedony precipitation
20. Pyritization
21. Calcite cementation

22. Emplacement of hydrocarbons

4.7 SUMMARY

Based on fabric relationships, there is considerable evidence for early diagenesis of the Nisku in the Wayne area. Specifically, interpretations of vadose silt and infiltrated green clay support the presence of a meteoric diagenetic system beneath an unconformity-related subaerial exposure surface at the end of Nisku 2 sub-unit deposition. Immediately below the exposure surface, coarse, corroded dolomite crystals (RD2b) with intercrystalline green clay flag the occurrence of early dolomitization. Figure 4.29 schematically summarizes the interpreted early diagenetic events.

Late diagenesis has also left its mark on the Nisku Formation. Most recognizable is the pervasive dolomitization (RD1) of the strata and the associated development of fossil molds. Other features are more host-specific such as the cavity formation and insitu sediment fill of Lithofacies J. Anhydrite cementation was episodic throughout the burial history of the Nisku, resulting in the occlusion of significant amounts of pore space.

There are limitations of this study, however. Since little geochemical analysis was performed, proposed timing and mechanisms of some diagenetic events are not as time constrained as possible. Isotope and fluid inclusion analysis, especially of dolomite cement and replacement phases, would likely assist in obtaining more precise interpretations on timing. Furthermore, the limited distribution and depths of core recovery have hindered an assessment of the possible diagenetic influences of processes after Nisku deposition on early formed Nisku structures.

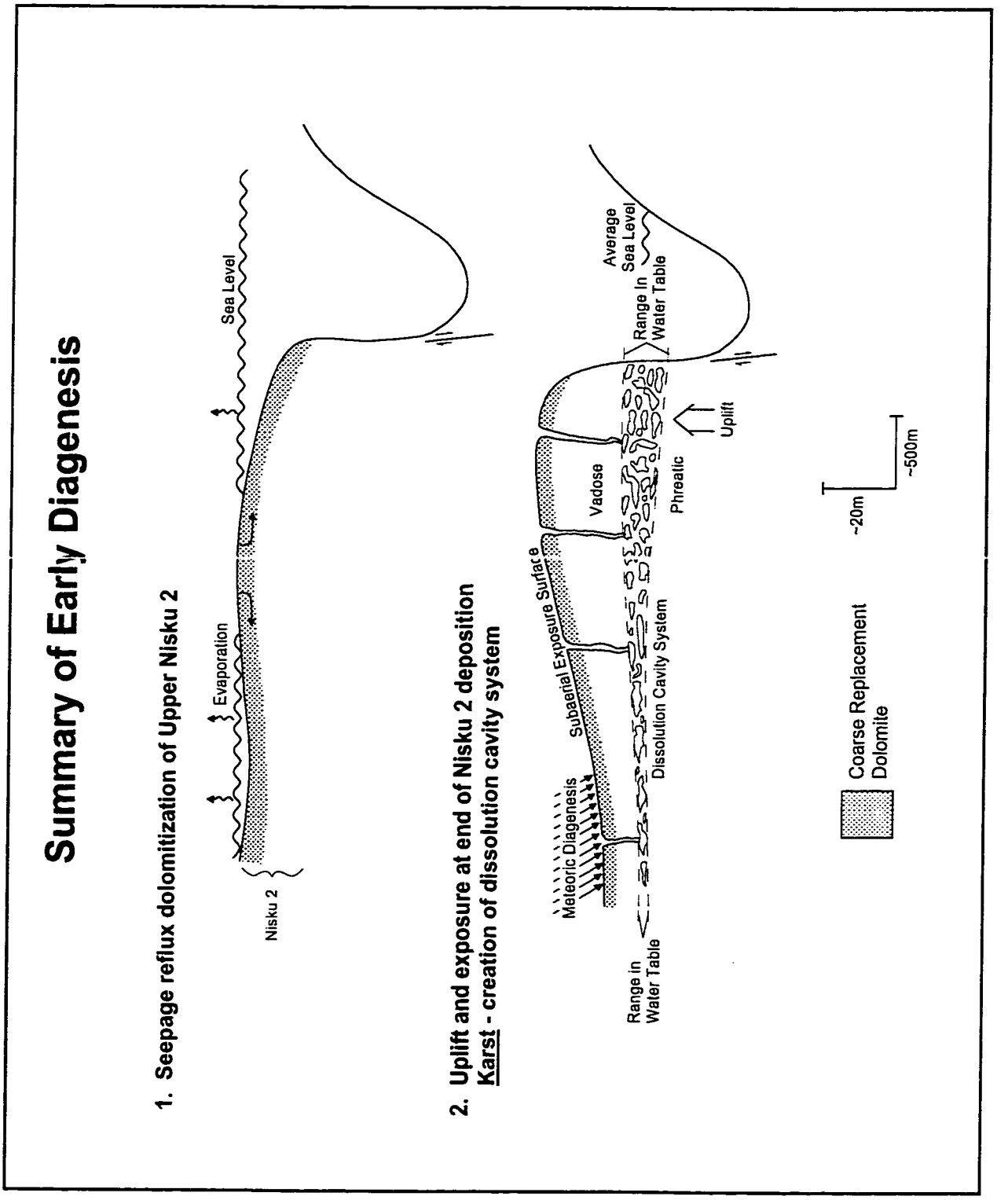

Figure 4.29 Schematic of early diagenetic influences on the Nisku 2 unit proximal to the Nisku 3 channel margin. Estimated average sea level positions are represented in the Nisku 3 channel.

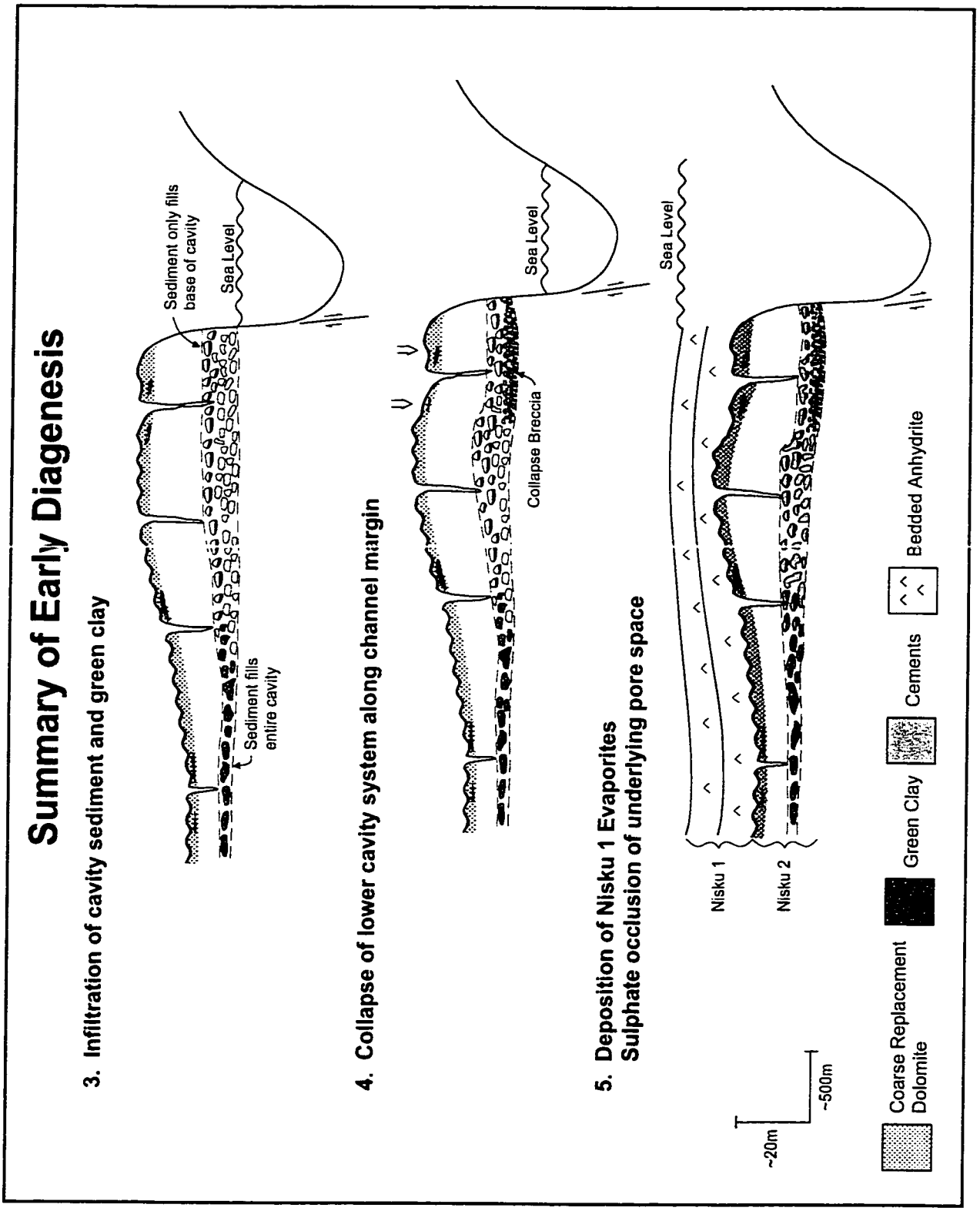

Figure 4.29 Continued.

Chapter 5 STRUCTURE

Potential structural influences on the Nisku Formation, before, during and after deposition, are of importance in unraveling the depositional and diagenetic history of the Nisku Formation. However, such influences are not readily apparent and therefore, indirect methods must be applied to discern their nature.

The northeasterly edge to all of the Wayne pools is straight and trends in a NW-SE orientation. This edge corresponds to the margin of the Nisku 3 sub-unit channel, which provides the updip trap for the hydrocarbon accumulations along the entire length of the Wayne field. The Nisku 3 sub-unit channel is linear over the 12 km that it stretches between pools and maintains a narrow, 600 to 800 m range in width along its extent (Figure 2.3). Such a long, narrow feature is likely not purely depositional in nature. It is probable that there is underlying structural involvement with the positioning of the Nisku 3 sub-unit channel and corresponding Wayne updip edges.

Salt dissolution is considered as a possible mechanism for the creation of the Nisku 3 sub-unit channel. Localized dissolution of salt-rich formations, such as the Prairie Evaporite of the Elk Point Group (Meijer Drees, 1994), may have occurred below the Nisku Formation in the study area. However, it does not seem likely that pure salt dissolution could have been responsible for the long, narrow channel within which Nisku 3 sub-unit sediments were deposited. Salt-dissolution along a conduit fault is a more likely option, or simply faulting without salt dissolution.

The Nisku Formation pools at Swalwell are aligned in similar fashion as to those along the Wayne trend (Figure 5.1). It may be no coincidence that the two fields parallel one another in the same NW-SE orientation. Babcock (1976) concludes that a regional orthogonal joint system, consisting of two sets of extension fractures parallel and normal to the Rocky Mountain fold belt, is present throughout southern Alberta (Figure 5.2). Greggs and Greggs (1989) also recognize the existence of an orthogonal fracture system throughout the Western Canada Sedimentary Basin. The fractures correspond to a global "regmatic" fracture system of NW-SE and NE-SW vertical faults (Greggs and Greggs,

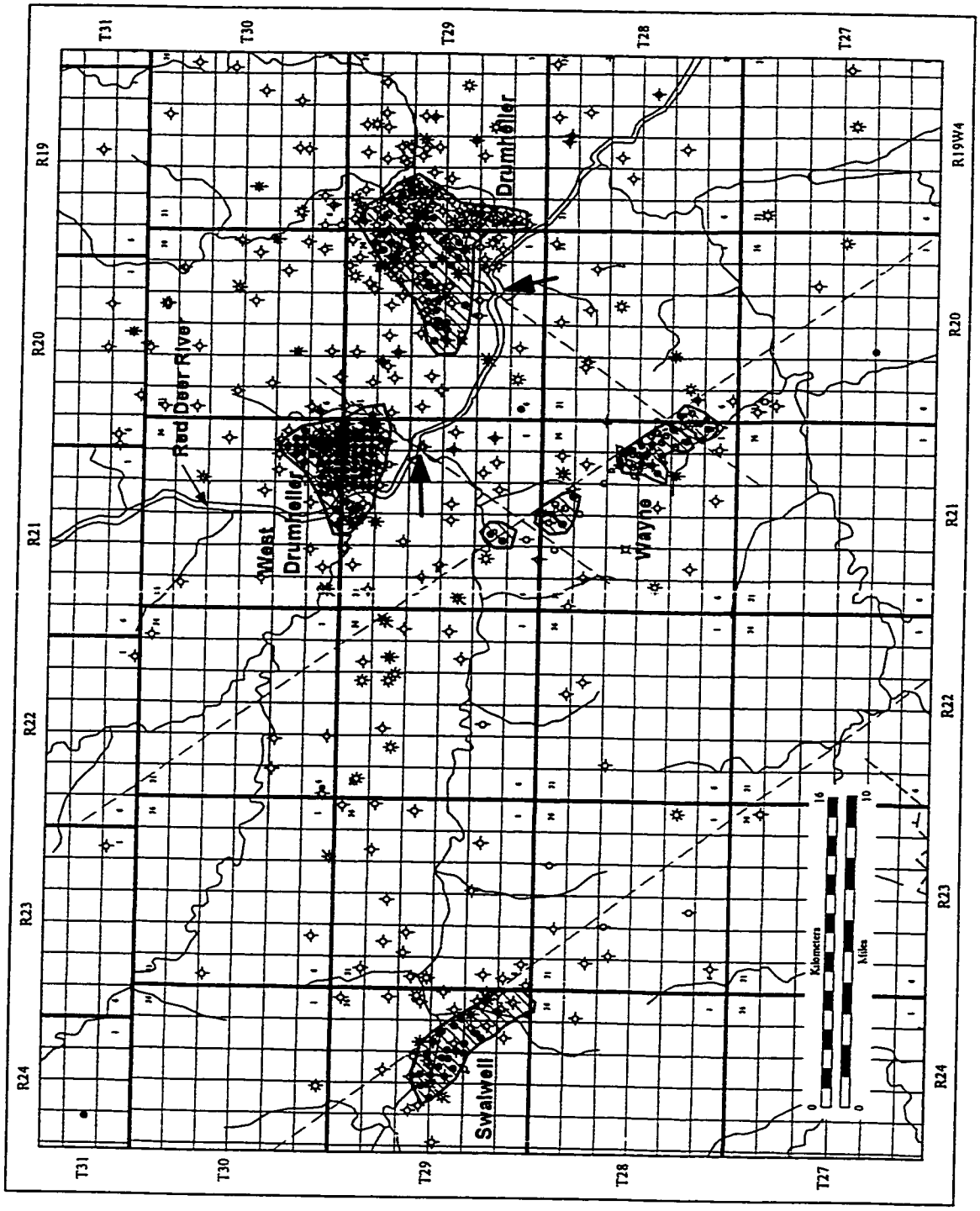

Figure 5.1 Location map of regional Nisku petroleum fields in relation to the Wayne field. Large arrows indicate where tributaries to the Red Deer River meet on opposite banks, likely related to underlying structural influences. Dashed lines are interpreted NE-SW and NW-SE structural lineaments.

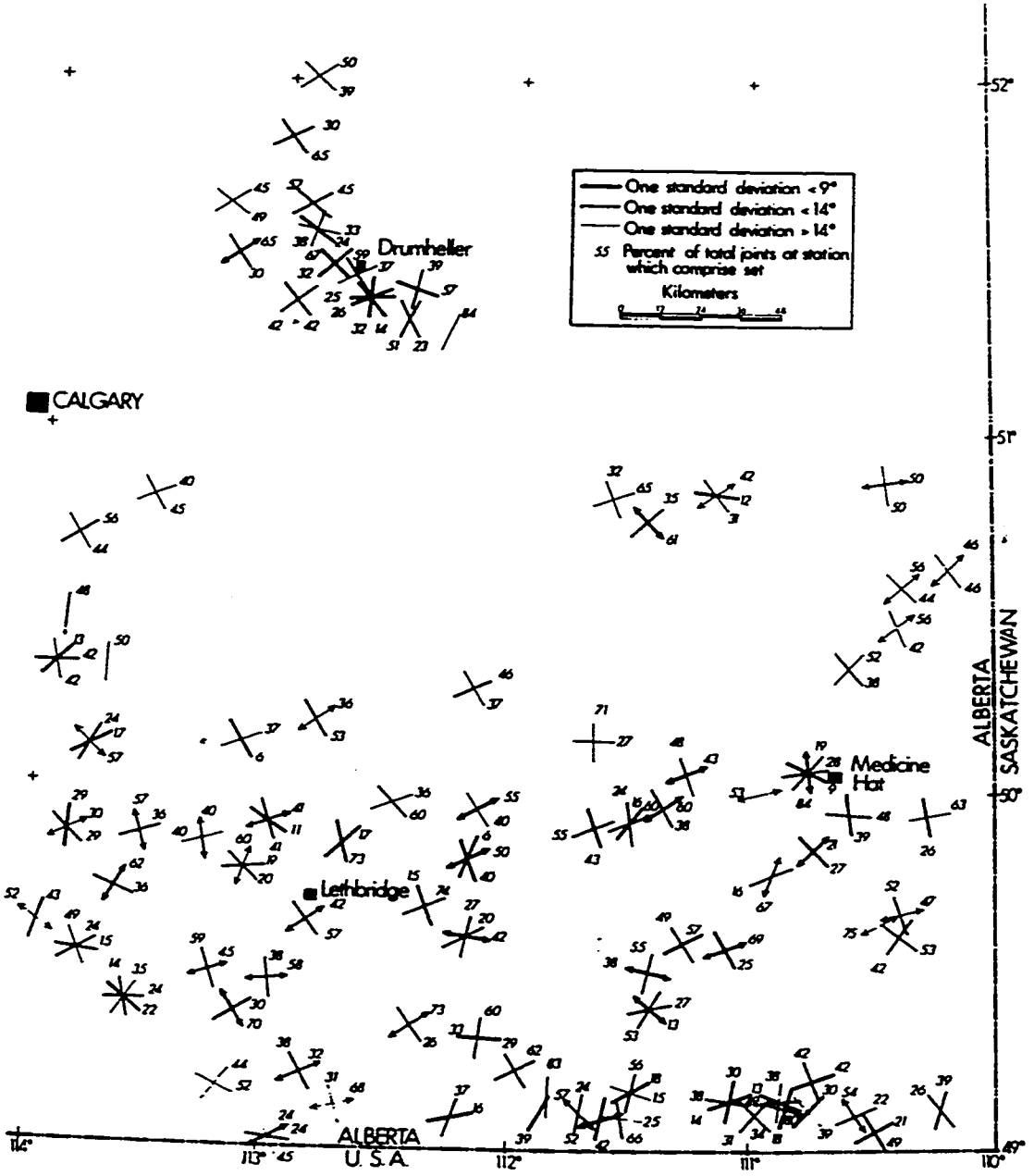

Figure 5.2 Mean strike and standard deviation about the mean of joint sets in southern Alberta. From Babcock (1976).

1989). In the Devonian subsurface of Western Canada the authors interpret the fractures to define a mosaic of fault blocks, with NW-SE the dominant breakout direction. Based on aeromagnetic data, Bower and Jain (1986) reveal two main fault trends in the Precambrian: first to develop was a NW-SE alignment and later a NE-SW trend evolved. Edwards et al. (1995) similarly distinguish a distinct NW-SE, NE-SW rectilinear grid of lineaments in central Alberta based on magnetic HGV (horizontal-gradient vector) and Bouger gravity maps (Figure 5.3). They believe the lineaments represent a pattern of fractures and faults originating in the shallow Precambrian basement and extending into the sedimentary cover. Collectively, a system of fault blocks are delineated, which have possibly experienced repeated reactivation and significant tilting over time (Edwards and Brown, 1993). Fault blocks and their movements have significant implications towards the style and distribution of overlying sediments. Kissling (1996) believes the NW-SE orientation of Nisku Formation porosity and isopach maps in southern Alberta correspond to frequently active faults in the crystalline basement during the Late Devonian. The shifting fault blocks controlled Nisku Formation paleotopography, deposition, reservoir development, and hydrocarbon entrapment (Kissling, 1996).

Within the Drumheller area, portions of the modern surface drainage channels commonly express linear patterns, with some streams directly paralleling the Wayne trend (Figure 5.1). The pronounced NW-SE linearity of the Red Deer River itself is believed to reflect underlying basement structure (Greggs and Greggs, 1989). Curiously, twice within an 8 km stretch, SW- and NE-flowing tributaries meet at the exact opposite sides of the Red Deer River (Figure 5.1). It is likely that an underlying structure controls the position where the streams join the main river. Extension of one of these NE-SW structural lineaments passes directly through the boundary between the Wayne 'A' and 'B' pools. The only significant difference between the two pools is their oil/water contacts, which differ by about 5 m. Such a barrier likely corresponds to one of the NE-SW fracture lineaments that are part of the orthogonal fracture system throughout Alberta. Arestad et al. (1995) recognize similar NE-SW-oriented features within the Nisku Formation at the Joffre field and interpret them to be faults or fractures based on 3-D seismic analysis.

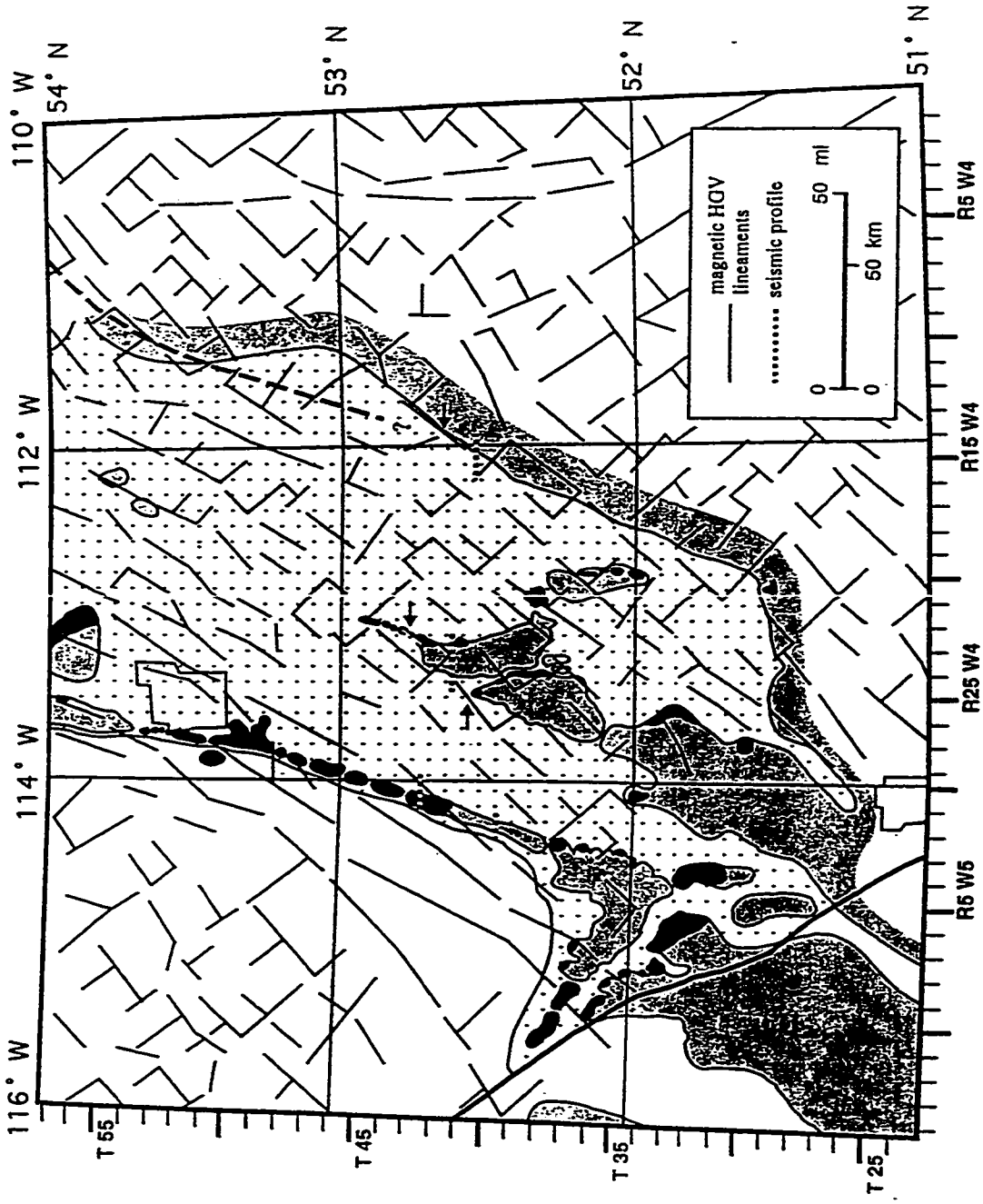

Figure 5.3 Rectilinear grid of magnetic HGV lineaments relative to the edge of the Leduc Formation in central Alberta. From Edwards et al. (1995).

It is then proposed that not only do underlying structures influence the positioning of the NW-SE trending Nisku 3 sub-unit channel, they also influence the segregation of the individual Wayne pools along NE-SW-oriented breaks. In combination, the two trends could delineate the boundaries of fault blocks, much like the fault block interpretations made by the authors previously mentioned and illustrated by Edwards and Brown (1993) (Figure 5.4). A basement-seated fault block interpretation for the study area has its merits: (a) the downthrown side of a fault block (or series of blocks) could have been the control on the position of the Nisku 3 sub-unit channel, (b) uplifted portions of fault blocks could have provided the means for increased exposure, dissolution, and brecciation at the contact between the Nisku 1 and 2 sub-units along the channel margin as well as decreased thickness of the overlying Nisku 1 sub-unit deposits, (c) lateral fault block edges may differentiate individual Wayne pools, and (d) the modern surface drainage pattern could be a reflection of the underlying fault block system.

Although only circumstantial evidence of faulting is available, the possibility that faults exist within the study area cannot be ruled out. The inferred presence of faults provide a means to explain certain depositional, diagenetic, and structural features observed within the Wayne field. Furthermore, detection of other fault-related structural lineaments within the study area has the potential to lead to the discovery of previously unrecognized Nisku Formation reservoirs.

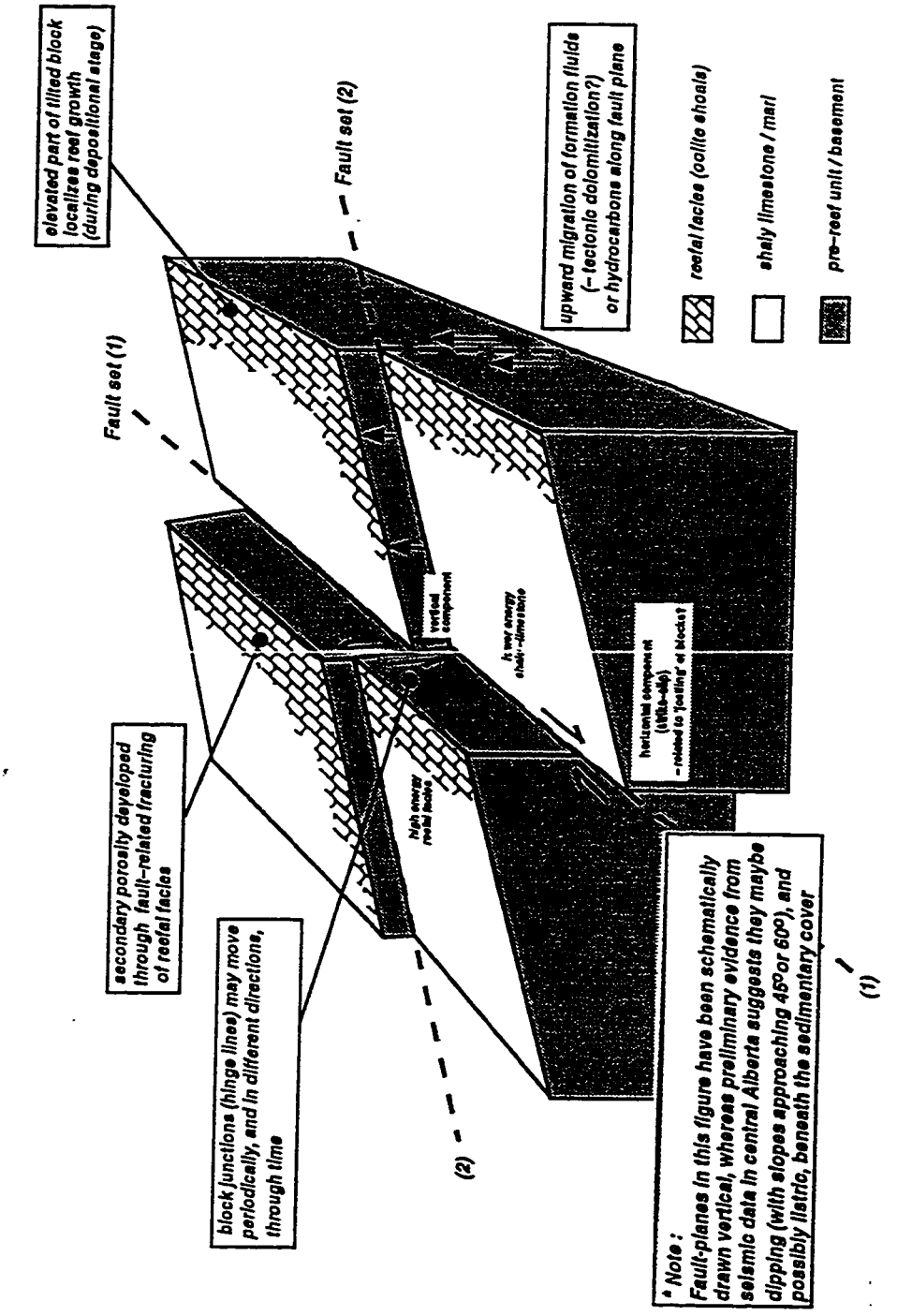

Figure 5.4 Schematic diagram of interaction between reefs and fault blocks. From Edwards and Brown (1993).

Chapter 6 SUMMARY AND CONCLUSIONS

6.1 SUMMARY

The Nisku Formation is informally divided into three sub-units within the Wayne study area. The uppermost sub-unit is distinguished as the Nisku 1. Lithofacies of the Nisku 1 sub-unit range from sulphate-rich hypersaline salina deposits to intertidally deposited dolograinstones. The evaporitic deposits of the Nisku 1 sub-unit are laterally continuous across the Wayne area.

Underlying the Nisku 1 sub-unit is the Nisku 2 sub-unit, which is sub-divided into lower and upper portions. The lower Nisku 2 sub-unit is comprised of open marine subtidal carbonate lithofacies and facies successions. The upper Nisku 2 sub-unit contains a combination of shallow subtidal and peritidal lithofacies, most of which are dolomite mud-rich, display low faunal diversities, and were deposited in restricted environments. Cycles in the upper Nisku 2 sub-unit vary with paleogeographic position and include lagoon, tidal flat, and channel margin successions. Cycles are not laterally correlatable within the study area to any significant degree.

Laterally adjacent to the Nisku 2 sub-unit platform deposits are deep subtidal deposits of the Nisku 3 sub-unit channel. Many of the channel lithofacies were deposited under quiet water, anoxic conditions. The position of the Nisku 3 sub-unit channel, which parallels the updip side of the pools of the Wayne field in a SE-NW orientation, is likely related to underlying structural influences. Based on the channel orientation and similar fill, the Nisku 3 sub-unit channel is probably connected to the Ghost Pine sub-basin.

Near the end of Nisku 2 sub-unit deposition relative sea level lowered and resulted in seepage reflux of dense brines through the topmost Nisku 2 sub-unit. Selective coarse-crystalline dolomite replacement (RD2a) of the limestone matrices took place. Continued relative sea level drop, partly due to local structural uplift, resulted in subaerial exposure following deposition of the Nisku 2 and 3 sub-units. Meteoric diagenesis caused partial dissolution of the RD2a dolomite, creation of corroded RD2b dolomite patches, and the generation of an underlying cavity system along a paleo water table. Vadose transported

DS dolomite crystal silt in the cavity sediment was sourced from the corroded RD2b dolomite. A layer of quartz-rich illite at the unconformable surface above the Nisku 2 sub-unit was the source for the infiltrated green clay in the corroded RD2b dolomite zones and between the DS dolomite crystal silt grains in the cavity sediment. Collapse of some cavity systems, particularly along the margin of the Nisku 3 sub-unit channel, resulted in collapse breccias. Cementation of cavity pore space by PFD1 dolomite and anhydrite occurred after flooding and initiation of Nisku 1 sub-unit deposition.

Large-scale seepage reflux dolomitization (RD1) of the Nisku Formation likely took place during the Famennian. The pervasive RD1 dolomite overprint obscured most depositional textures. Aggressive dolomitization resulted in the widespread creation of fossil molds and less commonly in the cementation of fossil molds by PFD2 dolomite. Late burial diagenesis included stylolitization, fracturing, pyritization, chalcedony replacement, anhydrite cementation, and calcite cementation.

6.2 CONCLUSIONS

(1) Three facies associations, the Nisku 1, 2 and 3, represent separate and distinct depositional complexes within the study area. The Nisku 1 comprises a shallow evaporitic salina to marginal salina complex, the Nisku 2 comprises a relatively shallow subtidal to peritidal carbonate platform complex, and the Nisku 3 comprises a deep subtidal carbonate channel complex.

(2) The upper Nisku 2 sub-unit contains the most diverse assemblage of lithofacies, which range from lagoonal *Amphipora* dolofloatstones, to shallow subtidal channel margin megalodont dolofloatstones, to peritidal gastropod wackestones and fenestral laminated dolomudstones. Many were deposited under stressed conditions, such as high temperatures, salinities, turbidity, and nutrient influx. Upper Nisku 2 sub-unit shallowing-upward facies successions stack upon one another at specific locations, a result of autocyclic mechanisms. Stratigraphic continuity between the cycles likely exists, but cannot be demonstrated.

(3) Laterally adjacent to the Nisku 2 sub-unit deposits, the Nisku 3 sub-unit channel is comprised of deep subtidal, massive and laminated dolomudstones and coarser-grained slope debris deposits. Zones of high total organic carbon content indicate that periods of anoxia were present during deposition. High levels of nutrient influx may have been responsible for the anoxia as well as the abundance of megalodont bivalves along the channel margin. The Nisku 3 sub-unit channel, which parallels the updip sides of the pools of the Wayne field, was probably connected with the Ghost Pine sub-basin to the northwest. Underlying structural activity likely influenced the position of the long and narrow, NW-SE trending Nisku 3 sub-unit channel.

(4) An unconformity-related subaerial exposure surface between the Nisku 1 and 2 sub-units resulted in early diagenesis of the underlying strata, including: coarse-crystalline dolomitization, meteoric corrosion, formation of an extensive water table-related dissolution cavity system, crystal silt and illite sedimentation within cavities, and collapse brecciation. Both dolomite and anhydrite were early pore-filling cements.

(5) Late diagenesis resulted in lithofacies-specific cavity formation and fill, pervasive dolomitization, fossil mold creation, and anhydrite cementation and replacement of significant portions of the Nisku Formation. Combined with the effects of early diagenesis, late diagenesis has drastically obscured the original sedimentary fabric of the Nisku Formation in the Wayne area.

(6) A tremendous amount of work can and still remains to be done on the Nisku Formation in the Wayne area. The next logical step would be to undertake a detailed geochemical study of the dolomites, particularly the C, O and Sr isotopes, as well as fluid inclusions. Cathodoluminescence and electron microprobe analyses would similarly be useful endeavors. Another line of pursuit could be towards the seemingly high total organic carbon contents of Lithofacies P and its source rock potential.

There are likely many more potential directions of scientific study, but the final suggestion regards the reservoir characteristics of the Wayne field, and includes the following potential topics of study: (a) porosity and permeability creation, evolution, and distribution, (b) hydrocarbon source and type, (c) timing and path of hydrocarbon migration, and (d) hydrogeology of the underlying aquifer and bottom-water influence on the reservoir.

REFERENCES

Adams, J.E. and Rhodes, M.G., 1960, Dolomitization by seepage refluxion: American Association of Petroleum Geologists Bulletin, v. 44, p. 1912-1920.

Adams, R.D. and Grotzinger, J.P., 1996, Lateral continuity of facies and parasequences in Middle Cambrian platform carbonates, Carrara Formation, southeastern California, U.S.A.: Journal of Sedimentary Research, v. 66, p. 1079-1090.

Aitken, J.D., 1967, Classification and environmental significance of cryptalgal limestones and dolomites, with illustrations from the Cambrian and Ordovician of southwestern Alberta: Journal of Sedimentary Petrology, v. 37, p. 1163-1178.

Algeo, T. and Maynard, J.B., 1993, The Late Devonian increase in vascular plant "rootedness": source of coeval shifts in seawater chemistry: Geological Society of America Abstracts with Programs, v. 25, p. A-83.

Arestad, J.F., Mattocks, B.W., Davis, T.L., and Benson, R.D., 1995, 3-D, 3-C seismic characterization of the Nisku carbonate reservoir, Joffre field, south-central Alberta: Canadian Society of Exploration Geophysicists Recorder, No. 4, p. 5-9.

Babcock, E.A., 1976, Bedrock jointing on the Alberta plains, *in* Hodgson, R.A., Gay, S.P. Jr., and Benjamins, J.Y., eds., Proceedings of the First International Conference on the New Basement Tectonics, Salt Lake City, Utah, June, 1974: Utah Geological Association Publication No. 5, p. 142-152.

Badiozamani, K., 1973, The Dorag dolomitization model-application to the Middle Ordovician of Wisconsin: Journal of Sedimentary Petrology, v. 43, p. 965-984.

Bathurst, R.G.C., 1975, Carbonate sediments and their diagenesis: Amsterdam, Elsevier, 658 p.

Belyea, H.R., 1955, Cross-sections through the Devonian system of the Alberta plains: Geological Survey of Canada, Paper 55-3, p. 1-29.

Bower, P. and Jain, S., 1986, Regional Precambrian surface structure in northern Alberta, from aeromagnetic maps (Abstract only): Canadian Society of Petroleum Geologists Reservoir, v. 13, p. 1-2.

Choquette, P.W. and James, N.P., 1990, Limestones – the burial diagenetic environment, *in* McIlreath, I.A. and Morrow, D.W., eds., Diagenesis: Geological Association of Canada, p. 75-111.

Chow, N., Wendte, J., and Stasiuk, L.D., 1995, Productivity versus preservation controls on two organic-rich carbonate facies in the Devonian of Alberta: sedimentological and organic petrological evidence: Bulletin of Canadian Petroleum Geology, v. 43, p. 433-460.

Clarkson, E.N.K., 1993, Invertebrate Palaeontology and Evolution, Third edition: Chapman and Hall, London.

Claypool, G.E., Holser, W.T., Kaplan, I.R., Sakai, H., and Zak, I., 1980, The age curves of sulfur and oxygen isotopes in marine sulfate and their mutual interpretation: Chemical Geology, v. 28, p. 199-260.

Cook, H.E. and Mullins, H.T., 1983, Basin margin environment, *in* Scholle, P.A., Bebout, D.G., and Moore, C.H., eds., Carbonate Depositional Environments: American Association of Petroleum Geologists, Memoir 33, p. 539-618.

Davies, G.R. and Ludlam, S.D., 1973, Origin of laminated and graded sediments, Middle Devonian of Western Canada: Geological Society of America Bulletin, v. 84, p. 3527-3546.

Deffeyes, K.S., Lucia, F.J., and Weyl, P.K., 1965, Dolomitization of Recent and Plio-Pleistocene sediments by marine evaporite waters on Bonaire, Netherlands Antilles, *in* Pray, L.C. and Murray, R.C., eds., Dolomitization and Limestone Diagenesis: Society of Economic Paleontologists and Mineralogists, Special Publication 13, p. 71-88.

de Freitas, T.A., Brunton, F., and Bernecker, T., 1993, Silurian megalodont bivalves of the Canadian Arctic and Australia: paleoecology and evolutionary significance: Palaios, v. 8, p. 450-464.

Dolphin, D.R. and Klovan, J.E., 1970, Stratigraphy and paleoecology of an Upper Devonian carbonate bank, Saskatchewan River Crossing, Alberta: Bulletin of Canadian Petroleum Geology, v. 18, p. 289-331.

Dooge, J., 1978, Stratigraphy of the Late Devonian (Frasnian) carbonate-shale transition in the Southesk Formation (Fairholme Group) at Cripple Creek (Front Ranges), *in* McIlreath, I.A. and Jackson, P.C., eds., The Fairholme Carbonate Complex at Hummingbird and Cripple Creek: Canadian Society of Petroleum Geologists, p. 53-75.

Dunham, R.J., 1962, Classification of carbonate rocks according to depositional texture, *in* Ham, W.E., ed., Classification of Carbonate Rocks: American Association of Petroleum Geologists, Memoir 1, p. 108-121.

Dunham, R.J., 1969, Early vadose silt in Townsend Mound (Reef), New Mexico. *in* Friedman, G.M., ed., Depositional Environments in Carbonate Rocks, Society of Economic Paleontologists and Mineralogists Special Publication 14, p. 139-181.

Edwards, D.J. and Brown, R.J., 1993, A geophysical investigation of basement control on reef growth, *in* Ross, G.M., ed., Alberta Basement Transects Workshop, LITHOPROBE report #31, LITHOPROBE Secretariat, University of British Columbia, p. 18-28.

Edwards, D.J., Lyatsky, H.V., and Brown, R.J., 1995, Basement fault control on Phanerozoic stratigraphy in the Western Canada Sedimentary Province: Integration of potential-field and lithostratigraphic data, *in* Ross, G.M., ed., Alberta Basement Transects Workshop, LITHOPROBE report #47, LITHOPROBE Secretariat, University of British Columbia, p. 181-224.

Eliuk, L.S., 1978, The Abenaki Formation, Nova Scotia Shelf, Canada – A depositional and diagenetic model for a Mesozoic carbonate platform: Canadian Society of Petroleum Geologists, Bulletin, v. 26, p. 424-514.

Eliuk, L.S., 1998, Big bivalves, algae and the nutrient poisoning of reefs: A tabulation with examples from the Devonian and Jurassic of Canada, *in* Johnston, P.A. and Haggart, J.W., eds., Bivalves: An Eon of Evolution, University of Calgary Press, p. 157-184.

Embry, A.F. and Klovan, J.E., 1971, A Late Devonian reef tract on northeastern Banks Island, Northwest Territories: Canadian Society of Petroleum Geologists, Bulletin, v. 19, p. 730-781.

Esteban, M. and Wilson, J.L., 1993, Introduction to karst systems and paleokarst reservoirs, *in* Fritz, R.D., Wilson, J.L., and Yurewicz, D.A., eds., Paleokarst Related Hydrocarbon Reservoirs, Society of Economic Paleontologists and Mineralogists, Core Workshop No. 18, New Orleans, p. 1-9.

Exploration Staff, Chevron Standard Limited, 1979, The geology geophysics and significance of the Nisku Reef discoveries, West Pembina area, Alberta, Canada: Canadian Society of Petroleum Geologists, Bulletin, v. 27, p. 326-359.

Folk, R.L., 1959, Practical petrographic classification of limestones: American Association of Petroleum Geologists Bulletin, v. 43, p. 1-38.

Gilhooly, M.G., 1987, Sedimentology and geologic history of the Upper Devonian (Frasnian) uppermost Ireton and Nisku Formations, Bashaw Area, Alberta. Unpublished M.Sc. Thesis, University of Calgary, 210 p.

Gilhooly, M.G., Potma, K., and Weissenberger, J.A.W., 1994, The Upper Devonian Cripple Creek reef margin: internal geometry and stratigraphic evolution: Canadian Society of Petroleum Geologists, Continuing Education Committee Field Guide, 44 p.

Greggs, R.G. and Greggs, D.H., 1989, Fault-block tectonism in the Devonian subsurface, western Canada basin: Journal of Petroleum Geology, v. 12, p. 377-404.

Hardie, L.A., Lowenstein, T.K., and Spencer, R.J., 1983, The problem of distinguishing between primary and secondary features in evaporites: Sixth International Symposium on Salt, v. 1, p. 11-39.

Havard, C.J., 1974, Sedimentary and early diagenetic cycles, Snipe Lake reef complex, Alberta. Unpublished M.Sc. Thesis, University of Calgary, 125 p.

Hearn, M.R., 1996, Stratigraphic and diagenetic controls on aquitard integrity and hydrocarbon entrapment, Bashaw reef complex, Alberta, Canada. Unpublished M.Sc. Thesis, University of Alberta, 135 p.

Hunter, I.G., 1995, Reservoir characterization of the Nisku Formation in the Swalwell area of southern Alberta: Canadian Society of Petroleum Geologists Annual Core Conference.

Imperial Oil Limited, Geological Staff, 1950, Devonian nomenclature in Edmonton area, Alberta, Canada: Bulletin of the American Association of Petroleum Geologists, v. 34, p. 1807-1825.

James, N.P., 1979, Shallowing-upward sequences in carbonates, *in* Walker, R.G., ed., Facies Models: Geoscience Canada Reprint Series 1, Toronto, p. 109-119.

James, N.P. and Choquette, P.W., 1990, Limestones – the meteoric diagenetic environment, *in* McIlreath, I.A. and Morrow, D.W., eds., Diagenesis: Geological Association of Canada, p. 35-75.

Johnson, J.G., Klapper, G., and Sandberg, C.A., 1985, Devonian eustatic fluctuations in Euramerica: Geological Society of America Bulletin, v. 96, p. 567-587.

Kendall, A.C., 1984, Evaporites, *in* Walker, R.G., ed., Facies Models: Geoscience Canada Reprint Series 1, Second edition, p. 259-296.

Kendall, A.C., 1992, Evaporites, *in* Walker, R.G. and James, N.P., eds., Facies Models: Response to Sea Level Change: Geological Association of Canada, p. 375-409.

Kirker, W.P., 1959, Devonian reef and off-reef relationships in the Drumheller area: Alberta Society of Petroleum Geologists, 9th Annual Field Conference, p. 92-102.

Kissling, D.L., 1996, The Nisku Formation of South Alberta and Northwest Montana: birth to burial of an Upper Devonian barrier-lagoon complex, *in* Longman, M.W. and Sonnenfeld, M.D., eds., Paleozoic Systems of the Rocky Mountain Region. Rocky Mountain Section, SEPM (Society for Sedimentary Geology), p. 97-116.

Klovan, J.E., 1964, Facies analysis of the Redwater reef complex, Alberta, Canada: Bulletin of Canadian Petroleum Geology, v. 12, p. 1-100.

Krumbein, W.E., 1983, Stromatolites – the challenge of a term in space and time: Precambrian Research, v. 20, p. 493-531.

Land, L.S., 1973, Contemporaneous dolomitization of Middle Pleistocene reefs by meteoric water, North Jamaica: Bulletin of Marine Sciences, v. 23, p. 64-92.

Leavitt, E.M., 1968, Petrology, palaeontology, Carson Creek north reef complex, Alberta: Bulletin of Canadian Petroleum Geology, v. 16, p. 298-413.

Logan, B.W., Hoffman, P., and Gebelein, C.D., 1974, Algal mats, cryptalgal fabrics and structures, Hamelin Pool, Western Australia: American Association of Petroleum Geologists, Memoir 22, p. 140-195.

Lucia, F.J., 1962, Diagenesis of a crinoidal sediment: Journal of Sedimentary Petrology, v. 32, p. 848-865.

Lucia, F.J., 1968, Recent sediments and diagenesis of South Bonaire, Netherlands Antilles: Journal of Sedimentary Petrology, v. 38, p. 845-858.

Lucia, F.J. and Major, R.P., 1994, Porosity evolution through hypersaline reflux dolomitization, *in* Purser, B., Tucker, M., and Zenger, D., eds., Dolomites, A volume in honour of Dolomieu: International Association of Sedimentologists, Special Publication No. 21, p. 309-324.

Meijer Drees, N.C., 1994, Devonian Elk Point Group of the Western Canada Sedimentary Basin, *in* Mossop, G.D. and Shetson, I., compilers, Geological Atlas of the Western Canada Sedimentary Basin: Canadian Society of Petroleum Geologists and Alberta Research Council, p. 129-163.

Murray, J.W., 1966, An oil producing reef-fringed carbonate bank in the Upper Devonian Swan Hills Member, Judy Creek, Alberta: Bulletin of Canadian Petroleum Geology, v. 14, p. 1-103.

Norton, W.H., 1917, A classification of breccias: Journal of Geology, v. 25, p. 160-194.

Palmer, A.N., 1991, Origin and morphology of limestone caves: Geological Society of America Bulletin, v. 103, p. 1-21.

Pederson, T.F. and Calvert, S.E., 1990, Anoxia vs. productivity: what controls the formation of organic-carbon-rich sediments and sedimentary rocks? American Association of Petroleum Geologists Bulletin, v. 74, p. 454-466.

Pemberton, S.G., MacEachern, J.A., and Frey, R.W., 1992, Trace fossil facies models: environmental and allostratigraphic significance, *in* Walker, R.G. and James, N.P., eds., Facies Models: Response to Sea Level Change: Geological Association of Canada, p. 47-72.

Peters, K.E., 1986, Guidelines for evaluating petroleum source rock using programmed pyrolysis: American Association of Petroleum Geologists Bulletin, v. 70, p. 318-329.

Pratt, B.R., 1982, Stromatolitic framework of carbonate mud-mounds: Journal of Sedimentary Petrology, v. 52, p. 1207-1227.

Pratt, B.R. and James, N.P., 1986, The St George Group (Lower Ordovician) of western Newfoundland: tidal flat island model for carbonate sedimentation in shallow epeiric seas: Sedimentology, v. 33, p. 313-343.

Pratt, B.R., James, N.P., and Cowan, C.A., 1992, Peritidal carbonates, *in* Walker, R.G. and James, N.P., eds., Facies Models: Response to Sea Level Change: Geological Association of Canada, p. 303-322.

Purser, B.H., Brown, A., and Aissaoui, D.M., 1994, Nature, origins and evolution of porosity in dolomites, *in* Purser, B., Tucker, M., and Zenger, D., eds., Dolomites, A volume in honour of Dolomieu: International Association of Sedimentologists, Special Publication No. 21, p. 283-308.

Schreiber, B.C., Friedman, G.M., Decima, A., and Schreiber, E., 1976, Depositional environments of Upper Miocene (Messinian) evaporite deposits of the Sicilian basin: Sedimentology, v. 23, p. 729-760.

Sears, S.O. and Lucia, F.J., 1980, Dolomitization of Northern Michigan Niagara reefs by brine refluxion and freshwater/seawater mixing, *in* Zenger, D.H., Dunham, J.B. and Ethington, R.L., eds., Concepts and Models of Dolomitization: Society of Economic Paleontologists and Mineralogists, Special Publication 28, p. 215-235.

Shearman, D.J. and Fuller, J.G., 1969, Anhydrite diagenesis, calcitization, and organic laminites, Winnipegosis Formation, Middle Devonian, Saskatchewan: Bulletin of Canadian Petroleum Geology, v. 17, p. 469-525.

Shields, M.J. and Brady, P.V., 1995, Mass balance and fluid flow constraints on regional-scale dolomitization, Late Devonian, Western Canada Sedimentary Basin: Bulletin of Canadian Petroleum Geology, v. 43, p. 371-392.

Shinn, E.A., 1968, Practical significance of birdseye structures in carbonate rocks: Journal of Sedimentary Petrology, v. 38, p. 215-223.

Shinn, E.A., 1983, Birdseyes, fenestrae, shrinkage pores and loferites: a reevaluation: Journal of Sedimentary Petrology, v. 53, p. 619-628.

Shinn, E.A., Robbin, D.M., and Steinen, R.P., 1980, Experimental compaction of lime sediment: Book of Abstracts, American Association of Petroleum Geologists-Society of Economic Paleontologists and Mineralogists, Annual Meeting, Denver, p. 120.

Slingsby, A. and Aukes, P.G., 1989, Geology and reservoir heterogeneity of the Enchant Arcs "F" and "G" Pools, *in* den Haan, J. and Webb, T., eds., 1989 Core Conference: Geology and Reservoir Heterogeneity: Canadian Society of Petroleum Geologists, p. 4.1-4.27.

Stoakes, F.A., 1992, Winterburn megasequence, *in* Stoakes, F.A. and Wendte, J.C., Devonian-Early Mississippian Carbonates of the Western Canada Sedimentary Basin: A Sequence Stratigraphic Framework, Society of Economic Paleontologists and Mineralogists, Short Course No. 28, p. 207-224.

Stoakes, F.A. and Creaney, S., 1984, Sedimentology of a carbonate source rock: the Duvernay Formation of central Alberta, *in* Eliuk, L., ed., Carbonates in Subsurface and Outcrop: Proceedings of the 1984 Canadian Society of Petroleum Geologists Core Conference, Calgary, p. 132-147.

Stoakes, F.A. and Creaney, S., 1985, Sedimentology of a carbonate source rock: the Duvernay Formation of Alberta, Canada, *in* Longman, M.W., Shanley, K.W., Lindsay, R.F., Eby, D.E., eds., Rocky Mountain Carbonate Reservoirs – a Core Workshop: Society of Economic Paleontologists and Mineralogists, Core Workshop No. 7, p. 343-374.

Switzer, S.B., Holland, W.G., Christie, D.S., Graf, G.C., Hedinger, A.S., McAuley, R.J., Wierzbicki, R.A., and Packard, J.J., 1994, Devonian Woodbend-Winterburn Strata of the Western Canada Sedimentary Basin, *in* Mossop, G.D. and Shetson, I., compilers, Geological Atlas of the Western Canada Sedimentary Basin: Canadian Society of Petroleum Geologists and Alberta Research Council, p. 165-202.

Van Wagoner, J.C., Posamentier, H.W., Mitchum, R.M., Vail, P.R., Sarg, J.F., Loutit, T.S., and Hardenbol, J., 1988, An overview of the fundamentals of sequence stratigraphy and key definitions, *in* Wilgus, C.K., Hastings, B.J., Posamentier, H.W., Van

Wagoner, J.C., Ross, C.A., and Kendall, C.G.St.C., eds., Sea-Level Change: An Integrated Approach: Society of Economic Paleontologists and Mineralogists, Special Publication No. 42, p. 39-46.

Warren, J.K., 1982, The hydrological setting, occurrence and significance of gypsum in late Quaternary salt lakes in South Australia: Sedimentology, v. 29, p. 609-637.

Warren, J.K. and Kendall, C.G.St.C., 1985, Comparison of sequences formed in marine sabkha (subaerial) and salina (subaqueous) settings – modern and ancient: American Association of Petroleum Geologists Bulletin, v. 69, p. 1013-1023.

Wendte, J., Qing, H., Dravis, J.J., Moore, S.L.O., Stasiuk, L.D., and Ward, G., 1998, High temperature saline (thermoflux) dolomitization of Devonian Swan Hills platform and bank carbonates, Wild River area, west-central Alberta: Bulletin of Canadian Petroleum Geology, v. 46, p. 210-265.

Weyl, P.K., 1960, Porosity through dolomitization: Conservation of mass requirements: Journal of Sedimentary Petrology, v. 30, p. 85-90.

Wilson, J.L., 1975, Carbonate Facies in Geologic History: Springer-Verlag, New York.

Whittaker, S.G. and Mountjoy, E.W., 1996, Diagenesis of an Upper Devonian carbonate-evaporite sequence: Birdbear Formation, Southern Interior Plains, Canada: Journal of Sedimentary Research, v. 66, p. 965-975.

Wood, R., 1993, Nutrients, predation and the history of reef-building: Palaios, v. 8, p. 529-543.

APPENDIX I

CORE DESCRIPTIONS:

Core descriptions of 14 cored wells within and near the Wayne 'A' and 'B' pools are provided in the following pages. Note that the rock types in the "LITHOLOGY" portion of the header of the core descriptions correspond to the lithofacies discussed in Chapter 3.

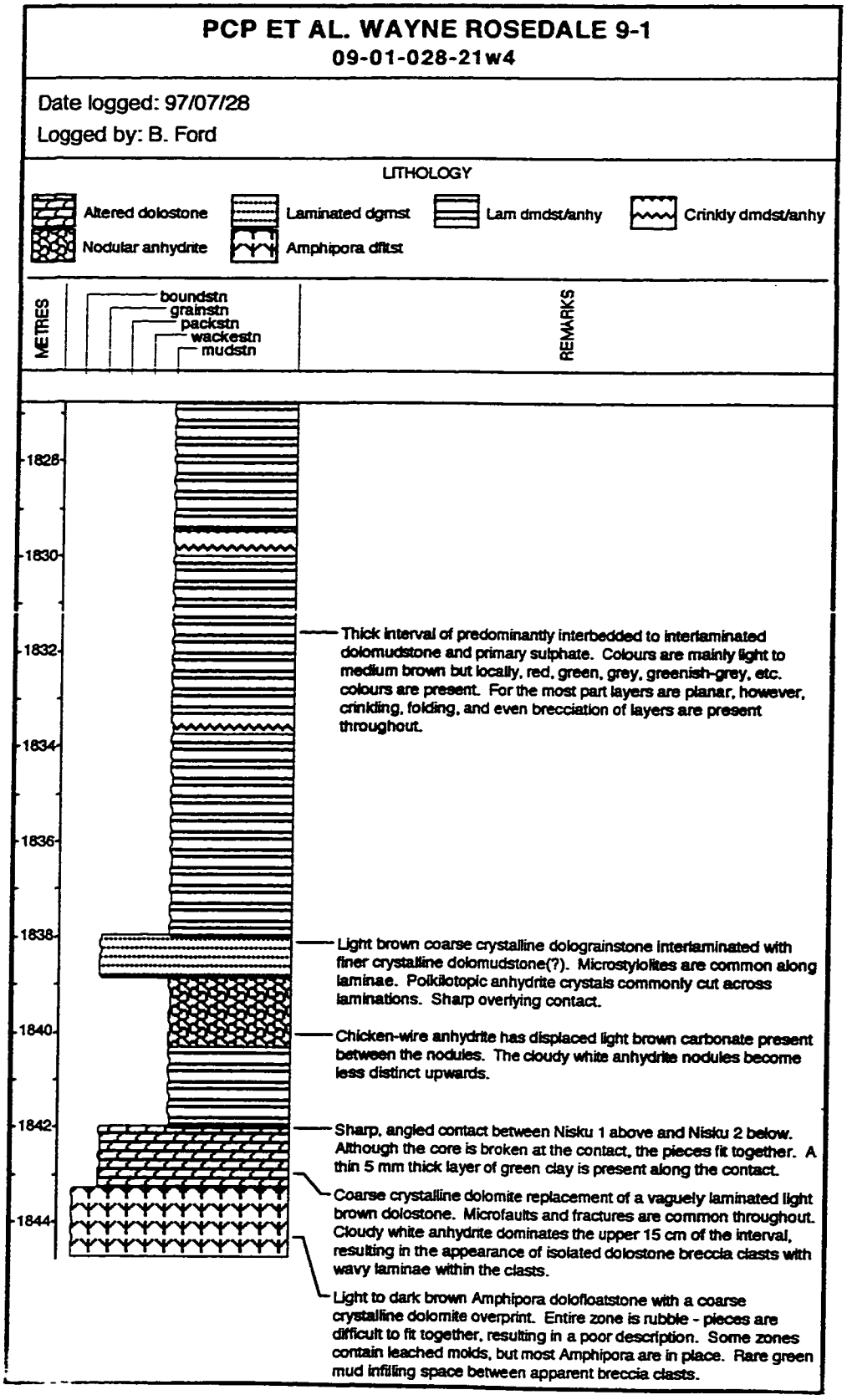
PCP ET AL. WAYNE ROSEDALE 9-1
09-01-028-21w4
Date logged: 97/07/28
Logged by: B. Ford
LITHOLOGY
Altered dolostone
Laminated dgmst
Lam dmdst/anhy
Crinkly dmdst/anhy
Nodular anhydrite
Amphipora dflst
METRES
boundstn
grainstn
packstn
wackestn
mudstn
REMARKS
1828
1830
1832
1834
1836
1838
1840
1842
1844
Thick interval of predominantly interbedded to interlaminated dolomudstone and primary sulphate. Colours are mainly light to medium brown but locally, red, green, grey, greenish-grey, etc. colours are present. For the most part layers are planar, however, crinkling, folding, and even brecciation of layers are present throughout.
Light brown coarse crystalline dolograinstone interlaminated with finer crystalline dolomudstone(?). Microstylolites are common along laminae. Poikilotopic anhydrite crystals commonly cut across laminations. Sharp overlying contact.
Chicken-wire anhydrite has displaced light brown carbonate present between the nodules. The cloudy white anhydrite nodules become less distinct upwards.
Sharp, angled contact between Nisku 1 above and Nisku 2 below. Although the core is broken at the contact, the pieces fit together. A thin 5 mm thick layer of green clay is present along the contact.
Coarse crystalline dolomite replacement of a vaguely laminated light brown dolostone. Microfaults and fractures are common throughout. Cloudy white anhydrite dominates the upper 15 cm of the interval, resulting in the appearance of isolated dolostone breccia clasts with wavy laminae within the clasts.
Light to dark brown Amphipora dolofloatstone with a coarse crystalline dolomite overprint. Entire zone is rubble - pieces are difficult to fit together, resulting in a poor description. Some zones contain leached molds, but most Amphipora are in place. Rare green mud infilling space between apparent breccia clasts.

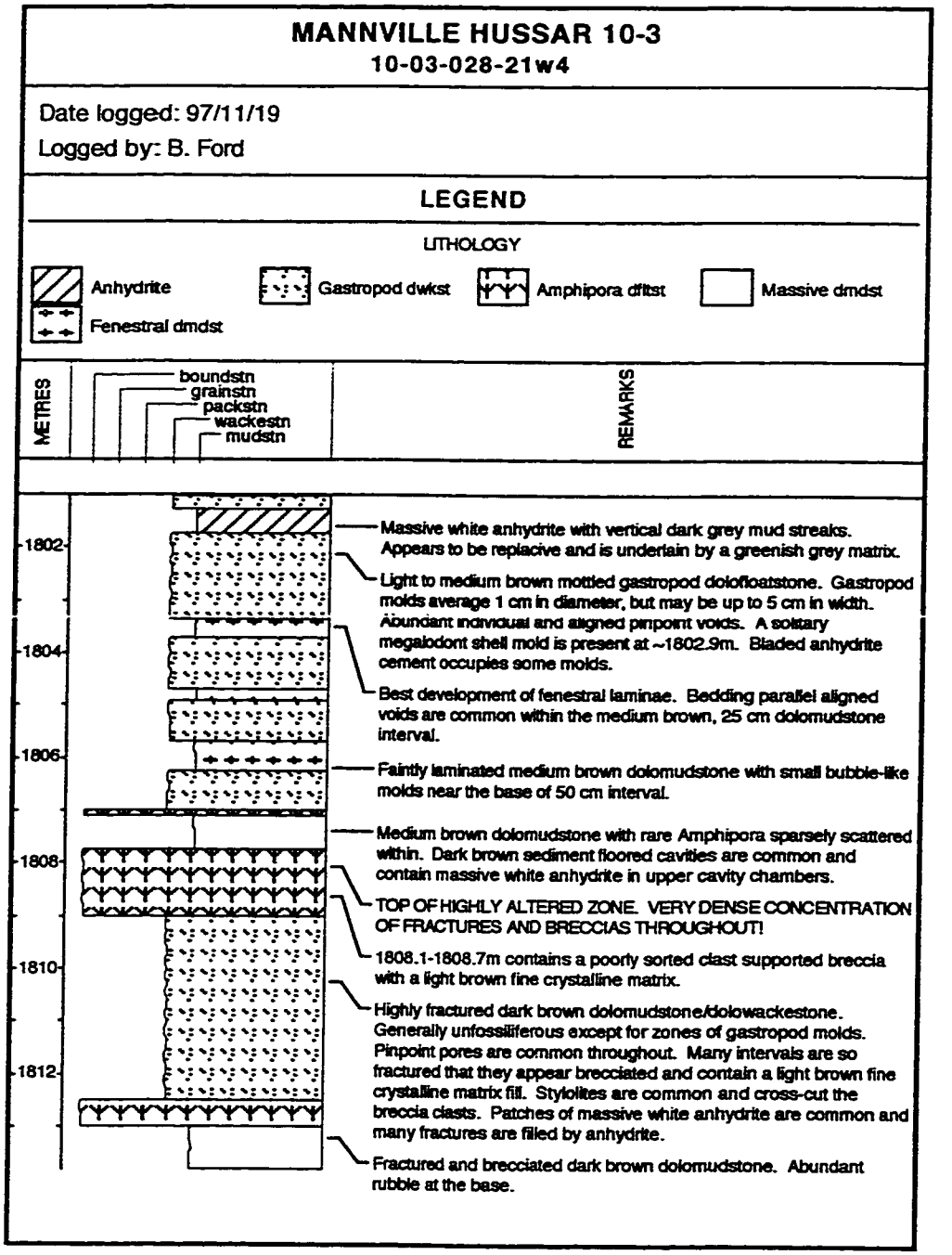
MANNVILLE HUSSAR 10-3
10-03-028-21w4
Date logged: 97/11/19
Logged by: B. Ford
LEGEND
LITHOLOGY
Anhydrite
Gastropod dwkst
Amphipora dfltst
Massive dmdst
Fenestral dmdst
METRES
boundstn
grainstn
packstn
wackestn
mudstn
REMARKS
1802
1804
1806
1808
1810
1812
Massive white anhydrite with vertical dark grey mud streaks. Appears to be replacive and is underlain by a greenish grey matrix.
Light to medium brown mottled gastropod dolofloatstone. Gastropod molds average 1 cm in diameter, but may be up to 5 cm in width. Abundant individual and aligned pinpoint voids. A solitary megalodont shell mold is present at ~1802.9m. Bladed anhydrite cement occupies some molds.
Best development of fenestral laminae. Bedding parallel aligned voids are common within the medium brown, 25 cm dolomudstone interval.
Faintly laminated medium brown dolomudstone with small bubble-like molds near the base of 50 cm interval.
Medium brown dolomudstone with rare Amphipora sparsely scattered within. Dark brown sediment floored cavities are common and contain massive white anhydrite in upper cavity chambers.
TOP OF HIGHLY ALTERED ZONE. VERY DENSE CONCENTRATION OF FRACTURES AND BRECCIAS THROUGHOUT!
1808.1-1808.7m contains a poorly sorted clast supported breccia with a light brown fine crystalline matrix.
Highly fractured dark brown dolomudstone/dolowackestone. Generally unfossiliferous except for zones of gastropod molds. Pinpoint pores are common throughout. Many intervals are so fractured that they appear brecciated and contain a light brown fine crystalline matrix fill. Stylolites are common and cross-cut the breccia clasts. Patches of massive white anhydrite are common and many fractures are filled by anhydrite.
Fractured and brecciated dark brown dolomudstone. Abundant rubble at the base.

PCP HUSSAR 14-11

14-11-028-21w4

Date logged: 97/07/28

Logged by: B. Ford

LEGEND

LITHOLOGY

Altered dolostone | Gastropod dwkst | Massive dmdst | Coarse cryst dolost

Cavity system | Amphipora dfltst | Thamnopora dfltst

boundstn
grainstn
packstn
wackestn
mudstn

METRES

REMARKS

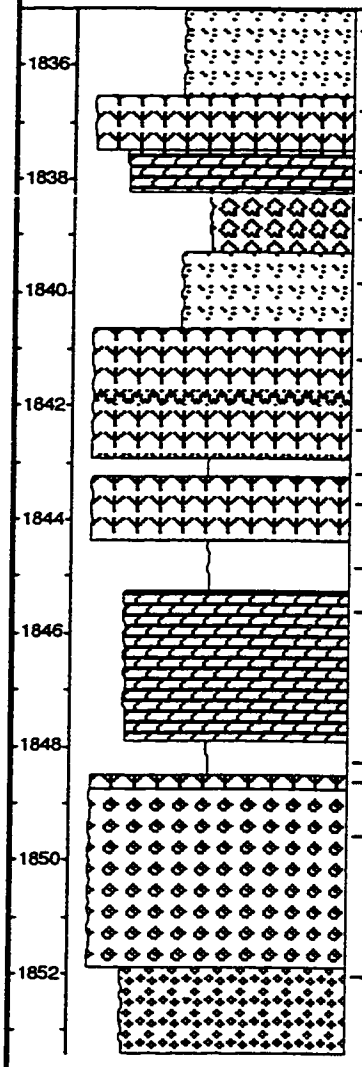

Light brown gastropod dolowackestone with abundant pinpoint pores.

Light brown Amphipora dolofloatstone contains thin intervals of breccias with dark brown mud fill

Diagenetically altered area overprints previous fabric; contains a breccia with dark brown mud and chalky light brown mud matrixes. Fractures are abundant. Cloudy white patches are common.

Irregular-shaped dissolution cavities, up to 8 cm in diameter, are filled by a green mud. Later anhydrite cross-cuts some of the cavity fills and the host rock.

Medium brown gastropod dolowackestone with abundant pinpoint pores. Dark brown/grey mottling is present throughout. Fractures display a distinct orientation, 30 degrees from vertical.

Amphipora dolofloatstone. Fossils are not abundant, resulting in a dolomudstone appearance in places. Microvugs are present throughout the medium brown to grey matrix.

Highly altered light to dark brown Amphipora dolofloatstone. Numerous fractures, grainy portions, small open vugs, and cloudy white anhydrite patches. Verges toward a breccia in places.

Light brown dolomudstone with irregular small vugs and dark brown mottling.

Similar to altered dolofloatstone above.

Similar to dolomudstone above.

Top of extremely diagenetically altered zone. Numerous matrix-supported breccias over a 2.5m interval. Angular clasts range from 1cm to over 5cm in diameter and may display inclined bedding, suggestive of tilting. Matrix is a light brown fine crystalline dolomite and cloudy white anhydrite. Fractures are abundant.

Massive dolomudstone with dark brown sediment-floored dissolution cavites and anhydrite cement.

Thin interval of light brown dolofloatstone with numerous Amphipora molds.

Medium brown Thamnopora dolofloatstone to dolorudstone. Snow white anhydrite patches dominate ~25% of the core. Fractures are abundant.

Light to medium brown coarse crystalline dolostone. Tight packing of crystals results in a massive appearance. Common orange/reddish staining, especially around stylolites. No anhydrite, therefore good porosity.

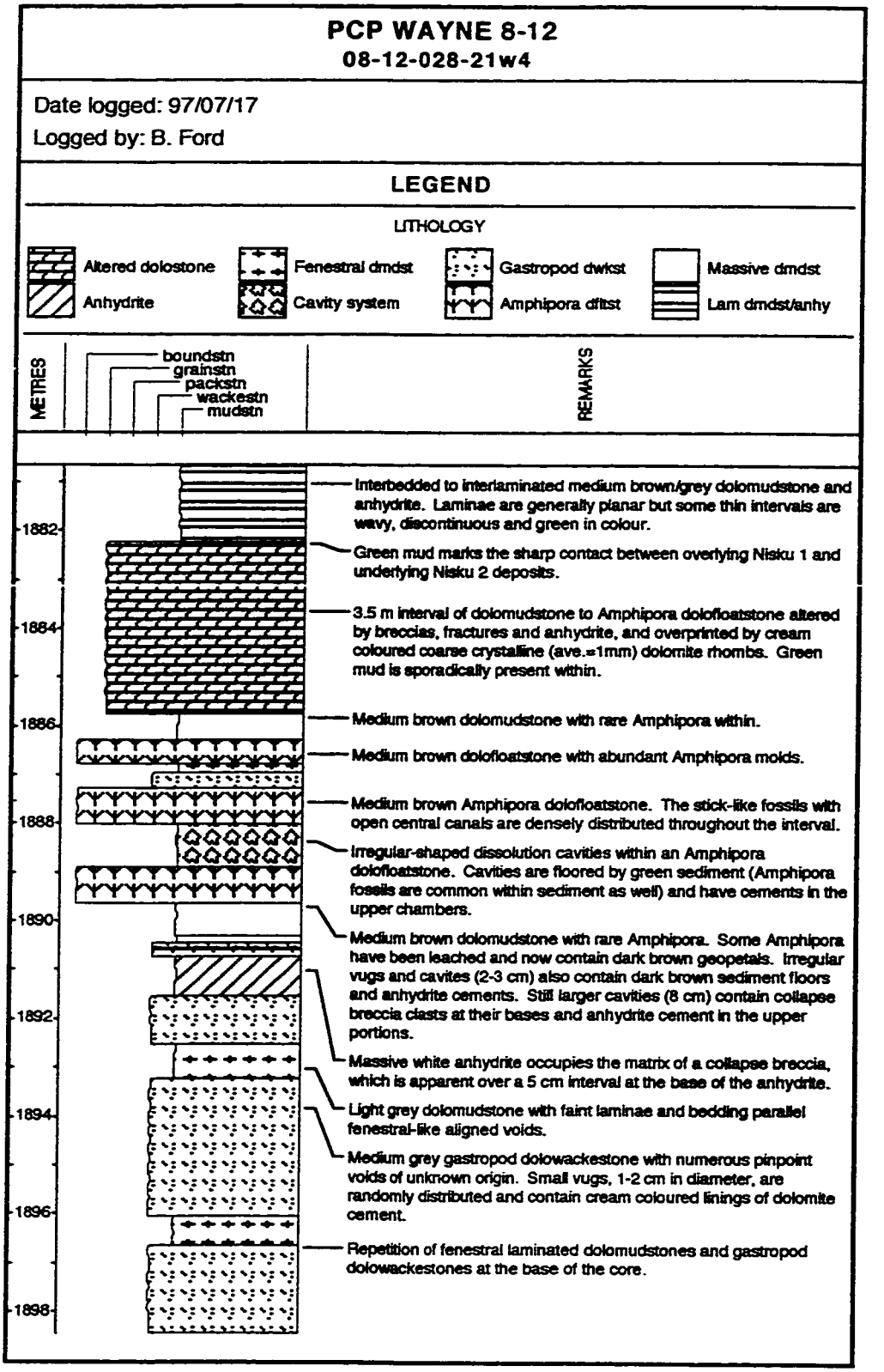
PCP WAYNE 8-12
08-12-028-21w4
Date logged: 97/07/17
Logged by: B. Ford
LEGEND
LITHOLOGY
Altered dolostone
Anhydrite
Fenestral dmdst
Cavity system
Gastropod dwkst
Amphipora dflst
Massive dmdst
Lam dmdst/anhy
METRES
boundstn
grainstn
packstn
wackestn
mudstn
REMARKS
1882
1884
1886
1888
1890
1892
1894
1896
1898
Interbedded to interlaminated medium brown/grey dolomudstone and anhydrite. Laminae are generally planar but some thin intervals are wavy, discontinuous and green in colour.
Green mud marks the sharp contact between overlying Nisku 1 and underlying Nisku 2 deposits.
3.5 m interval of dolomudstone to Amphipora dolofloatstone altered by breccias, fractures and anhydrite, and overprinted by cream coloured coarse crystalline (ave.=1mm) dolomite rhombs. Green mud is sporadically present within.
Medium brown dolomudstone with rare Amphipora within.
Medium brown dolofloatstone with abundant Amphipora molds.
Medium brown Amphipora dolofloatstone. The stick-like fossils with open central canals are densely distributed throughout the interval.
Irregular-shaped dissolution cavities within an Amphipora dolofloatstone. Cavities are floored by green sediment (Amphipora fossils are common within sediment as well) and have cements in the upper chambers.
Medium brown dolomudstone with rare Amphipora. Some Amphipora have been leached and now contain dark brown geopetals. Irregular vugs and cavites (2-3 cm) also contain dark brown sediment floors and anhydrite cements. Still larger cavities (8 cm) contain collapse breccia clasts at their bases and anhydrite cement in the upper portions.
Massive white anhydrite occupies the matrix of a collapse breccia, which is apparent over a 5 cm interval at the base of the anhydrite.
Light grey dolomudstone with faint laminae and bedding parallel fenestral-like aligned voids.
Medium grey gastropod dolowackestone with numerous pinpoint voids of unknown origin. Small vugs, 1-2 cm in diameter, are randomly distributed and contain cream coloured linings of dolomite cement.
Repetition of fenestral laminated dolomudstones and gastropod dolowackestones at the base of the core.

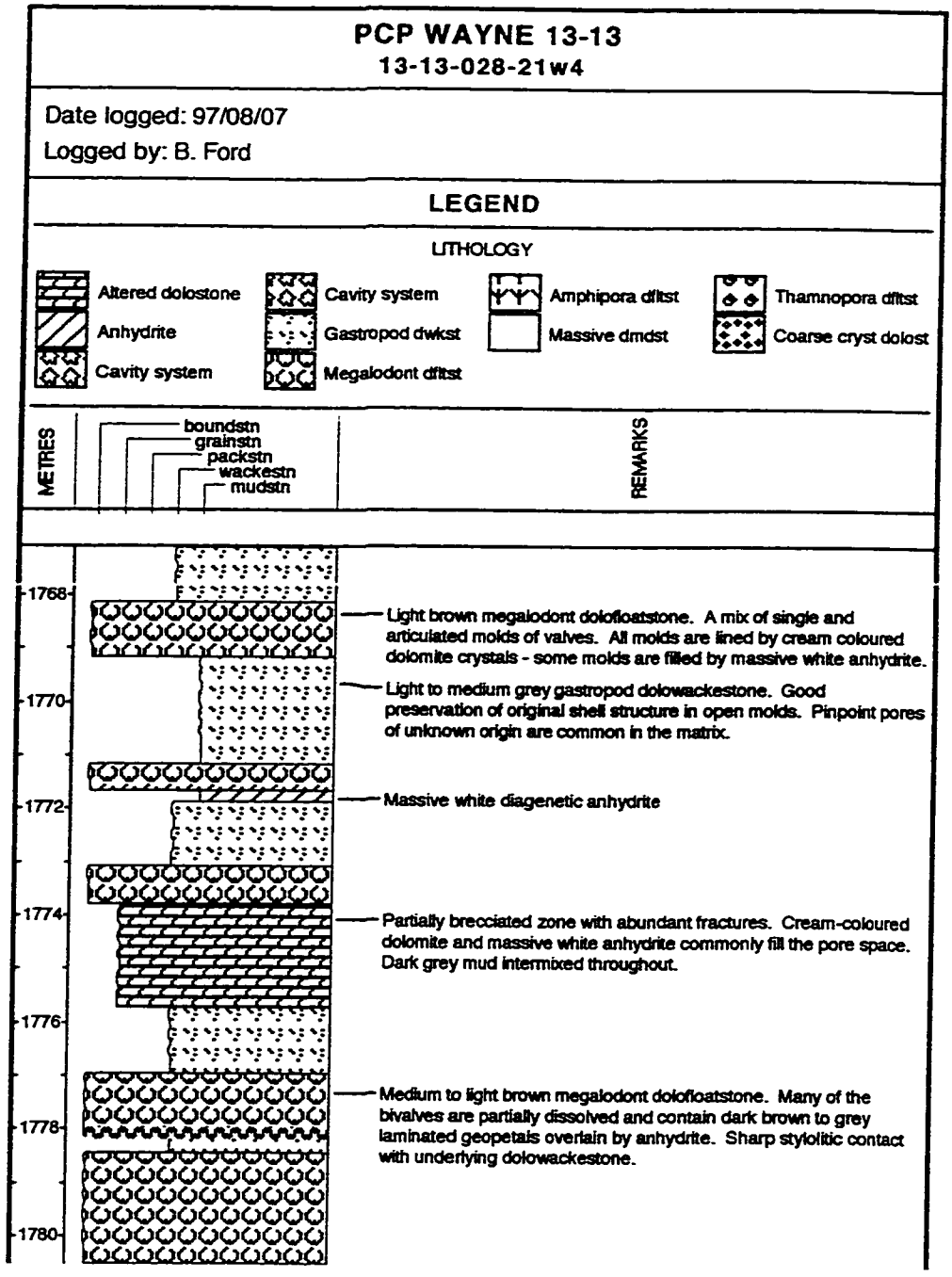
PCP WAYNE 13-13
13-13-028-21w4
Date logged: 97/08/07
Logged by: B. Ford
LEGEND
LITHOLOGY
Altered dolostone
Anhydrite
Cavity system
Cavity system
Gastropod dwkst
Megalodont dflst
Amphipora dflst
Massive dmdst
Thamnopora dflst
Coarse cryst dolost
METRES
boundstn
grainstn
packstn
wackestn
mudstn
REMARKS
1768
1770
1772
1774
1776
1778
1780
Light brown megalodont dolofloatstone. A mix of single and articulated molds of valves. All molds are lined by cream coloured dolomite crystals - some molds are filled by massive white anhydrite.
Light to medium grey gastropod dolowackestone. Good preservation of original shell structure in open molds. Pinpoint pores of unknown origin are common in the matrix.
Massive white diagenetic anhydrite
Partially brecciated zone with abundant fractures. Cream-coloured dolomite and massive white anhydrite commonly fill the pore space. Dark grey mud intermixed throughout.
Medium to light brown megalodont dolofloatstone. Many of the bivalves are partially dissolved and contain dark brown to grey laminated geopetals overlain by anhydrite. Sharp stylolitic contact with underlying dolowackestone.

13-13-28-21W4 Continued

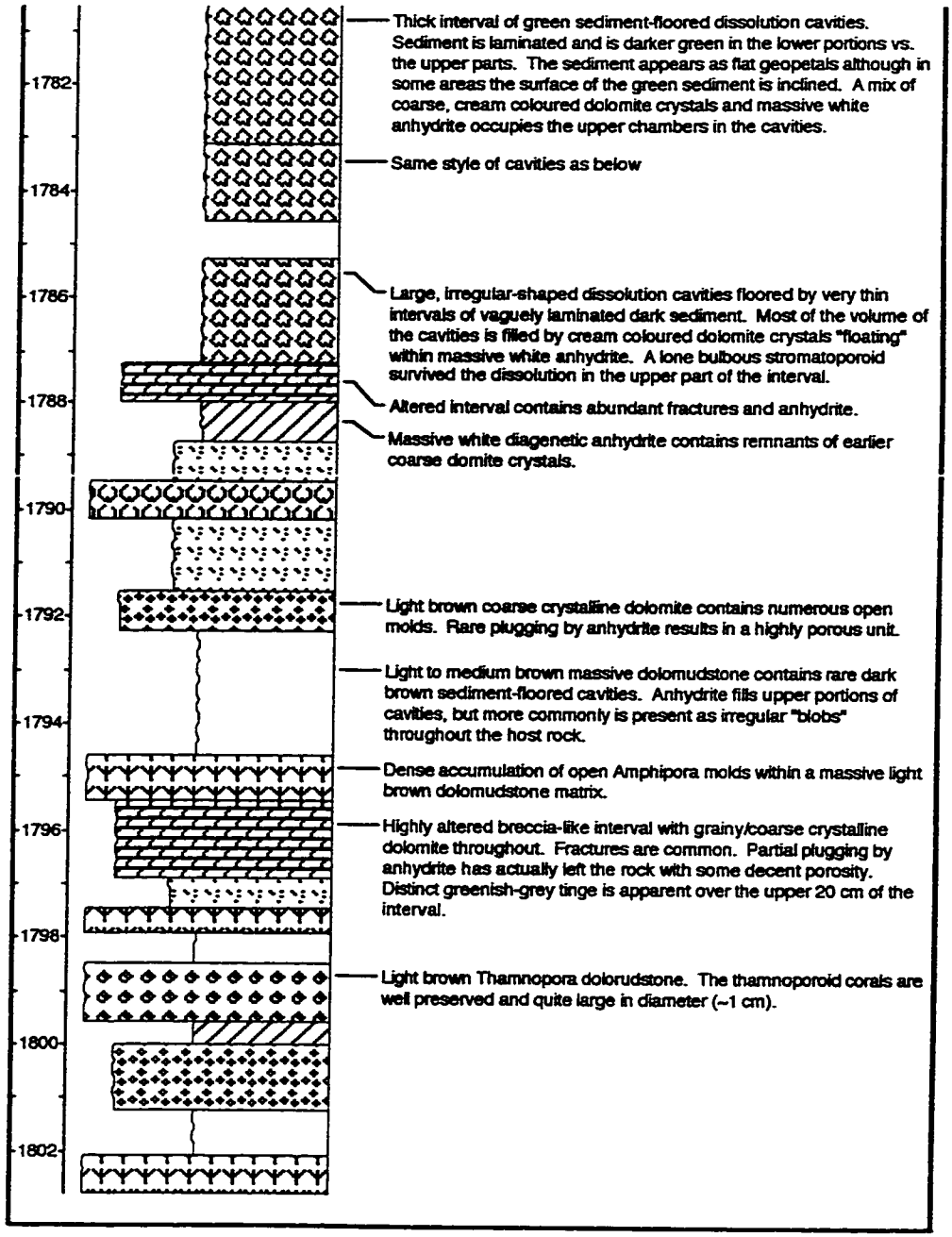

PCP WAYNE 14-13

14-13-028-21w4

Date logged: 97/08/07

Logged by: B. Ford

LEGEND

LITHOLOGY

Altered dolostone | Megalodont dfltst | Massive dmdst | Thamnopora dfltst | Gastropod dwkst

boundstn
grainstn
packstn
wackestn
mudstn

METRES | REMARKS

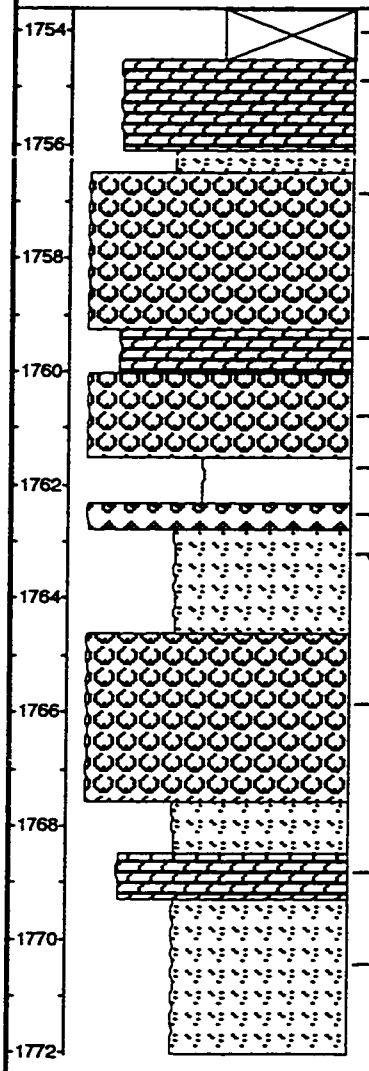

Rubble zone.

Crackle breccia: heavily fractured but little displacement of dark brown clasts. Coarse crystalline infill along fractures. A large (15 cm in height) bulbous stromatoporoid is present within a less altered zone in the middle of the breccia

Light brown megalodont dolofloatstone. Large open molds, with cream coloured dolomite linings, are common throughout the interval except for the lowermost 50 cm in which molds are completely cemented. Large gastropod molds are an accessory fossil. Pinpoint pores are common within the matrix.

Combination of coarse crystalline dolomite, skeletal fragments, and dolowackestone clasts are suggestive of a breccia matrix. Massive white anhydrite patches are common.

Light brown megalodont dolofloatstone - same as above.

Medium brown dolomudstone with abundant anhydrite patches. Rare pinpoint voids. Moderately fractured.

Medium brown Thamnopora dolorudstone. Most corals are ~5 mm in diameter. Patches of white anhydrite commonly surround the thamnoporoid corals.

Medium grey dolowackestone contains numerous pinpoint voids and random small (~1mm) to large (3cm) vugs with cream coloured dolomite crystal linings.

Light to medium brown megalodont dolofloatstone. Excellent porosity with only minor dolomite crystal linings along the interiors of the abundant megalodont molds. No anhydrite is present, except for the lower 60 cm of the interval which is highly fractured and has its pore space occluded by cements.

Breccia: angular dolowackestone clasts (up to 6 cm in diameter) supported by a coarse crystalline/grainy dark brown matrix of mainly dolomite. Anhydrite patches are common.

Light brown mottled dolowackestone with pinpoint pores throughout. No obvious fossil evidence. Abundant vugs, many with cream coloured dolomite crystal linings. Fractures are common.

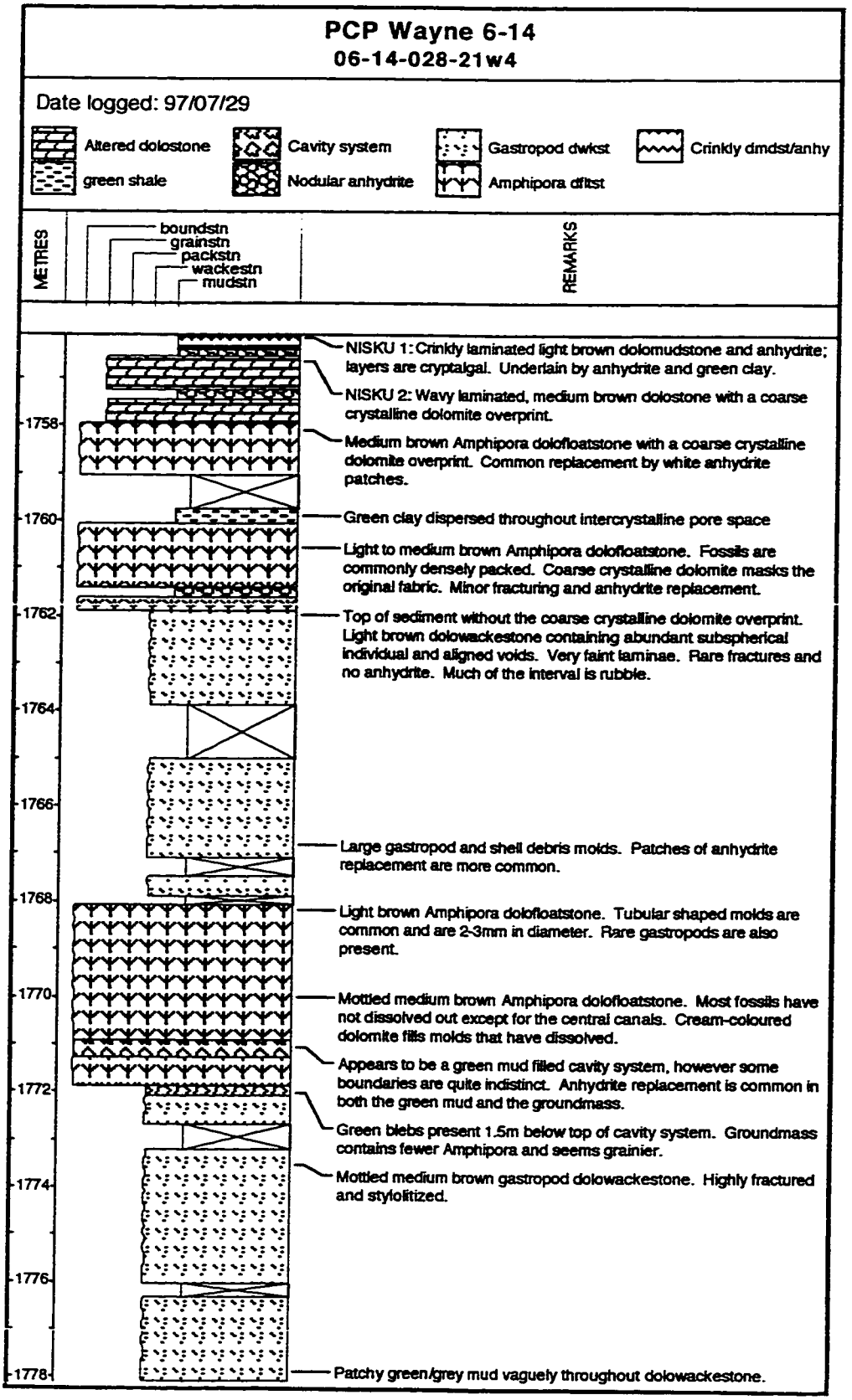
PCP Wayne 6-14
06-14-028-21w4
Date logged: 97/07/29
Altered dolostone
green shale
Cavity system
Nodular anhydrite
Gastropod dwkst
Amphipora dflst
Crinkly dmdst/anhy
METRES
boundstn
grainstn
packstn
wackestn
mudstn
REMARKS
1758
1760
1762
1764
1766
1768
1770
1772
1774
1776
1778
NISKU 1: Crinkly laminated light brown dolomudstone and anhydrite; layers are cryptalgal. Underlain by anhydrite and green clay.
NISKU 2: Wavy laminated, medium brown dolostone with a coarse crystalline dolomite overprint.
Medium brown Amphipora dolofloatstone with a coarse crystalline dolomite overprint. Common replacement by white anhydrite patches.
Green clay dispersed throughout intercrystalline pore space
Light to medium brown Amphipora dolofloatstone. Fossils are commonly densely packed. Coarse crystalline dolomite masks the original fabric. Minor fracturing and anhydrite replacement.
Top of sediment without the coarse crystalline dolomite overprint. Light brown dolowackestone containing abundant subspherical individual and aligned voids. Very faint laminae. Rare fractures and no anhydrite. Much of the interval is rubble.
Large gastropod and shell debris molds. Patches of anhydrite replacement are more common.
Light brown Amphipora dolofloatstone. Tubular shaped molds are common and are 2-3mm in diameter. Rare gastropods are also present.
Mottled medium brown Amphipora dolofloatstone. Most fossils have not dissolved out except for the central canals. Cream-coloured dolomite fills molds that have dissolved.
Appears to be a green mud filled cavity system, however some boundaries are quite indistinct. Anhydrite replacement is common in both the green mud and the groundmass.
Green blebs present 1.5m below top of cavity system. Groundmass contains fewer Amphipora and seems grainier.
Mottled medium brown gastropod dolowackestone. Highly fractured and stylolitized.
Patchy green/grey mud vaguely throughout dolowackestone.

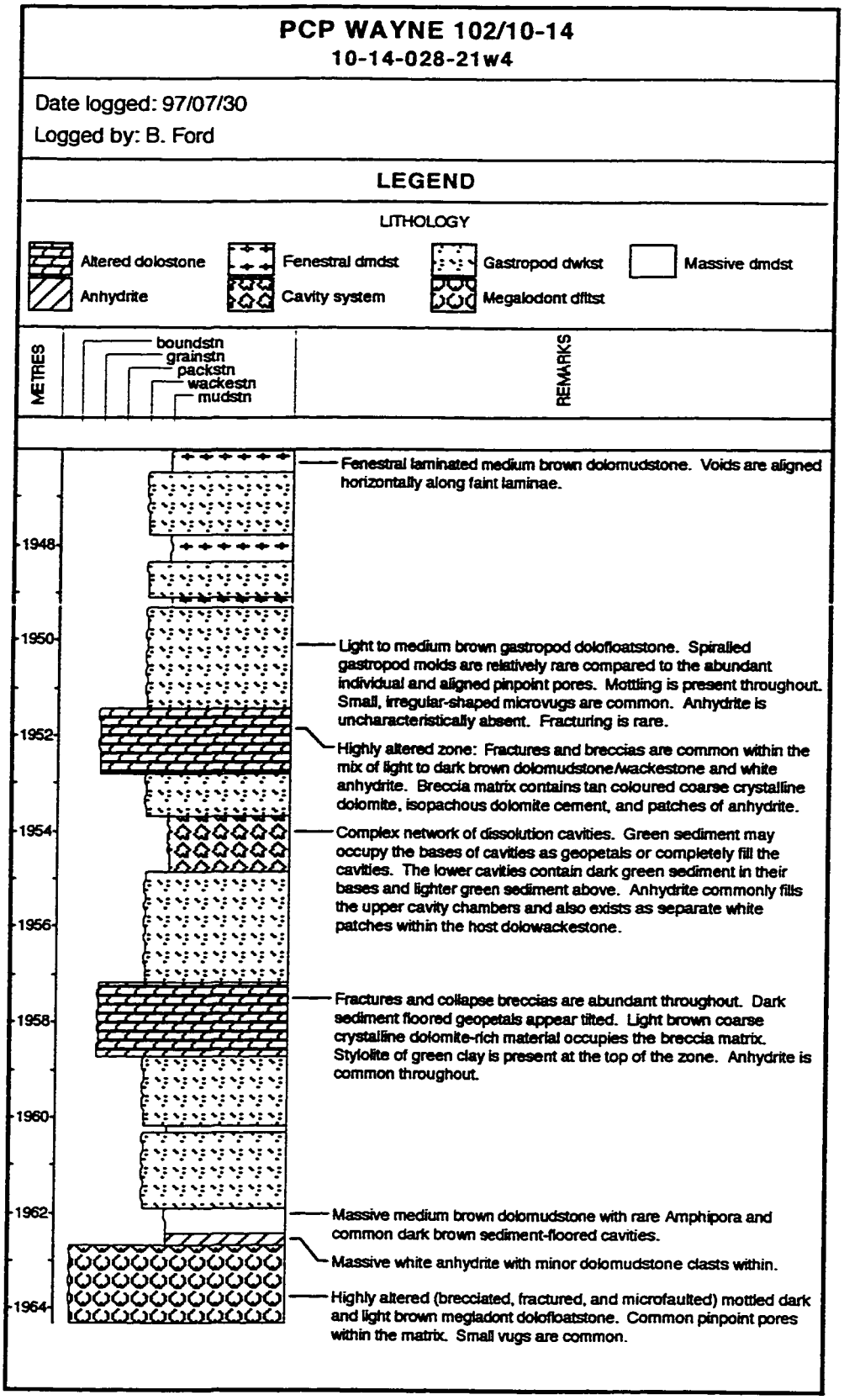
PCP WAYNE 102/10-14
10-14-028-21w4
Date logged: 97/07/30
Logged by: B. Ford
LEGEND
LITHOLOGY
Altered dolostone
Anhydrite
Fenestral dmdst
Cavity system
Gastropod dwkst
Megalodont dflst
Massive dmdst
METRES
boundstn
grainstn
packstn
wackestn
mudstn
REMARKS
1948
1950
1952
1954
1956
1958
1960
1962
1964
Fenestral laminated medium brown dolomudstone. Voids are aligned horizontally along faint laminae.
Light to medium brown gastropod dolofloatstone. Spiralled gastropod molds are relatively rare compared to the abundant individual and aligned pinpoint pores. Mottling is present throughout. Small, irregular-shaped microvugs are common. Anhydrite is uncharacteristically absent. Fracturing is rare.
Highly altered zone: Fractures and breccias are common within the mix of light to dark brown dolomudstone/wackestone and white anhydrite. Breccia matrix contains tan coloured coarse crystalline dolomite, isopachous dolomite cement, and patches of anhydrite.
Complex network of dissolution cavities. Green sediment may occupy the bases of cavities as geopetals or completely fill the cavities. The lower cavities contain dark green sediment in their bases and lighter green sediment above. Anhydrite commonly fills the upper cavity chambers and also exists as separate white patches within the host dolowackestone.
Fractures and collapse breccias are abundant throughout. Dark sediment floored geopetals appear tilted. Light brown coarse crystalline dolomite-rich material occupies the breccia matrix. Stylolite of green clay is present at the top of the zone. Anhydrite is common throughout.
Massive medium brown dolomudstone with rare Amphipora and common dark brown sediment-floored cavities.
Massive white anhydrite with minor dolomudstone clasts within.
Highly altered (brecciated, fractured, and microfaulted) mottled dark and light brown megladont dolofloatstone. Common pinpoint pores within the matrix. Small vugs are common.

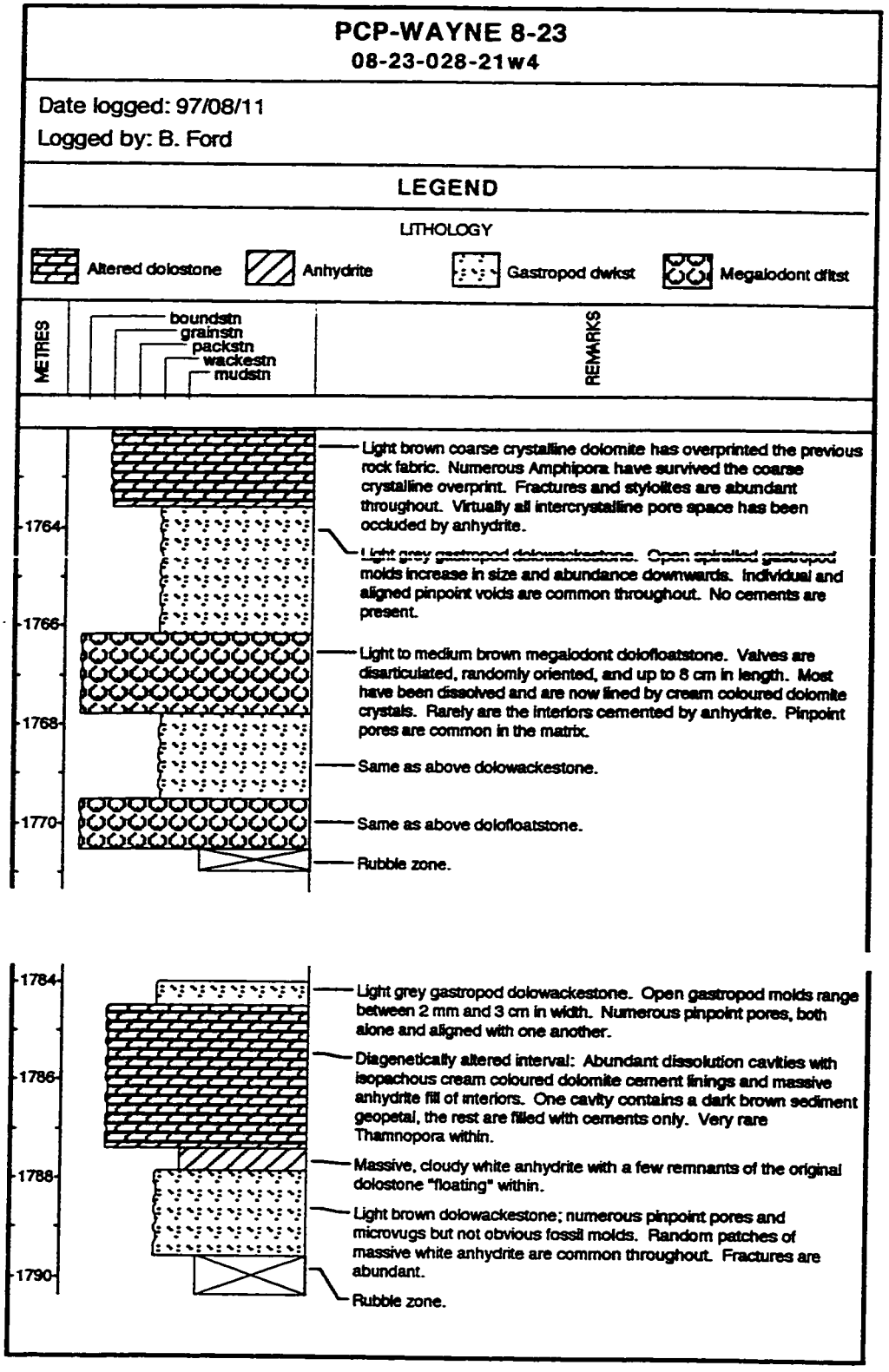
PCP-WAYNE 8-23
08-23-028-21w4
Date logged: 97/08/11
Logged by: B. Ford
LEGEND
LITHOLOGY
Altered dolostone
Anhydrite
Gastropod dwkst
Megalodont dfltst
METRES
boundstn
grainstn
packstn
wackestn
mudstn
REMARKS
1764
1766
1768
1770
1784
1786
1788
1790
Light brown coarse crystalline dolomite has overprinted the previous rock fabric. Numerous Amphipora have survived the coarse crystalline overprint. Fractures and stylolites are abundant throughout. Virtually all intercrystalline pore space has been occluded by anhydrite.
Light grey gastropod dolowackestone. Open spiralled gastropod molds increase in size and abundance downwards. Individual and aligned pinpoint voids are common throughout. No cements are present.
Light to medium brown megalodont dolofloatstone. Valves are disarticulated, randomly oriented, and up to 8 cm in length. Most have been dissolved and are now lined by cream coloured dolomite crystals. Rarely are the interiors cemented by anhydrite. Pinpoint pores are common in the matrix.
Same as above dolowackestone.
Same as above dolofloatstone.
Rubble zone.
Light grey gastropod dolowackestone. Open gastropod molds range between 2 mm and 3 cm in width. Numerous pinpoint pores, both alone and aligned with one another.
Diagenetically altered interval: Abundant dissolution cavities with isopachous cream coloured dolomite cement linings and massive anhydrite fill of interiors. One cavity contains a dark brown sediment geopetal, the rest are filled with cements only. Very rare Thamnopora within.
Massive, cloudy white anhydrite with a few remnants of the original dolostone "floating" within.
Light brown dolowackestone; numerous pinpoint pores and microvugs but not obvious fossil molds. Random patches of massive white anhydrite are common throughout. Fractures are abundant.
Rubble zone.

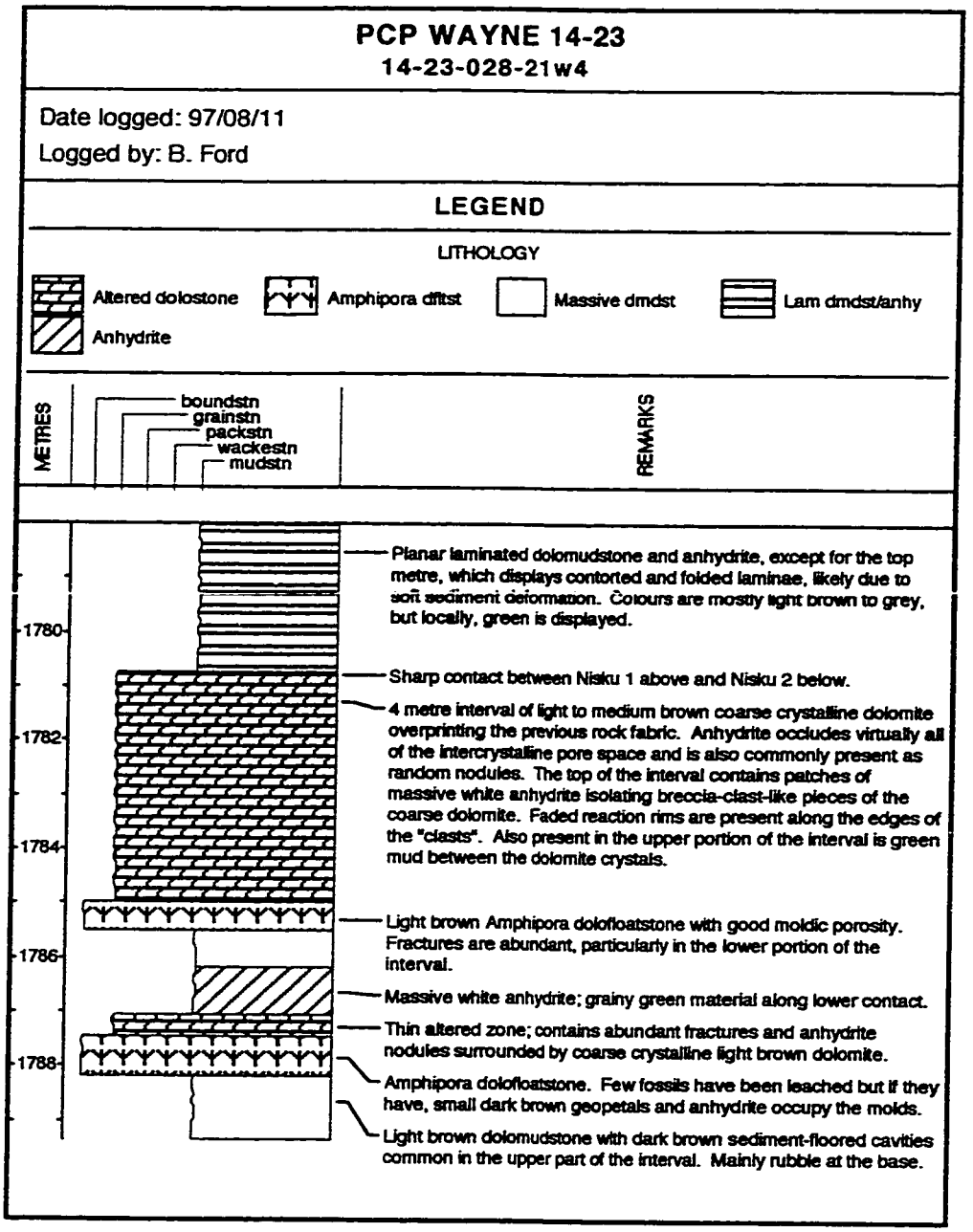
PCP WAYNE 14-23
14-23-028-21w4
Date logged: 97/08/11
Logged by: B. Ford
LEGEND
LITHOLOGY
Altered dolostone
Amphipora dfltst
Massive dmdst
Lam dmdst/anhy
Anhydrite
METRES
boundstn
grainstn
packstn
wackestn
mudstn
REMARKS
1780
1782
1784
1786
1788
Planar laminated dolomudstone and anhydrite, except for the top metre, which displays contorted and folded laminae, likely due to soft sediment deformation. Colours are mostly light brown to grey, but locally, green is displayed.
Sharp contact between Nisku 1 above and Nisku 2 below.
4 metre interval of light to medium brown coarse crystalline dolomite overprinting the previous rock fabric. Anhydrite occludes virtually all of the intercrystalline pore space and is also commonly present as random nodules. The top of the interval contains patches of massive white anhydrite isolating breccia-clast-like pieces of the coarse dolomite. Faded reaction rims are present along the edges of the "clasts". Also present in the upper portion of the interval is green mud between the dolomite crystals.
Light brown Amphipora dolofloatstone with good moldic porosity. Fractures are abundant, particularly in the lower portion of the interval.
Massive white anhydrite; grainy green material along lower contact.
Thin altered zone; contains abundant fractures and anhydrite nodules surrounded by coarse crystalline light brown dolomite.
Amphipora dolofloatstone. Few fossils have been leached but if they have, small dark brown geopetals and anhydrite occupy the molds.
Light brown dolomudstone with dark brown sediment-floored cavities common in the upper part of the interval. Mainly rubble at the base.

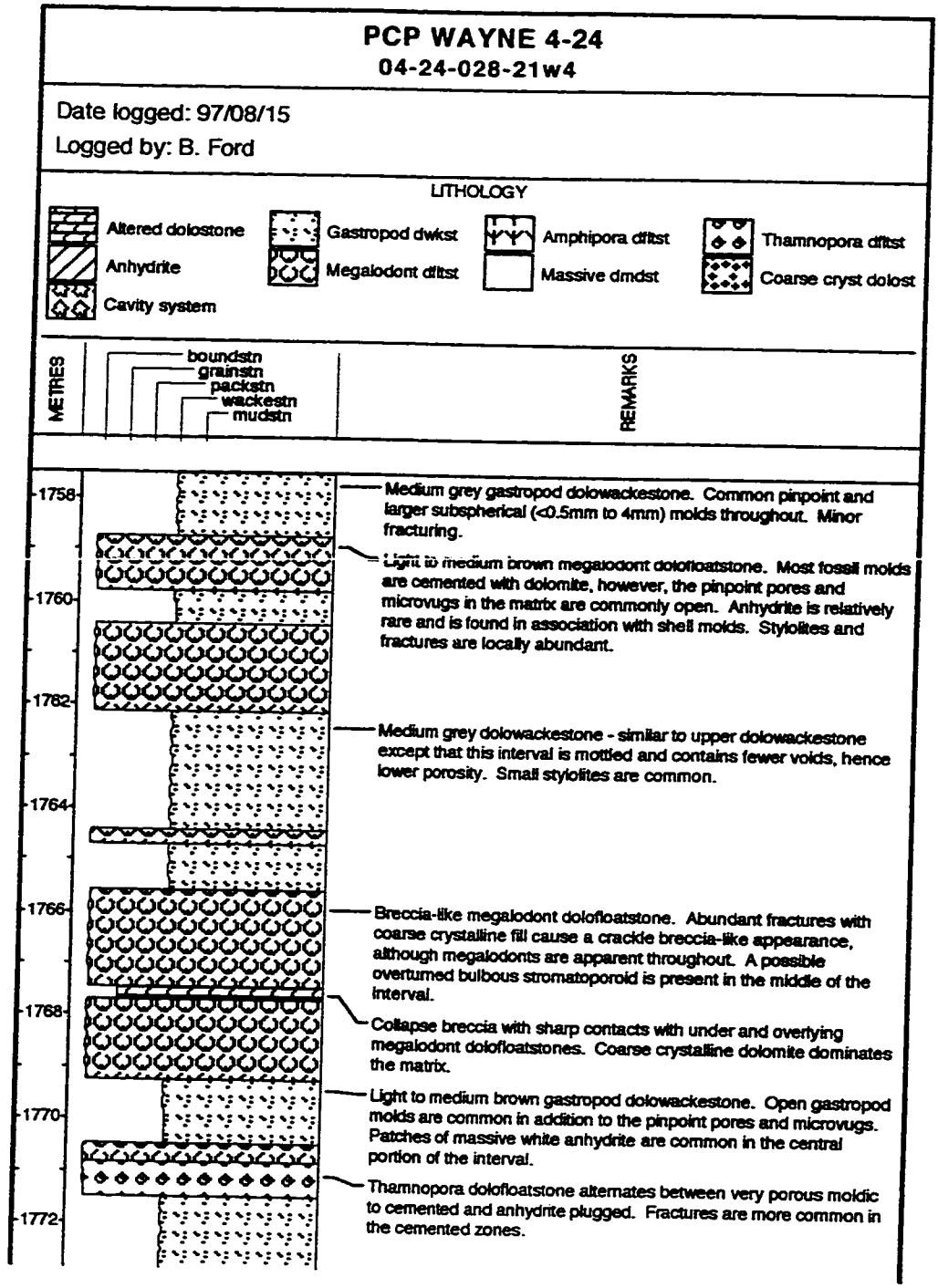
PCP WAYNE 4-24
04-24-028-21w4
Date logged: 97/08/15
Logged by: B. Ford
LITHOLOGY
Altered dolostone
Anhydrite
Cavity system
Gastropod dwkst
Megalodont dflst
Amphipora dflst
Massive dmdst
Thamnopora dflst
Coarse cryst dolost
METRES
boundstn
grainstn
packstn
wackestn
mudstn
REMARKS
1758
1760
1762
1764
1766
1768
1770
1772
Medium grey gastropod dolowackestone. Common pinpoint and larger subspherical (<0.5mm to 4mm) molds throughout. Minor fracturing.
Light to medium brown megalodont dolofloatstone. Most fossil molds are cemented with dolomite, however, the pinpoint pores and microvugs in the matrix are commonly open. Anhydrite is relatively rare and is found in association with shell molds. Stylolites and fractures are locally abundant.
Medium grey dolowackestone - similar to upper dolowackestone except that this interval is mottled and contains fewer voids, hence lower porosity. Small stylolites are common.
Breccia-like megalodont dolofloatstone. Abundant fractures with coarse crystalline fill cause a crackle breccia-like appearance, although megalodonts are apparent throughout. A possible overturned bulbous stromatoporoid is present in the middle of the interval.
Collapse breccia with sharp contacts with under and overlying megalodont dolofloatstones. Coarse crystalline dolomite dominates the matrix.
Light to medium brown gastropod dolowackestone. Open gastropod molds are common in addition to the pinpoint pores and microvugs. Patches of massive white anhydrite are common in the central portion of the interval.
Thamnopora dolofloatstone alternates between very porous moldic to cemented and anhydrite plugged. Fractures are more common in the cemented zones.

4-24-28-21W4 Continued

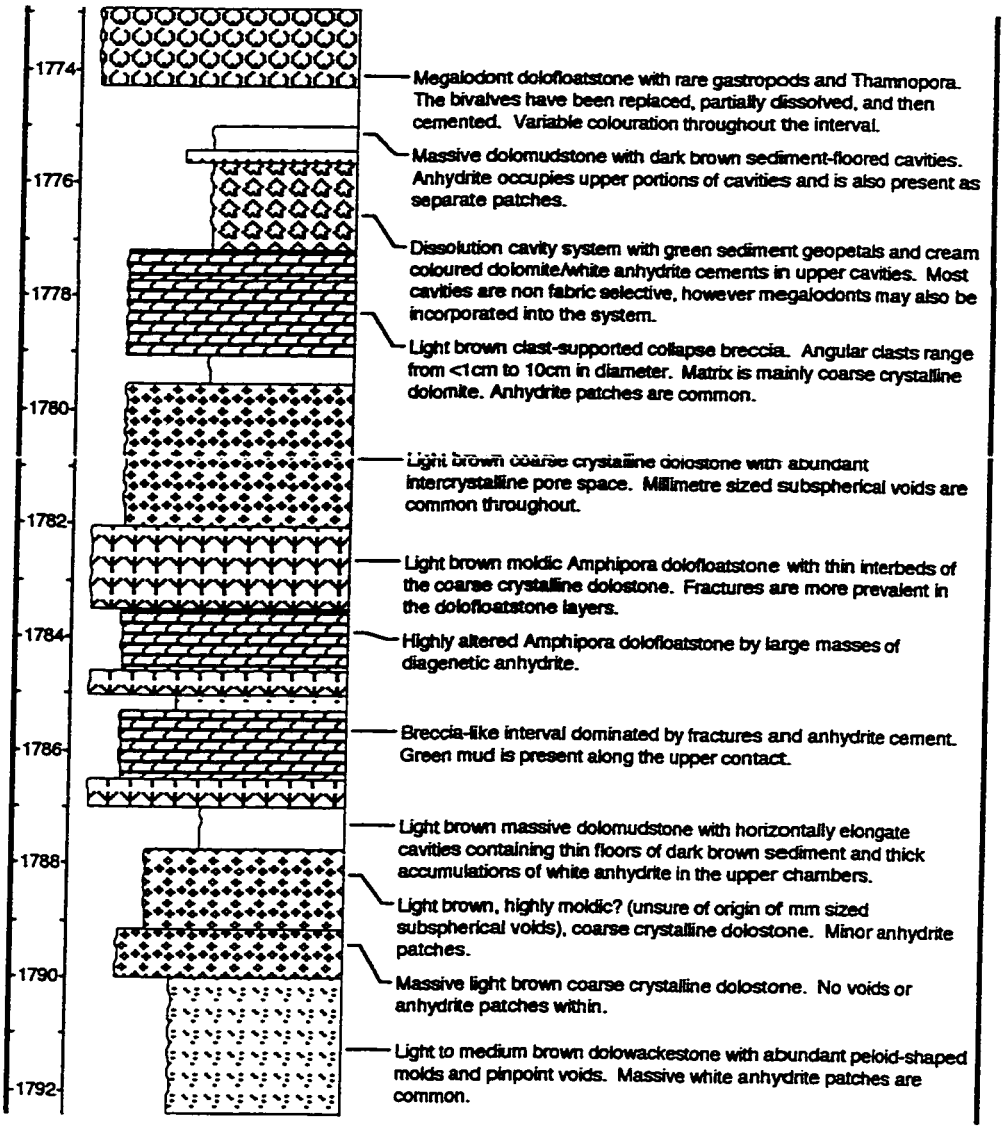

4-24-28-21W4 Continued

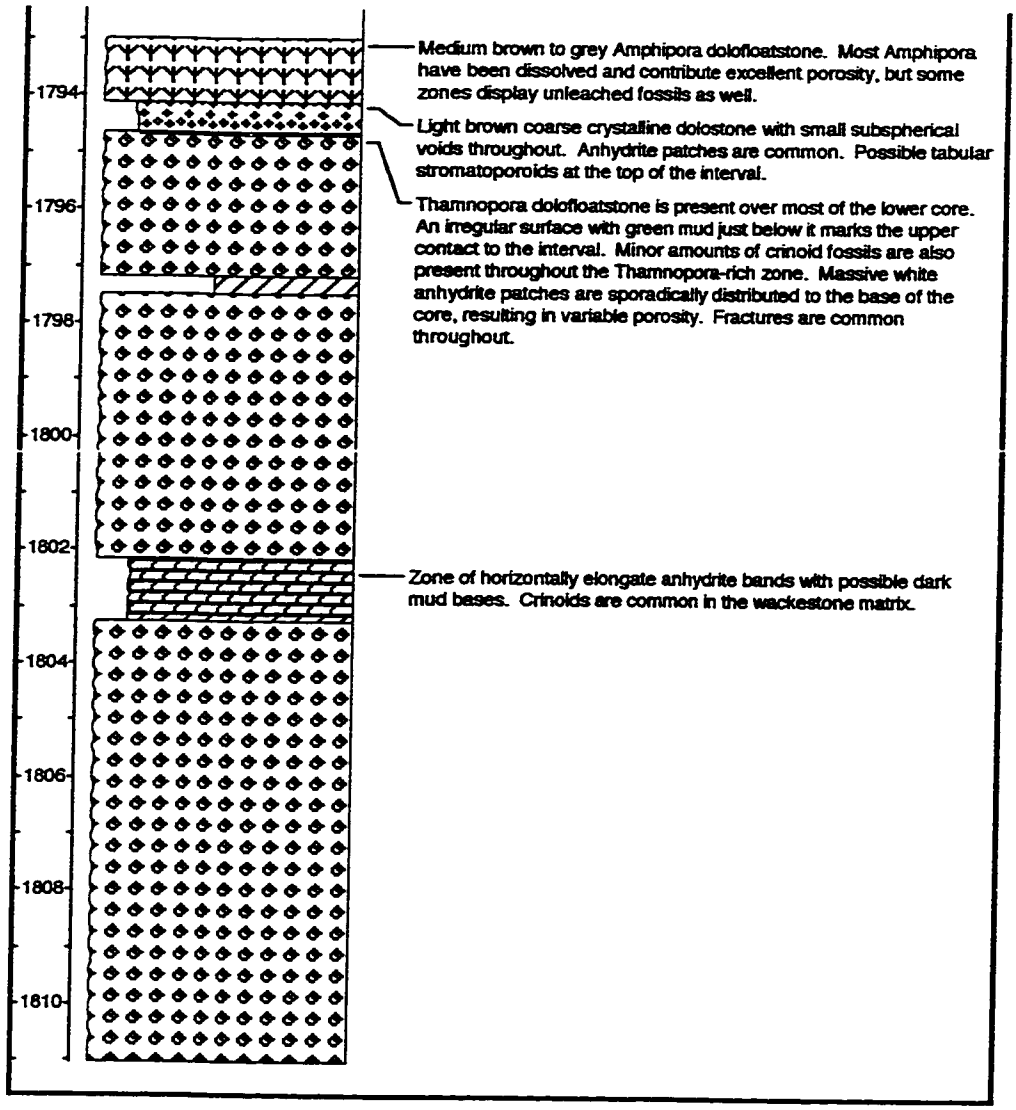

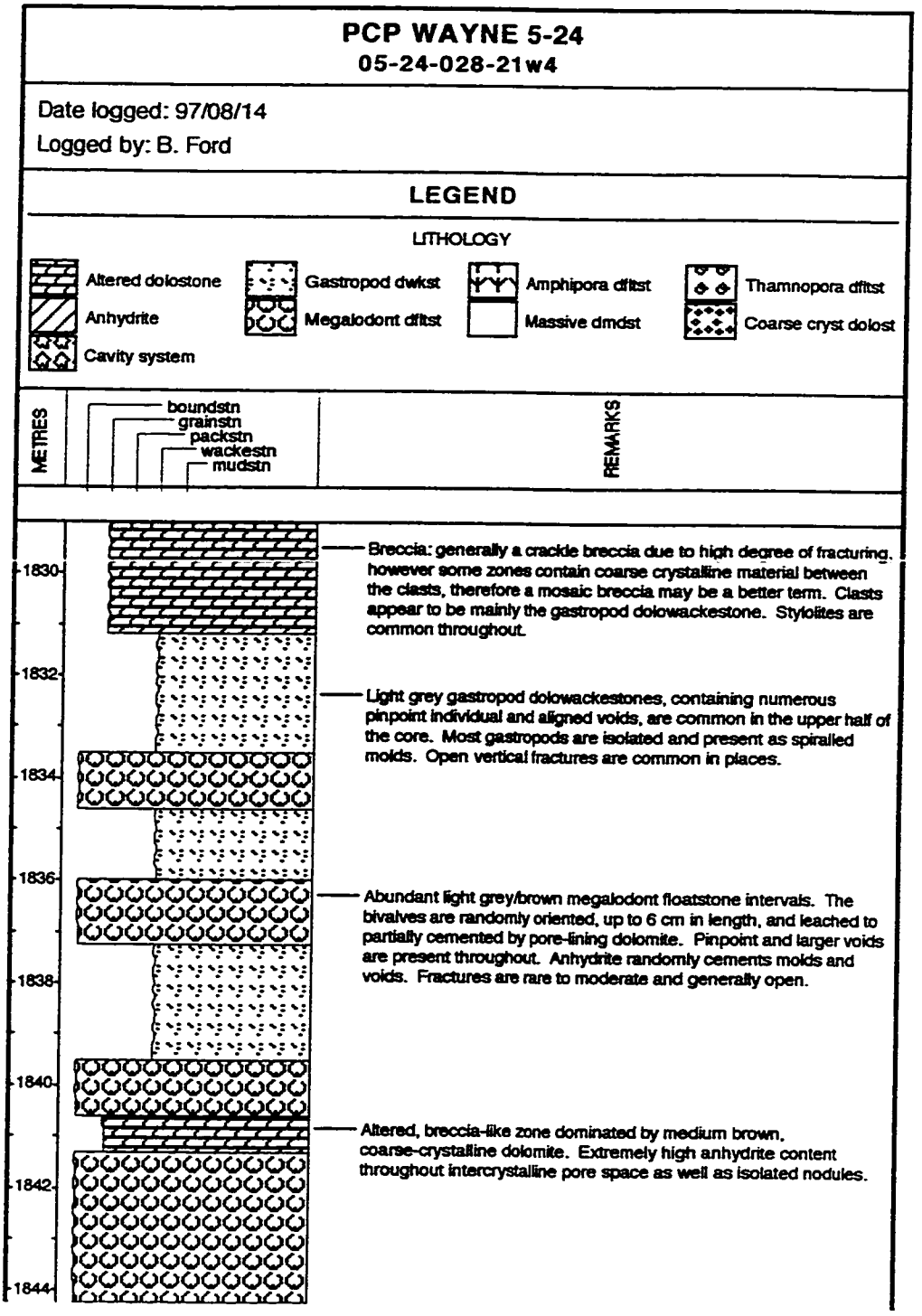
PCP WAYNE 5-24
05-24-028-21w4
Date logged: 97/08/14
Logged by: B. Ford
LEGEND
LITHOLOGY
Altered dolostone
Anhydrite
Cavity system
Gastropod dwkst
Megalodont dfltst
Amphipora dfltst
Massive dmdst
Thamnopora dfltst
Coarse cryst dolost
METRES
boundstn
grainstn
packstn
wackestn
mudstn
REMARKS
1830
1832
1834
1836
1838
1840
1842
1844
Breccia: generally a crackle breccia due to high degree of fracturing, however some zones contain coarse crystalline material between the clasts, therefore a mosaic breccia may be a better term. Clasts appear to be mainly the gastropod dolowackestone. Stylolites are common throughout.
Light grey gastropod dolowackestones, containing numerous pinpoint individual and aligned voids, are common in the upper half of the core. Most gastropods are isolated and present as spiralled molds. Open vertical fractures are common in places.
Abundant light grey/brown megalodont floatstone intervals. The bivalves are randomly oriented, up to 6 cm in length, and leached to partially cemented by pore-lining dolomite. Pinpoint and larger voids are present throughout. Anhydrite randomly cements molds and voids. Fractures are rare to moderate and generally open.
Altered, breccia-like zone dominated by medium brown, coarse-crystalline dolomite. Extremely high anhydrite content throughout intercrystalline pore space as well as isolated nodules.

5-24-28-21W4 Continued

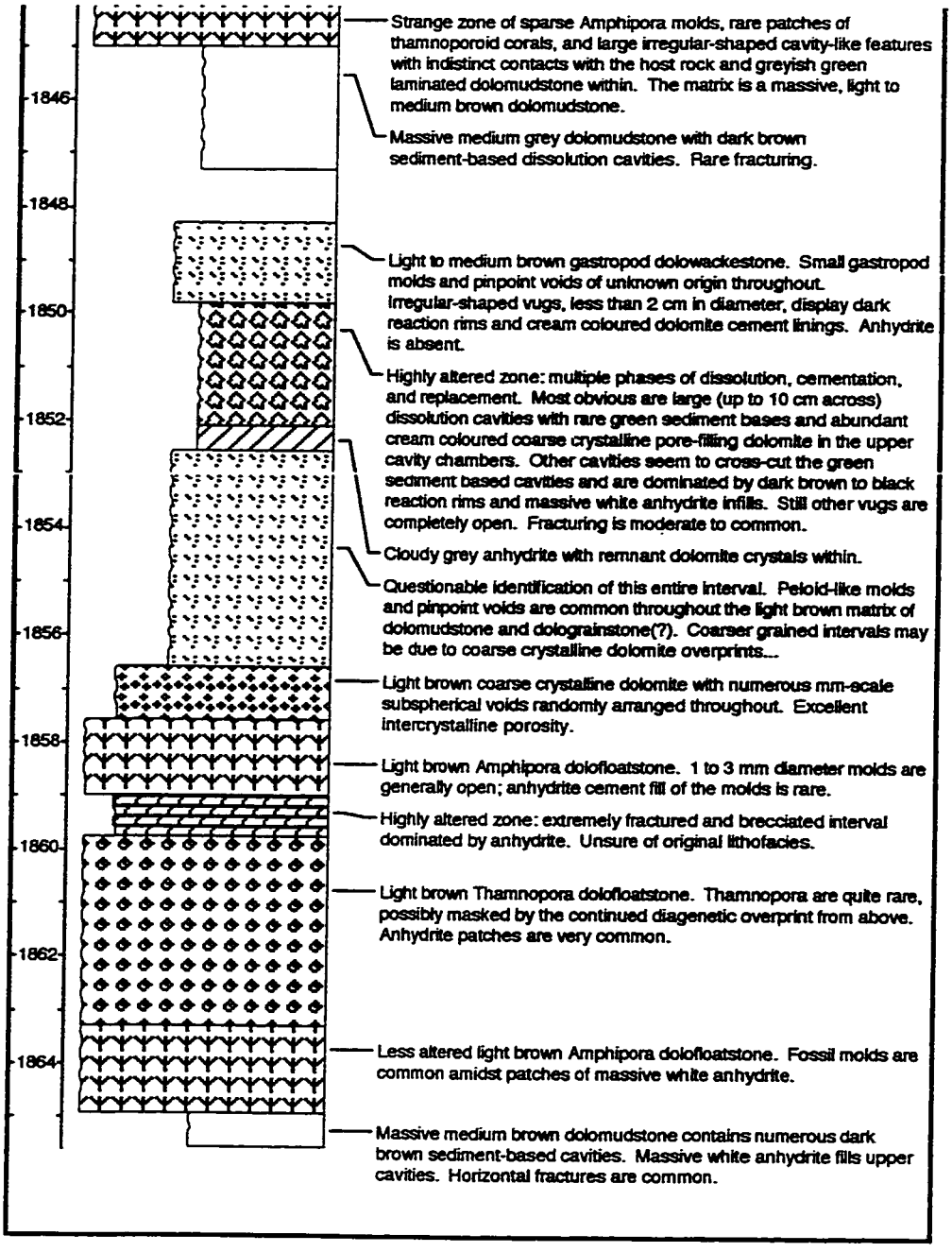

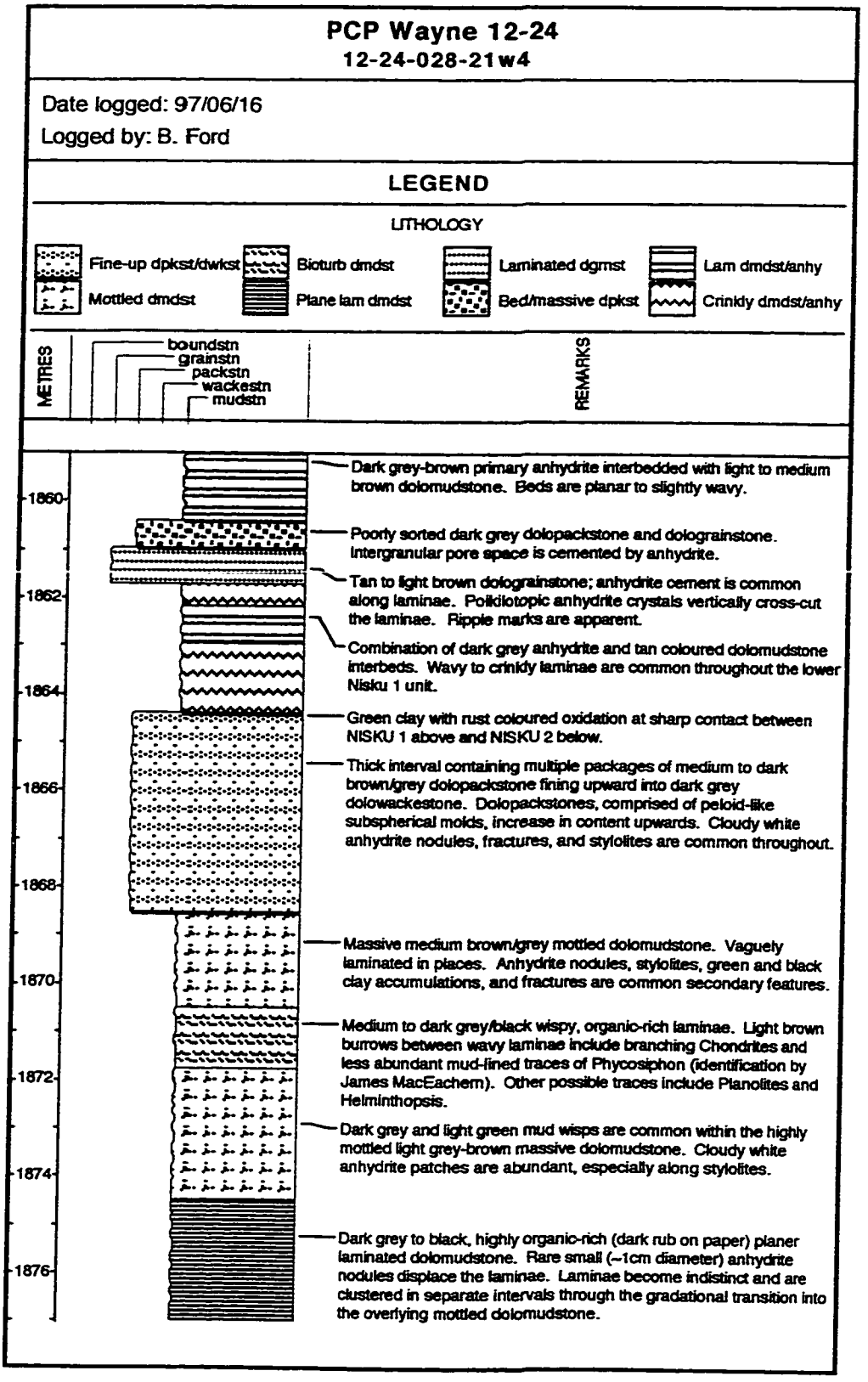
PCP Wayne 12-24
12-24-028-21w4
Date logged: 97/06/16
Logged by: B. Ford
LEGEND
LITHOLOGY
Fine-up dpkst/dwkst
Mottled dmdst
Bioturb dmdst
Plane lam dmdst
Laminated dgmst
Bed/massive dpkst
Lam dmdst/anhy
Crinkly dmdst/anhy
METRES
boundstn
grainstn
packstn
wackestn
mudstn
REMARKS
1860
1862
1864
1866
1868
1870
1872
1874
1876
Dark grey-brown primary anhydrite interbedded with light to medium brown dolomudstone. Beds are planar to slightly wavy.
Poorly sorted dark grey dolopackstone and dolograinstone. Intergranular pore space is cemented by anhydrite.
Tan to light brown dolograinstone; anhydrite cement is common along laminae. Poikilotopic anhydrite crystals vertically cross-cut the laminae. Ripple marks are apparent.
Combination of dark grey anhydrite and tan coloured dolomudstone interbeds. Wavy to crinkly laminae are common throughout the lower Nisku 1 unit.
Green clay with rust coloured oxidation at sharp contact between NISKU 1 above and NISKU 2 below.
Thick interval containing multiple packages of medium to dark brown/grey dolopackstone fining upward into dark grey dolowackestone. Dolopackstones, comprised of peloid-like subspherical molds, increase in content upwards. Cloudy white anhydrite nodules, fractures, and stylolites are common throughout.
Massive medium brown/grey mottled dolomudstone. Vaguely laminated in places. Anhydrite nodules, stylolites, green and black clay accumulations, and fractures are common secondary features.
Medium to dark grey/black wispy, organic-rich laminae. Light brown burrows between wavy laminae include branching Chondrites and less abundant mud-lined traces of Phycosiphon (identification by James MacEachern). Other possible traces include Planolites and Helminthopsis.
Dark grey and light green mud wisps are common within the highly mottled light grey-brown massive dolomudstone. Cloudy white anhydrite patches are abundant, especially along stylolites.
Dark grey to black, highly organic-rich (dark rub on paper) planer laminated dolomudstone. Rare small (~1cm diameter) anhydrite nodules displace the laminae. Laminae become indistinct and are clustered in separate intervals through the gradational transition into the overlying mottled dolomudstone.

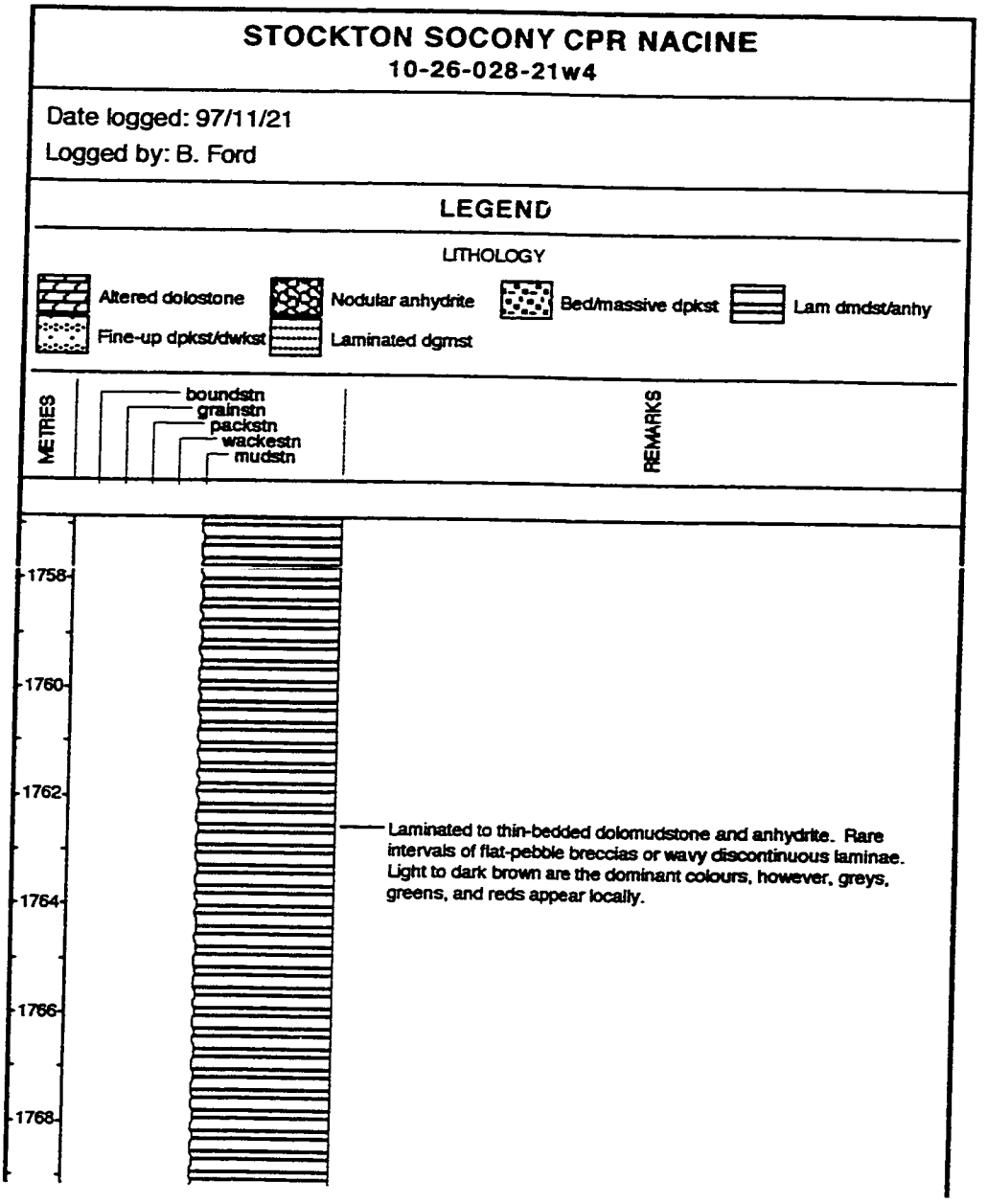
STOCKTON SOCONY CPR NACINE
10-26-028-21w4
Date logged: 97/11/21
Logged by: B. Ford
LEGEND
LITHOLOGY
Altered dolostone
Fine-up dpkst/dwkst
Nodular anhydrite
Laminated dgmst
Bed/massive dpkst
Lam dmdst/anhy
METRES
boundstn
grainstn
packstn
wackestn
mudstn
REMARKS
1758
1760
1762
1764
1766
1768
Laminated to thin-bedded dolomudstone and anhydrite. Rare intervals of flat-pebble breccias or wavy discontinuous laminae. Light to dark brown are the dominant colours, however, greys, greens, and reds appear locally.

10-26-28-21W4 Continued